

Advances

in Clinical and Experimental Medicine

MONTHLY ISSN 1899-5276 (PRINT) ISSN 2451-2680 (ONLINE)

advances.umw.edu.pl

2024, Vol. 33, No. 4 (April)

Impact Factor (IF) – 2.1
Ministry of Science and Higher Education – 70 pts
Index Copernicus (ICV) – 161.11 pts



WROCLAW
MEDICAL UNIVERSITY

Advances
in Clinical and Experimental
Medicine



Advances in Clinical and Experimental Medicine

ISSN 1899-5276 (PRINT)

ISSN 2451-2680 (ONLINE)

advances.umw.edu.pl

MONTHLY 2024
Vol. 33, No. 4
(April)

Advances in Clinical and Experimental Medicine (*Adv Clin Exp Med*) publishes high-quality original articles, research-in-progress, research letters and systematic reviews and meta-analyses of recognized scientists that deal with all clinical and experimental medicine.

Editorial Office

ul. Marcinkowskiego 2–6
50-368 Wrocław, Poland
Tel.: +48 71 784 12 05
E-mail: redakcja@umw.edu.pl

Editor-in-Chief

Prof. Donata Kurpas

Deputy Editor

Prof. Wojciech Kosmala

Managing Editor

Marek Misiak, MA

Statistical Editors

Wojciech Bombała, MSc

Łucja Janek, MSc

Anna Kopszak, MSc

Dr. Krzysztof Kujawa

Jakub Wronowicz, MSc

Manuscript editing

Marek Misiak, MA

Paulina Piątkowska, MA

Publisher

Wrocław Medical University
Wybrzeże L. Pasteura 1
50-367 Wrocław, Poland

Online edition is the original version
of the journal

Scientific Committee

Prof. Sandra Maria Barbalho

Prof. Antonio Cano

Prof. Chong Chen

Prof. Breno Diniz

Prof. Erwan Donal

Prof. Chris Fox

Prof. Yuko Hakamata

Prof. Carol Holland

Prof. Sabine Bährer-Kohler

Prof. Markku Kurkinen

Prof. Christos Lionis

Prof. Raimundo Mateos

Prof. Zbigniew W. Raś

Prof. Jerzy W. Rozenblit

Prof. Silvina Santana

Prof. Sajee Sattayut

Prof. James Sharman

Prof. Jamil Shibli

Prof. Michał J. Toborek

Prof. László Vécsei

Prof. Cristiana Vitale

Prof. Hao Zhang

Section Editors

Basic Sciences

Prof. Iwona Bil-Lula

Prof. Bartosz Kempisty

Dr. Wiesława Kranc

Dr. Anna Lebedeva

Clinical Anatomy, Legal Medicine, Innovative Technologies

Prof. Rafael Boscolo-Berto

Dentistry

Prof. Marzena Dominiak

Prof. Tomasz Gedrange

Prof. Jamil Shibli

Laser Dentistry

Assoc. Prof. Kinga Grzech-Leśniak

Dermatology

Prof. Jacek Szepietowski

Emergency Medicine, Innovative Technologies

Prof. Jacek Smereka

Gynecology and Obstetrics

Prof. Olimpia Sipak-Szmigiel

Histology and Embryology

Dr. Mateusz Olbromski

Internal Medicine

Angiology

Dr. Angelika Chachaj

Cardiology

Prof. Wojciech Kosmala

Dr. Daniel Morris

Endocrinology

Prof. Marek Bolanowski

Gastroenterology

Assoc. Prof. Katarzyna Neubauer

Hematology

Prof. Andrzej Deptała
Prof. Dariusz Wołowicz

Nephrology and Transplantology

Assoc. Prof. Dorota Kamińska
Prof. Krzysztof Letachowicz

Pulmonology

Prof. Anna Brzecka

Microbiology

Prof. Marzenna Bartoszewicz
Assoc. Prof. Adam Junka

Molecular Biology

Dr. Monika Bielecka

Prof. Jolanta Sączko

Neurology

Assoc. Prof. Magdalena Koszewicz
Assoc. Prof. Anna Pokryszko-Dragan

Dr. Masaru Tanaka

Neuroscience

Dr. Simone Battaglia
Dr. Francesco Di Gregorio

Oncology

Prof. Andrzej Deptała
Prof. Adam Maciejczyk

Gynecological Oncology

Dr. Marcin Jędryka

Ophthalmology

Dr. Małgorzata Gajdzis

Orthopedics

Prof. Paweł Reichert

Otolaryngology

Assoc. Prof. Tomasz Zatoński

Pediatrics

Pediatrics, Metabolic Pediatrics, Clinical Genetics, Neonatology, Rare Disorders

Prof. Robert Śmigiel

Pediatric Nephrology

Prof. Katarzyna Kiliś-Pstrusińska

Pediatric Oncology and Hematology

Assoc. Prof. Marek Ussowicz

Pharmaceutical Sciences

Assoc. Prof. Marta Kepińska
Prof. Adam Matkowski

Pharmacoeconomics, Rheumatology

Dr. Sylwia Szafraniec-Buryło

Psychiatry

Dr. Melike Küçükkarapınar
Prof. Jerzy Leszek
Assoc. Prof. Bartłomiej Stańczykiewicz

Public Health

Prof. Monika Sawhney
Prof. Izabella Uchmanowicz

Qualitative Studies, Quality of Care

Prof. Ludmiła Marcinowicz

Radiology

Prof. Marek Szaśiadek

Rehabilitation

Dr. Elżbieta Rajkowska-Labon

Surgery

Assoc. Prof. Mariusz Chabowski
Assoc. Prof. Mirosław Kozłowski
Prof. Renata Taboła

Telemedicine, Geriatrics, Multimorbidity

Assoc. Prof. Maria Magdalena
Bujnowska-Fedak

Editorial Policy

Advances in Clinical and Experimental Medicine (Adv Clin Exp Med) is an independent multidisciplinary forum for exchange of scientific and clinical information, publishing original research and news encompassing all aspects of medicine, including molecular biology, biochemistry, genetics, biotechnology and other areas. During the review process, the Editorial Board conforms to the "Uniform Requirements for Manuscripts Submitted to Biomedical Journals: Writing and Editing for Biomedical Publication" approved by the International Committee of Medical Journal Editors (www.ICMJE.org). The journal publishes (in English only) original papers and reviews. Short works considered original, novel and significant are given priority. Experimental studies must include a statement that the experimental protocol and informed consent procedure were in compliance with the Helsinki Convention and were approved by an ethics committee.

For all subscription-related queries please contact our Editorial Office: redakcja@umw.edu.pl

For more information visit the journal's website: advances.umw.edu.pl

Pursuant to the ordinance of the Rector of Wrocław Medical University No. 12/XVI R/2023, from February 1, 2023, authors are required to pay a fee for each manuscript accepted for publication in the journal Advances in Clinical and Experimental Medicine. The fee amounts to 1600 EUR for all types of papers.

Advances in Clinical and Experimental Medicine has received financial support from the resources of Ministry of Science and Higher Education within the "Social Responsibility of Science – Support for Academic Publishing" project based on agreement No. RCN/SP/0584/2021.



Ministry of Education and Science
Republic of Poland

Czasopismo Advances in Clinical and Experimental Medicine korzysta ze wsparcia finansowego ze środków Ministerstwa Edukacji i Nauki w ramach programu „Społeczna Odpowiedzialność Nauki – Rozwój Czasopism Naukowych” na podstawie umowy nr RCN/SP/0584/2021.



Ministerstwo
Edukacji i Nauki

Indexed in: MEDLINE, Science Citation Index Expanded, Journal Citation Reports/Science Edition, Scopus, EMBASE/Excerpta Medica, Ulrich's™ International Periodicals Directory, Index Copernicus

Typographic design: Piotr Gil, Monika Kołęda

DTP: Wydawnictwo UMW

Cover: Monika Kołęda

Printing and binding: PRINT PROFIT Sp. z o.o., Koźmin 27, 59-900 Zgorzelec

Contents

Editorial

- 321 Francesco Di Gregorio, Simone Battaglia
The intricate brain–body interaction in psychiatric and neurological diseases

Meta-analysis

- 327 Liansheng Hao, Shengkai Mu, Junyan Yin, Jun Liu
A meta-analysis of the risk of osteoporotic fractures in inflammatory bowel disease

Original papers

- 335 Xinyue Zhang, Xiaotong Zhuang, Jie Dong, Bo Fu, Genghua Zhang, Li Xu
Clinical efficacy of conbercept injection on neovascular age-related macular degeneration under different levels of inflammation
- 343 Zhiqin Liu, Wentao Gao, Xiping Zhang, Weifeng Wang, Miduo Tan, Eryue Qiu, Anlie Cai
The distance between the anterior and posterior edges of the fibula at a lateral internal rotation of 15° is associated with postoperative malreduction in patients with an ankle joint fracture combined with a lower tibiofibular syndesmosis injury
- 351 Haotang Wei, Jialei Wang, Zhengkai Jiang, Yu Liu, Sheng Jiang, Bangli Hu
Preoperative prognostic nutritional index associated with anastomotic leakage in colorectal cancer patients after surgery
- 361 Anna Repczyńska, Katarzyna Jułga, Anđzelika Lorenc, Jolanta Skalska-Sadowska, Mariusz Wysocki, Agnieszka Zaucha-Prażmo, Katarzyna Drabko, Artur Bossowski, Bożena Dembowska-Bagińska, Jacek Wachowiak, Adam Bucirski, Olga Haus
Cytogenetic findings in Polish patients with suspected Fanconi anemia
- 369 Joanna Kosalka-Węgiel, Sabina Lichołaj, Sylwia Dziedzina, Mamert Milewski, Piotr Kuzmiersz, Anna Korona, Mariusz Korkosz, Jolanta Gašior, Aleksandra Matyja-Bednarczyk, Helena Kwiatkowska, Anđzelika Siwiec-Kozlik, Wojciech Sydor, Joanna Wilańska, Lech Zaręba, Weronika Pocięj-Marciak, Jerzy Dropiński, Marek Sanak, Jacek Musiał, Stanisława Bazan-Socha
Association between clinical features and course of systemic sclerosis and serum interleukin-8, vascular endothelial growth factor, basic fibroblast growth factor, and interferon alpha
- 379 Jakub Stępień, Żanna Pastuszek
Distal symmetrical polyneuropathy in diabetes mellitus patients: Proposition of a new scoring system based on electroneurography findings
- 387 Katarzyna Olszewska, Agnieszka Ptak, Agnieszka Rusak, Agnieszka Dębiec-Bąk, Małgorzata Stefańska
Changes in the scar tissue structure after cesarean section as a result of manual therapy
- 397 Ewelina Stelcer, Karol Jopek, Małgorzata Błatkiewicz, Anna Olechnowicz, Kacper Kamiński, Marta Szyszka, Wiktoria Maria Suchorska, Marcin Ruciński
Gene expression profile of hiPSC-derived cells differentiated with growth factors, forskolin and conditioned medium from human adrenocortical cell line

Reviews

- 409 Agata Tyczyńska, Jan Zaucha
At what point are we on the way to optimally treat multiple myeloma patients over 75 years of age in 2023?

The intricate brain–body interaction in psychiatric and neurological diseases

Francesco Di Gregorio^{A,D–F}, Simone Battaglia^{A,D–F}

Center for Studies and Research in Cognitive Neuroscience, Department of Psychology “Renzo Canestrari”, University of Bologna, Italy

A – research concept and design; B – collection and/or assembly of data; C – data analysis and interpretation; D – writing the article; E – critical revision of the article; F – final approval of the article

Advances in Clinical and Experimental Medicine, ISSN 1899–5276 (print), ISSN 2451–2680 (online)

Adv Clin Exp Med. 2024;33(4):321–326

Address for correspondence

Francesco Di Gregorio
E-mail: francesco.digregori5@unibo.it

Funding sources

The study was supported by Next Generation EU (NGEU) and funded by the Ministry of University and Research (MUR), National Recovery and Resilience Plan (NRRP) and the MNESYS project (grant No. PE0000006): A multiscale integrated approach to the study of the nervous system in health and disease (grant No. DN. 1553 11.10.2022) granted to Simone Battaglia.

Conflict of interest

None declared

Received on February 13, 2024

Reviewed on March 1, 2024

Accepted on March 5, 2024

Published online on March 21, 2024

Abstract

A harmonic brain–body communication is fundamental to individual wellbeing and is the basis of human cognition and behavior. In the last 2 decades, the interaction between the brain and body functioning has become a central area of study for neurologists and neuroscientists in clinical and non-clinical contexts. Indeed, brain–body axis dysfunctions occur in many psychiatric, neurological and neurodegenerative diseases. This editorial will focus on recent advances and future therapeutic perspectives for studying brain–body interactions in health and diseases.

Key words: psychiatric disorders, central nervous system, neurodegeneration, autonomic nervous system, neurological disorders

Cite as

Di Gregorio F, Battaglia S. The intricate brain–body interaction in psychiatric and neurological diseases. *Adv Clin Exp Med.* 2024;33(4):321–326. doi:10.17219/acem/185689

DOI

10.17219/acem/185689

Copyright

Copyright by Author(s)

This is an article distributed under the terms of the Creative Commons Attribution 3.0 Unported (CC BY 3.0) (<https://creativecommons.org/licenses/by/3.0/>)

The brain–body balance

Coordinated interactions between the brain and the body are crucial for survival. The human body is a complex system of interconnected structures and functions, each playing a crucial role in maintaining brain–body homeostasis and driving behavior and cognition. However, brain–body balance disruption can lead to neurological or psychological diseases. Indeed, several psychiatric, neurological and neurodegenerative disorders present with dysregulations of brain and body functioning.^{1–3} In this context, the combined assessment of brain and body functioning becomes fundamental in clinical practice, as it offers valuable insights into the relationship between brain function and body regulation.^{4,5}

In this manuscript, we will delve into the profound interplay between the brain and the body, examining how disruptions in this dynamic relationship contribute to the onset and/or progression of debilitating conditions. Despite extensive research on dysfunctional brain–body interactions in neurological and psychiatric disorders, it is not currently possible to establish causative and/or hierarchical links between dysfunctional brain–body interactions and neuropsychiatric disease onset.

The onset and progression of many psychiatric and neurological diseases often involve intricate molecular, cellular and systemic changes that impact the central and autonomic nervous systems.⁶ Neuronal damage, inflammation and aberrant protein accumulation can disrupt the normal flow of signals within brain networks. Such brain-level dysfunctions are linked to a cascade of symptoms and dysregulation of the autonomic nervous system while concurrently revealing the interplay between neural substrates and neuropsychiatric diseases.⁶ For instance, dysfunctional cardiac activity was linked to impaired cognitive functioning in healthy and neurological populations,^{7–9} and heart rate variability (i.e., a measure of cardiac functioning) was recently used as a biomarker to differentiate Alzheimer's disease from Lewy body dementia in patients with mild cognitive impairment.¹⁰ Moreover, the degeneration of dopaminergic neurons in Parkinson's disease results in motor fluctuations and dyskinetic movements. However, relevant works have also highlighted the role of the gut microbiome in the maladaptive immune and inflammatory responses that accelerate Parkinson's pathogenesis.^{11,12} Crucially, preclinical and clinical studies indicate that gut microbiome alterations may be susceptibility factors for the progression of several neurodegenerative disorders, including Alzheimer's disease and Parkinson's disease, and major psychiatric disorders.^{13–17} For instance, recent findings demonstrate a consistent decrease in microbial richness in bipolar disorder patients, while differences in beta diversity were observed in major depressive disorder, schizophrenia and psychosis, compared with controls.¹⁶ Similarly, liver diseases such as cirrhosis and hepatic encephalopathy are closely related to neurological symptoms through the liver–brain axis.^{18,19}

The immune system plays a crucial role in multiple sclerosis (MS) etiology and progression.^{20,21} Specifically, immunological mechanisms acting at the brain and body levels can interact through multiple pathways^{22–24} and, in MS, chronic immunological dysregulations may reflect a long-term stress response to homeostatic dysregulation in the central nervous system, ultimately leading to neurodegeneration.²⁵ However, the role of central and peripheral immunological events in the early inflammatory phase of MS is under debate. In particular, it is unclear whether a primary immunological process occurs in the brain and extends to the periphery or vice versa, where the immune activation initiates in the periphery before transferring to the as-yet unaffected central nervous system.^{26,27} Importantly, peripheral and central inflammatory processes likely play a crucial role in fatigue during MS.^{27,28}

Recent advances in neuroscience and physiology have shed light on the dynamic brain–body relationship in psychiatric disorders, emphasizing the bidirectional communication between the brain and various physiological systems. Dysregulations of specific neural circuits and neurotransmitter systems and structural and functional brain changes contribute to the pathophysiology of various psychiatric disorders.^{2,29–32} For instance, dysfunction in the prefrontal–limbic circuitry and alterations in neurotransmitter systems such as dopamine and glutamate are implicated in mood disorders and schizophrenia.^{33–37} Moreover, epigenetic and genetic influences shape susceptibility to neuropsychiatric disorders, with genome-wide association studies identifying risk genes associated with conditions such as bipolar disorder.^{31,38,39} Epigenetic modifications, including DNA methylation and histone modification, further regulate gene expression patterns linked to psychiatric phenotypes.^{40,41}

Dysregulations of the neuroendocrine and immune systems have been reported in depression, anxiety and elevated stress,^{42,43} with a key role for the hypothalamus–pituitary–adrenal axis (HPA).^{44,45} In particular, post-traumatic stress disorder (PTSD) was related to abnormal dynamics in HPA axis activation,^{46,47} which was responsible for increased cortisol levels.^{48,49} This abnormal activity may lead to impairments in cognitive functions like attention, memory and cognitive control,^{50–52} in PTSD patients. Moreover, dysfunctions in the heart rate, blood pressure and respiratory rate have been observed in several psychiatric disorders, including panic and generalized anxiety disorders.^{53–56} The research framework highlighted the significance of heart rate variability (HRV) in the context of psychiatric disorders, adding a new dimension to our understanding of the dynamic brain–body relationship.⁵⁷ Decreased HRV has been identified as a contributing factor in heart failure patients with psychiatric conditions; furthermore, abnormal HRV has been reported in various mental disorders, emphasizing the role of the autonomic nervous system in these conditions.^{58–60} Increased sympathetic activity and reduced parasympathetic tone are

common findings in psychiatric disorders, highlighting the role of autonomic dysregulation in the manifestation and progression of mental health conditions, as the autonomic imbalance contributes to the resulting pro-inflammatory state of depression.^{42,44,61–64} Finally, chronic inflammation, characterized by elevated levels of pro-inflammatory cytokines, has also been linked to conditions like schizophrenia.^{65–67}

Diagnostic and therapeutic prospective

Integrating different markers from brain and body functioning would enhance diagnostic and prognostic accuracy across various clinical domains. Definitively, an integrative brain–body assessment approach may enable a more comprehensive understanding of the neurobiological mechanisms and help guide treatment strategies, such as selecting appropriate medications or implementing targeted interventions for personalized medical approaches.^{5,68,69} As such, recent studies highlighted how combining electroencephalography (EEG) and cardiac activity may provide detailed information about the interaction between neural activity and the autonomic nervous system during cognitive processes⁷⁰ and neurological and psychiatric disorders.⁷¹ Specifically, EEG biomarkers, such as aberrant oscillatory patterns or reduced connectivity,^{37,72,73} can indicate early signs of cognitive decline, while cardiac measures may reflect autonomic dysfunction associated with neurodegenerative processes.^{58,59,74,75} By integrating these measures, it is possible to improve diagnostic accuracy and track disease progression, facilitating the development of personalized treatment plans.^{5,76–80}

Advancements in neuroscience and technology have opened new frontiers for treating neurological and psychiatric-related symptoms by integrating different approaches.^{81–83} Neurostimulation techniques, such as deep brain stimulation, transcranial magnetic stimulation (TMS), transcranial direct current stimulation (tDCS), transcranial electrical stimulation, and vagus nerve stimulation, are being explored as potential interventions for various neurological disorders.^{84–89} These approaches aim to modulate neural activity within large neural networks, but the effects of these treatments on brain–body communication are scarcely investigated.⁹⁰

Understanding the multifaceted interactions between the brain and the body in neurological and psychiatric diseases is essential for developing effective therapeutic approaches.⁵ Current treatments often focus on mitigating symptoms, slowing disease progression or modulating specific pathways. In Parkinson's disease, for example, medications aim to target the dopaminergic system to alleviate motor symptoms.⁹¹ However, new therapeutic approaches are becoming available for the wide range of non-motor symptoms, which are often very disabling


and include neuropsychiatric, autonomic, sleep, and pain symptoms (for a review, see Foltynie et al. and Tajti et al.).^{91,92} In depression, the crosstalk between inflammation, metabolic pathways and neural circuits can ultimately affect neural network activity, which is responsible for regulating behavioral and emotional responses.⁶³ Accordingly, several studies reported the antidepressant effects of anti-inflammatory treatments in patients with depression.^{93–95} Furthermore, recent advances in exercise physiology have yielded crucial insights into the interplay between the brain and body concerning the advantageous effects of physical activity on cognition and mood in states of health and disease.^{77,78,96–100} Finally, neurostimulation techniques, including TMS and tDCS, have shown efficacy in alleviating depressive symptoms when combined with psychosocial intervention.^{101–103} Thus, integrated multidisciplinary approaches are generally recommended to holistically address the disease-related symptoms and ensure the best outcomes for individuals at brain and body levels.

Tip the scale

The synergistic utilization of brain and body functioning measures in clinical practice offers a multidimensional perspective on brain function and physiological regulation.⁵ This integrative approach holds promise for enhancing diagnostic accuracy, treatment selection and monitoring of various neuropsychiatric and neurodegenerative conditions, ultimately improving patient outcomes and advancing the field of clinical neuroscience.^{71,104} The brain–body interaction in neurological and psychiatric diseases is a complex and dynamic system that extends beyond the traditional boundaries of the nervous system,¹⁰⁵ including disrupted communication pathways, the influence of the immune and endocrine systems, and the role of the gut–brain axis, though our understanding of these intricate connections continues to evolve. In conclusion, unraveling dysfunctional brain–body interactions in neurological and psychiatric diseases would be the basis for innovative therapeutic interventions.^{5,104} The proposal of synergistic approaches to investigating and treating brain–body communication remains at the forefront of scientific research and clinical exploration, with the potential to transform the landscape of health care in years to come. Indeed, a holistic and synergistic approach could enhance diagnostic accuracy, treatment selection, and psychological and neurological health monitoring across the lifespan.

ORCID iDs

Francesco Di Gregorio  <https://orcid.org/0000-0002-3587-3149>

Simone Battaglia  <https://orcid.org/0000-0003-4133-654X>

References

1. Candia-Rivera D. Brain–heart interactions in the neurobiology of consciousness. *Curr Res Neurobiol.* 2022;3:100050. doi:10.1016/j.crneur.2022.100050

2. Ibanez A, Northoff G. Intrinsic timescales and predictive allostatic interoception in brain health and disease. *Neurosci Biobehav Rev.* 2024;157:105510. doi:10.1016/j.neubiorev.2023.105510
3. Silvani A, Calandra-Buonaura G, Dampney RAL, Cortelli P. Brain–heart interactions: Physiology and clinical implications. *Phil Trans R Soc A.* 2016;374(2067):20150181. doi:10.1098/rsta.2015.0181
4. Di Gregorio F, Petrone V, Casanova E, et al. Hierarchical psychophysiological pathways subtend perceptual asymmetries in neglect. *NeuroImage.* 2023;270:119942. doi:10.1016/j.neuroimage.2023.119942
5. Ibanez A, Kringelbach ML, Deco G. A synergetic turn in cognitive neuroscience of brain diseases [published online as ahead of print on January 20, 2024]. *Trends Cogn Sci.* 2024;S1364661323003066. doi:10.1016/j.tics.2023.12.006
6. Forstenpointner J, Elman I, Freeman R, Borsook D. The omnipresence of autonomic modulation in health and disease. *Prog Neurobiol.* 2022;210:102218. doi:10.1016/j.pneurobio.2022.102218
7. Molloy C, Choy EH, Arechavala RJ, et al. Resting heart rate (variability) and cognition relationships reveal cognitively healthy individuals with pathological amyloid/tau ratio. *Front Epidemiol.* 2023;3:1168847. doi:10.3389/fevid.2023.1168847
8. Skora LI, Livermore JJA, Roelofs K. The functional role of cardiac activity in perception and action. *Neurosci Biobehav Rev.* 2022;137:104655. doi:10.1016/j.neubiorev.2022.104655
9. Thayer JF, Hansen AL, Saus-Rose E, Johnsen BH. Heart rate variability, prefrontal neural function, and cognitive performance: The neurovisceral integration perspective on self-regulation, adaptation, and health. *Ann Behav Med.* 2009;37(2):141–153. doi:10.1007/s12160-009-9101-z
10. Kim MS, Yoon JH, Hong JM. Early differentiation of dementia with Lewy bodies and Alzheimer's disease: Heart rate variability at mild cognitive impairment stage. *Clin Neurophysiol.* 2018;129(8):1570–1578. doi:10.1016/j.clinph.2018.05.004
11. Morris HR, Spillantini MG, Sue CM, Williams-Gray CH. The pathogenesis of Parkinson's disease. *Lancet.* 2024;403(10423):293–304. doi:10.1016/S0140-6736(23)01478-2
12. Romano S, Savva GM, Bedard JR, Charles IG, Hildebrand F, Narbad A. Meta-analysis of the Parkinson's disease gut microbiome suggests alterations linked to intestinal inflammation. *NPJ Parkinsons Dis.* 2021;7(1):27. doi:10.1038/s41531-021-00156-z
13. Andrioaie IM, Duhaniuc A, Nastase EV, et al. The role of the gut microbiome in psychiatric disorders. *Microorganisms.* 2022;10(12):2436. doi:10.3390/microorganisms10122436
14. Cryan JF, O'Riordan KJ, Sandhu K, Peterson V, Dinan TG. The gut microbiome in neurological disorders. *Lancet Neurol.* 2020;19(2):179–194. doi:10.1016/S1474-4422(19)30356-4
15. Góralczyk-Bińkowska A, Szmajda-Krygier D, Kozłowska E. The microbiota–gut–brain axis in psychiatric disorders. *Int J Mol Sci.* 2022;23(19):11245. doi:10.3390/ijms231911245
16. Nikolova VL, Smith MRB, Hall LJ, Cleare AJ, Stone JM, Young AH. Perturbations in gut microbiota composition in psychiatric disorders: A review and meta-analysis. *JAMA Psychiatry.* 2021;78(12):1343. doi:10.1001/jamapsychiatry.2021.2573
17. Ullah H, Arbab S, Tian Y, et al. The gut microbiota–brain axis in neurological disorder. *Front Neurosci.* 2023;17:1225875. doi:10.3389/fnins.2023.1225875
18. Yan M, Man S, Sun B, et al. Gut liver brain axis in diseases: The implications for therapeutic interventions. *Signal Transduct Target Ther.* 2023;8(1):443. doi:10.1038/s41392-023-01673-4
19. Loh JS, Mak WQ, Tan LKS, et al. Microbiota–gut–brain axis and its therapeutic applications in neurodegenerative diseases. *Signal Transduct Target Ther.* 2024;9(1):37. doi:10.1038/s41392-024-01743-1
20. Reich DS, Lucchinetti CF, Calabresi PA. Multiple sclerosis. *N Engl J Med.* 2018;378(2):169–180. doi:10.1056/NEJMra1401483
21. Thompson AJ, Baranzini SE, Geurts J, Hemmer B, Ciccarelli O. Multiple sclerosis. *Lancet.* 2018;391(10130):1622–1636. doi:10.1016/S0140-6736(18)30481-1
22. Dantzer R. Neuroimmune interactions: From the brain to the immune system and vice versa. *Physiol Rev.* 2018;98(1):477–504. doi:10.1152/physrev.00039.2016
23. Dinet V, Petry KG, Badaut J. Brain–immune interactions and neuroinflammation after traumatic brain injury. *Front Neurosci.* 2019;13:1178. doi:10.3389/fnins.2019.01178
24. Savitz J, Harrison NA. Interoception and inflammation in psychiatric disorders. *Biol Psychiatry Cogn Neurosci Neuroimaging.* 2018;3(6):514–524. doi:10.1016/j.bpsc.2017.12.011
25. Dendrou CA, Fugger L, Friese MA. Immunopathology of multiple sclerosis. *Nat Rev Immunol.* 2015;15(9):545–558. doi:10.1038/nri3871
26. Hemmer B, Kerschensteiner M, Korn T. Role of the innate and adaptive immune responses in the course of multiple sclerosis. *Lancet Neurol.* 2015;14(4):406–419. doi:10.1016/S1474-4422(14)70305-9
27. Manjaly ZM, Harrison NA, Critchley HD, et al. Pathophysiological and cognitive mechanisms of fatigue in multiple sclerosis. *J Neurol Neurosurg Psychiatry.* 2019;90(6):642–651. doi:10.1136/jnnp-2018-320050
28. Rouault M, Pereira I, Galiouline H, Fleming SM, Stephan KE, Manjaly Z. Interoceptive and metacognitive facets of fatigue in multiple sclerosis. *Eur J Neurosci.* 2023;58(2):2603–2622. doi:10.1111/ejn.16048
29. Battaglia S, Di Fazio C, Mazzà M, Tamietto M, Avenanti A. Targeting human glucocorticoid receptors in fear learning: A multiscale integrated approach to study functional connectivity. *Int J Mol Sci.* 2024;25(2):864. doi:10.3390/ijms25020864
30. Quadt L, Esposito G, Critchley HD, Garfinkel SN. Brain–body interactions underlying the association of loneliness with mental and physical health. *Neurosci Biobehav Rev.* 2020;116:283–300. doi:10.1016/j.neubiorev.2020.06.015
31. Tanaka M, Szabó Á, Spekker E, Polyák H, Tóth F, Vécsei L. Mitochondrial impairment: A common motif in neuropsychiatric presentation? The link to the tryptophan–kynurenine metabolic system. *Cells.* 2022;11(16):2607. doi:10.3390/cells11162607
32. Tanaka M, Szabó Á, Vécsei L. Integrating armchair, bench, and bedside research for behavioral neurology and neuropsychiatry: Editorial. *Biomedicines.* 2022;10(12):2999. doi:10.3390/biomedicines10122999
33. Paul IA, Skolnick P. Glutamate and depression: Clinical and preclinical studies. *Ann N Y Acad Sci.* 2003;1003(1):250–272. doi:10.1196/annals.1300.016
34. Polyák H, Galla Z, Nánási N, et al. The tryptophan–kynurenine metabolic system is suppressed in cuprizone-induced model of demyelination simulating progressive multiple sclerosis. *Biomedicines.* 2023;11(3):945. doi:10.3390/biomedicines11030945
35. Tanaka M, Szabó Á, Vécsei L, Giménez-Llort L. Emerging translational research in neurological and psychiatric diseases: From in vitro to in vivo models. *Int J Mol Sci.* 2023;24(21):15739. doi:10.3390/ijms242115739
36. Tortora F, Hadipour AL, Battaglia S, Falzone A, Avenanti A, Vicario CM. The role of serotonin in fear learning and memory: A systematic review of human studies. *Brain Sci.* 2023;13(8):1197. doi:10.3390/brainsci13081197
37. Trajkovic J, Di Gregorio F, Ferri F, Marzi C, Diciotti S, Romei V. Resting state alpha oscillatory activity is a valid and reliable marker of schizotypy. *Sci Rep.* 2021;11(1):10379. doi:10.1038/s41598-021-89690-7
38. McEwen BS. Redefining neuroendocrinology: Epigenetics of brain–body communication over the life course. *Front Neuroendocrinol.* 2018;49:8–30. doi:10.1016/j.yfrne.2017.11.001
39. Tanaka M, Vécsei L. Editorial of special issue 'Dissecting Neurological and Neuropsychiatric Diseases: Neurodegeneration and Neuroprotection.' *Int J Mol Sci.* 2022;23(13):6991. doi:10.3390/ijms23136991
40. Tanaka M, Szabó Á, Körtési T, Szok D, Tajti J, Vécsei L. From CGRP to PACAP, VIP, and beyond: Unraveling the next chapters in migraine treatment. *Cells.* 2023;12(22):2649. doi:10.3390/cells12222649
41. Tanaka M, Szabó Á, Vécsei L. Preclinical modeling in depression and anxiety: Current challenges and future research directions. *Adv Clin Exp Med.* 2023;32(5):505–509. doi:10.17219/acem/165944
42. Miller AH. Neuroendocrine and immune system interactions in stress and depression. *Psychiatr Clin North Am.* 1998;21(2):443–463. doi:10.1016/S0193-953X(05)70015-0
43. Oglódek E, Szota A, Just M, Moś D, Araszkievicz A. The role of the neuroendocrine and immune systems in the pathogenesis of depression. *Pharmacol Rep.* 2014;66(5):776–781. doi:10.1016/j.pharep.2014.04.009
44. Kim YK, Na KS, Myint AM, Leonard BE. The role of pro-inflammatory cytokines in neuroinflammation, neurogenesis and the neuroendocrine system in major depression. *Prog Neuropsychopharmacol Biol Psychiatry.* 2016;64:277–284. doi:10.1016/j.pnpbpb.2015.06.008
45. Tanaka M, Bohár Z, Vécsei L. Are kynurenines accomplices or principal villains in dementia? Maintenance of kynurenine metabolism. *Molecules.* 2020;25(3):564. doi:10.3390/molecules25030564

46. Pervanidou P. Biology of post-traumatic stress disorder in childhood and adolescence. *J Neuroendocrinol.* 2008;20(5):632–638. doi:10.1111/j.1365-2826.2008.01701.x
47. Pervanidou P, Chrousos GP. Neuroendocrinology of post-traumatic stress disorder. *Prog Brain Res.* 2010;182:149–160. doi:10.1016/S0079-6123(10)82005-9
48. Lehrner A, Daskalakis N, Yehuda R. Cortisol and the hypothalamic–pituitary–adrenal axis in PTSD. In: Bremner JD, ed. *Posttraumatic Stress Disorder.* Hoboken, USA: Wiley & Sons; 2016:265–290. doi:10.1002/9781118356142.ch11
49. Yehuda R. Current status of cortisol findings in post-traumatic stress disorder. *Psychiatr Clin North Am.* 2002;25(2):341–368. doi:10.1016/S0193-953X(02)00002-3
50. Blair KS, Vythilingam M, Crowe SL, et al. Cognitive control of attention is differentially affected in trauma-exposed individuals with and without post-traumatic stress disorder. *Psychol Med.* 2013;43(1):85–95. doi:10.1017/S0033291712000840
51. Flaks MK, Malta SM, Almeida PP, et al. Attentional and executive functions are differentially affected by post-traumatic stress disorder and trauma. *J Psychiatr Res.* 2014;48(1):32–39. doi:10.1016/j.jpsy-chires.2013.10.009
52. Neylan TC, Lenoci M, Rothlind J, et al. Attention, learning, and memory in posttraumatic stress disorder. *J Trauma Stress.* 2004;17(1):41–46. doi:10.1023/B:JOTS.0000014675.75686.ee
53. Alvares GA, Quintana DS, Hickie IB, Guastella AJ. Autonomic nervous system dysfunction in psychiatric disorders and the impact of psychotropic medications: A systematic review and meta-analysis. *J Psychiatry Neurosci.* 2016;41(2):89–104. doi:10.1503/jpn.140217
54. Bär KJ. Cardiac autonomic dysfunction in patients with schizophrenia and their healthy relatives: A small review. *Front Neurol.* 2015;6:139. doi:10.3389/fneur.2015.00139
55. Bassi A, Bozzali M. Potential interactions between the autonomic nervous system and higher level functions in neurological and neuropsychiatric conditions. *Front Neurol.* 2015;6:182. doi:10.3389/fneur.2015.00182
56. Bryant RA, Creamer M, O'Donnell M, Silove D, McFarlane AC. A multi-site study of initial respiration rate and heart rate as predictors of post-traumatic stress disorder. *J Clin Psychiatry.* 2008;69(11):1694–1701. doi:10.4088/JCP.v69n1104
57. Jung W, Jang KI, Lee SH. Heart and brain interaction of psychiatric illness: A review focused on heart rate variability, cognitive function, and quantitative electroencephalography. *Clin Psychopharmacol Neurosci.* 2019;17(4):459–474. doi:10.9758/cpn.2019.17.4.459
58. Battaglia S, Nazzi C, Thayer JF. Heart's tale of trauma: Fear-conditioned heart rate changes in post-traumatic stress disorder. *Acta Psychiatr Scand.* 2023;148(5):463–466. doi:10.1111/acps.13602
59. Battaglia S, Nazzi C, Thayer JF. Genetic differences associated with dopamine and serotonin release mediate fear-induced bradycardia in the human brain. *Transl Psychiatry.* 2024;14(1):24. doi:10.1038/s41398-024-02737-x
60. Glannon W. Biomarkers in psychiatric disorders. *Camb Q Healthc Ethics.* 2022;31(4):444–452. doi:10.1017/S0963180122000056
61. Halaris A. Inflammation and depression but where does the inflammation come from? *Curr Opin Psychiatry.* 2019;32(5):422–428. doi:10.1097/YCO.0000000000000531
62. Leonard BE. Inflammation and depression: A causal or coincidental link to the pathophysiology? *Acta Neuropsychiatr.* 2018;30(1):1–16. doi:10.1017/neu.2016.69
63. Miller AH, Raison CL. The role of inflammation in depression: From evolutionary imperative to modern treatment target. *Nat Rev Immunol.* 2016;16(1):22–34. doi:10.1038/nri.2015.5
64. Zunszain PA, Hepgul N, Pariante CM. Inflammation and depression. In: Cowen PJ, Sharp T, Lau JYF, eds. *Behavioral Neurobiology of Depression and Its Treatment.* Vol. 14. Current Topics in Behavioral Neurosciences. Berlin–Heidelberg, Germany: Springer Berlin Heidelberg; 2012:135–151. doi:10.1007/7854_2012_211
65. Dawidowski B, Górniak A, Podwalski P, Lebiecka Z, Misiak B, Samochowiec J. The role of cytokines in the pathogenesis of schizophrenia. *J Clin Med.* 2021;10(17):3849. doi:10.3390/jcm10173849
66. Na KS, Jung HY, Kim YK. The role of pro-inflammatory cytokines in the neuroinflammation and neurogenesis of schizophrenia. *Prog Neuropsychopharmacol Biol Psychiatry.* 2014;48:277–286. doi:10.1016/j.pnpbbp.2012.10.022
67. Uptegrove R, Khandaker GM. Cytokines, oxidative stress and cellular markers of inflammation in schizophrenia. In: Khandaker GM, Meyer U, Jones PB, eds. *Neuroinflammation and Schizophrenia.* Vol. 44. Current Topics in Behavioral Neurosciences. Cham, Switzerland: Springer International Publishing; 2019:49–66. doi:10.1007/7854_2018_88
68. Hardy-Sosa A, León-Arcia K, Llibre-Guerra JJ, et al. Diagnostic accuracy of blood-based biomarker panels: A systematic review. *Front Aging Neurosci.* 2022;14:683689. doi:10.3389/fnagi.2022.683689
69. Songsaeng D, Nava-apisak P, Wongsripumtet J, et al. The diagnostic accuracy of artificial intelligence in radiological markers of normal-pressure hydrocephalus (NPH) on non-contrast CT scans of the brain. *Diagnostics.* 2023;13(17):2840. doi:10.3390/diagnostics13172840
70. Di Gregorio F, Steinhäuser M, Maier ME, Thayer JF, Battaglia S. Error-related cardiac deceleration: Functional interplay between error-related brain activity and autonomic nervous system in performance monitoring. *Neurosci Biobehav Rev.* 2024;157:105542. doi:10.1016/j.neubiorev.2024.105542
71. Suhail TA, Indiradevi KP, Suhara EM, Poovathinal SA, Ayyappan A. Distinguishing cognitive states using electroencephalography local activation and functional connectivity patterns. *Biomed Signal Process Control.* 2022;77:103742. doi:10.1016/j.bspc.2022.103742
72. Di Gregorio F, La Porta F, Petrone V, et al. Accuracy of EEG biomarkers in the detection of clinical outcome in disorders of consciousness after severe acquired brain injury: Preliminary results of a pilot study using a machine learning approach. *Biomedicines.* 2022;10(8):1897. doi:10.3390/biomedicines10081897
73. Di Gregorio F, Battaglia S. Advances in EEG-based functional connectivity approaches to the study of the central nervous system in health and disease. *Adv Clin Exp Med.* 2023;32(6):607–612. doi:10.17219/acem/166476
74. Alba G, Vila J, Rey B, Montoya P, Muñoz MÁ. The relationship between heart rate variability and electroencephalography functional connectivity variability is associated with cognitive flexibility. *Front Hum Neurosci.* 2019;13:64. doi:10.3389/fnhum.2019.00064
75. Battaglia S, Nazzi C, Thayer JF. Fear-induced bradycardia in mental disorders: Foundations, current advances, future perspectives. *Neurosci Biobehav Rev.* 2023;149:105163. doi:10.1016/j.neubiorev.2023.105163
76. Ashton NJ, Brum WS, Di Molfetta G, et al. Diagnostic accuracy of a plasma phosphorylated Tau 217 immunoassay for Alzheimer disease pathology [published online as ahead of print on January 22, 2024]. *JAMA Neurol.* 2024:e235319. doi:10.1001/jamaneurol.2023.5319
77. Chen C, Nakagawa S. Physical activity for cognitive health promotion: An overview of the underlying neurobiological mechanisms. *Ageing Res Rev.* 2023;86:101868. doi:10.1016/j.arr.2023.101868
78. Chen C, Nakagawa S. Recent advances in the study of the neurobiological mechanisms behind the effects of physical activity on mood, resilience and emotional disorders. *Adv Clin Exp Med.* 2023;32(9):937–942. doi:10.17219/acem/171565
79. Liloia D, Cauda F, Uddin LQ, et al. Revealing the selectivity of neuroanatomical alteration in autism spectrum disorder via reverse inference. *Biol Psychiatry Cogn Neurosci Neuroimaging.* 2023;8(11):1075–1083. doi:10.1016/j.bpspc.2022.01.007
80. Rocha RP, Koçillari L, Suweis S, et al. Recovery of neural dynamics criticality in personalized whole-brain models of stroke. *Nat Commun.* 2022;13(1):3683. doi:10.1038/s41467-022-30892-6
81. Di Gregorio F, La Porta F, Casanova E, et al. Efficacy of repetitive transcranial magnetic stimulation combined with visual scanning treatment on cognitive and behavioral symptoms of left hemispatial neglect in right hemispheric stroke patients: Study protocol for a randomized controlled trial. *Trials.* 2021;22(1):24. doi:10.1186/s13063-020-04943-6
82. Di Gregorio F, La Porta F, Lullini G, et al. Efficacy of repetitive transcranial magnetic stimulation combined with visual scanning treatment on cognitive–behavioral symptoms of unilateral spatial neglect in patients with traumatic brain injury: Study protocol for a randomized controlled trial. *Front Neurol.* 2021;12:702649. doi:10.3389/fneur.2021.702649
83. Trajkovic J, Di Gregorio F, Marcantoni E, Thut G, Romei V. A TMS/EEG protocol for the causal assessment of the functions of the oscillatory brain rhythms in perceptual and cognitive processes. *STAR Protoc.* 2022;3(2):101435. doi:10.1016/j.xpro.2022.101435

84. Corazzol M, Lio G, Lefevre A, et al. Restoring consciousness with vagus nerve stimulation. *Curr Biol*. 2017;27(18):R994–R996. doi:10.1016/j.cub.2017.07.060
85. Demirtas-Tatlidede A, Vahabzadeh-Hagh AM, Bernabeu M, Tormos JM, Pascual-Leone A. Noninvasive brain stimulation in traumatic brain injury. *J Head Trauma Rehab*. 2012;27(4):274–292. doi:10.1097/HTR.0b013e318217df55
86. Formica C, De Salvo S, Corallo F, et al. Role of neurorehabilitative treatment using transcranial magnetic stimulation in disorders of consciousness. *J Int Med Res*. 2021;49(2):030006052097647. doi:10.1177/0300060520976472
87. Karatzetzou S, Tsiptsios D, Terzoudi A, Aggeloussis N, Vadikolias K. Transcranial magnetic stimulation implementation on stroke prognosis. *Neurol Sci*. 2022;43(2):873–888. doi:10.1007/s10072-021-05791-1
88. Rossi S, Hallett M, Rossini PM, Pascual-Leone A; Safety of TMS Consensus Group. Safety, ethical considerations, and application guidelines for the use of transcranial magnetic stimulation in clinical practice and research. *Clin Neurophysiol*. 2009;120(12):2008–2039. doi:10.1016/j.clinph.2009.08.016
89. Schulz R, Gerloff C, Hummel FC. Non-invasive brain stimulation in neurological diseases. *Neuropharmacology*. 2013;64:579–587. doi:10.1016/j.neuropharm.2012.05.016
90. Chaves AR, Snow NJ, Alcock LR, Ploughman M. Probing the brain-body connection using transcranial magnetic stimulation (TMS): Validating a promising tool to provide biomarkers of neuroplasticity and central nervous system function. *Brain Sci*. 2021;11(3):384. doi:10.3390/brainsci11030384
91. Foltynie T, Bruno V, Fox S, Kühn AA, Lindop F, Lees AJ. Medical, surgical, and physical treatments for Parkinson's disease. *Lancet*. 2024;403(10423):305–324. doi:10.1016/S0140-6736(23)01429-0
92. Tajti J, Szok D, Csáti A, Szabó Á, Tanaka M, Vécsei L. Exploring novel therapeutic targets in the common pathogenic factors in migraine and neuropathic pain. *Int J Mol Sci*. 2023;24(4):4114. doi:10.3390/ijms24044114
93. Bai S, Guo W, Feng Y, et al. Efficacy and safety of anti-inflammatory agents for the treatment of major depressive disorder: A systematic review and meta-analysis of randomised controlled trials. *J Neurol Neurosurg Psychiatry*. 2020;91(1):21–32. doi:10.1136/jnnp-2019-320912
94. Köhler O, Benros ME, Nordentoft M, et al. Effect of anti-inflammatory treatment on depression, depressive symptoms, and adverse effects: A systematic review and meta-analysis of randomized clinical trials. *JAMA Psychiatry*. 2014;71(12):1381. doi:10.1001/jamapsychiatry.2014.1611
95. Köhler-Forsberg O, Lydholm CN, Hjorthøj C, Nordentoft M, Mors O, Benros ME. Efficacy of anti-inflammatory treatment on major depressive disorder or depressive symptoms: Meta-analysis of clinical trials. *Acta Psychiatr Scand*. 2019;139(5):404–419. doi:10.1111/acps.13016
96. Ellis TD, Colón-Semenza C, DeAngelis TR, et al. Evidence for early and regular physical therapy and exercise in Parkinson's disease. *Semin Neurol*. 2021;41(2):189–205. doi:10.1055/s-0041-1725133
97. Ernst M, Folkerts AK, Gollan R, et al. Physical exercise for people with Parkinson's disease: A systematic review and network meta-analysis. *Cochrane Database Syst Rev*. 2023;2023(5):CD013856. doi:10.1002/14651858.CD013856.pub2
98. Motl RW, Sandroff BM, Kwakkel G, et al. Exercise in patients with multiple sclerosis. *Lancet Neurol*. 2017;16(10):848–856. doi:10.1016/S1474-4422(17)30281-8
99. Schuch FB, Vancampfort D. Physical activity, exercise, and mental disorders: It is time to move on. *Trends Psychiatry Psychother*. 2021;43(3):177–184. doi:10.47626/2237-6089-2021-0237
100. Sun W, Yu M, Zhou X. Effects of physical exercise on attention deficit and other major symptoms in children with ADHD: A meta-analysis. *Psychiatry Res*. 2022;311:114509. doi:10.1016/j.psychres.2022.114509
101. Battaglia S, Schmidt A, Hassel S, Tanaka M. Editorial: Case reports in neuroimaging and stimulation. *Front Psychiatry*. 2023;14:1264669. doi:10.3389/fpsy.2023.1264669
102. Liu S, Sheng J, Li B, Zhang X. Recent advances in non-invasive brain stimulation for major depressive disorder. *Front Hum Neurosci*. 2017;11:526. doi:10.3389/fnhum.2017.00526
103. Tanaka M, Diano M, Battaglia S. Editorial: Insights into structural and functional organization of the brain: Evidence from neuroimaging and non-invasive brain stimulation techniques. *Front Psychiatry*. 2023;14:1225755. doi:10.3389/fpsy.2023.1225755
104. Owolabi MO, Leonardi M, Bassetti C, et al. Global synergistic actions to improve brain health for human development. *Nat Rev Neurol*. 2023;19(6):371–383. doi:10.1038/s41582-023-00808-z
105. Signorelli CM, Boils JD, Tagliazucchi E, Jarraya B, Deco G. From brain-body function to conscious interactions. *Neurosci Biobehav Rev*. 2022;141:104833. doi:10.1016/j.neubiorev.2022.104833

A meta-analysis of the risk of osteoporotic fractures in inflammatory bowel disease

*Liansheng Hao^{1,B,C}, *Shengkai Mu^{1,C,D}, Junyan Yin^{2,B,D}, Jun Liu^{3,4,A,E,F}

¹ 2nd Department of Trauma, Liaocheng Hospital of Traditional Chinese Medicine, China

² Department of Chinese Traditional Medicine, Liaocheng People's Hospital, China

³ Department of Geriatric Medicine, Affiliated Hospital of Shandong University of Traditional Chinese Medicine, Shandong Province Hospital of Traditional Chinese Medicine, Jinan, China

⁴ Postdoctoral Research Station, Shandong University of Traditional Chinese Medicine, Jinan, China

A – research concept and design; B – collection and/or assembly of data; C – data analysis and interpretation;

D – writing the article; E – critical revision of the article; F – final approval of the article

Advances in Clinical and Experimental Medicine, ISSN 1899–5276 (print), ISSN 2451–2680 (online)

Adv Clin Exp Med. 2024;33(4):327–333

Address for correspondence

Jun Liu

E-mail: sliujun2022@126.com

Funding sources

None declared

Conflict of interest

None declared

*Liansheng Hao and Shengkai Mu contributed equally to this work.

Received on October 24, 2022

Reviewed on March 23, 2023

Accepted on June 22, 2023

Published online on August 7, 2023

Abstract

Background. There are a variety of perspectives on the risk of osteoporotic fractures in inflammatory bowel disease (IBD), and few thorough assessments that are pertinent.

Objectives. We conducted a meta-analysis to assess the risk of osteoporotic fractures in IBD.

Materials and methods. A systematic literature search up to September 2022 was performed, and 1,158,982 subjects participated in the baseline trials of the selected studies. A total of 261,829 patients had IBD, while 897,153 were controls. Odds ratio (OR) and mean difference (MD) with 95% confidence intervals (95% CIs) were calculated to measure the risk of osteoporotic fractures in IBD patients using contentious and dichotomous approaches with a random or fixed influence model.

Results. The presence of IBD resulted in significantly higher frequency of osteoporotic fractures (OR: 1.42, 95% CI: 1.21–1.66, $p < 0.001$) compared to controls. Nevertheless, no significant differences in terms of osteoporotic fractures were found between ulcerative colitis (OR: 2.79, 95% CI: 0.88–8.87, $p = 0.08$) and Crohn's disease (OR: 1.84, 95% CI: 0.81–4.18, $p = 0.14$) compared to controls.

Conclusions. This study found a strong correlation between the risk of osteoporotic fractures and inflammatory bowel disease. The small number of studies in certain comparisons requires care when analyzing the results.

Key words: inflammatory bowel disease, osteoporotic fractures, Crohn's disease, ulcerative colitis

Cite as

Hao L, Mu S, Yin J, Liu J. A meta-analysis of the risk of osteoporotic fractures in inflammatory bowel disease.

Adv Clin Exp Med. 2024;33(4):327–333.

doi:10.17219/acem/168684

DOI

10.17219/acem/168684

Copyright

Copyright by Author(s)

This is an article distributed under the terms of the Creative Commons Attribution 3.0 Unported (CC BY 3.0)

(<https://creativecommons.org/licenses/by/3.0/>)

Introduction

The development of osteoporosis and osteoporotic fractures is significantly influenced by inflammatory bowel disease (IBD), particularly ulcerative colitis and Crohn's disease.¹ The probability of developing osteoporosis varies from 17% to 41%.² Patients with IBD have higher rates of peripheral cortical and spinal trabecular osteoporosis. Young, amenorrheic women have clinical osteoporosis that is more severe.³ Patients are more likely to sustain osteoporotic fractures due to the increased chance of developing osteoporosis. When compared to the general population, IBD patients may have a 40% higher incidence of fractures, which lowers their quality of life and increases their morbidity.⁴ The mechanism by which IBD increases a patient's risk of osteoporosis and osteoporotic fractures is complex. Numerous studies examining glucocorticoid use have not found a statistically significant increase in osteoporosis in patients taking this medication.⁴ Patients with IBD are frequently prescribed steroids, and this can predispose them to osteoporosis. Moreover, there seems to be a process affecting bone metabolism in IBD patients, such as a chronic inflammatory state that causes bone loss by activating the tumor necrosis factor alpha (TNF- α)-mediated RANK/RANKL/osteoprotegerin pathway, which encourages osteoclastogenesis.⁴ Secondary hyperparathyroidism, which is frequently prevalent due to the decreased absorption of vital nutrients including calcium and vitamin D, is another cause of osteoporosis.⁵ The goal of this study was to compile the most reliable data comparing IBD patients with control patients in terms of likelihood of developing osteoporotic fractures.

Objectives

The aim of the study was to determine the risk of osteoporotic fractures in patients with IBD.

Materials and methods

Information sources

The main goal of the current meta-analysis was to appraise the risk of osteoporotic fractures in IBD. Every selected study involved human research. Inclusion was unaffected by study size or language. Commentaries, review papers and papers that did not provide a measure of a relationship were excluded from the study. The complete course of the study is presented in Fig. 1. The following inclusion criteria had to be met for the publications to be selected for the meta-analysis:

1. The study was either a controlled trial, observational, prospective, or retrospective study;
2. Subjects with osteoporotic fractures make up the intended selected subjects for the meta-analysis;
3. The intervention program included IBD;
4. The study was about the risk of osteoporotic fractures in IBD.

Studies that had no comparison of outcomes within its protocol, research that did not examine IBD in subjects with osteoporotic fractures, and studies in subjects without osteoporotic fractures or without IBD were excluded from the study.⁶

Search strategy

A protocol of search strategy followed the Population, Intervention, Comparison, Outcomes and Study (PICOS) concept, and was characterized as follows: "population" comprised patients with osteoporotic fractures "intervention" or "exposure" concerned IBD treatment, whereas the "comparison" pertained IBD patients compared to controls, osteoporotic fractures were the "outcomes", and there were no restrictions regarding the study's design.⁷

We conducted a thorough search of the OVID, Embase, Cochrane Library, PubMed, and Google Scholar databases up until September 2022, using an arrangement of keywords and terms correlated with IBD, Crohn's disease, osteoporotic fractures, and ulcerative colitis (cf. Table 1). To identify studies that did not show a relationship between

Table 1. Search strategy for each database

Database	Search strategy
PubMed	#1 "inflammatory bowel disease" (MeSH terms) OR "osteoporotic fractures" (all fields) #2 "ulcerative colitis" (MeSH terms) OR "Crohn's disease new" (all fields) #3 #1 AND #2
Embase	#1 "inflammatory bowel disease"/exp OR "osteoporotic fractures" #2 "ulcerative colitis"/exp OR "Crohn's disease" #3 #1 AND #2
Cochrane Library	#1 "inflammatory bowel disease": ti,ab,kw OR "osteoporotic fractures": ti,ab,kw (word variations have been searched) #2 "ulcerative colitis": ti,ab,kw OR "Crohn's disease": ti,ab,kw (word variations have been searched) #3 #1 AND #2

MeSH – medical subject headings; ti,ab,kw – terms in either title or abstract or keyword fields; exp – exploded indexing term.

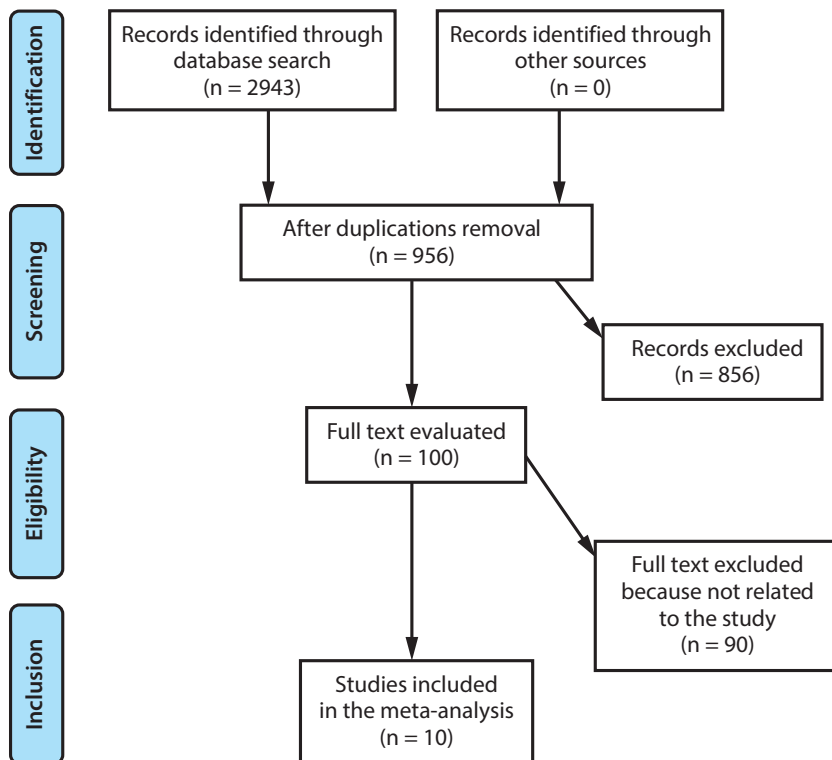


Fig. 1. Flowchart of the study process

IBD patients and the controls regarding the risk of osteoporotic fractures, all retrieved papers were joined into an EndNote file, duplicates were eliminated, and the titles and abstracts were reviewed.

Selection process

The present study followed the meta-analysis of studies in the epidemiology statement, which was performed following an established protocol.

Data collection process

The criteria used to gather the data included the last name of the first author, country, population, the quantitative and qualitative assessment technique, the information source, the assessment of the results, and statistical analysis.⁸

Data items

When there were disparate findings from a single study on the risk of osteoporotic fractures in IBD, such data were collected independently.

Risk of bias assessment

Two authors individually evaluated the methodology of the designated articles to ascertain the possibility of bias in each study. The procedural quality was assessed using the “risk of bias instrument” from the Cochrane Handbook

for Systematic Reviews of Interventions Version 5.1.0 (<https://handbook-5-1.cochrane.org/>). Each study was classified according to the appraisal criteria and was assigned with one of the 3 levels of the bias. A study was rated as having a low risk of bias if all the quality standards were met; if one or more requirements were not met or were not taken into account in a given study, such study was rated as having a moderate risk of bias. The study was considered to have a high risk of bias when one or more quality criteria were not met at all or were only partially met. Any discrepancies were addressed through a reassessment of a given analyzed article.

Effect measures

Only studies that reported and assessed the influence of IBD in comparison to controls on the risk of osteoporotic fractures were subjected to sensitivity studies. A sensitivity and subclass analysis was utilized to compare the risk of osteoporotic fractures in IBD.

Synthesis methods

The current meta-analysis used a random-effects model with dichotomous and continuous techniques to calculate the odds ratio (OR) with a 95% confidence interval (95% CI). Additionally, we decided to evaluate the I^2 index, with a range of 0–100%. Meta-analyses use either a fixed-effect or a random-effects statistical model. A fixed-effect meta-analysis assumes that all studies are estimating the same (fixed) treatment effect, whereas a random-effects

meta-analysis allows for the differences in the treatment effect from study to study. The choice of method affects the interpretation of the summary estimates.⁹

Reporting bias assessment

Publication bias was measured both qualitatively and statistically using funnel plots and the Egger's regression test that displays the logarithm of ORs or mean differences (MDs) compared to their standard errors (publication bias existed if the p -value was <0.05), if the number of selected studies was bigger than 4. However, if the number of selected studies for the comparison was 4 or less, the Begg's rank correlation test was used.¹⁰

Certainty assessment

Two-tailed tests were used to analyze all p -values. The graphs and statistical analysis were created using Reviewer Manager v. 5.3 (The Nordic Cochrane Centre, The Cochrane Collaboration, Copenhagen, Denmark).

Results

From the total of 2943 related research studies, 10 articles published between 2000 and 2022 met the requirements and were included in the meta-analysis.^{11–20} Table 2 presents the findings from these studies. A total of 1,158,982 subjects participated in the baseline trials of the selected studies, of which 261,829 had IBD, while 897,153 were controls. The number of controls ranged from 105 to 463,576. Ten studies presented data related to IBD, 3 studies presented data organized by ulcerative colitis, and 4 studies presented data organized by Crohn's disease.

The presence of IBD resulted in significantly higher number of osteoporotic fractures (OR: 1.42, 95% CI: 1.21–1.66, $p < 0.001$) with high heterogeneity ($I^2 = 81%$) compared to controls, as shown in Fig. 2. Nevertheless, no

significant differences were found amongst ulcerative colitis patients (OR: 2.79, 95% CI: 0.88–8.87, $p = 0.08$) with high heterogeneity ($I^2 = 99%$), and Crohn's disease patients (OR: 1.84, 95% CI: 0.81–4.18, $p = 0.14$) with high heterogeneity ($I^2 = 97%$) compared to the control group for osteoporotic fractures, as shown in Fig. 3 and Fig. 4.

Stratified models could not be utilized to examine the influence of some factors on comparison outcomes, such as gender, age and ethnicity, due to no available data for these parameters. Quantitative evaluations using the Egger's regression test for the 1st comparison and Begg's rank correlation test for the 2nd and 3rd comparisons, as well as visual inspection of the funnel plot were conducted (Fig. 5–7). There was no evidence of publication bias ($p = 0.86$). However, most of the included randomized controlled trials were found to have subpar methodological quality, no bias in selective reporting and scant outcome data.

Discussion

A total of 1,158,982 subjects participated in the baseline trials of the studies selected for this meta-analysis, of which 261,829 had IBD and 897,153 were controls.^{11–20} Inflammatory bowel disease resulted in significantly higher number of osteoporotic fractures compared to controls. Nevertheless, no significant differences regarding osteoporotic fractures were found between ulcerative colitis and Crohn's disease patients compared to controls. Particular attention should be paid when evaluating the results due to the small number of studies included in some comparisons, e.g., ulcerative colitis and Crohn's disease.

Numerous pieces of information have been gathered to evaluate the connection between IBD and osteoporosis; the latter is characterized by decreased bone mineral density. The only related outcome that has considerable morbidity, mortality and healthcare expense is the probability of suffering bone fractures.¹¹ These findings demonstrate

Table 2. Characteristics of the studies selected for the meta-analysis

Study, year, reference	Country	Total	Inflammatory bowel disease	Control
Bernstein et al. (2000) ¹¹	Canada	66,297	6027	60,270
Loftus et al. (2002) ¹²	USA	476	238	238
van Staa et al. (2003) ¹³	UK	463,576	231,788	231,788
Targownik et al. (2013) ¹⁴	Canada	46,404	1230	45,174
Tsai et al. (2015) ¹⁵	China	15,705	3141	12,564
Bartko et al. (2020) ¹⁶	Austria	350,078	531	349,547
Lo et al. (2020) ¹⁷	Denmark	11,080	513	10,567
Soare et al. (2021) ¹⁸	Romania	162	81	81
Soare et al. (2022) ¹⁹	Romania	105	52	53
Ahn et al. (2022) ²⁰	South Korea	205,099	18,228	186,871
Total		1,158,982	261,829	897,153

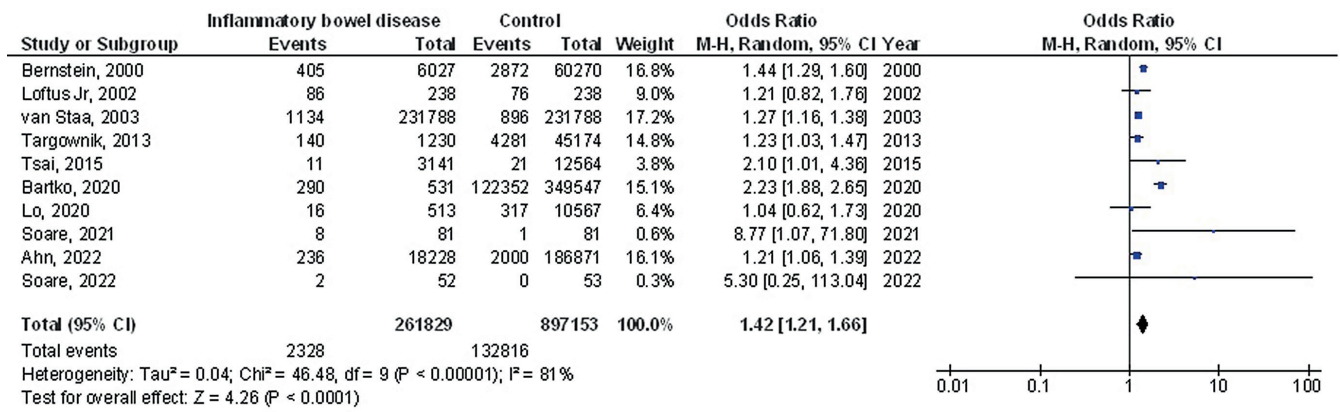


Fig. 2. Forest plot showing the impact of inflammatory bowel disease compared to controls on osteoporotic fractures

95% CI – 95% confidence interval; df – degrees of freedom.

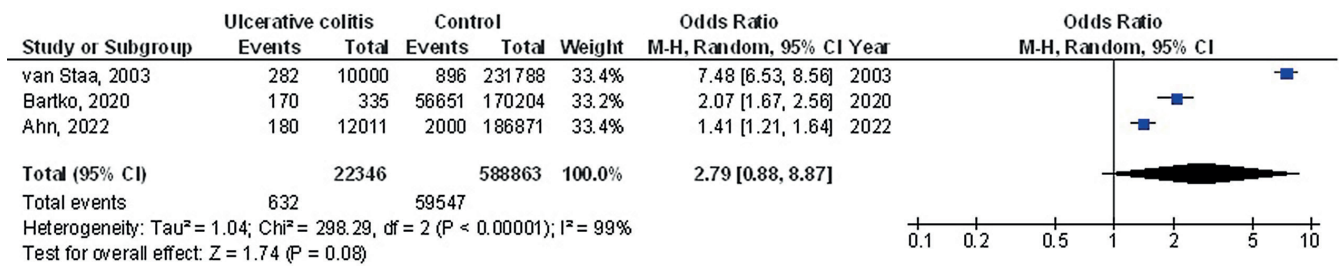


Fig. 3. Forest plot showing the impact of ulcerative colitis compared to controls on osteoporotic fractures

95% CI – 95% confidence interval; df – degrees of freedom.

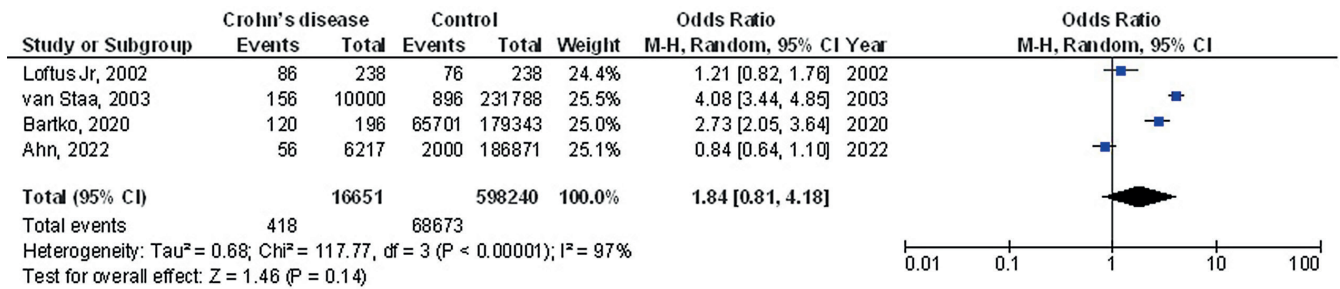


Fig. 4. Forest plot showing the impact of Crohn's disease compared to controls on osteoporotic fractures

95% CI – 95% confidence interval; df – degrees of freedom.

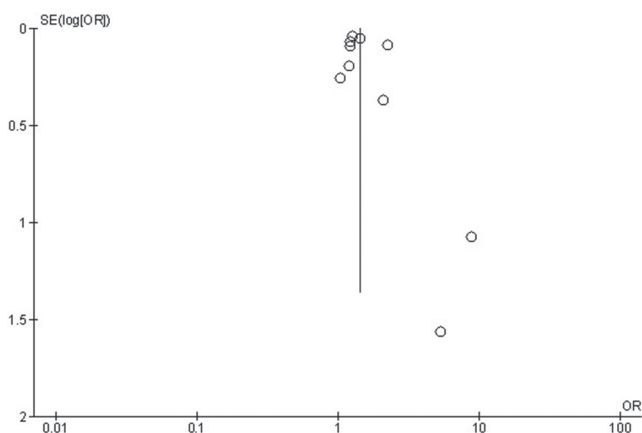


Fig. 5. Funnel plot showing the impact of inflammatory bowel disease compared to controls on osteoporotic fractures (Egger's test p-value = 0.88)

SE – standard error; OR – odds ratio.

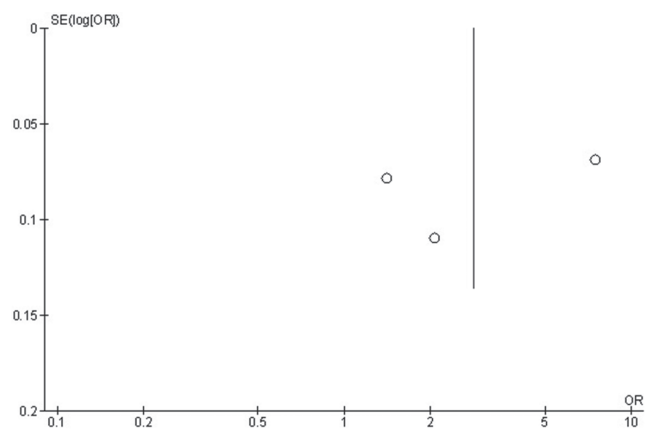


Fig. 6. Funnel plot showing the impact of ulcerative colitis compared to controls on osteoporotic fractures (Egger's test p-value = 0.85)

SE – standard error; OR – odds ratio.

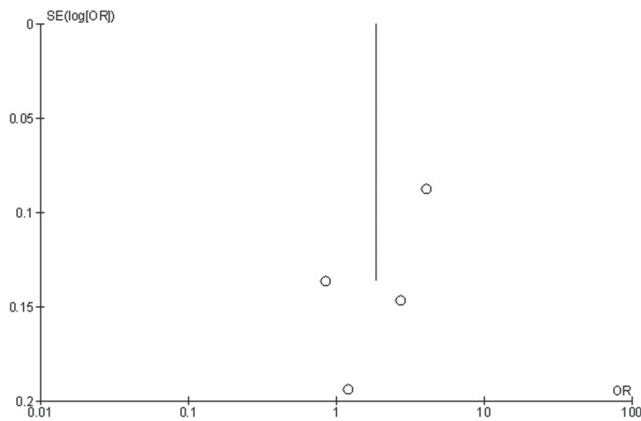


Fig. 7. Funnel plot showing the impact of Crohn's disease compared to controls on osteoporotic fractures (Egger's test p-value = 0.83)

SE – standard error; OR – odds ratio.

that the risk of osteoporotic fractures increases with age and that even people with IBD often do not exhibit accelerated bone disease symptoms until the disease has significantly advanced.²¹ The use of corticosteroids in the data utilized for this meta-analysis was matched. Patients who took steroids alone were more likely to suffer from fractures. The biggest impact of steroids on bone health is the reduction of osteoblastic activity, which decreases bone growth. The reduction in osteoblast production is a result of both a decline in the generation of new osteoblasts and an increase in the mortality of mature osteoblasts. Glucocorticoids also suppress the production of insulin-like growth factor 1, which reduces the function of the remaining osteoblasts, both directly and indirectly.²² Since most IBD patients are currently using or have previously used steroids, this could be a confounding issue. For this confounder, direct standardization was utilized as an adjustment. After accounting for the usage of this medicine, the decrease in bone mass and the increased number of bone fractures confirmed that an inflammatory condition is sufficient to alter bone metabolism. Since early detection, risk factor modification and treatment can reduce the risk of bone mass loss and improve morbidity in this particular demographic, further research is needed to determine the risk of developing fractures in the pediatric population.

This meta-analysis assesses the risk of osteoporotic fractures in IBD. More investigation is needed to clarify probable associations of the consequences under discussion. Larger and more homogeneous samples are obligatory for this investigation.^{23–28} This was likewise emphasized in a previous work that employed a related meta-analysis technique and reported similar advantageous outcomes for IBD on osteoporotic fractures.^{29–32} Since our meta-analysis was incapable of defining whether differences in gender, age and ethnicity are connected to the outcomes, well conducted randomized controlled trials are required to evaluate these factors and the mixture of variables such as gender, ethnicity, age, and other variants of subjects.

Limitations


Since several studies identified during this systemic review were not encompassed in the meta-analysis, there might have been a selection bias. The removed publications, nevertheless, did not meet the necessary inclusion criteria for this systemic review. Furthermore, we were incapable to determine whether factors such as age, gender or ethnicity affected the outcomes. The study aimed to compare the results regarding osteoporotic fractures between a control group and an IBD group. The incorporation of data from earlier studies could have added bias due to incomplete or inaccurate data. Potential sources of bias included the nutritional status of the participants as well as their age and gender characteristics. Regrettably, some unpublished papers and missing data can bias the study outcomes.


Conclusions

Inflammatory bowel disease resulted in significantly higher osteoporotic fractures compared to controls. Nevertheless, no significant differences regarding osteoporotic fractures were found between ulcerative colitis patients and Crohn's disease patients compared to controls. Particular attention should be paid when evaluating the results due to the small number of studies included in some comparisons, e.g., ulcerative colitis and Crohn's disease.

ORCID iDs

Liansheng Hao  <https://orcid.org/0000-0001-5853-7642>

Shengkai Mu  <https://orcid.org/0000-0003-0688-1534>

Junyan Yin  <https://orcid.org/0009-0001-9813-2727>

Jun Liu  <https://orcid.org/0000-0001-9515-3699>

References

- Lima CA, Lyra AC, Mendes CMC, et al. Bone mineral density and inflammatory bowel disease severity. *Braz J Med Biol Res.* 2017;50(12):e6374. doi:10.1590/1414-431x20176374
- Ali T, Lam D, Bronze MS, Humphrey MB. Osteoporosis in inflammatory bowel disease. *Am J Med.* 2009;122(7):599–604. doi:10.1016/j.amjmed.2009.01.022
- Mundy GR. Osteoporosis and inflammation. *Nutr Rev.* 2007;65(12 Pt 2):S147–S151. doi:10.1111/j.1753-4887.2007.tb00353.x
- Madney YM, Laz NI, Elberry AA, Rabea H, Abdelrahim MEA. The influence of changing interfaces on aerosol delivery within high flow oxygen setting in adults: An in-vitro study. *J Drug Deliv Sci Technol.* 2020;55:101365. doi:10.1016/j.jddst.2019.101365
- Ross AC, Manson JE, Abrams SA, et al. The 2011 report on dietary reference intakes for calcium and vitamin D from the Institute of Medicine: What clinicians need to know. *J Clin Endocrinol Metab.* 2011;96(1):53–58. doi:10.1210/jc.2010-2704
- Stroup DF, Berlin J, Morton S, et al. Meta-analysis of observational studies in epidemiology: A proposal for reporting. Meta-analysis Of Observational Studies in Epidemiology (MOOSE) group. *JAMA.* 2000;283(15):2008–2012. doi:10.1001/jama.283.15.2008
- Liberati A, Altman DG, Tetzlaff J, et al. The PRISMA statement for reporting systematic reviews and meta-analyses of studies that evaluate health care interventions: Explanation and elaboration. *J Clin Epidemiol.* 2009;62(10):e1–e34. doi:10.1016/j.jclinepi.2009.06.006

8. Gupta S, Rout G, Patel AH, et al. Efficacy of generic oral directly acting agents in patients with hepatitis C virus infection. *J Viral Hepat*. 2018;25(7):771–778. doi:10.1111/jvh.12870
9. Sheikhabahaei S, Trahan TJ, Xiao J, et al. FDG-PET/CT and MRI for evaluation of pathologic response to neoadjuvant chemotherapy in patients with breast cancer: A meta-analysis of diagnostic accuracy studies. *Oncologist*. 2016;21(8):931–939. doi:10.1634/theoncologist.2015-0353
10. Higgins JPT, Thompson S, Deeks J, Altman D. Measuring inconsistency in meta-analyses. *BMJ*. 2003;327(7414):557–560. doi:10.1136/bmj.327.7414.557
11. Bernstein CN, Blanchard J, Leslie W, Wajda A, Yu B. The incidence of fracture among patients with inflammatory bowel disease: A population-based cohort study. *Ann Intern Med*. 2000;133(10):795–799. doi:10.7326/0003-4819-133-10-200011210-00012
12. Loftus EV, Crowson CS, Sandborn WJ, Tremaine WJ, O'Fallon WM, Melton LJ. Long-term fracture risk in patients with Crohn's disease: A population-based study in Olmsted County, Minnesota. *Gastroenterology*. 2002;123(2):468–475. doi:10.1053/gast.2002.34779
13. van Staa TP, Cooper C, Samuels Brusse L, Leufkens H, Javaid MK, Arden NK. Inflammatory bowel disease and the risk of fracture. *Gastroenterology*. 2003;125(6):1591–1597. doi:10.1053/j.gastro.2003.09.027
14. Targownik LE, Bernstein CN, Nugent Z, Leslie WD. Inflammatory bowel disease has a small effect on bone mineral density and risk for osteoporosis. *Clin Gastroenterol Hepatol*. 2013;11(3):278–285. doi:10.1016/j.cgh.2012.10.022
15. Tsai MS, Lin CL, Tu YK, Lee PH, Kao CH. Risks and predictors of osteoporosis in patients with inflammatory bowel diseases in an Asian population: A nationwide population-based cohort study. *Int J Clin Pract*. 2015;69(2):235–241. doi:10.1111/ijcp.12526
16. Bartko J, Reichardt B, Kocijan R, Klaushofer K, Zwerina J, Behanova M. Inflammatory bowel disease: A nationwide study of hip fracture and mortality risk after hip fracture. *J Crohns Colitis*. 2020;14(9):1256–1263. doi:10.1093/ecco-jcc/jjaa052
17. Lo B, Holm JP, Vester-Andersen MK, Bendtsen F, Vind I, Burisch J. Incidence, risk factors and evaluation of osteoporosis in patients with inflammatory bowel disease: A Danish population-based inception cohort with 10 years of follow-up. *J Crohns Colitis*. 2020;14(7):904–914. doi:10.1093/ecco-jcc/jjaa019
18. Soare I, Sirbu A, Martin S, et al. Assessment of bone quality with trabecular bone score in patients with inflammatory bowel disease. *Sci Rep*. 2021;11(1):20345. doi:10.1038/s41598-021-99669-z
19. Soare I, Sirbu A, Diculescu M, et al. Therapies and bone impairment in inflammatory bowel disease young adults. *Farmacologia*. 2022;70(2):355–359. doi:10.31925/farmacologia.2022.2.22
20. Ahn HJ, Kim YJ, Lee HS, et al. High risk of fractures within 7 years of diagnosis in Asian patients with inflammatory bowel diseases. *Clin Gastroenterol Hepatol*. 2022;20(5):e1022–e1039. doi:10.1016/j.cgh.2021.06.026
21. Sakellariou GT, Moschos J, Berberidis C, et al. Bone density in young males with recently diagnosed inflammatory bowel disease. *Joint Bone Spine*. 2006;73(6):725–728. doi:10.1016/j.jbspin.2006.01.017
22. Canalis E. Mechanisms of glucocorticoid-induced osteoporosis. *Curr Opin Rheumatol*. 2003;15(4):454–457. doi:10.1097/00002281-200307000-00013
23. Saeed H, Mohsen M, Salah Eldin A, et al. Effects of fill volume and humidification on aerosol delivery during single-limb noninvasive ventilation. *Respir Care*. 2018;63(11):1370–1378. doi:10.4187/respcare.06022
24. Nicola M, Elberry A, Sayed O, Hussein R, Saeed H, Abdelrahim M. The impact of adding a training device to familiar counselling on inhalation technique and pulmonary function of asthmatics. *Adv Ther*. 2018;35(7):1049–1058. doi:10.1007/s12325-018-0737-6
25. Rabea H, Ali AMA, Salah Eldin R, Abdelrahman MM, Said ASA, Abdelrahim ME. Modelling of in-vitro and in-vivo performance of aerosol emitted from different vibrating mesh nebulisers in non-invasive ventilation circuit. *Eur J Pharm Sci*. 2017;97:182–191. doi:10.1016/j.ejps.2016.11.018
26. Moustafa IOF, Ali MRAA, Al Hallag M, et al. Lung deposition and systemic bioavailability of different aerosol devices with and without humidification in mechanically ventilated patients. *Heart Lung*. 2017;46(6):464–467. doi:10.1016/j.hrtlng.2017.08.004
27. Madney YM, Fathy M, Elberry AA, Rabea H, Abdelrahim MEA. Nebulizers and spacers for aerosol delivery through adult nasal cannula at low oxygen flow rate: An in-vitro study. *J Drug Deliv Sci Technol*. 2017;39:260–265. doi:10.1016/j.jddst.2017.04.014
28. Elgendy MO, Abdelrahim ME, Salah Eldin R. Potential benefit of repeated MDI inhalation technique counselling for patients with asthma. *Eur J Hosp Pharm*. 2015;22(6):318–322. doi:10.1136/ejhp-2015-000648
29. Rajput S, Mehta P, Mittal M, Rajender S, Chattopadhyay N. Human relevance of preclinical studies on the skeletal impact of inflammatory bowel disease: A systematic review and meta-analysis. *Calcif Tissue Int*. 2021;108(6):708–724. doi:10.1007/s00223-021-00808-5
30. Shen X, Wan Q, Zhao R, et al. Inflammatory bowel diseases and the risk of adverse health outcomes: Umbrella review of meta-analyses of observational studies. *Dig Liver Dis*. 2021;53(7):809–816. doi:10.1016/j.dld.2021.01.018
31. Hidalgo DF, Boonpheng B, Phemister J, Hidalgo J, Young M. Inflammatory bowel disease and risk of osteoporotic fractures: A meta-analysis. *Cureus*. 2019;11(9):e5810. doi:10.7759/cureus.5810
32. Kärnsund S, Lo B, Bendtsen F, Holm J, Burisch J. Systematic review of the prevalence and development of osteoporosis or low bone mineral density and its risk factors in patients with inflammatory bowel disease. *World J Gastroenterol*. 2020;26(35):5362–5374. doi:10.3748/wjg.v26.i35.5362

Clinical efficacy of conbercept injection on neovascular age-related macular degeneration under different levels of inflammation

Xinyue Zhang^{1,2,A,D}, Xiaotong Zhuang^{1,B}, Jie Dong^{1,C}, Bo Fu^{1,C}, Genghua Zhang^{1,E}, Li Xu^{1,F}

¹ Department of Ophthalmology, Fourth People's Hospital of Shenyang, China

² Department of Ophthalmology, Shengjing Hospital of China Medical University, Shenyang, China

A – research concept and design; B – collection and/or assembly of data; C – data analysis and interpretation; D – writing the article; E – critical revision of the article; F – final approval of the article

Advances in Clinical and Experimental Medicine, ISSN 1899–5276 (print), ISSN 2451–2680 (online)

Adv Clin Exp Med. 2024;33(4):335–342

Address for correspondence

Li Xu

E-mail: xu-li1149@163.com

Funding sources

None declared

Conflict of interest

None declared

Received on September 5, 2022

Reviewed on December 12, 2022

Accepted on June 26, 2023

Published online on September 25, 2023

Cite as

Zhang X, Zhuang X, Dong J, Fu B, Zhang G, Xu L. Clinical efficacy of conbercept injection on neovascular age-related macular degeneration under different levels of inflammation. *Adv Clin Exp Med.* 2024;33(4):335–342. doi:10.17219/acem/168808

DOI

10.17219/acem/168808

Copyright

Copyright by Author(s)

This is an article distributed under the terms of the Creative Commons Attribution 3.0 Unported (CC BY 3.0) (<https://creativecommons.org/licenses/by/3.0/>)

Abstract

Background. Age-related macular degeneration (AMD) is considered one of the most common causes of irreversible blindness among elderly patients. Neovascular AMD, which accounts for 10% of all AMD cases, can cause devastating vision loss due to choroidal neovascularization (CNV). The clinical effects and safety of intravitreal injection of conbercept in patients suffering from neovascular AMD have not been fully evaluated.

Objectives. The aim of the study was to evaluate the efficacy and safety of intravitreal injection of conbercept in patients with neovascular AMD with different levels of inflammation.

Materials and methods. A total of 120 consecutive patients with neovascular AMD who underwent intravitreal injection of conbercept (3 injections per month + pro re nata (3 + PRN)) were included and stratified based on the intraocular level of high-sensitivity C-reactive protein (hs-CRP). The level of inflammation was defined as low, medium or high, based on the concentration of hs-CRP prior to injection. Before and after conbercept injections, best-corrected visual acuity (BCVA) and central retinal thickness (CRT) were compared, respectively. Moreover, cytokine markers as well as the frequency of injections and adverse events (AEs) were measured.

Results. There were significant differences in BCVA and CRT between low, medium and high tertiles. Compared to the baseline, improved BCVA was observed, and CRT declined significantly after operation. Adverse events were most observed in high tertiles. A significant decrease in vascular endothelial growth factor (VEGF), interleukin (IL)-6 and IL-8 was observed after 1 year.

Conclusions. The effectiveness of conbercept on neovascular AMD varies depending on the level of inflammation, which could be achieved by administering different injection frequencies at different levels of inflammation. Furthermore, conbercept is associated with the reduction of inflammatory factor (IL-6 and IL-8) levels after intravitreal injection, which suggests that suppressing inflammatory response might contribute to the clinical efficacy of anti-VEGF treatment. Our results provide a novel mechanism for conbercept in patients with neovascular AMD.

Key words: inflammation, age-related macular degeneration, hs-CRP, intravitreal injection, conbercept

Introduction

Elderly patients in developing countries commonly suffer from age-related macular degeneration (AMD), one of the leading causes of irreversible blindness.¹ As a result of choroidal neovascularization (CNV), 10% of AMD cases can cause devastating vision loss.² Studies have shown that numerous cytokine pathways are involved in CNV formation and leakage. Several treatments have been developed for CNV, including transpupillary thermotherapy, focal laser therapy, verteporfin ocular photodynamic therapy, intravitreal steroids, and surgical removal of the choroidal neovascular membranes.³ Nonetheless, adverse reactions and low cure rates persisted. However, advanced anti-vascular endothelial growth factor (VEGF) therapy has eliminated these problems completely.⁴ Intravitreal anti-VEGF injections are the first-line treatment for neovascular AMD.⁵

Age-related macular degeneration is characterized by complement activation, inflammation, and choroidal endothelial cell loss. Additionally, researchers have suggested that C-reactive protein (CRP), a prototypical acute phase reactant, plays a role in AMD pathogenesis.⁶ Markers of inflammation, namely interleukin (IL)-6 and IL-8, have also been associated with AMD.⁷ Inflammatory ophthalmopathy can result in neovascularization, which is similar to the most debilitating form of neovascularization in AMD.⁸

The interaction between VEGF and inflammation in the clinical setting has not been extensively studied. Additionally, researchers do not know in what way the degree of inflammation affects the levels of VEGF and high-sensitivity CRP (hs-CRP). In this study, the clinical effect and safety of intravitreal injection of conbercept were evaluated in patients with neovascular AMD with different levels of inflammation.

Objectives

The aim of this study was to determine whether intravitreal injection of conbercept was effective and safe in patients with neovascular AMD with different levels of inflammation.

Materials and methods

Study design and participants

We enrolled 120 consecutive patients diagnosed with neovascular AMD who underwent anti-VEGF therapy at the Fourth People's Hospital of Shenyang (Shenyang, China) from September 2020 to January 2022. The inclusion criteria were as follows: 1) patients over 50 years old; 2) any type of fundus fluorescein angiography (FFA)

– diagnosing CNV induced by AMD under or near the fovea; and 3) treatment in accordance with the treatment plan. The following criteria were used for exclusion: 1) previous treatment with intravitreal anti-VEGF or laser photocoagulation; 2) history of ophthalmic surgery except for cataracts; 3) CNV due to a reason other than AMD; 4) CNV with diseases of the retina such as diabetic retinopathy; 5) diseases that affect intravitreal injections in a severe manner; and 6) no clear indication of the severity of refractive effects of the stroma.

The study protocol adhered to the ethical guidelines of the 1975 Declaration of Helsinki and its subsequent amendments. The ethics committee of the First Affiliated Hospital of China Medical University and the Institutional Review Board of Fourth People's Hospital of Shenyang approved the study (approval No. KY2020-105). Each patient gave informed consent to participate in the study, and for their data to be collected and analyzed for research purposes.

Settings

Based on the hs-CRP levels, the patients were grouped into 3 tertiles: high, medium and low. The cut-off hs-CRP levels between the low, medium and high tertiles were 1.99 and 10.22 mg/L, respectively. All patients received the following tests: a measurement of best-corrected visual acuity (BCVA), intraocular pressure, color fundus photography, optical coherence tomography (OCT), and a FFA (Fig. 1). The BCVA was determined by using an international standard logarithmic visual acuity chart, and letter scores were collected from participants. Intraocular pressure measurements were performed using a tonometer without contact (Huvitz HNT-7000; Huvitz, Seoul, South Korea). Color fundus photography and the FFA were performed using a Topcon Fundus Camera (Topcon TRC-50X; Topcon, Tokyo, Japan). Spectral domain OCT products were used to perform the OCT test (Heidelberg Engineering, Heidelberg, Germany).

Data collection

The patient's eyeball was anesthetized, and the eyelid was opened. Next, the anterior chamber was punctured using a 0.45-mm needle, which was then inserted at the limbus and advanced to the middle of the anterior chamber. The eyeball was gently pressed to make approx. 0.1 mL of aqueous humor enter into a disposable syringe via the needle. The obtained aqueous humor samples were kept in a freezer at -76°C until analysis. The IL-6, IL-8 and VEGF levels were analyzed by performing an enzyme-linked immunosorbent assay (ELISA) at the Biochemistry Laboratory of China Medical University, Shenyang, China.

Measurement of cytokine levels

Inflammatory levels were determined by using a commercially available immunonephelometric kinetic assay

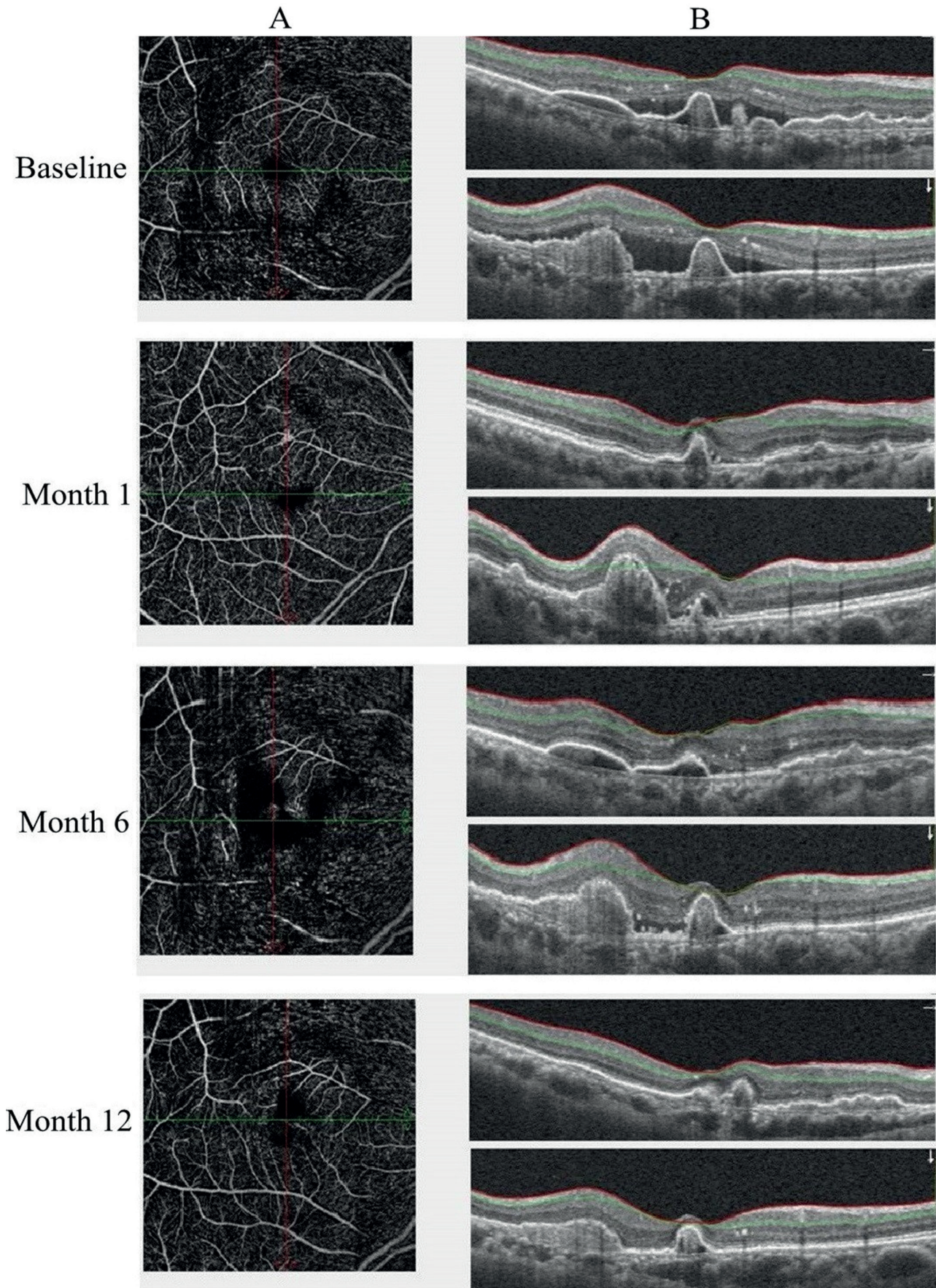


Fig. 1. Fundus fluorescein angiography (FFA) (A) and horizontal (up) and vertical (down) optical coherence tomography (OCT) scans (B) at baseline and up to 12-month follow-up, conducted after 6 conbercept injections over 12 months in an eye with neovascular age-related macular degeneration (AMD) characterized as retinal angiomatous proliferation

(BN ProSpec; Siemens, Tarrytown, USA), and hs-CRP levels were determined using CardioPhase (Siemens). In this study, cytokine-specific ELISA kits were used to measure plasma and supernatant cytokine levels (Abcam, Cambridge, UK). A 0.025-mL sample of aqueous humor was used for each measurement. Absorbances were read at 450 nm using a microplate reader (ELx800; BioTek Instruments Inc., Winooski, USA). The assay ranges for VEGF, IL-6 and IL-8 were 15.6–1000, 2–250 and 2–300 pg/mL, respectively.

Drug treatment

As described previously, the same senior physician administered intravitreal injections of conbercept (0.5 mg/0.05 mL solution was obtained from Chengdu Kanghong Biotechnology Co., Ltd., Chengdu, China) to all patients' eyes.⁹ Three days before the injection, a dose of 5 µg (2 drops) of 0.5% levofloxacin was administered 4 times daily to the patient's eye. A three-month course of intravitreal injections of conbercept was administered. The pro re nata (PRN) administration was retracted in the presence of any of the following changes: OCT scan revealing a persistent or recurrent intraretinal or subretinal fluid, new hemorrhage of the macula, new leakage or onset of classic CNV on FFA, a loss of vision greater than 1 line, or a decrease in conscious vision.^{9,10} The eyes were bandaged with tobramycin–dexamethasone ointment after injecting conbercept into the conjunctival sacs. For 3 days after the surgery, eye drops were applied 4 times a day using 0.5% levofloxacin.

Follow-up

The patients were followed up for 12 months. Optical coherence tomography examinations and visual acuity tests were performed on a monthly basis. Every third monthly exam was conducted using FFA. The BCVA and central retinal thickness (CRT), as well as the leakage area of CNV were measured before and after the treatment in all patients. In addition, the adverse events (AEs) and cytokine markers (VEGF, IL-6 and IL-8) were recorded

at admission and at 12-month follow-up. The trial was conducted according to the Technical Guidelines for Clinical Research of Drugs for Treatment of Age-Related Macular Degeneration (Center for Drug Evaluation, National Medical Products Administration, Beijing, China).

Statistical analyses

Mean value ± standard deviation was used for data with a normal distribution, and median (interquartile range) was used for data with a non-normal distribution. The Shapiro–Wilk test was utilized to check the normal distribution of data. One-way analysis of variance (ANOVA) tests were used to assess the differences between multiple sets of data. The Mann–Whitney U tests were conducted to compare sets of non-normally distributed data. The Wilcoxon test for matched pairs was performed to test the differences between baseline and follow-up for each cytokine in all hs-CRP groups. Categorical variables were compared using the χ^2 or Fisher's exact tests, as appropriate. A two-sided p-value <0.05 was considered statistically significant. The study utilized SPSS v. 22.0 software (IBM Corp., Armonk, USA) for all statistical analyses.

Results

Baseline data

A total of 120 consecutive patients suffering from neovascular AMD who underwent injection of intravitreal conbercept (3 + PRN) were included in the study. The participants were stratified based on the concentrations of hs-CRP in the intraocular fluid. As a result of pre-injection hs-CRP concentrations, patients' inflammation levels were set as high, medium and low. The baseline demographic characteristics and ophthalmoscopic examination results of the 3 groups are shown in Table 1 and Supplementary Table 1. There were no significant differences observed in the basic characteristics of the patients.

Table 1. Baseline demographic characteristics of the patients

Characteristic		hs-CRP ≤ 2 mg/L (n = 40)	2 mg/L < hs-CRP < 10 mg/L (n = 40)	hs-CRP ≥ 10 mg/L (n = 40)	χ^2 or F	p-value
Male, n (%)		26 (65.00)	25 (62.50)	23 (57.50)	0.494	0.781
Age [years]		66.30 (64.53–68.07)	66.33 (64.68–69.97)	66.68 (65.52–68.13)	0.068	0.935
Right eye, n (%)		14 (35.00)	9 (22.50)	15 (37.50)	2.388	0.303
Mean BCVA, letter score		48.10 (45.24–50.96)	47.15 (44.52–49.78)	46.50 (43.97–49.03)	0.370	0.692
CRT [µm]		426.50 (406.72–446.28)	428.50 (405.57–451.43)	441.30 (420.65–461.95)	0.589	0.556
CNV location, n (%)	extrafoveal	13 (32.50)	10 (25.00)	14 (35.00)	1.016	0.602
	juxtafoveal	16 (40.00)	15 (37.50)	18 (45.00)	–	–
	subfoveal	11 (27.50)	15 (37.50)	8 (20.00)	–	–

Mean values (95% confidence intervals (95% CIs)) and n (%) were reported for variables, respectively. hs-CRP – hypersensitive C-reactive protein; BCVA – best-corrected visual acuity; CRT – central retinal thickness; CNV – choroidal neovascularization. Categorical variables were compared using the χ^2 test. One-way analysis of variance (ANOVA) was used to assess the differences between 3 groups.

Visual acuity

As depicted in Fig. 2 and Supplementary Tables 2 and 3, BCVA letter scores improved on average in all post-baseline assessments. The BCVA letter scores significantly improved between the 3 groups after 1 month of treatment ($p < 0.001$), which averaged increments of 5.92 ± 1.19 , 5.85 ± 1.12 and 6.25 ± 1.01 , respectively. The improvements in BCVA continued up to 3 months and were maintained for 6 months, which averaged increments of 12.68 ± 1.94 , 11.20 ± 1.95 and 10.10 ± 1.13 at 3 months, respectively. There were no significant differences in BCVA letter scores between the 3 groups at 7, 10 and 12 months.

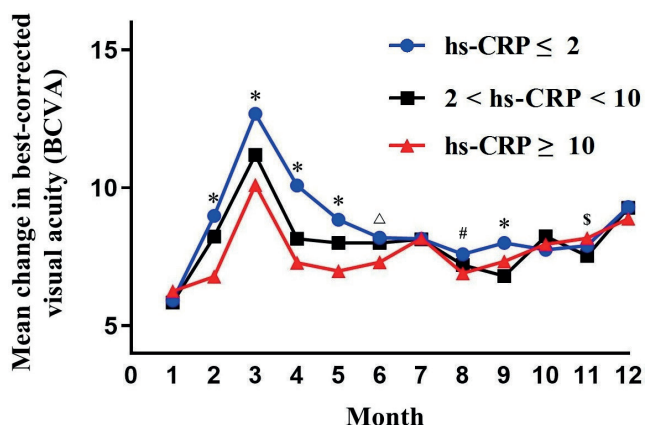


Fig. 2. Mean change in best-corrected visual acuity (BCVA)

hs-CRP – hypersensitive C-reactive protein; * $p < 0.0001$; $\Delta p = 0.002$; # $p = 0.014$; $\S p = 0.027$. The detailed data with a post-hoc test are shown in Supplementary Table 1.

Central retinal thickness

Table 2 and Supplementary Table 4 summarize the characteristics of CRT at admission and follow-up across the 3 groups. There were no significant differences between the 3 groups at 1-, 6- and 12-month follow-ups. However, there was a trend for CRT levels to decrease more rapidly in the group with a $hs-CRP \leq 2$.

Choroidal neovascularization

In the group with a $hs-CRP \leq 2$, FFA examinations at the last follow-up indicated that 24 eyes no longer had leakage areas within the CNV (60%), 14 eyes had

reduced CNV (35%), and 2 eyes had enlarged CNV (5%). In the group with a $hs-CRP > 2$ but < 10 , 20 eyes no longer had leakage areas of CNV (50%), 14 eyes had reduced CNV (35%), and 6 eyes had enlarged CNV (15%). In the group with a $hs-CRP \geq 10$, 16 eyes no longer had leakage areas of CNV (40%), 18 eyes had reduced CNV (45%), and 6 eyes had enlarged CNV (15%). In groups with low inflammation, conbercept had a better effect on leakage areas of CNV compared to groups with high inflammation, but no significant difference was observed.

Cytokine

Conbercept injections significantly reduced levels of VEGF and proinflammatory cytokines IL-6 and IL-8 at low- and medium levels of inflammation (Table 3). Compared to medium- and high levels of inflammation, conbercept had a significantly higher anti-VEGF and inflammatory effect at low inflammation levels (Table 3 and Supplementary Table 5).

Clinical outcomes and ocular adverse events at 12-month follow-up

The number of conbercept injections on average between the 3 groups was 5.93 (5.55–6.30), 5.85 (5.49–6.21) and 6.25 (5.93–6.57) in the low, medium and high inflammation groups, respectively. There was a trend for a greater number of injections in the high inflammation group (Table 4 and Supplementary Table 6). Ocular AEs were summarized in Table 4. An intravitreal injection did not result in serious complications, such as porogen detachment or endophthalmitis, during the 12-month follow-up period. Increased intraocular pressure, pain in the eye and conjunctival hemorrhage were ocular AEs. In the low-tertile group, cumulative AEs were significantly lower than in the medium- and high-tertile groups.

Discussion

To date, the efficacy of conbercept in treating neovascular AMD at different levels of inflammation and anti-inflammatory effects of anti-VEGF agents are still unclear. Approximately 8% of the world population suffers from

Table 2. Central retinal thickness results at follow-up

Follow-up timepoint	hs-CRP ≤ 2 mg/L (n = 40)	2 mg/L < hs-CRP < 10 mg/L (n = 40)	hs-CRP ≥ 10 mg/L (n = 40)	df	F	p-value
1 month	282.20 (269.12–295.28)	283.55 (268.36–298.74)	292.05 (278.39–305.71)	2	0.595	0.553
6 months	255.28 (243.42–267.13)	256.43 (242.68–270.17)	259.85 (248.97–270.73)	2	0.155	0.856
12 months	243.30 (233.30–253.30)	253.88 (240.28–267.47)	254.55 (243.72–265.38)	2	1.215	0.300

Mean values (95% confidence intervals (95% CIs)) were reported for variables. hs-CRP – hypersensitive C-reactive protein; CRT – central retinal thickness; df – degrees of freedom. One-way analysis of variance (ANOVA) was used to assess the differences between 3 groups.

Table 3. Cytokine levels at baseline and follow-up

Characteristic		hs-CRP ≤ 2 mg/L (n = 40)	2 mg/L < hs-CRP < 10 mg/L (n = 40)	hs-CRP ≥ 10 mg/L (n = 40)	df	F	p-value
VEGF [pg/mL]	baseline	12.34 (9.03–15.66)	69.08 (60.70–77.46)	473.53 (201.53–745.53)	2	10.482	<0.001
	12-month follow-up	3.88 (2.84–4.92)	23.03 (20.23–25.82)	265.01 (73.46–456.56)	2	7.085	0.001
	p-value	<0.001	<0.001	<0.001	–	–	–
IL-6 [pg/mL]	baseline	25.70 (20.95–30.44)	171.48 (146.84–196.11)	3794.12 (1646.07–5942.16)	2	12.112	<0.001
	12-month follow-up	19.16 (14.85–23.47)	114.32 (97.89–130.74)	2918.55 (1266.21–4570.90)	2	12.196	<0.001
	p-value	<0.001	<0.001	0.001	–	–	–
IL-8 [pg/mL]	baseline	22.27 (20.91–23.63)	46.63 (41.82–51.45)	317.75 (155.19–480.31)	2	12.483	<0.001
	12-month follow-up	5.97 (5.21–6.74)	19.74 (17.01–22.46)	172.91 (81.07–264.75)	2	12.483	<0.001
	p-value	<0.001	<0.001	<0.001	–	–	–

Mean values (95% confidence intervals (95% CIs)) were reported for variables. hs-CRP – hypersensitive C-reactive protein; VEGF – vascular endothelial growth factor; IL – interleukin; df – degrees of freedom. One-way analysis of variance (ANOVA) was used to assess the differences between 3 groups. The Wilcoxon test for matched pairs was performed to evaluate the differences between baseline and follow-up for each cytokine in all hs-CRP groups.

Table 4. Clinical outcomes and ocular adverse events (AEs) over 12 months

Characteristic		hs-CRP ≤ 2 mg/L (n = 40)	2 mg/L < hs-CRP < 10 mg/L (n = 40)	hs-CRP ≥ 10 mg/L (n = 40)	χ ² or F	p-value
Clinical outcomes	mean change in BCVA, letter score	9.30 (8.65–9.95)	9.28 (8.66–9.89)	8.88 (8.21–9.54)	0.558	0.574
	number of injections	5.93 (5.55–6.30)	5.85 (5.49–6.21)	6.25 (5.93–6.57)	3.618	0.164
	change in BCVA ≥ 10 letter score, n (%)	18 (45.00)	17 (42.50)	15 (37.50)	0.480	0.787
Ocular AEs, n (%)	cumulative AEs	8 (20.00)	13 (32.50)	25 (62.50)	16.146	<0.001
	increased intraocular pressure	2 (5.00)	4 (10.00)	6 (15.00)	2.164	0.329
	eye pain	3 (7.50)	3 (7.50)	6 (15.00)	1.667	0.435
	conjunctival hemorrhage	2 (5.00)	4 (10.00)	6 (15.00)	2.164	0.329
	vitreous hemorrhage	0 (0.00)	0 (0.00)	1 (2.50)	1.834	0.365
	vitreous floaters	0 (0.00)	1 (2.50)	1 (2.50)	1.259	0.601
	vitreous detachment	1 (2.50)	0 (0.00)	1 (2.50)	1.259	0.601
	macular fibrosis	0 (0.00)	1 (2.50)	2 (5.00)	1.868	0.359
	corneal abrasion	0 (0.00)	0 (0.00)	1 (2.50)	1.834	0.365
	dry eye	0 (0.00)	0 (0.00)	1 (2.50)	1.834	0.365

Mean values (95% confidence intervals (95% CIs)) and n (%) were reported for variables, respectively. hs-CRP – hypersensitive C-reactive protein; BCVA – best-corrected visual acuity. Categorical variables were compared using the χ² or Fisher exact tests, as appropriate. One-way analysis of variance (ANOVA) was used to assess the differences between 3 groups. The Kruskal–Wallis test was used to assess the differences regarding the number of injections.

AMD, a progressive neurodegenerative disease.¹¹ Developed countries have the highest rate of elderly blindness caused by AMD. Neovascular growth of patients suffering from neovascular AMD, featuring CNV, should be driven by a complex process that involves VEGF-A, a signal protein.¹² The development of AMD is closely associated with neovascularization and abnormal vessel permeability in the eye, mediated by VEGF.¹³ In recent years, conbercept has become a leading anti-VEGF drug.¹⁴ A major benefit of conbercept is that it inhibits retinal angiogenesis and reduces vascular permeability.¹⁵ Additionally, inflammation leading to VEGF-A expression also contributes to AMD pathology.¹⁶

Regulatory factors associated with AMD, including smoking, dietary factors, obesity, and lipid levels,^{17–19} which are also related to cardiovascular disease (CVD), have become

better understood in the past decade. Despite the fact that CVD and AMD have common risk factors, the evaluation of the potential relationship between CVD-related biomarkers and AMD is strongly advised.⁸ As a physiological marker of systemic inflammation, hs-CRP is associated with advanced AMD, which is also consistently associated with CVD. Although there may be new detection methods of other inflammatory markers in the future, with better accuracy, standardization, and characteristics other than those observed in the current detection methods, present clinical practice utilizes hs-CRP detection as a useful marker.²⁰ In our study, conbercept showed a greater reduction in inflammation (IL-6 and IL-8) at lower levels of hs-CRP and a much more stable anti-VEGF effect. Conbercept is a large protein molecule and is known as the extracellular domains of VEGF receptors 1 and 2, which were combined

with the human immunoglobulin Fc region to construct a new bait receptor protein.¹⁵ In addition, conbercept binds to placental growth factor (PIGF), VEGF-B and VEGF-A, which regulate inflammation.^{21,22} Meanwhile, by increasing the number of injections, conbercept is expected to provide a similar clinical effect in patients with high levels of hs-CRP.

In our study, intravitreal injections of conbercept rapidly improved eyesight in neovascular AMD patients. After receiving 3 scheduled conbercept injections, improvements were observed, and these improvements were sustained over a 12-month variable dosing regimen. This study found that conbercept was well tolerated without systemic serious adverse events (SAEs). The intravitreal injections were associated with a high rate of AEs, including conjunctival hemorrhages and increased intraocular pressure. Due to the high molecular weight (143 kDa) of conbercept, systemic AEs are reduced, and the drug's activity is prolonged, limiting its permeability through the blood–eye barrier, with less systemic exposure than systemic medication.²³

Limitations

Our study had some limitations. First of all, only a small number of patients participated in the study. Secondly, referral bias may have been present since the study was conducted in a single hospital setting. Also, there was no long-term data or follow-ups, which will be addressed in a future study. Finally, the small sample size of our study prevented us from detecting any AEs related to the drug. Continuous monitoring of short-term effects will be carried out during the post-marketing phase.

Conclusions

The effectiveness of conbercept on neovascular AMD varies depending on the level of inflammation, which could be achieved by administering different injection frequencies at different levels of inflammation. Furthermore, conbercept is related to reduced inflammation (IL-6 and IL-8) at follow-up after intravitreal injections, indicating an anti-inflammatory function for conbercept as anti-VEGF treatment, which could provide another explanation for conbercept treatment in neovascular AMD patients.

Availability of data and materials

The authors of the study are willing to make the raw data supporting their conclusions readily accessible.

Supplementary data

The Supplementary materials are available at <https://doi.org/10.5281/zenodo.8330239>. The package contains the following files:

Supplementary Table 1. One-way ANOVA test for basic characteristics with post-hoc results.

Supplementary Table 2. Changes of BCVA letter scores in all post-baseline assessments.

Supplementary Table 3. One-way ANOVA test for BCVA letter scores with post-hoc results.

Supplementary Table 4. One way ANOVA test for central retinal thickness outcome with post-hoc results.

Supplementary Table 5. One-way ANOVA test for cytokine levels with post-hoc results.

Supplementary Table 6. One-way ANOVA test for clinical outcomes with post-hoc results.

ORCID iDs

Xinyue Zhang  <https://orcid.org/0000-0002-3686-0382>
 Xiaotong Zhuang  <https://orcid.org/0009-0008-9075-3546>
 Jie Dong  <https://orcid.org/0000-0002-4043-8192>
 Bo Fu  <https://orcid.org/0000-0001-6058-9513>
 Genghua Zhang  <https://orcid.org/0009-0003-1902-4571>
 Li Xu  <https://orcid.org/0000-0003-0421-253X>

References

- Hanus J, Zhao F, Wang S. Current therapeutic developments in atrophic age-related macular degeneration. *Br J Ophthalmol*. 2016;100(1):122–127. doi:10.1136/bjophthalmol-2015-306972
- Arepalli S, Kaiser PK. Pipeline therapies for neovascular age related macular degeneration. *Int J Retina Vitreous*. 2021;7(1):55. doi:10.1186/s40942-021-00325-5
- Spaide RF, Jaffe GJ, Sarraf D, et al. Consensus nomenclature for reporting neovascular age-related macular degeneration data: Consensus on neovascular age-related macular degeneration nomenclature study group. *Ophthalmology*. 2020;127(5):616–636. doi:10.1016/j.ophtha.2019.11.004
- Hussain RM, Shaukat BA, Ciulla LM, Berrocal AM, Sridhar J. Vascular endothelial growth factor antagonists: Promising players in the treatment of neovascular age-related macular degeneration. *Drug Des Devel Ther*. 2021;15:2653–2665. doi:10.2147/DDDT.S295223
- Yang S, Zhao J, Sun X. Resistance to anti-VEGF therapy in neovascular age-related macular degeneration: A comprehensive review. *Drug Des Devel Ther*. 2016;1857–1867. doi:10.2147/DDDT.S97653
- Chirco KR, Potempa LA. C-reactive protein as a mediator of complement activation and inflammatory signaling in age-related macular degeneration. *Front Immunol*. 2018;9:539. doi:10.3389/fimmu.2018.00539
- Nahavandipour A, Krogh Nielsen M, Sørensen TL, Subhi Y. Systemic levels of interleukin-6 in patients with age-related macular degeneration: A systematic review and meta-analysis. *Acta Ophthalmol*. 2020;98(5):434–444. doi:10.1111/aos.14402
- Seddon JM, George S, Rosner B, Rifai N. Progression of age-related macular degeneration: Prospective assessment of C-reactive protein, interleukin 6, and other cardiovascular biomarkers. *Arch Ophthalmol*. 2005;123(6):774–782. doi:10.1001/archophth.123.6.774
- Lalwani GA, Rosenfeld PJ, Fung AE, et al. A variable-dosing regimen with intravitreal ranibizumab for neovascular age-related macular degeneration: Year 2 of the PrONTO Study. *Am J Ophthalmol*. 2009;148(1):43–58.e1. doi:10.1016/j.ajo.2009.01.024
- Giacomelli G, Giansanti F, Finocchio L, et al. Results of intravitreal ranibizumab with a prn regimen in the treatment of extrafoveal and juxtafoveal neovascular membranes in age-related macular degeneration. *Retina*. 2014;34(5):860–867. doi:10.1097/IAE.0000000000000007
- Wong WL, Su X, Li X, et al. Global prevalence of age-related macular degeneration and disease burden projection for 2020 and 2040: A systematic review and meta-analysis. *Lancet Glob Health*. 2014;2(2):e106–e116. doi:10.1016/S2214-109X(13)70145-1
- Sarwar S, Maya JR, Hanout M, Sepah YJ, Do DV, Nguyen QD. Aflibercept for neovascular age-related macular degeneration. In: *Cochrane Database of Systematic Reviews*. John Wiley & Sons, Ltd; 2014:CD011346. doi:10.1002/14651858.CD011346

13. Xia JP, Liu SQ, Wang S. Intravitreal conbercept improves outcome of proliferative diabetic retinopathy through inhibiting inflammation and oxidative stress. *Life Sci.* 2021;265:118795. doi:10.1016/j.lfs.2020.118795
14. Mao J, Wu H, Chen Y, et al. Effect of intravitreal conbercept treatment before vitrectomy in proliferative diabetic retinopathy. *Int J Ophthalmol.* 2018;11(7):1217–1221. doi:10.18240/ijo.2018.07.23
15. Wang Q, Li T, Wu Z, et al. Novel VEGF decoy receptor fusion protein conbercept targeting multiple VEGF isoforms provide remarkable anti-angiogenesis effect in vivo. *PLoS One.* 2013;8(8):e70544. doi:10.1371/journal.pone.0070544
16. Nagineni CN, Kommineni VK, William A, Detrick B, Hooks JJ. Regulation of VEGF expression in human retinal cells by cytokines: Implications for the role of inflammation in age-related macular degeneration. *J Cell Physiol.* 2012;227(1):116–126. doi:10.1002/jcp.22708
17. Smith W, Assink J, Klein R, et al. Risk factors for age-related macular degeneration: Pooled findings from three continents. *Ophthalmology.* 2001;108(4):697–704. doi:10.1016/S0161-6420(00)00580-7
18. Seddon JM, Cote J, Rosner B. Progression of age-related macular degeneration: Association with dietary fat, transunsaturated fat, nuts, and fish intake. *Arch Ophthalmol.* 2003;121(12):1728–1737. doi:10.1001/archophth.121.12.1728
19. Seddon JM, Cote J, Davis N, Rosner B. Progression of age-related macular degeneration: Association with body mass index, waist circumference, and waist-hip ratio. *Arch Ophthalmol.* 2003;121(6):785–792. doi:10.1001/archophth.121.6.785
20. Jeong HS, Hong SJ, Cho SA, et al. Comparison of ticagrelor versus prasugrel for inflammation, vascular function, and circulating endothelial progenitor cells in diabetic patients with non-ST-segment elevation acute coronary syndrome requiring coronary stenting: A prospective, randomized, crossover trial. *JACC Cardiovasc Interv.* 2017;10(16):1646–1658. doi:10.1016/j.jcin.2017.05.064
21. Gragoudas ES, Adamis AP, Cunningham ET, Feinsod M, Guyer DR. Pegaptanib for neovascular age-related macular degeneration. *N Engl J Med.* 2004;351(27):2805–2816. doi:10.1056/NEJMoa042760
22. Carnevale D, Lembo G. Placental growth factor and cardiac inflammation. *Trends Cardiovasc Med.* 2012;22(8):209–212. doi:10.1016/j.tcm.2012.07.022
23. Liu K, Song Y, Xu G, et al. Conbercept for treatment of neovascular age-related macular degeneration: Results of the randomized phase 3 PHOENIX study. *Am J Ophthalmol.* 2019;197:156–167. doi:10.1016/j.ajo.2018.08.026

The distance between the anterior and posterior edges of the fibula at a lateral internal rotation of 15° is associated with postoperative malreduction in patients with an ankle joint fracture combined with a lower tibiofibular syndesmosis injury

Zhiqin Liu^{B–D}, Wentao Gao^{B,C}, Xiping Zhang^B, Weifeng Wang^B, Miduo Tan^{B,E}, Eryue Qiu^{B,C}, Anlie Cai^{A,C,E,F}

Department of Orthopedic Surgery, Zhuzhou Central Hospital, Zhuzhou Hospital Affiliated to Xiangya School of Medicine, Central South University, Changsha, China

A – research concept and design; B – collection and/or assembly of data; C – data analysis and interpretation; D – writing the article; E – critical revision of the article; F – final approval of the article

Advances in Clinical and Experimental Medicine, ISSN 1899–5276 (print), ISSN 2451–2680 (online)

Adv Clin Exp Med. 2024;33(4):343–350

Address for correspondence

Anlie Cai
E-mail: anlie_cai@163.com

Funding sources

The study was funded by 2020 Natural Science Foundation of Hunan Province – Provincial and Municipal Joint Fund (grant No. 2020JJ6107): Evaluation of the reduction of the syndesmotom joint during the operation based on the projection X-ray measurement data from different angles of the ankle joint.

Conflict of interest

None declared

Received on December 31, 2022

Reviewed on June 18, 2023

Accepted on July 3, 2023

Published online on August 14, 2023

Cite as

Liu Z, Gao W, Zhang X, et al. The distance between the anterior and posterior edges of the fibula at a lateral internal rotation of 15° is associated with postoperative malreduction in patients with an ankle joint fracture combined with a lower tibiofibular syndesmosis injury. *Adv Clin Exp Med.* 2024;33(4):343–350. doi:10.17219/acem/169190

DOI

10.17219/acem/169190

Copyright

Copyright by Author(s)

This is an article distributed under the terms of the Creative Commons Attribution 3.0 Unported (CC BY 3.0) (<https://creativecommons.org/licenses/by/3.0/>)

Abstract

Background. Malreduction remains a problem in patients with an ankle joint fracture combined with a lower tibiofibular syndesmosis injury. Current methods of malreduction evaluation have many limitations, and novel techniques are required.

Objectives. The aim of the study was to investigate the association between the distance between the anterior and posterior edges of the fibula at a 15° lateral internal rotation and postoperative malreduction in patients with an ankle joint fracture combined with a lower tibiofibular syndesmosis injury.

Materials and methods. This prospective observational cohort study enrolled 187 patients diagnosed with an ankle joint fracture combined with a lower tibiofibular syndesmosis injury between January 2020 and January 2022. The patients were divided into 2 groups according to their postoperative malreduction condition: the malreduction group and the non-malreduction group. After tibiofibular syndesmosis reduction, a computed tomography (CT) scan was used to measure the distance between the anterior and posterior edges of the fibula at a standard lateral position and a position with a lateral internal rotation of 15°. Demographic data and basic clinical characteristics were recorded for all patients.

Results. The mean distance between the anterior and posterior edges of the fibula was longer in malreduction patients than non-malreduction patients at the standard lateral and 15° lateral internal rotation positions. At a lateral internal rotation of 15°, the distance between the anterior and posterior edges correlated negatively with the postoperative Mazur and American Orthopaedic Foot and Ankle Society (AOFAS) scores, and correlated positively with the length of hospitalization and fracture healing time. Receiver operating characteristic (ROC) curves revealed the potential postoperative malreduction diagnostic value of fibular anterior–posterior edge distance using an internal rotation of 15°. Postoperative AOFAS score, length of hospitalization, fracture healing time, and the distance between the anterior and posterior edges of the fibula at a lateral internal rotation of 15° were independent risk factors of malreduction.

Conclusions. The fibular anterior–posterior edge distance at an internal rotation of 15° is associated with postoperative ankle joint function and the occurrence of malreduction.

Key words: fibular anterior–posterior edge distance, malreduction, tibiofibular syndesmosis reduction, ankle joint fracture

Background

The lower tibiofibular syndesmosis is vital for ankle joint structural stability and is a site of frequent damage, accounting for 1–11% of all orthopedic ankle joint injuries.^{1,2} Despite the development of surgical strategies, malreduction remains a problem in patients with an ankle joint fracture combined with a lower tibiofibular syndesmosis injury.^{3,4} The occurrence of malreduction is related to many factors. A recent study reported that malreduction was influenced by incisura morphology, with more shallow syndesmoses likely causing a higher malreduction rate.⁵ However, even without considering these factors, it is widely accepted that achieving anatomic reduction remains a significant clinical challenge, even for experienced surgeons.⁶

Current standard malreduction evaluation methods involve measuring the tibiofibular clear space and tibiofibular overlap.⁷ However, the fibula is located at the posterolateral side of the tibia; thus, there are few non-overlapping parts of the tibia and fibula in standard ankle joint lateral imaging.⁸ When evaluated during surgery, fractures with posterior malleolus and internal fixation can affect the measurement of the lateral fibula position relative to the tibia, affecting the judgment of whether the fibula has a malreduction in the sagittal position.^{9,10}

The malreduction rate after the reduction of tibiofibular syndesmosis injury can be as high as 50%, indicating limitations of the current evaluation methods.^{11–13} In recent years, many novel potential methods for evaluating malreduction after lower tibiofibular syndesmosis injury have been developed.^{3,14} However, most of the studies on the subject were cadaver-based investigations.

Objectives

The present study aimed to investigate the clinical significance of the distance between the anterior and posterior edge of the fibula at a standard lateral internal rotation of 15° in patients with postoperative malreduction after lower tibiofibular syndesmosis injury. The findings may provide a novel method to predict and reduce malreduction in tibiofibular syndesmosis injury.

Materials and methods

Study design and participants

This prospective observational cohort study enrolled 187 patients diagnosed with an ankle joint fracture combined with a lower tibiofibular syndesmosis injury between January 2020 and January 2022. The diagnosis was confirmed in all cases with imaging evidence, such

as computed tomography (CT) scan, X-ray and magnetic resonance imaging (MRI). The inclusion criteria were as follows: 1) adults with their first diagnosis of an ankle joint fracture combined with a lower tibiofibular syndesmosis injury; 2) tibiofibular separation requiring reduction of tibiofibular syndesmosis; 3) no ankle joint injury before the study; 4) closed fracture. The following patients were excluded: 1) those with ankle joint injury before the study or previous lower tibiofibular syndesmosis injury; 2) open fracture patients; 3) patients with a surgical contraindication, such as severe cardiovascular, renal or liver dysfunctions. Written informed consent was obtained from all participants. The ethical committee of Zhuzhou Hospital, affiliated to Xiangya School of Medicine (Central South University, Changsha, China) approved the study (approval No. 201905029).

All patients received routine surgeries, with the tibiofibular syndesmosis reduction conducted using either tibiofibular screw or button fixation, as reported elsewhere.^{15,16} Follow-up occurred 6 months after surgery, during which patients were divided into malreduction and non-malreduction groups based on postoperative malreduction condition.

Sample size calculation

For sample size calculation, we used the distance between the anterior and posterior edges of the fibula at a standard lateral internal rotation of 15° as the primary observational factor. The formula to calculate sample size of cohort study, $(Z_{1-\alpha/2} \times \sigma / \delta)^2$, was used, in which $Z_{1-\alpha/2}$ represents standardized value for the corresponding level of confidence, σ represents predicted standard error, and δ represents allowable error. In this study, the value of $Z_{1-\alpha/2} = 1.96$ (at 95% CI), $\sigma = 8.31$ according to our previous experience, and $\delta = 1.19$. Thus $n = (1.96 \times 8.31 / 1.19)^2 = 187$.

Measurement of the distance between the anterior and posterior edges of the fibula during surgery

Since the fibula has a posterior arch at the lower end, we rotated the ankle joint 15° inward on the standard lateral position to obtain an overlapping image of the distal posterior edge of the fibula and the posterior edge of the tibia. Then, we measured the distance between the anterior and posterior edges of the most prominent tibia of the ankle joint and the anterior and posterior edges of the fibula on the image obtained at that position.

After the tibiofibular syndesmosis reduction, a CT scan measured the distance between the anterior and posterior edges of the fibula at 2 positions, the standard lateral position and a lateral internal rotation of 15°. The CT scans were obtained with the use of an SCT-7000TS CT scanner (Shimadzu Corp., Kyoto, Japan). Figure 1 depicts typical examples of the images captured.

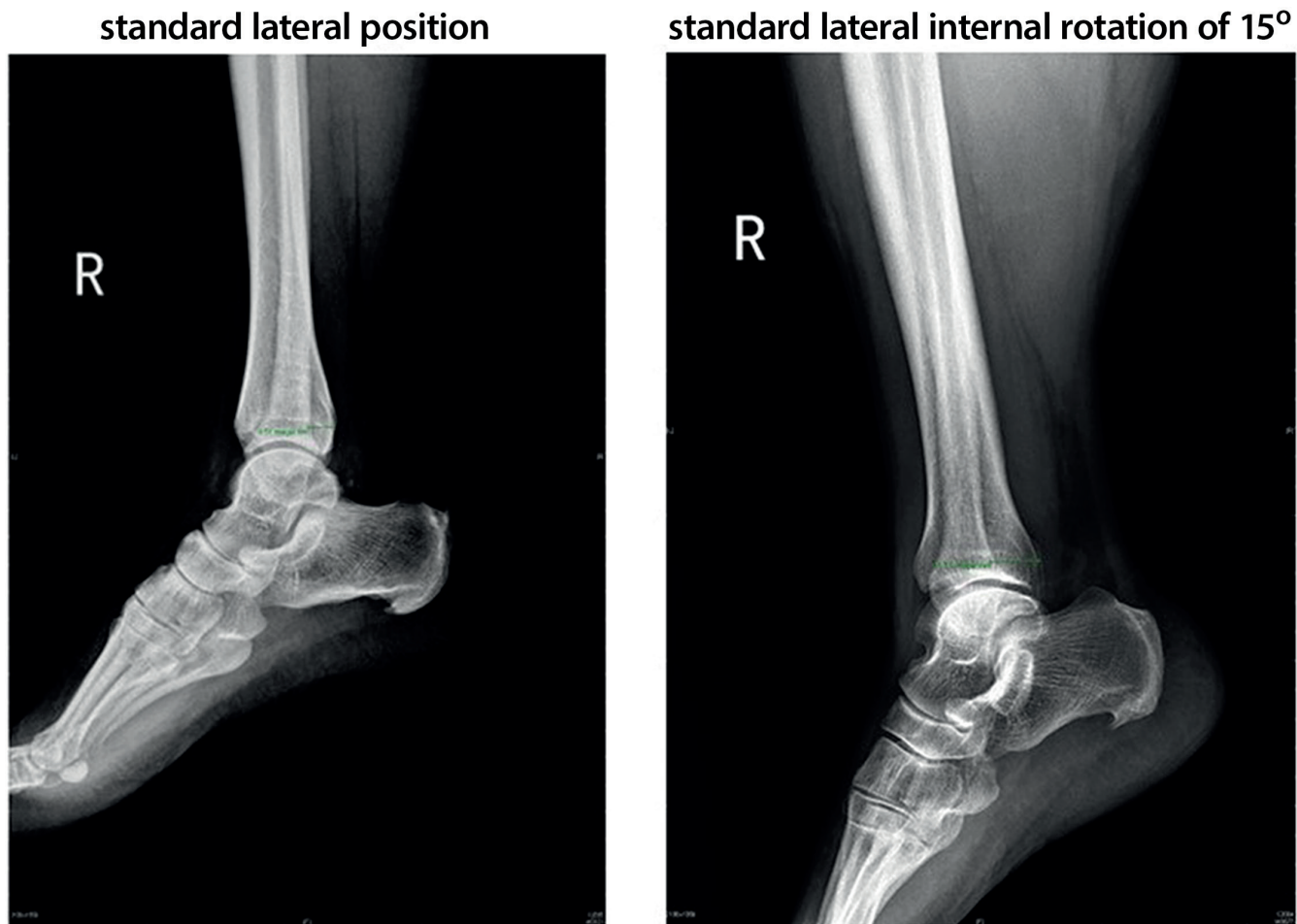


Fig. 1. Typical examples of images showing the distance between the anterior and posterior edges of the fibula at the standard lateral position (a 32-year-old female, on the left) and with a lateral internal rotation of 15° (a 53-year-old female, on the right)

Measurement of postoperative recovery

Demographic data and basic clinical characteristics were recorded for all patients, including age, sex, body mass index (BMI), cause of fracture, Lauge–Hansen type, and reduction methods. The modified Mazur score and American Orthopaedic Foot and Ankle Society (AOFAS) score evaluated the ankle function before and 6 months after the surgery. The duration of hospitalization and fracture healing time were also recorded. Postoperative complications during the follow-up were noted, and a CT scan confirmed the malreduction after surgery.

Statistical analyses

Normally distributed data were expressed as mean \pm standard deviation ($M \pm SD$), and non-normally distributed data were presented as median (range and interquartile range (IQR)). The Kolmogorov–Smirnov method was used to analyze data distribution. Intergroup comparisons were performed with Student’s *t*-test or Mann–Whitney *U* test for normally or non-normally distributed data, respectively. The *t*-test employing Levene’s method was used to assess the homogeneity of variance. The χ^2 test was utilized

to compare rates, while the relationship between variables was evaluated with Spearman’s correlation analysis. A receiver operating characteristic (ROC) curve allowed for assessing the diagnostic value, and the logistic regression analysis was used to evaluate the malreduction risk factor. The Box–Tidwell test was employed to measure continuous data linear relationships, with the variance inflation factor (VIF) assessing multicollinearity. Detailed statistical data are listed in the Supplementary materials. Statistical significance was indicated by $p < 0.05$. All calculations employed IBM Statistical Package for Social Sciences (SPSS) v. 22.0 (IBM Corp., Armonk, USA) and GraphPad Prism v. 6.0 (GraphPad Software Inc., San Diego, USA).

Results

Comparison of clinical characteristics between malreduction and non-malreduction patients

Table 1 lists the clinical outcomes for all patients and the comparisons between malreduction and non-malreduction patients. Malreduction was found in 68 cases

Table 1. Basic clinical characteristics between malreduction and non-malreduction patients

Variables		All patients (n = 187)	Malreduction (n = 68)	Non-malreduction (n = 119)	t/Z/ χ^2	p-value*
Age [years]		40.36 ±12.00	41.63 ±11.28	39.64 ±12.38	1.094	0.275
Female sex, n (%)		80 (42.78)	29 (42.65)	51 (42.86)	0.001	0.976
BMI [kg/m ²]		26.37 (18.05–34.97, 8.41)	27.53 (18.11–34.36, 7.60)	26.16 (18.05–34.97, 8.82)	−0.667	0.505
Cause of fracture, n (%)	traffic accident	118 (63.10)	45 (66.18)	73 (61.34)	0.507	0.476
	full	69 (36.90)	23 (33.82)	46 (38.66)		
Lauge–Hansen type, n (%)	supination external rotation	62 (33.16)	23 (33.82)	39 (32.77)	0.434	0.933
	supination adduction	33 (17.65)	12 (17.65)	21 (17.65)		
	pronation external rotation	52 (27.81)	20 (29.41)	32 (26.89)		
	pronation abduction	40 (21.39)	13 (19.12)	27 (22.69)		
Reduction methods, n (%)	tibiofibular screw	102 (54.55)	39 (57.35)	63 (52.94)	0.393	0.531
	button fixation	85 (45.45)	29 (42.65)	56 (47.06)		
Mazur score	before surgery	46.00 (30.00–60.00, 15.00)	48.50 (31.00–60.00, 14.75)	45.00 (30.00–60.00, 15.00)	−1.636	0.102
	6 months after surgery	79.00 (61.00–98.00, 15.00)	74.50 (61.00–88.00, 11.75)	84.00 (70.00–98.00, 16.00)	−6.174	<0.001
AOFAS score	before surgery	42.00 (25.00–59.00, 17.00)	42.50 (26.00–59.00, 16.50)	42.00 (25.00–59.00, 18.00)	−0.429	0.668
	6 months after surgery	82.00 (65.00–97.00, 11.00)	75.00 (65.00–88.00, 10.75)	86.00 (75.00–97.00, 10.00)	−7.906	<0.001
	hospitalization [days]	11.00 (7.00–15.00, 3.00)	13.00 (10.00–15.00, 2.00)	9.00 (7.00–12.00, 3.00)	−9.851	<0.001
	fracture healing [days]	57.00 (50.00–70.00, 6.00)	60.00 (50.00–70.00, 9.00)	56.00 (50.00–60.00, 5.00)	−5.347	<0.001
Postoperative complications, n (%)	infection	17 (9.09)	7 (10.29)	10 (8.40)	0.438	0.803
	pain	8 (4.28)	3 (4.41)	5 (4.20)		
	exclusive granuloma	4 (2.14)	1 (1.47)	3 (2.52)		

*p-values were calculated for comparison between malreduction and non-malreduction patients. Normally distributed data (only age) were compared using the Student's t-test. Non-normally distributed data were analyzed using the Mann–Whitney U test. Rates were compared using the χ^2 test. The measurement data were expressed as mean ± standard deviation (M ± SD) for normally distributed data or median (interquartile range (IQR), distance) for non-normally distributed data. AOFAS – American Orthopaedic Foot and Ankle Society; BMI – body mass index.

(36.36%). No significant differences were found for demographic data and basic clinical characteristics, including age, sex, BMI, cause of fracture, Lauge–Hansen type, and reduction methods, as well as Mazur and AOFAS scores before the surgery. However, both Mazur and AOFAS scores significantly increased in non-malreduction patients compared with the malreduction patients 6 months after surgery ($p < 0.001$). In addition, hospitalization length and fracture healing time were substantially longer in malreduction patients than in non-malreduction patients ($p < 0.001$). No significant difference was found for other postoperative complications.

Comparison of the distance between the anterior and posterior edges of the fibula between malreduction and non-malreduction patients

Investigations focused on comparing the distance between the anterior and posterior edges of the fibula

between malreduction and non-malreduction patients. As shown in Fig. 2A,B, the mean distance between the anterior and posterior edges of the fibula was significantly longer in malreduction patients than in non-malreduction patients at the standard lateral position and at a lateral internal rotation of 15° ($p < 0.05$).

The relationship between postoperative recovery and the distance between the anterior and posterior edges

To further investigate the clinical significance of the distance between the anterior and posterior edges, Spearman's correlation analysis evaluated the relationship between anterior and posterior edge distance and postoperative recovery indices. Findings demonstrated that the distance between the anterior and posterior edges correlated negatively with the postoperative Mazur and AOFAS scores when using a lateral internal rotation of 15°, and correlated positively with hospitalization and fracture healing

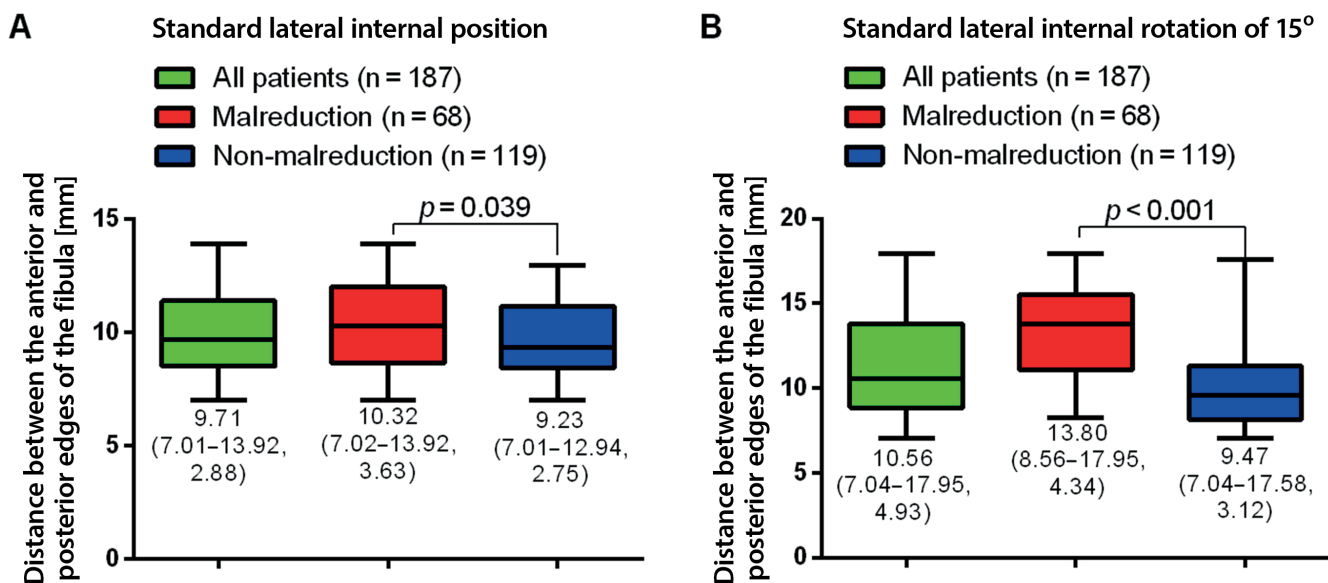


Fig. 2. The distance between the anterior and posterior edges of the fibula between malreduction and non-malreduction patients at the standard lateral position (A) and with a lateral internal rotation of 15° (B). Comparison between the malreduction and non-malreduction groups was evaluated using the Mann–Whitney U test. Data are depicted as median with interquartile range (IQR) and distance

Table 2. Spearman’s analysis for correlation between postoperative recovery and distance between the anterior and posterior edges

Variables		Spearman’s correlation	p-value
Standard lateral position	postoperative Mazur score	−0.104	0.158
	postoperative AOFAS score	−0.170	0.020
	hospitalization	0.139	0.057
	fracture healing	0.018	0.806
Standard lateral internal rotation of 15°	postoperative Mazur score	−0.208	0.004
	postoperative AOFAS score	−0.277	<0.001
	hospitalization	0.378	<0.001
	fracture healing	0.238	0.001

AOFAS – American Orthopaedic Foot and Ankle Society.

duration (Table 2). However, a negative correlation was found between the anterior and posterior edge distances and postoperative AOFAS score for the standard lateral position. These results indicated that more extensive anterior and posterior edge distances were associated with poor postoperative recovery, especially for the 15° lateral internal rotation position.

The diagnostic potential of the distance between the anterior and posterior edge for postoperative malreduction

The ROC curves explored the diagnostic value of the distance between the anterior and posterior edges for postoperative malreduction. As shown in Fig. 3, the area under the curve (AUC) at the standard lateral position was 0.581, with a sensitivity of 60.50% (51.13–69.34%), specificity of 53.62% (41.20–65.72%), and cutoff value >10.06 mm. When using a 15° lateral internal rotation, the AUC was 0.822, with a sensitivity of 75.36%

(63.51–84.94%), specificity of 73.95% (65.11–81.56%), and cutoff value >11.18 mm. These results suggested that the distance between the anterior and posterior edges showed potential diagnostic value for postoperative malreduction, particularly for the 15° lateral internal rotation images.

Logistic regression for risk factors of postoperative malreduction

The risk factors of postoperative malreduction were investigated using univariate and multivariate logistic regression analyses. The postoperative Mazur score, postoperative AOFAS score, length of hospitalization, fracture healing duration, and the distance between the anterior and posterior edges of the fibula at the standard lateral and 15° internal rotation positions were risk factors in the univariate model. In the multivariate regression model, preoperative factors (age, sex, BMI, cause of fracture, Lauge–Hansen type, restoration methods,

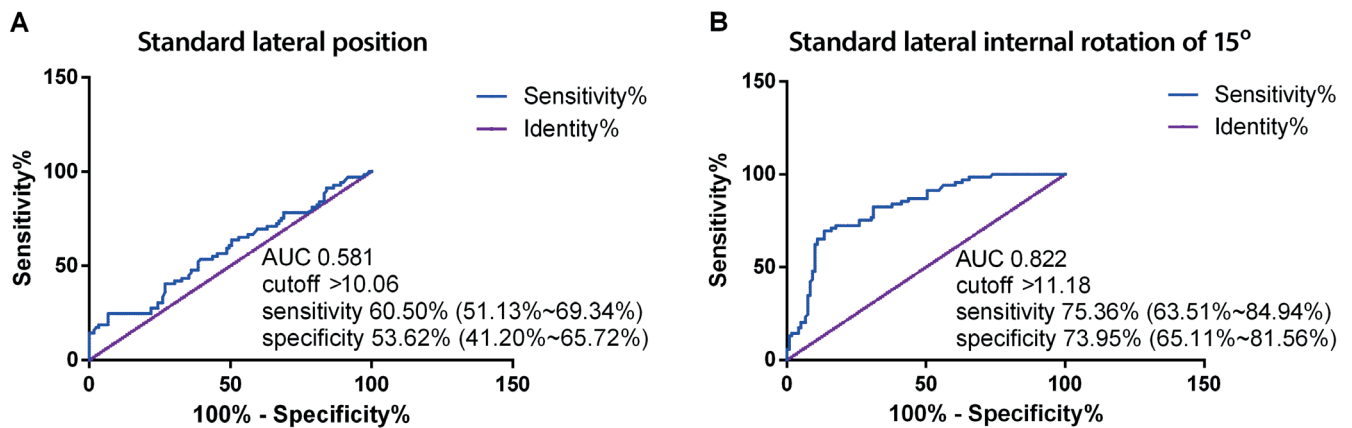


Fig. 3. Receiver operating characteristic (ROC) curves of the distance between the anterior and posterior edges of the fibula for diagnosis of postoperative malreduction using a standard lateral position (A) and a 15° lateral internal rotation (B)

AUC – area under the curve.

Table 3. Binary logistic regression analysis for risk factors of postoperative malreduction

Variables	Univariate				Multivariate			
	OR	95% CI	R ²	p-value	OR	95% CI	R ²	p-value
Age	0.986	0.962–1.011	0.009	0.274	0.989	0.961–1.011	0.037	0.269
Sex	0.991	0.543–1.811	<0.001	0.978	1.036	0.554–1.936		0.913
BMI	0.980	0.922–1.041	0.003	0.509	0.979	0.920–1.042		0.512
Cause of fracture	1.233	0.661–2.299	0.003	0.510	1.255	0.663–2.374		0.486
Lauge–Hansen type	1.044	0.806–1.352	0.001	0.746	1.084	0.831–1.413		0.552
Restoration methods	1.195	0.656–2.179	0.002	0.560	1.152	0.617–2.151		0.657
Preoperative Mazur score	0.972	0.939–1.006	0.019	0.106	0.974	0.940–1.009		0.141
Preoperative AOFAS score	0.994	0.964–1.024	0.001	0.685	0.996	0.966–1.028	0.818	
Postoperative Mazur score	1.142	1.092–1.195	0.301	<0.001	1.138	0.971–1.333	0.926	0.110
Postoperative AOFAS score	1.270	1.183–1.363	0.479	<0.001	1.345	1.109–1.633		0.003
Hospitalization	0.276	0.189–0.403	0.691	<0.001	0.236	0.114–0.490		<0.001
Fracture healing	0.790	0.726–0.858	0.284	<0.001	0.718	0.548–0.942		0.017
Postoperative complications	1.022	0.635–1.644	<0.001	0.930	0.685	0.201–2.338		0.546
Anterior and posterior edge distance 1*	0.831	0.706–0.977	0.037	0.025	1.235	0.707–2.156		0.458
Anterior and posterior edge distance 2 [#]	0.634	0.554–0.726	0.388	<0.001	0.465	0.297–0.729		0.001

*standard lateral position; [#]standard lateral internal rotation of 15°; BMI – body mass index; AOFAS – American Orthopaedic Foot and Ankle Society; OR – odds ratio; 95% CI – 95% confidence interval.

preoperative Mazur score, preoperative AOFAS score) and postoperative factors (postoperative Mazur score, postoperative AOFAS score, length of hospitalization, fracture healing duration, postoperative complications, and the distance between the anterior and posterior edges of the fibula for the diagnosis of postoperative malreduction at the standard lateral and 15° lateral internal rotation positions) were analyzed using 2 different models. Postoperative AOFAS score, length of hospitalization, fracture healing time, and the distance between the anterior and posterior edges of the fibula at the 15° internal lateral rotation position were independent risk factors of postoperative malreduction, according to the multivariate analysis (Table 3).

Discussion

In ankle joint fracture, lower tibiofibular syndesmosis injury is a common complication that, if not appropriately treated, affects ankle joint function.¹⁴ Despite many therapeutic options available for lower tibiofibular syndesmosis, postoperative complications such as infection and malreduction limit their application.¹⁷ Furthermore, traditional methods for evaluating malreduction are insufficient.¹⁸ In the present study, we proposed a novel method for evaluating malreduction by measuring the distance between the anterior and posterior edges of the fibula using a lateral internal rotation of 15°. The distance was longer in patients with postoperative malreduction, which is associated with

patient recovery of ankle joint function, and the method has a potential to predict postoperative malreduction.

Postoperative malreduction is a common complication after surgery of lower tibiofibular syndesmosis injury, with malreduction rates reportedly ranging from 15% to 50%. There is no specific effective method to reduce malreduction.¹⁴ In a randomized controlled trial, the authors reported a malreduction rate of 39% for screw fixation and 15% using TightRope fixation for reducing tibiofibular syndesmosis.¹⁹ In addition, a meta-analysis found that malreduction occurred in 12.6% of patients treated with a syndesmotom screw for distal tibiofibular syndesmosis injury.²⁰ In the present study, malreduction occurred in 36.36% (68/187) of patients.

Currently, the evaluation of postoperative malreduction relies on measuring the tibiofibular clear space and tibiofibular overlap.²¹ However, traditional methods have failed to reduce the malreduction rate to an acceptable level. In recent years, some new methods have reported reduced malreduction rates. Futamura et al. demonstrated that using intraoperative perspective mortise views, based on Weber's 3 indexes, could avoid the malreduction of syndesmosis, with an AUC of 0.857 in the diagnosis potential.²² Another study reported using the Leporjärvi clear space for lateral translation, the Nault anterior tibiofibular distance for posterior translation, and the Nault talar dome angle for external rotation of the fibula as potential measuring methods for detecting isolated malreduction in distal tibiofibular syndesmosis injury.²³ In a recent study, Bai et al. found that when the syndesmosis was fixed at an internal rotation of 20°, the tibiofibular clear space and the anteroposterior ratio could achieve a diagnostic value of 92.3% and a sensitivity of 100% for syndesmosis malreduction.²⁴

The current research proposed a novel method for measuring the distance between the anterior and posterior edges of the fibula using a lateral internal rotation of 15°. We found that the distance between the anterior and posterior edges of the fibula was associated with postoperative ankle joint function and malreduction occurrence, in which a longer distance predicted a higher rate of malreduction and worse ankle joint function.

Limitations

The present study was limited by being a single-center trial with a small sample size that only analyzed short-term efficacy after surgery. As such, the relationship between the fibular anterior and posterior edge distance and long-term surgical efficacy is unclear. These issues require further study to provide adequate evidence.

Conclusions

In summary, the distance between the anterior and posterior edges of the fibula was associated with postoperative

ankle joint function and malreduction occurrence when using a lateral internal rotation of 15°. These findings may prove a novel method for evaluating postoperative malreduction after reduction surgery in patients with an ankle joint fracture combined with a lower tibiofibular syndesmosis injury.

Supplementary data

The supplementary materials are available at <https://doi.org/10.5281/zenodo.8087392>. The package contains the following files:


Supplementary Table 1. Information on t-test from Table 1.


Supplementary Table 2. Assumptions for logistic regression from Table 3.


Supplementary Fig. 1. Normality test for continuous data.

ORCID iDs


Zhiqin Liu  <https://orcid.org/0009-0007-7233-0569>


Wentao Gao  <https://orcid.org/0009-0008-9790-2911>

Xiping Zhang  <https://orcid.org/0009-0001-4746-5038>

Weifeng Wang  <https://orcid.org/0009-0004-1758-9015>

Miduo Tan  <https://orcid.org/0009-0007-9748-5022>

Eryue Qiu  <https://orcid.org/0009-0006-3896-2346>

Anlie Cai  <https://orcid.org/0009-0007-4852-8081>

References

- Liu G, Chen L, Gong M, Xing F, Xiang Z. Clinical evidence for treatment of distal tibiofibular syndesmosis injury: A systematic review of clinical studies. *J Foot Ankle Surg.* 2019;58(6):1245–1250. doi:10.1053/j.jfas.2019.01.015
- Marasco D, Russo J, Izzo A, et al. Static versus dynamic fixation of distal tibiofibular syndesmosis: A systematic review of overlapping meta-analyses. *Knee Surg Sports Traumatol Arthrosc.* 2021;29(11):3534–3542. doi:10.1007/s00167-021-06721-6
- Kubik JF, Rollick NC, Bear J, et al. Assessment of malreduction standards for the syndesmosis in bilateral CT scans of uninjured ankles. *Bone Joint J.* 2021;103-B(1):178–183. doi:10.1302/0301-620X.103B1.BJJ-2020-0844.R1
- Fan X, Zheng P, Zhang Y, Hou Z. Dynamic fixation versus static fixation in treatment effectiveness and safety for distal tibiofibular syndesmosis injuries: A systematic review and meta-analysis. *Orthop Surg.* 2019;11(6):923–931. doi:10.1111/os.12523
- Cherney SM, Spraggs-Hughes AG, McAndrew CM, Ricci WM, Gardner MJ. Incisura morphology as a risk factor for syndesmotom malreduction. *Foot Ankle Int.* 2016;37(7):748–754. doi:10.1177/1071100716637709
- van den Heuvel SB, Dingemans SA, Gardenbroek TJ, Schepers T. Assessing quality of syndesmotom reduction in surgically treated acute syndesmotom injuries: A systematic review. *J Foot Ankle Surg.* 2019;58(1):144–150. doi:10.1053/j.jfas.2018.08.038
- Xu Y, Kang R, Li M, et al. The clinical efficacy of suture-button fixation and trans-syndesmotom screw fixation in the treatment of ankle fracture combined with distal tibiofibular syndesmosis injury: A retrospective study. *J Foot Ankle Surg.* 2022;61(1):143–148. doi:10.1053/j.jfas.2021.07.009
- Gifford PB, Lutz M. The tibiofibular line: An anatomical feature to diagnose syndesmosis malposition. *Foot Ankle Int.* 2014;35(11):1181–1186. doi:10.1177/1071100714546187
- Dikos GD, Heisler J, Choplin RH, Weber TG. Normal tibiofibular relationships at the syndesmosis on axial CT imaging. *J Orthop Trauma.* 2012;26(7):433–438. doi:10.1097/BOT.0b013e3182535f30
- Marmor M, Hansen E, Han HK, Buckley J, Matiyahu A. Limitations of standard fluoroscopy in detecting rotational malreduction of the syndesmosis in an ankle fracture model. *Foot Ankle Int.* 2011;32(6):616–622. doi:10.3113/FAI.2011.0616

11. Lucas DE, Watson BC, Simpson GA, Berlet GC, Hyer CF. Arthroscopic evaluation of syndesmotric instability and malreduction. *Foot Ankle Spec.* 2016;9(6):500–505. doi:10.1177/1938640016666913
12. Gardner MJ, Demetrakopoulos D, Briggs SM, Helfet DL, Lorch DG. Malreduction of the tibiofibular syndesmosis in ankle fractures. *Foot Ankle Int.* 2006;27(10):788–792. doi:10.1177/107110070602701005
13. Franke J, von Recum J, Suda AJ, Grützner PA, Wendl K. Intraoperative three-dimensional imaging in the treatment of acute unstable syndesmotric injuries. *J Bone Joint Surg Am.* 2012;94(15):1386–1390. doi:10.2106/JBJS.K.01122
14. Stenquist DS, Kwon JY. Strategies to avoid syndesmosis malreduction in ankle fractures. *Foot Ankle Clin.* 2020;25(4):613–630. doi:10.1016/j.fcl.2020.08.001
15. Song L, Liao Z, Kuang Z, et al. Comparison of tendon suture fixation and cortical screw fixation for treatment of distal tibiofibular syndesmosis injury: A case-control study. *Medicine (Baltimore).* 2020;99(34):e21573. doi:10.1097/MD.00000000000021573
16. Kurtoglu A, Kochai A, Inanmaz ME, et al. A comparison of double single suture-button fixation, suture-button fixation, and screw fixation for ankle syndesmosis injury: A retrospective cohort study. *Medicine (Baltimore).* 2021;100(13):e25328. doi:10.1097/MD.00000000000025328
17. Bai L, Zhang W, Guan S, Liu J, Chen P. Syndesmotric malreduction may decrease fixation stability: A biomechanical study. *J Orthop Surg Res.* 2020;15(1):64. doi:10.1186/s13018-020-01584-y
18. Ntalos D, Rupprecht M, Grossterlinden LG, et al. Incidence and severity of malreduction of the tibiofibular syndesmosis following surgical treatment of displaced ankle fractures and impact on the function: Clinical study and MRI evaluation. *Injury.* 2018;49(6):1220–1227. doi:10.1016/j.injury.2018.04.027
19. Sanders D, Schneider P, Taylor M, Tieszer C, Lawendy AR. Improved reduction of the tibiofibular syndesmosis with TightRope compared with screw fixation: Results of a randomized controlled study. *J Orthop Trauma.* 2019;33(11):531–537. doi:10.1097/BOT.0000000000001559
20. Zhang P, Liang Y, He J, Fang Y, Chen P, Wang J. A systematic review of suture-button versus syndesmotric screw in the treatment of distal tibiofibular syndesmosis injury. *BMC Musculoskelet Disord.* 2017;18(1):286. doi:10.1186/s12891-017-1645-7
21. Fort NM, Aiyer AA, Kaplan JR, Smyth NA, Kadakia AR. Management of acute injuries of the tibiofibular syndesmosis. *Eur J Orthop Surg Traumatol.* 2017;27(4):449–459. doi:10.1007/s00590-017-1956-2
22. Futamura K, Baba T, Mogami A, et al. Malreduction of syndesmosis injury associated with malleolar ankle fracture can be avoided using Weber's three indexes in the mortise view. *Injury.* 2017;48(4):954–959. doi:10.1016/j.injury.2017.02.004
23. Schon JM, Brady AW, Krob JJ, et al. Defining the three most responsive and specific CT measurements of ankle syndesmotric malreduction. *Knee Surg Sports Traumatol Arthrosc.* 2019;27(9):2863–2876. doi:10.1007/s00167-019-05457-8
24. Bai L, Zhou W, Cheng Z, Liu J, Liu P, Zhang W. A radiological study for assessing syndesmosis malreduction: Its validity and limitation. *J Foot Ankle Surg.* 2020;59(6):1181–1185. doi:10.1053/j.jfas.2020.04.014

Preoperative prognostic nutritional index associated with anastomotic leakage in colorectal cancer patients after surgery

Haotang Wei^{1,A–C}, Jialei Wang^{1,B–D}, Zhengkai Jiang^{1,E,F}, Yu Liu^{1,B–D}, Sheng Jiang^{1,B,C}, Bangli Hu^{2,A,D}

¹ Department of Gastrointestinal Surgery, Third Affiliated Hospital of Guangxi Medical University, Nanning, China

² Department of Research, Guangxi Medical University Cancer Hospital, Nanning, China

A – research concept and design; B – collection and/or assembly of data; C – data analysis and interpretation; D – writing the article; E – critical revision of the article; F – final approval of the article

Advances in Clinical and Experimental Medicine, ISSN 1899–5276 (print), ISSN 2451–2680 (online)

Adv Clin Exp Med. 2024;33(4):351–359

Address for correspondence

Bangli Hu

E-mail: hubangli@gxmu.edu.cn

Funding sources

The study was funded by National Natural Science Foundation of China (grant No. 82160446); Scientific Research Project of Guangxi Health Commission (grant No. Z20190717).

Conflict of interest

None declared

Received on February 21, 2023

Reviewed on July 1, 2023

Accepted on July 11, 2023

Published online on August 4, 2023

Abstract

Background. Anastomotic leakage (AL) is a severe complication of colorectal cancer (CRC) surgery and is associated with the immune and nutritional status.

Objectives. This study aimed to investigate the role of the prognostic nutritional index (PNI) in AL in CRC patients after surgery.

Materials and methods. A retrospective case–control study was designed in a single center. The clinicopathological features and preoperative laboratory data of 124 CRC patients and 120 non-cancer patients who underwent surgery were collected and examined. Among the CRC patients, 24 had AL.

Results. Nutritional indicators were lower in CRC patients than in non-cancer patients ($p < 0.05$), but the clinical parameters analysis showed that only metastasis (M) stage, albumin, carcinoembryonic antigen (CEA), CA153, and PNI were associated with AL in CRC after surgery ($p < 0.05$). Prognostic nutritional index had a moderate predictive value for AL, with an area under the curve (AUC) of 0.625. Using the median value as a cutoff point, a high PNI was associated with a longer survival time in CRC patients ($p = 0.033$), and AL showed marginal significance ($p = 0.048$). The nomogram showed that PNI has a better prognostic value than tumor–node–metastasis (TNM) staging in CRC patients who underwent surgery.

Conclusions. Prognostic nutritional index is a useful supplement for predicting AL in CRC patients after colorectal surgery. It also helps predict the prognosis of CRC patients.

Key words: colorectal cancer, anastomotic leakage, prognostic nutritional index

Cite as

Wei H, Wang J, Jiang Z, Liu Y, Jiang S, Hu B. Preoperative prognostic nutritional index associated with anastomotic leakage of colorectal cancer patients after surgery.

Adv Clin Exp Med. 2024;33(4):351–359.

doi:10.17219/acem/169495

DOI

10.17219/acem/169495

Copyright

Copyright by Author(s)

This is an article distributed under the terms of the Creative Commons Attribution 3.0 Unported (CC BY 3.0) (<https://creativecommons.org/licenses/by/3.0/>)

Background

Surgery is a major treatment approach for colorectal cancer (CRC), and anastomotic leakage (AL) is one of the most severe early complications of colorectal surgery, with an incidence rate of 1–30%, depending on the site of anastomosis (rectum > colon).¹ Anastomotic leakage causes abdominal infections, sepsis and prolonged hospital stays, and is associated with a high reoperation rate, increased short- and long-term morbidity and mortality rates,^{2,3} as well as reduced quality of life. Thus, identifying the risk factors associated with AL after colorectal surgery remains a critical need for doctors.⁴

The exact etiology of AL remains unclear. Current evidence indicates that AL is a result of multiple factors, including operation time,⁵ steroidal anti-inflammatory drug use⁶ and surgical experience.⁷ In addition, nutritional status,⁸ inflammation status⁹ and immune system status¹⁰ contribute to the occurrence of AL after colorectal surgery. Several indicators, such as the neutrophil-to-lymphocyte ratio (NLR), platelet-to-lymphocyte ratio (PLR) and lymphocyte-to-monocyte ratio (LMR), have reportedly been associated with AL.¹¹ In addition, some novel indicators, including the systemic immune-inflammation index (SII),¹² prognostic nutritional index (PNI), pan-immune-inflammation value (PIV),¹³ as well as systemic inflammation response index (SIRI),¹⁴ have been reported to be associated with the survival of various cancers.

Given that AL is associated with nutrition, inflammation and immune status, finding indicators that can be incorporated into routine blood examination to predict AL in CRC patients after colorectal surgery can help prevent the occurrence of AL, thus improving treatment efficacy.

Objectives

This study aimed to determine the association of NLR, LMR, PLR, PNI, SII, PIV, SIRI, and PNI with AL in CRC patients after colorectal surgery to identify reliable indicators that predict AL, and explore their association with the survival of CRC patients.

Materials and methods

Data collection

This study has a case–control design. The data were retrospectively collected from CRC patients who underwent surgery between March 2013 and July 2022 at Third Affiliated Hospital of Guangxi Medical University (Nanning, China). The inclusion criteria were as follows: 1) histopathologically validated CRC diagnosis; 2) surgical resection of the primary CRC tumor; and 3) complete clinicopathological and postoperative follow-up data.

The exclusion criteria included 1) complications with other primary tumors; 2) complications with severe autoimmune diseases, infectious diseases, blood diseases, or injury; and 3) complications with severe liver or kidney malfunction. We also collected data from 120 non-cancer control patients who underwent abdominal surgery.

Clinical data collection and definitions

Clinicopathological features and preoperative laboratory data were collected from the patient's electronic medical records, and laboratory data used were collected within 3 days of surgery. As part of the clinicopathological analysis of CRC, data on patient's age, sex, body mass index (BMI), tumor–node–metastasis (TNM) stage, routine blood tests, liver function tests, and tumor biomarkers were collected. A summary of the surgical information included data on the surgical approach (laparoscopic or open), the operation time and the volume of bleeding that occurred during the surgery. The NLR, LMR, PLR, PNI, SII, PIV, SIRI, and PNI were calculated as previously described.^{14–17} Anastomotic leakage was defined based on the statement of the International Study Group of Rectal Cancer,¹⁸ in which the integrity of the intestinal wall fails at the anastomosis site, and the communication between the intraintestinal and extraintestinal compartments is established.

Follow-up

The follow-up for patients with CRC after surgery was performed every 3 months for the first 2 years, followed by a 6-month follow-up frequency for the next 2 years. The last follow-up date was July 12, 2022. In this study, overall survival (OS) was defined as the number of years between the date of surgery and the date of death or last follow-up of the patient.

Statistical analyses

The distribution of data was tested using the Shapiro–Wilk test, with a p-value <0.05 indicating a normal distribution. The results are listed in Supplementary Table 1. Student's t-tests with Welch's correction were used to compare normally distributed continuous data. Median and interquartile range (IQR) as well as the Mann–Whitney U test were used to compare data that were non-normally distributed. Data from categorical variables are presented as absolute numbers (percentages) and compared using the χ^2 test or Fisher's exact test if the sample size was small (when the expected frequency count in any cell of the table was less than 5). The survival analysis was conducted using the Kaplan–Meier plots and log-rank tests. The predictive advantage was distinguished using the receiver operating characteristic (ROC) and area under the curve (AUC). A value of p < 0.05 was considered statistically significant.

Table 1. Clinical characteristics of the included participants

Clinical variables		CRC (n = 124)	Non-cancer (n = 120)	$\chi^2/t/Z$ -value	p-value
Gender	male	61 (49.2%)	64 (53.3%)	–	–
	female	63 (50.8%)	56 (46.7%)	–	–
Age		63.5 ±13.3	61.4 ±8.45	1.4617	0.145*
BMI		22.1 (19.7–24.7)	22.8 (20.4–24.8)	4684.5	0.328
WBC		6.80 (5.80–8.43)	6.70 (5.50–8.03)	6871	0.302
Hemoglobin		116 (99.8–130)	138 (122–148)	10886	<0.001
Platelet		288 (224–361)	244 (222–279)	5536	0.001
Neutrophil		4.29 (3.29–5.87)	3.53 (2.79–4.70)	5709.5	0.002
Lymphocyte		1.58 (1.06–1.90)	2.01 (1.59–2.45)	10323	<0.001
Monocyte		0.55 (0.43–0.80)	0.60 (0.50–0.75)	7966.5	0.339
Fibrinogen		4.09 (3.45–4.69)	2.95 (2.58–3.40)	2732.5	<0.001
Albumin		36.7 ±4.26	40.5 ±3.80	7.433	<0.001*
Globulin		27.0 (24.9–29.9)	26.0 (23.8–28.2)	6097	0.015
AGR		1.36 (1.21–1.48)	1.52 (1.41–1.74)	10963.5	<0.001
Total protein		63.6 (60.1–68.3)	66.9 (62.9–69.8)	9216	0.001
Prealbumin		182 ±52.5	255 ±62.3	9.860	<0.001*
Ferritin		120 (34.2–258)	171 (69.1–295)	8653.5	0.028
CEA		4.60 (2.29–13.7)	1.75 (1.10–2.82)	3149.5	<0.001
AFP		2.40 (1.80–3.10)	2.25 (1.70–3.00)	6975	0.399
CA125		10.3 (7.50–19.0)	8.62 (6.82–12.6)	5805.5	0.003
CA153		10.4 (6.84–16.2)	10.2 (7.20–14.6)	6910	0.456
CA199		11.9 (6.85–24.8)	8.60 (4.62–12.7)	5561	0.001
PLR		184 (130–270)	126 (95.4–162)	4094	<0.001
NLR		3.02 (1.76–4.71)	1.69 (1.32–2.42)	4632	<0.001
LMR		2.53 (1.82–3.65)	3.32 (2.48–4.35)	9192	0.001
SII		1672 (1098–3001)	1717 (1086–2826)	7252	0.733
PIV		997 (540–2122)	1021 (589–2210)	7767	0.553
SIRI		1.54 (0.94–3.27)	1.05 (0.73–1.96)	5680	0.001
PNI		43.8 (41.5–47.3)	51.5 (47.2–54.3)	11961.5	<0.001

CRC – colorectal cancer; BMI – body mass index; CEA – carcinoembryonic antigen; WBC – white blood cells; NLR – neutrophil-to-lymphocyte ratio; LMR – lymphocyte-to-monocyte ratio; PLR – platelet-to-lymphocyte ratio; SII – systemic immune-inflammation index; PNI – prognostic nutritional index; PIV – pan-immune-inflammation value; SIRI – systemic inflammation response index; * data were compared using Student's t-test; # data were compared using the χ^2 test; the other parameters were compared using the Mann–Whitney U test. AGR – albumin-to-globulin ratio.

All studies were performed with the use of R language (v. 4.1.3; R Foundation for Statistical Computing, Vienna, Austria).

Results

Clinical characteristics of the included participants

A total of 124 CRC patients and 120 non-cancer patients who underwent abdominal surgery were included in the study. Adenocarcinoma was the histological type of all CRCs. The results of variance homogeneity t-tests for patients with and without CRC are listed

in Supplementary Table 2. A comparison of clinicopathological and preoperative laboratory data between CRC and non-cancer patients is listed in Table 1. Age, gender and BMI of CRC patients showed little significance between cancer and non-cancer patients ($p > 0.05$). Blood nutritional indicators, including hemoglobin, albumin, globulin, total protein, and prealbumin levels, were lower in CRC patients than in non-cancer patients ($p < 0.05$). The levels of tumor biomarkers, including carcinoembryonic antigen (CEA), CA125 and CA199, were significantly higher in CRC patients than in non-cancer patients. Other blood indicators, including PLR, NLR, albumin-to-globulin ratio (AGR), and PNI, were substantially elevated in CRC patients compared to non-cancer patients ($p < 0.05$).

Patients who exhibited risk factors related to AL underwent surgeries for CRC

The results of the variance homogeneity t-tests between patients with and without AL are presented in Supplementary

Table 3. As listed in Table 2, M0 stage and laparoscopic surgery were associated with AL in patients who underwent surgeries for CRC. Patients complicated with AL exhibited low levels of albumin, CEA, CA153, and PNI as compared to patients without AL ($p < 0.05$). Age, sex, tumor type,

Table 2. Risk factors related to anastomotic leakage (AL) for patients who underwent colorectal cancer (CRC) surgery

Clinical variables		Non-AL (n = 100)	AL (n = 24)	$\chi^2/t/Z$ -value	p-value
Sex	male	53 (53.0%)	8 (33.3%)	2.260	0.133 [#]
	female	47 (47.0%)	16 (66.7%)		
Age		64.7 ± 12.9	58.5 ± 13.7	2.031	0.050*
Cancer type	colon cancer	67 (67.0%)	11 (45.8%)	2.864	0.091 [#]
	rectal cancer	33 (33.0%)	13 (54.2%)		
Tumor location	right side	31 (31.0%)	3 (12.5%)	4.508	0.105 [#]
	left side	35 (35.0%)	8 (33.3%)		
	rectal	34 (34.0%)	13 (54.2%)		
Tumor grade	high	8 (8%)	3 (12.5%)	0.790	0.674 [#]
	middle	79 (79%)	19 (79.2%)		
	low	13 (13%)	2 (8.3%)		
Surgery type	laparoscope	77 (77.0%)	13 (54.2%)	3.988	0.046 [#]
	open	23 (23.0%)	11 (45.8%)		
Operation time		180 (159–235)	235 (175–286)	911.5	0.068
Intraoperative bleeding		50.0 (20.0–100)	50.0 (20.0–200)	954.0	0.113
T stage	T1	3 (3.00%)	0 (0.00%)	3.341	0.359 [#]
	T2	12 (12.0%)	4 (16.7%)		
	T3	31 (31.0%)	11 (45.8%)		
	T4	54 (54.0%)	9 (37.5%)		
N stage	N0	45 (45.0%)	12 (50.0%)	0.947	0.977 [#]
	N1	32 (32.0%)	8 (33.3%)		
	N2	20 (20.0%)	4 (16.7%)		
	NX	3 (3.00%)	0 (0.00%)		
M stage	M0	68 (68.0%)	22 (91.7%)	6.117	0.038 [#]
	M1	16 (16.0%)	2 (8.33%)		
	MX	16 (16.0%)	0 (0.00%)		
Tumor stage	I	13 (13.0%)	2 (8.33%)	2.356	0.607 [#]
	II	30 (30.0%)	11 (45.8%)		
	III	44 (44.0%)	9 (37.5%)		
	IV	13 (13.0%)	2 (8.33%)		
BMI		21.8 (19.6–24.0)	24.4 (20.6–26.4)	1579.5	0.057
WBC		7.10 (5.97–8.53)	6.10 (5.02–6.85)	1243.5	0.016
Hemoglobin		113 ± 24.6	114 ± 32.6	0.150	0.882*
Platelet		282 (220–348)	290 (259–374)	1546	0.333
Neutrophil		4.50 (3.53–6.12)	3.34 (2.50–4.90)	1296	0.029
Lymphocyte		1.60 (1.05–1.95)	1.50 (1.24–1.80)	1402.5	0.544
Monocyte		0.57 (0.44–0.80)	0.50 (0.40–0.64)	1166.5	0.199
Fibrinogen		4.12 (3.45–4.65)	4.02 (3.50–5.17)	1570.5	0.832
Albumin		37.1 (33.9–39.7)	35.9 (33.2–37.1)	995.5	0.019
Globulin		26.7 (24.7–29.5)	28.4 (25.4–32.1)	1379.5	0.196
AGR		1.36 (1.24–1.50)	1.31 (1.16–1.45)	1072.5	0.256

Table 2. Risk factors related to anastomotic leakage (AL) for patients who underwent colorectal cancer (CRC) surgery – cont

Clinical variables	Non-AL (n = 100)	AL (n = 24)	$\chi^2/t/Z$ -value	p-value
Total protein	63.5 (60.0–68.2)	65.6 (60.2–68.6)	1328.5	0.420
Prealbumin	185 ±51.8	171 ±55.1	1.081	0.287*
Ferritin	144 (35.6–277)	70.6 (16.9–193)	1316	0.124
CEA	4.93 (2.30–12.3)	3.40 (2.00–16.7)	1496.5	0.463
AFP	2.50 (1.83–3.11)	2.01 (1.58–2.52)	1269	0.061
CA125	10.8 (7.59–18.7)	9.13 (6.91–27.8)	1551	0.663
CA153	11.4 (7.28–17.0)	8.36 (4.74–12.9)	1320.5	0.026
CA199	12.0 (6.92–26.6)	9.75 (6.70–15.9)	1250	0.446
PLR	179 (128–271)	198 (146–268)	1043	0.321
NLR	3.12 (1.79–4.53)	2.03 (1.58–4.74)	1356	0.324
LMR	2.46 (1.61–3.70)	2.84 (2.31–3.60)	1077.5	0.438
SII	1944 (1121–3097)	1432 (1080–1957)	1404	0.197
PIV	1077 (546–2383)	710 (481–1058)	1446	0.120
SIRI	1.69 (0.97–3.27)	1.12 (0.76–2.07)	1463	0.096
PNI	43.9 (41.7–48.6)	41.4 (40.8–44.5)	1491	0.007

BMI – body mass index; WBC – white blood cells; CEA – carcinoembryonic antigen; NLR – neutrophil-to-lymphocyte ratio; LMR – lymphocyte-to-monocyte ratio; PLR – platelet-to-lymphocyte ratio; SII – systemic immune-inflammation index; PNI – prognostic nutritional index; PIV – pan-immune-inflammation value; SIRI – systemic inflammation response index; * data were compared using Student's t-test; # data were compared using the χ^2 test; other parameters were compared using the Mann–Whitney U test. The values in bold indicated statistically significant change.

tumor location, TNM stage, and other blood indicators were not significantly associated with AL ($p > 0.05$). Using a ROC curve analysis, we found that albumin, CA153 and PNI had a moderate predictive value for AL, with AUC values of 0.662 (95% confidence interval (95% CI): 0.55–0.76), 0.648 (95% CI: 0.52–0.78) and 0.625 (95% CI: 0.52–0.73), respectively, whereas the predictive value of CEA was low, with an AUC of 0.535 (95% CI: 0.42–0.68) (Fig. 1).

Survival analysis of the blood biomarkers and anastomotic leakage in CRC patients

Previous studies have indicated that SII,¹⁹ PIV,²⁰ SIRI,²¹ and PNI²² were associated with the survival of patients with CRC who underwent surgery. In this study, we determined the association of the 4 biomarkers and AL with the survival of patients with CRC. Using the median value as a cutoff point, we found that high PNI was associated with a longer survival time in CRC patients ($p = 0.033$), and AL was marginally associated with the survival of CRC patients ($p = 0.048$), while SII, PIV and SIRI did not show an obvious association with the patients' survival ($p > 0.05$) (Fig. 2).

Association of PNI with clinicopathological features in CRC

Next, we explored the association of PNI with clinicopathological features in CRC patients. As illustrated in Fig. 3, PNI was significantly associated with T stage ($p = 0.044$), but was not associated with sex, cancer type, N stage, M stage, and tumor stage ($p > 0.05$).

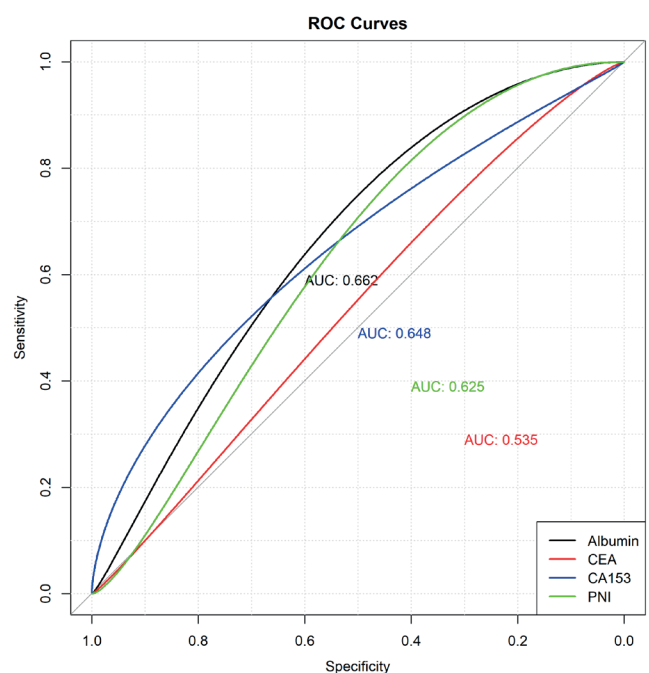


Fig. 1. Predictive value of albumin, carcinoembryonic antigen (CEA), CA153, and prognostic nutritional index (PNI) on anastomotic leakage (AL) in colorectal cancer (CRC) patients after surgery

ROC – receiver operating characteristic; AUC – area under the curve.

Comparison of the prognostic value of clinical parameters in CRC patients

To compare the prognostic value of clinical features in CRC patients who underwent surgery, the nomogram was prepared after analyzing age, TNM stage, tumor stage,

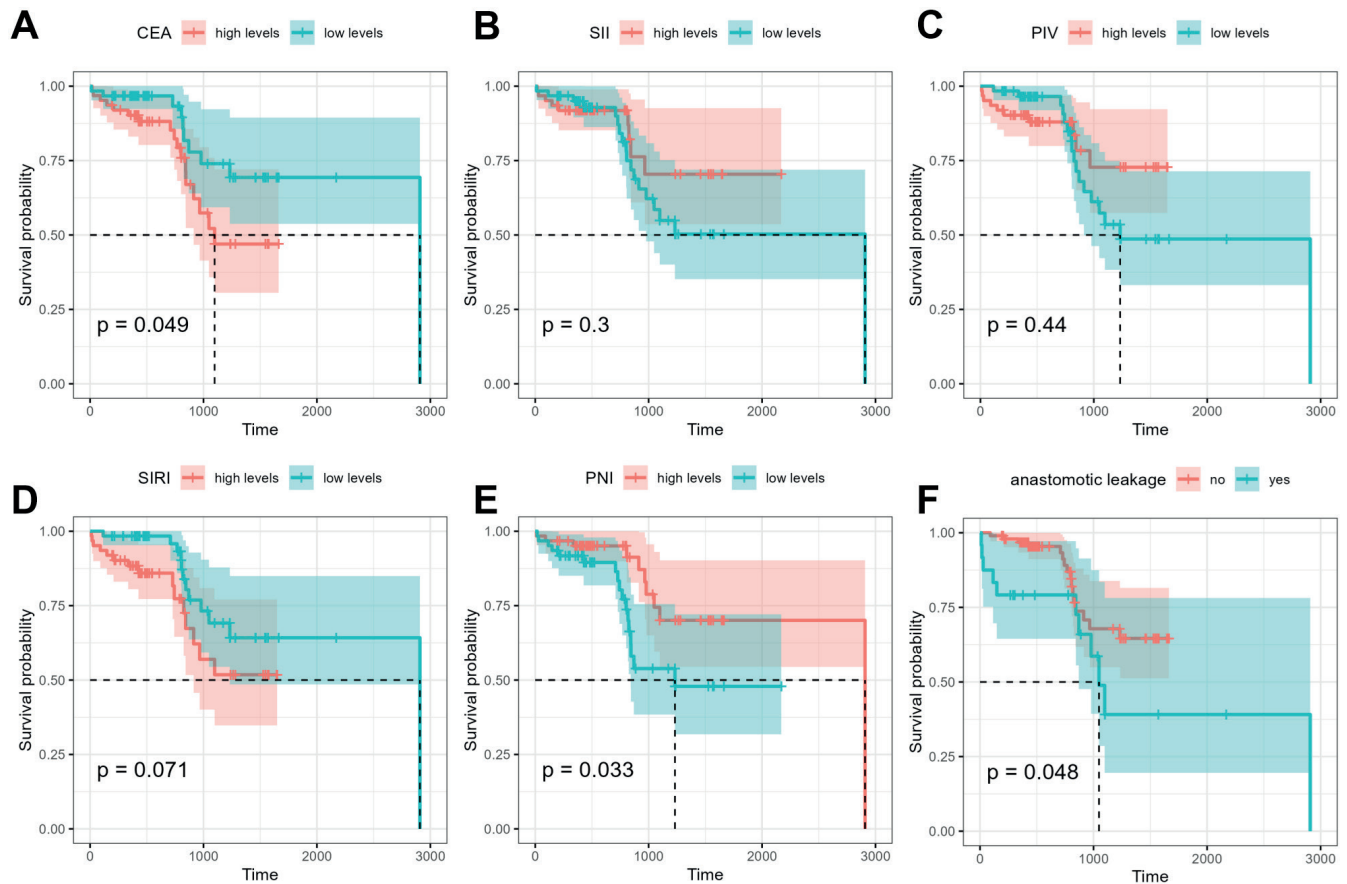


Fig. 2. Survival analysis of the blood biomarkers and anastomotic leakage (AL) in colorectal cancer (CRC) patients. A. Carcinoembryonic antigen (CEA); B. Systemic immune-inflammation index (SII); C. Pan-immune-inflammation value (PIV); D. Systemic inflammation response index (SIRI); E. Prognostic nutritional index (PNI); F. AL

AL, and PNI. As shown in Fig. 4, PNI showed a better prognostic value in CRC patients who underwent surgery for 1-, 3- and 5-year survival time as compared to other clinicopathological features such as age, TNM stage, tumor stage, and AL.

Discussion

Due to the high risk of AL in patients after colorectal surgery, this study explored the indicators that could serve as predictive biomarkers for AL. By comparing the data between CRC and non-cancer patients, we found that several blood cell count indicators were increased, while the nutritional status was decreased in CRC patients. Next, we compared the clinicopathological features of CRC patients with and without AL after colorectal surgery, and found that female sex, M stage, albumin, CEA, CA153 and PNI were associated with AL, and albumin, CA153 and PNI had a moderate predictive value for AL, suggesting that these indicators may help screen patients at high risk of AL after colorectal surgery. Subsequently, we explored the association between SII, PIV, SIRI and PNI, and found that high PNI was associated with longer survival time in CRC patients. Moreover, the nomogram showed that

PNI had a better prognostic value for 1-, 3- and 5-year survival time compared with other clinicopathological features in CRC patients who underwent surgery. Taken together, these results demonstrate that CRC patients with AL present with lower nutritional status and that PNI could help predict AL. Prognostic nutritional index was associated with the survival of CRC patients and showed a better prognostic value in CRC patients who underwent surgery.

Prognostic nutritional index is calculated based on serum albumin levels and peripheral blood lymphocyte counts, and is an indicator that reflects both the nutritional and immune status of patients.^{23,24} Our results showed that patients with AL had lower albumin levels than those without AL, although no significant difference was noted in lymphocyte counts. The role of PNI in predicting AL in gastrointestinal tumors had been reported before. A previous study²⁵ stated that preoperative PNI showed no significant prognostic value for short-term outcomes in patients with AL after cancerous esophagectomy. Another study²⁶ reported that PNI is useful for predicting the onset of postoperative complications (including AL) in patients with esophageal cancer after resection. Recently, a study²⁷ concluded that PNI was a predictor of AL (risk ratio (RR): 0.151; 95% CI: 0.036–0.640) in CRC

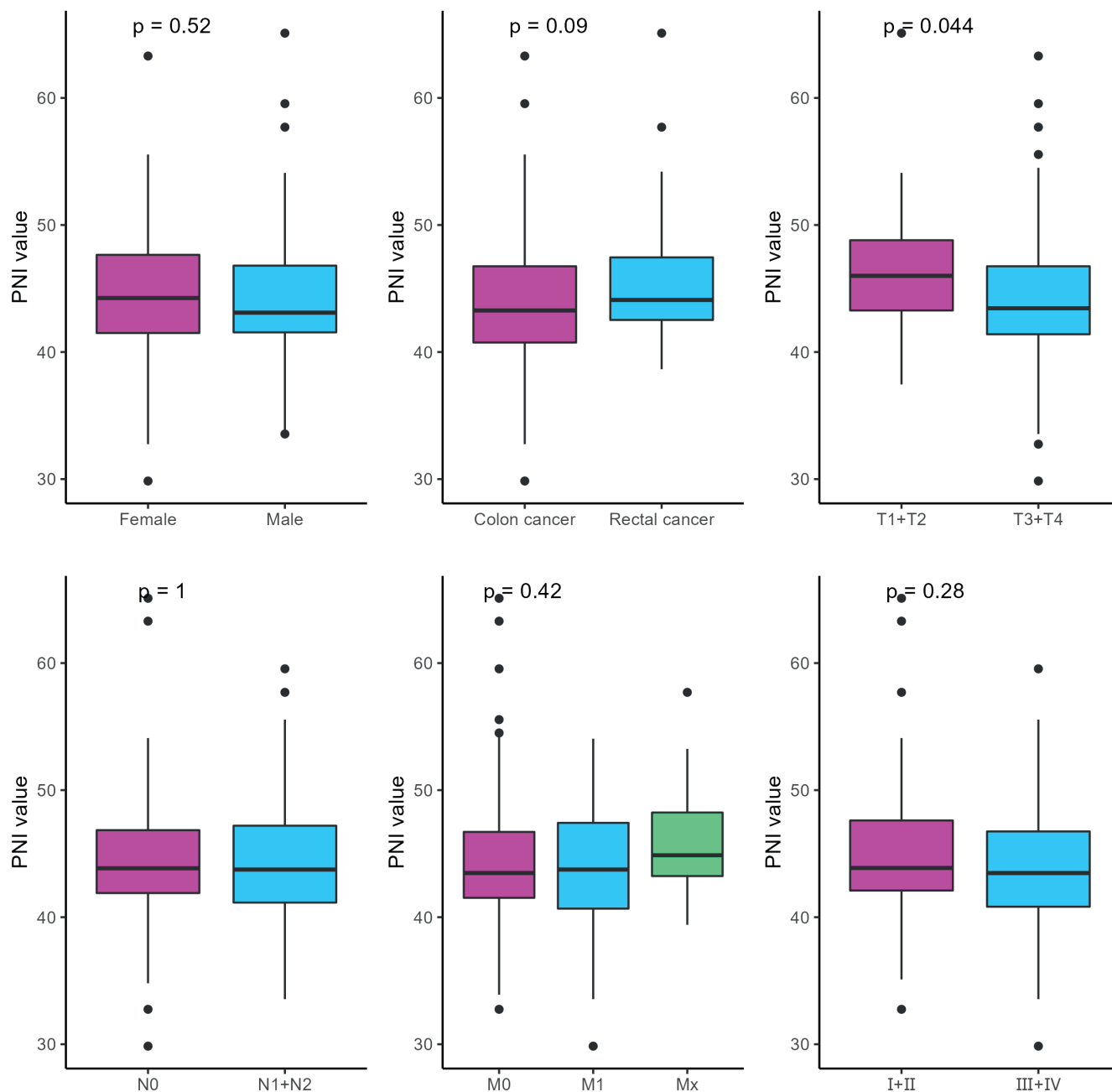


Fig. 3. Association of prognostic nutritional index (PNI) with clinicopathological features in colorectal cancer (CRC). Data were compared using the Mann–Whitney U test. The whiskers extend from the box to the minimum and maximum values of the dataset, excluding any outliers. Outliers are data points that fall more than 1.5 times of the interquartile range (IQR) beyond the nearest quartile. They are represented by individual points outside the whiskers

patients after curative surgery. In this study, we found that, similar to the result of CA153, PNI exhibited a moderate predictive value for AL, but was superior to CEA, suggesting that high PNI and CA153 could help screen patients at risk of AL, but CEA showed little significance in this aspect. However, the number was small, with only 11 patients having an AL; thus, the reliability of PNI in predicting AL needs to be further validated.

After confirming the association between PNI and AL in CRC patients after colorectal surgery, we investigated the prognostic value of PNI in CRC. Prognostic nutritional index has been reported to be associated with the treatment response and survival of various malignant tumors

such as CRC,²⁸ breast cancer¹⁷ and esophageal cancer,²⁹ suggesting that PNI could be a novel prognostic indicator for patients with cancer. Our results are in line with those of previous studies,³⁰ which confirmed the association of PNI and AL with the survival of CRC patients after colorectal surgery. More importantly, PNI-based nomograms showed better prognostic accuracy than TNM stage, tumor stage and AL, which has not been reported in previous studies, indicating that PNI could act as an auxiliary indicator to predict the prognosis of CRC patients. Moreover, the nomograms revealed that PNI showed a much better predictive accuracy; thus, it could serve as a reliable indicator to estimate the prognosis of CRC patients.

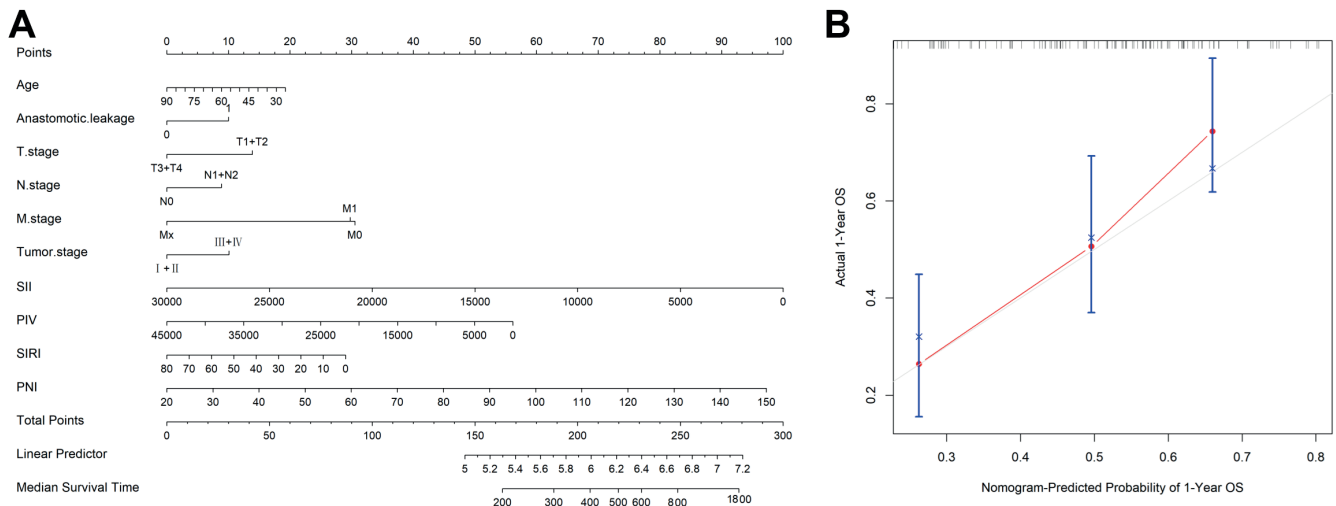


Fig. 4. Comparison of the prognostic value of clinicopathological features for colorectal cancer (CRC) patients. A. Nomogram; B. Calibration curve

SII – systemic immune-inflammation index; PNI – prognostic nutritional index; PIV – pan-immune-inflammation value; SIRI – systemic inflammation response index; OS – overall survival.

Limitations

The present study has some limitations. First, it had a retrospective design and was a single-center study, which inevitably led to selection bias. Second, even though we retrieved a long period of medical records, the number of ALs was relatively small, and the robustness of the results was undermined. Third, some factors that might affect nutritional status, such as genetics and intestinal microbiota, were not taken into consideration in this study; thus, the reliability of our results might be reduced. Fourth, molecular status, such as microsatellite instability (MSI), is an important prognostic and predictive factor in patients with CRC. However, due to the limited data of our study, we could not analyze the effect of molecular status on AL after surgery. Therefore, our results need to be validated in prospective, larger, multicenter cohorts.

Conclusions

This study demonstrated that preoperative PNI is a useful supplement for predicting AL in CRC patients after colorectal surgery and it also helps predict the prognosis of CRC patients. However, considering the limitations of this study, a larger study is required to validate these results.

Supplementary data

The supplementary materials are available at <https://doi.org/10.5281/zenodo.8106981>. The package contains the following files:

Supplementary Table 1. Continuous data distribution analysis with Shapiro–Wilk normality test.

Supplementary Table 2. Variance homogeneity t-test results between patients with or without CRC.

Supplementary Table 3. Variance homogeneity t-test results between patients with or without anastomotic leakage.

ORCID iDs

Haotang Wei <https://orcid.org/0000-0003-2977-9866>
 Jialei Wang <https://orcid.org/0009-0006-7803-4544>
 Zhengkai Jiang <https://orcid.org/0009-0004-5611-459X>
 Yu Liu <https://orcid.org/0009-0002-9824-9914>
 Sheng Jiang <https://orcid.org/0009-0005-0789-315X>
 Bangli Hu <https://orcid.org/0000-0002-4401-0601>

References

- Foppa C, Ng SC, Montorsi M, Spinelli A. Anastomotic leak in colorectal cancer patients: New insights and perspectives. *Eur J Surg Oncol.* 2020;46(6):943–954. doi:10.1016/j.ejso.2020.02.027
- Hoek VT, Buettner S, Sparreboom CL, et al. A preoperative prediction model for anastomotic leakage after rectal cancer resection based on 13,175 patients. *Eur J Surg Oncol.* 2022;48(12):2495–2501. doi:10.1016/j.ejso.2022.06.016
- Chiarello MM, Fransvea P, Cariati M, Adams NJ, Bianchi V, Brisinda G. Anastomotic leakage in colorectal cancer surgery. *Surg Oncol.* 2022; 40:101708. doi:10.1016/j.suronc.2022.101708
- Ishizuka M, Shibuya N, Takagi K, et al. Impact of anastomotic leakage on postoperative survival of patients with colorectal cancer: A meta-analysis using propensity score matching studies. *Surg Oncol.* 2021;37:101538. doi:10.1016/j.suronc.2021.101538
- González-Valverde FM, Vicente-Ruiz M, Gómez-Ramos MJ. Risk factors of anastomotic leakage in colon cancer. *Cir Cir.* 2019;87(3):347–352. doi:10.24875/CIRU.18000616
- Klein M, Gogenur I, Rosenberg J. Postoperative use of non-steroidal anti-inflammatory drugs in patients with anastomotic leakage requiring reoperation after colorectal resection: Cohort study based on prospective data. *BMJ.* 2012;345:e6166. doi:10.1136/bmj.e6166
- Vasiliu ECZ, Zarnescu NO, Costea R, Neagu S. Review of risk factors for anastomotic leakage in colorectal surgery. *Chirurgia (Bucur).* 2015; 110(4):319–326. PMID:26305194.
- Yamano T, Yoshimura M, Kobayashi M, et al. Malnutrition in rectal cancer patients receiving preoperative chemoradiotherapy is common and associated with treatment tolerability and anastomotic leakage. *Int J Colorectal Dis.* 2016;31(4):877–884. doi:10.1007/s00384-016-2507-8

9. Wu CX, Rao DY, Sang CP, et al. Peripheral blood inflammation indices are effective predictors of anastomotic leakage in elective esophageal surgery. *J Gastrointest Oncol*. 2021;12(6):2675–2684. doi:10.21037/jgo-21-812
10. Mauser M, Bartsokas C, Brand M, Plani F. Postoperative CD4 counts predict anastomotic leaks in patients with penetrating abdominal trauma. *Injury*. 2019;50(1):167–172. doi:10.1016/j.injury.2018.11.028
11. Paliogiannis P, Deidda S, Maslyankov S, et al. Blood cell count indexes as predictors of anastomotic leakage in elective colorectal surgery: A multicenter study on 1432 patients. *World J Surg Oncol*. 2020;18(1):89. doi:10.1186/s12957-020-01856-1
12. Yilmaz H, Yersal Ö. Prognostic significance of novel inflammatory markers in extensive-stage small-cell lung cancer. *J Can Res Ther*. 2022;18(3):691–696. doi:10.4103/jcrt.jcrt_1937_21
13. Lin F, Zhang LP, Xie SY, et al. Pan-immune-inflammation value: A new prognostic index in operative breast cancer. *Front Oncol*. 2022;12:830138. doi:10.3389/fonc.2022.830138
14. Feng Y, Zhang N, Wang S, et al. Systemic inflammation response index is a predictor of poor survival in locally advanced nasopharyngeal carcinoma: A propensity score matching study. *Front Oncol*. 2020;10:575417. doi:10.3389/fonc.2020.575417
15. Özkan U, Gürdoğan M, Öztürk C, et al. Systemic immune-inflammation index: A novel predictor of coronary thrombus burden in patients with non-ST acute coronary syndrome. *Medicina (Kaunas)*. 2022;58(2):143. doi:10.3390/medicina58020143
16. Zeng R, Liu F, Fang C, et al. PIV and PILE score at baseline predict clinical outcome of Anti-PD-1/PD-L1 inhibitor combined with chemotherapy in extensive-stage small cell lung cancer patients. *Front Immunol*. 2021;12:724443. doi:10.3389/fimmu.2021.724443
17. Chen L, Bai P, Kong X, et al. Prognostic nutritional index (PNI) in patients with breast cancer treated with neoadjuvant chemotherapy as a useful prognostic indicator. *Front Cell Dev Biol*. 2021;9:656741. doi:10.3389/fcell.2021.656741
18. Rahbari NN, Weitz J, Hohenberger W, et al. Definition and grading of anastomotic leakage following anterior resection of the rectum: A proposal by the International Study Group of Rectal Cancer. *Surgery*. 2010;147(3):339–351. doi:10.1016/j.surg.2009.10.012
19. Polk N, Budai B, Hitre E, Patócs A, Mersich T. High neutrophil-to-lymphocyte ratio (NLR) and systemic immune-inflammation index (SII) are markers of longer survival after metastasectomy of patients with liver-only metastasis of rectal cancer. *Pathol Oncol Res*. 2022;28:1610315. doi:10.3389/pore.2022.1610315
20. Pérez-Martelo M, González-García A, Vidal-Ínsua Y, et al. Clinical significance of baseline pan-immune-inflammation value and its dynamics in metastatic colorectal cancer patients under first-line chemotherapy. *Sci Rep*. 2022;12(1):6893. doi:10.1038/s41598-022-10884-8
21. Yatabe S, Eto K, Haruki K, et al. Signification of systemic immune-inflammation index for prediction of prognosis after resecting in patients with colorectal cancer. *Int J Colorectal Dis*. 2020;35(8):1549–1555. doi:10.1007/s00384-020-03615-w
22. Takamizawa Y, Shida D, Boku N, et al. Nutritional and inflammatory measures predict survival of patients with stage IV colorectal cancer. *BMC Cancer*. 2020;20(1):1092. doi:10.1186/s12885-020-07560-3
23. Johannet P, Sawyers A, Qian Y, et al. Baseline prognostic nutritional index and changes in pretreatment body mass index associate with immunotherapy response in patients with advanced cancer. *J Immunother Cancer*. 2020;8(2):e001674. doi:10.1136/jitc-2020-001674
24. Wang X, Cheng G, Tao R, et al. Clinical characteristics and predictors of permanent stoma in rectal cancer patients underwent anterior resections: The value of preoperative prognostic nutritional index. *Int J Clin Oncol*. 2020;25(11):1960–1968. doi:10.1007/s10147-020-01743-5
25. Lai GHA, Deng HY, Song TN, et al. Preoperative prognostic nutritional index shows no significant prognostic value for short-term outcomes of anastomosis-leakage patients after cancerous esophagectomy. *Ann Palliat Med*. 2019;8(5):698–707. doi:10.21037/apm.2019.11.08
26. Shimakawa T, Asaka S, Sagawa M, et al. Nutritional screening before surgery for esophageal cancer: Current status and evaluation results [in Japanese]. *Gan To Kagaku Ryoho*. 2014;41(10):1301–1303. PMID:25335724.
27. Bailón-Cuadrado M, Pérez-Saborido B, Sánchez-González J, et al. Prognostic nutritional index predicts morbidity after curative surgery for colorectal cancer. *Cir Esp (Engl Ed)*. 2019;97(2):71–80. doi:10.1016/j.ciresp.2018.08.015
28. Tamai M, Kiuchi J, Kuriu Y, et al. Clinical impact of postoperative prognostic nutritional index in colorectal cancer patients undergoing adjuvant chemotherapy. *Am J Cancer Res*. 2021;11(10):4947–4955. PMID:34765302.
29. Kang J, Yang G, Wang D, Lin Y, Wang Q, Luo H. The clinical application value of the prognostic nutritional index for the overall survival prognosis of patients with esophageal cancer: A robust real-world observational study in China. *Comput Math Methods Med*. 2022;2022:3889588. doi:10.1155/2022/3889588
30. Xie H, Wei L, Yuan G, Liu M, Tang S, Gan J. Prognostic value of prognostic nutritional index in patients with colorectal cancer undergoing surgical treatment. *Front Nutr*. 2022;9:794489. doi:10.3389/fnut.2022.794489

Cytogenetic findings in Polish patients with suspected Fanconi anemia

Anna Repczyńska^{1,A–D}, Katarzyna Jułga^{1,B,C}, Andżelika Lorenc^{2,B,C}, Jolanta Skalska-Sadowska^{3,B,C},
Mariusz Wysocki^{4,B,C}, Agnieszka Zaucha-Prażmo^{5,B,C}, Katarzyna Drabko^{5,B,C}, Artur Bossowski^{6,B,C},
Bożena Dembowska-Bagińska^{7,B,C}, Jacek Wachowiak^{3,B,C}, Adam Buciński^{2,B,C}, Olga Haus^{1,D–F}

¹ Department of Clinical Genetics, Faculty of Medicine, Collegium Medicum in Bydgoszcz, Nicolaus Copernicus University in Toruń, Poland

² Department of Biopharmacy, Faculty of Pharmacy, Collegium Medicum in Bydgoszcz, Nicolaus Copernicus University in Toruń, Poland

³ Department of Oncology, Hematology and Pediatric Transplantology, Poznan University of Medical Sciences, Poland

⁴ Department of Pediatric Hematology and Oncology, Faculty of Medicine, Collegium Medicum in Bydgoszcz, Nicolaus Copernicus University in Toruń, Poland

⁵ Department of Pediatric Haematology, Oncology and Transplantology, Medical University of Lublin, Poland

⁶ Department of Pediatrics, Endocrinology, Diabetology with Cardiology Division, Medical University of Białystok, Poland

⁷ Department of Oncology, Children's Memorial Health Institute, Warsaw, Poland

A – research concept and design; B – collection and/or assembly of data; C – data analysis and interpretation;

D – writing the article; E – critical revision of the article; F – final approval of the article

Advances in Clinical and Experimental Medicine, ISSN 1899–5276 (print), ISSN 2451–2680 (online)

Adv Clin Exp Med. 2024;33(4):361–368

Address for correspondence

Anna Repczyńska
E-mail: annasz@cm.umk.pl

Funding sources

None declared

Conflict of interest

None declared

Acknowledgements

We would like to thank the families for the participation in the study and for their consent to publish the data.

Received on February 12, 2023

Reviewed on April 6, 2023

Accepted on June 26, 2023

Published online on August 4, 2023

Cite as

Repczyńska A, Jułga K, Lorenc A, et al. Cytogenetic findings in Polish patients with suspected Fanconi anemia. *Adv Clin Exp Med.* 2024;33(4):361–368. doi:10.17219/acem/168825

DOI

10.17219/acem/168825

Copyright

Copyright by Author(s)

This is an article distributed under the terms of the Creative Commons Attribution 3.0 Unported (CC BY 3.0) (<https://creativecommons.org/licenses/by/3.0/>)

Abstract

Background. The high sensitivity of cells of Fanconi anemia (FA) patients to DNA cross-linking agents (clastogens), such as mitomycin C (MMC), was used as a screening tool in Polish children with clinical suspicion of FA.

Objectives. The aim of the study was to compare chromosome fragility between 3 groups, namely non-FA, possible mosaic FA and FA patients.

Materials and methods. The study included 100 children with hematological manifestations and/or congenital defects characteristic of FA, and 100 healthy controls. Blood samples obtained from participants were analyzed using an MMC-induced chromosomal breakage test.

Results. Patients with clinical suspicion of FA were divided into 3 subgroups based on the MMC test results, namely FA, possible mosaic FA and non-FA. Thirteen out of 100 patients had a true FA cellular phenotype. The mean value of MMC-induced chromosome breaks/cell for FA patients was higher than for non-FA patients (6.67 ± 3.92 compared to 0.23 ± 0.18). In addition, the percentage of cells with spontaneous aberrations was more than 9 times higher in FA patients than in non-FA patients.

Conclusions. Our results confirmed that the MMC sensitivity test distinguishes between individuals affected by FA, those with possible somatic mosaicism, and patients with bone marrow failure for other reasons, who were classified as non-FA in the first diagnostic step. However, a definitive differential diagnosis requires follow-up mutation testing and chromosome breakage analysis of skin fibroblasts.

Key words: Fanconi anemia, mitomycin C, chromosome breakage test

Background

Fanconi anemia (FA) is the most prevalent cancer-prone inherited bone marrow failure syndrome (IBMF). The phenotype of FA patients is characterized by microcephaly, radial ray defects, skin pigmentation abnormalities, short stature, and genitourinary defects,^{1–4} although 25% of patients do not present abnormalities or pancytopenia at birth. In this patient population, the diagnosis is often not established until they develop cancers typical of adults with FA or family studies are conducted.^{5–7}

Fanconi anemia is a rare genetic disease caused by pathogenic variants in any of the 23 FA complementation group A (*FANC*) genes, which are involved in the FA/breast cancer gene (*BRCA*) pathway. An autosomal recessive inheritance was demonstrated for 21 *FANC* genes, an autosomal dominant inheritance was demonstrated for 1 gene (*FANCR/RAD51*), and an X-linked recessive inheritance for another (*FANCB*). The incidence of FA is 1 in 300,000 live births, affecting from 1 to 9 people in 1,000,000, with a carrier frequency in the general population of around 1 in 181.⁸

The consequences of FA pathway failure manifest at the chromosomal, cellular and clinical levels, with characteristic structural aberrations formed at the chromosomal level. Cellular outcomes include increased apoptosis, cell cycle changes and heightened sensitivity to DNA cross-linking agents such as exogenous mitomycin C (MMC) and diepoxybutane (DEB), and endogenous aldehydes. At the clinical level, FA patients present a triad of symptoms that involve bone marrow failure, a high risk of cancer and congenital defects.⁹

Chromosomal aberrations found in metaphase spreads from FA patients include gaps, chromatid or isochromatid breaks, chromosome breaks, acentric fragments, dicentric chromosomes, chromatid interchange, and characteristic triradial and tetradial figures.¹⁰

The hallmark of FA cells is high genomic instability, first described in 1966 by Schroeder as a high level of spontaneous chromosome breaks.¹¹ Some years later, studies showed that hypersensitivity to DNA cross-linking agents caused this genomic instability, leading to the development of the MMC and DEB tests, which are the “gold standard” diagnostic tests for FA. Although the high sensitivity to DNA cross-linking agents is the hallmark of peripheral blood T-lymphocytes of FA patients, it is not observed in all FA cases.^{12,13}

Around 10–20% of FA patients present with a special type of hematopoietic somatic mosaicism that reduces or eliminates lymphocyte sensitivity to clastogens. Identifying individuals affected with mosaicism using a chromosome breakage test can be difficult. Various mechanisms, such as back mutation, gene conversion, intragenic crossover, and second-site mutation, may result in the restoration of the affected gene to wild type, and these mechanisms have been identified in cells of mosaic FA patients. Gene reversion may affect all hematopoietic cell lineages,

causing a “natural gene therapy” with a stable phenotype or only individual cell lines and leading to a limited effect. The success of reversion depends on the stage of differentiation of the cell at which the gene correction occurs.^{14,15}

Determining the level of chromosomal abnormalities is crucial for identifying patients with FA. The most challenging problem when interpreting the results of chromosome breakage tests is distinguishing between non-FA and mosaic FA patients. Some non-FA patients may have a proportion of T-lymphocytes with chromosome breaks after chemotherapy treatment, which can be interpreted by inexperienced cytogeneticists as mosaicism, leading to false-positive results. In contrast, a high proportion of reverted T-lymphocytes in FA mosaic patients can lead to false negatives.^{16,17}

A spontaneous chromosome breakage analysis of cells not treated with MMC is also required since various levels occur among patients with different FA subtypes. Individuals with variants in *FANCD1/BRCA2* or *FANCN/partner* and localizer of *BRCA2 (PALB2)* genes have very high levels of spontaneous breakage and atypical aberrations compared with other groups of FA patients. Other DNA repair deficiency syndromes also show increased levels of spontaneous fragility, and it is possible to reveal specific types of chromosomal abnormalities for these syndromes. For example, telomeric rearrangements are present in cells of patients with dyskeratosis congenita, premature centromere separation occurs in Roberts syndrome, and Warsaw breakage syndrome and aberrations of chromosomes 7 and 14 are frequent in Nijmegen breakage syndrome and ataxia–telangiectasia. Additionally, analyzing breakages on G-banded chromosome preparations makes it possible to diagnose constitutional chromosome aberrations that may be responsible for the patient’s clinical features in around 1–2% of patients with suspected FA.^{10,18}

Objectives

The aim of the study was to assess chromosomal fragility using chromosome aberration analysis, including the number of chromosomal breaks and/or radial figures/cell, percentage of cells with aberrations, and breaks or radials/aberrant cell in Polish patients with suspected FA.

Materials and methods

Patients

One hundred patients (52 females and 48 males) with suspected FA were referred to the Department of Clinical Genetics of Collegium Medicum in Bydgoszcz (Nicolaus Copernicus University in Toruń, Poland). The age at diagnosis ranged from 1 month to 32 years (median: 15.36 years).

Sampling and culture conditions

Peripheral blood samples were collected with heparin (≥ 5 mL) to prepare cultures for routine cytogenetic analysis upon receiving signed consent forms from the parents of examined children and healthy controls. Four cultures were set up for each participant by adding 0.5 mL of blood to 4.5 mL of Roswell Park Memorial Institute (RPMI) 1640 culture medium containing 15% fetal bovine serum (FBS), phytohemagglutinin (PHA) and gentamicin (all from Thermo Fisher Scientific, Waltham, USA), according to the procedure described by Oostra et al.¹⁰ Cultures were incubated for 72 h with 0, 50, 150, or 300 nM of MMC (Sigma-Aldrich, St. Louis, USA). Cells were harvested after the treatment with colcemid (0.1 $\mu\text{g}/\text{mL}$) for 50 min. The next step involved incubation with 0.075 M KCl for 20 min at 37°C, followed by fixation with methanol and acetic acid (3:1). Lastly, microscope slide were prepared by staining cytogenetic preparations in 5% Giemsa solution for 2 min (Sigma-Aldrich) using the no banding technique. Chromosome breakage was analyzed using the Nikon E600 microscope (Nikon Corp., Tokyo, Japan) with a computer-assisted metaphase system (ASI Technologies, Netzer Sereni, Israel).

Cytogenetic analysis

The analysis included at least 50 metaphases from MMC-treated and untreated cultures of every patient and healthy control (Table 1,2). According to the recommendations for chromosomal breakage testing with MMC, it is necessary to set up the cell cultures from healthy controls concurrent with the samples from patients with suspected FA.¹⁰ The chromosome breakage analysis was performed using the aberrations outlined in Table 3, though chromosome and chromatid gaps were not scored.

The data were analyzed and scored for each patient and healthy control as a percentage of aberrant cells, mean chromosome breaks/cell, mean chromosome breaks/aberrant cell, and triradial, tetradial and chromatid interchange figure frequency (Table 1,2).

Statistical analysis

The Shapiro–Wilk (S–W) test, with a statistical significance level of 0.05, was used to determine the distribution of MMC test data across all investigated groups – control, non-FA, possible mosaic FA, and FA. The highest p-value for all S–W tests was 0.04, indicating that the data were non-normally distributed. As such, further analysis required non-parametric statistical methods, with the Mann–Whitney U test with Bonferroni correction applied to compare FA, possible mosaic FA and non-FA groups to the control group. A statistical significance level of 0.05 was established for this test. All analyses employed PQStat v. 1.8.2 (PQStat Software, Poznań, Poland).

Results

The results of the chromosome breakage examination and cytogenetic analysis of a population of Polish patients presented herein were systematically obtained in the same laboratory under controlled conditions over a 6-year period (2015–2020). There are no studies on FA conducted in Poland, except for a small number of case reports.

The MMC test results included the percentage of aberrant cells, the number of breaks/analyzed cell, the number of breaks/aberrant cell, and the presence of radial figures characteristic of FA, which allowed for the stratification of patients into 3 subgroups: FA, displaying a typical MMC-sensitive cellular response, possible mosaic FA, and non-FA. The results of the spontaneous and MMC-induced breakage for all subgroups and controls are presented in Table 1 and Table 2.

Thirteen out of 100 examined patients (13%) had a cellular FA phenotype, with increased MMC-induced chromosomal breaks at 50-nM, 150-nM and 300-nM MMC concentrations (Fig. 1). Twelve of the 13 FA patients showed an increased rate of spontaneous breaks, while 1 patient had no spontaneous breaks. Meanwhile, 27 patients had possible mosaic FA, as they presented with only a slightly higher number of aberrant cells and breaks/aberrant cell and characteristic radial figures. The remaining patients presented with single chromosome breaks only, similar to the control group, and they were classified as non-FA.

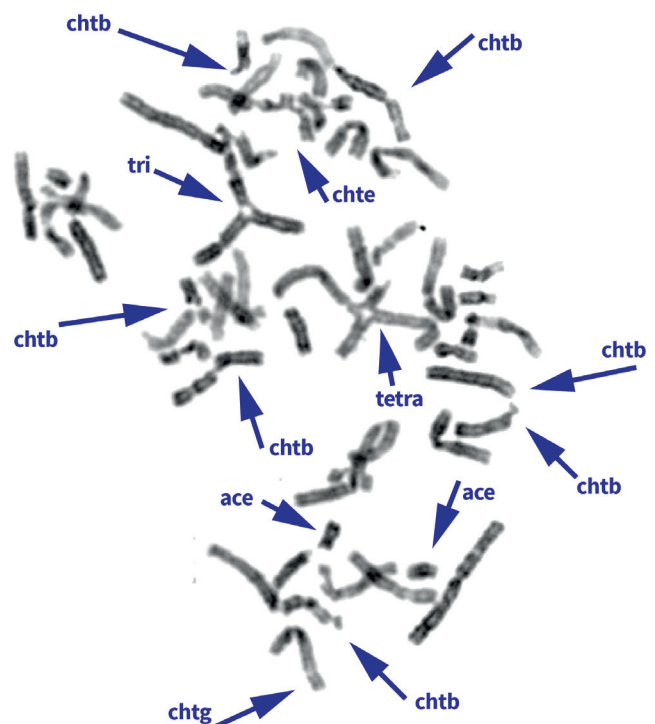


Fig. 1. Metaphase spread from a Fanconi anemia (FA) patient

ace – acentric fragment; chtb – chromatid break; chtg – chromatid gap; tri – triradial figure; tetra – tetradial figure; chte – chromatid interchange figure.

Table 1. Evaluation of spontaneous and MMC-induced chromosome breakage in Fanconi anemia (FA), possible mosaic FA and non-FA patients

Culture type	Group	Analyzed cells, n	Ace (%)	Ace (%)	Dic (%)	Dic (%)	Chtb (%)	Chtb (%)	Gaps	Triradial	Triradial (%)	Tetradial	Tetradial (%)	Multiradial	Multiradial (%)
Spontaneous chromosome breakage test	controls	3940	0	0.00	0	0.00	24	100.00	3	0	0.00	0	0.00	0	0.00
	non-FA	1914	0	0.00	1	3.85	25	96.15	0	0	0.00	0	0.00	0	0.00
	possible mosaic FA	854	2	5.56	0	0.00	31	86.11	9	1	2.78	1	2.78	1	2.78
Mitomycin C – 50 nM	FA	551	2	3.57	0	0.00	50	89.29	1	2	3.57	1	1.79	1	1.79
	controls	4496	0	0.00	0	0.00	386	99.48	34	1	0.26	1	0.26	0	0.00
	non-FA	2246	2	1.02	0	0.00	187	95.41	39	3	1.53	4	2.04	0	0.00
Mitomycin C – 150 nM	possible mosaic FA	1088	0	0.00	0	0.00	170	92.90	8	4	2.19	8	4.37	1	0.55
	FA	578	4	0.58	2	0.29	626	90.59	115	23	3.33	26	3.76	10	1.45
	controls	4605	0	0.00	0	0.00	972	98.38	57	1	0.10	13	1.32	2	0.20
Mitomycin C – 300 nM	non-FA	2238	1	0.26	4	1.03	368	94.36	32	7	1.79	8	2.05	2	0.51
	possible mosaic FA	1076	0	0.00	0	0.00	245	93.87	37	4	1.53	11	4.21	1	0.38
	FA	543	32	1.48	2	0.09	1852	85.62	174	90	4.16	115	5.32	72	3.33
Mitomycin C – 300 nM	controls	5003	1	0.05	0	0.00	1822	96.91	119	25	1.33	31	1.65	1	0.05
	non-FA	2973	2	0.29	0	0.00	656	94.80	135	12	1.73	20	2.89	2	0.29
	possible mosaic FA	1333	6	0.59	1	0.10	882	86.81	111	31	3.05	85	8.37	11	1.08
FA	672	74	1.65	0	0.00	3748	83.55	376	195	4.35	223	4.97	246	5.48	

chtb – chromatid break (the interruption which is more than 2 times the width of the chromatid, or displacement of the fragment of chromatid); ace – acentric fragment (fragment of a chromosome with 2 chromatids without a centromere); dic – dicentric (a chromosome with 2 centromeres). Triradial figure is a chromosome arrangement formed by fusion of broken translocated chromatids in a three-armed way. Tetradial figure is a chromosome arrangement formed by the incorrect joining of 2 chromosomal breaks involving 2 homologous or non-homologous chromosomes.

Table 2. Results of statistical analysis of spontaneous and mitomycin C (MMC)-induced chromosome breakage in Fanconi anemia (FA), possible mosaic FA and non-FA patients

Culture type	Group	Analyzed cells, n	Sample size, n	Analyzed cell numbers per patient (range; Me; Q1; Q3)	General number of breaks in the analyzed group	Abnormal cells, n	Aberrant cells (%)	Number of breaks/cell (Me; Q1; Q3)	Mann-Whitney U test with Bonferroni correction (Z; p) for number of breaks/cell	Number of breaks/aberrant cell (Me; Q1; Q3)	Mann-Whitney U test with Bonferroni correction (Z; p) for number of breaks/aberrant cell
Spontaneous chromosome breakage test	controls	3940	100	12–100; 20; 50	24	26	0.55	0; 0; 0	4.87; <0.01	0; 0; 0	4.87; <0.01
	non-FA	1914	60	0–100; 21; 20; 25.75	26	20	0.84	0; 0; 0	5.59; <0.01	0; 0; 0	5.32; <0.01
	possible mosaic FA	854	27	19–100; 21; 20; 30	36	24	1.55	0; 0; 0.02	3.76; <0.01	0; 0; 0.50	2.83; <0.01
	FA	551	13	16–100; 22; 21; 50	56	44	8.31	0.09; 0.07; 0.17	–	1.00; 1.00; 1.40	–
Mitomycin C – 50 nM	controls	4496	100	0–117; 50; 50; 50	388	389	8.66	0.06; 0.00; 0.12	10.25; <0.01	1.00; 0.00; 1.00	10.32; <0.01
	non-FA	2246	60	0–50; 50; 34.5; 50	196	172	7.66	0.04; 0.00; 0.08	4.10; <0.01	1.00; 0.00; 1.00	3.83; <0.01
	possible mosaic FA	1088	27	0–50; 50; 50; 50	183	121	11.55	0.10; 0.00; 0.19	3.45; <0.01	1.00; 0.00; 1.48	2.91; <0.01
	FA	578	13	0–80; 50; 50; 50	691	259	44.58	1.09; 0.5; 1.44	–	2.18; 1.92; 3.00	–
Mitomycin C – 150 nM	controls	4605	100	0–100; 50; 50; 50	988	872	18.87	0.14; 0.06; 0.28	12.08; <0.01	1.00; 1.00; 1.17	12.13; <0.01
	non-FA	2238	60	0–51; 50; 27.75; 50	390	321	14.29	0.08; 0.00; 0.19	4.12; <0.01	1.00; 0.00; 1.17	4.06; <0.01
	possible mosaic FA	1076	27	0–50; 50; 50; 50	261	200	19.78	0.14; 0.03; 0.29	3.57; <0.01	1.00; 0.42; 1.42	3.49; <0.01
	FA	543	13	0–57; 50; 50; 50	2163	386	71.36	2.54; 1.10; 5.02	–	3.55; 2.89; 6.26	–
Mitomycin C – 300 nM	controls	5003	100	11–94; 50; 50; 50	1880	1421	28.24	0.30; 0.16; 0.54	13.29; <0.01	1.22; 1.00; 1.28	13.30; <0.01
	non-FA	2973	60	14–60; 50; 50; 50	692	605	20.12	0.18; 0.10; 0.30	5.63; <0.01	1.00; 0.79; 1.31	5.63; <0.01
	possible mosaic FA	1333	27	0–50; 50; 50; 50	1016	442	33.81	0.64; 0.55; 1.02	5.06; <0.01	2.18; 1.92; 2.74	5.05; <0.01
	FA	672	13	36–86; 50; 50; 50	4486	575	85.62	4.86; 4.24; 8.34	–	6.18; 5.14; 8.34	–

Me – median; Q1 – 1st quartile; Q3 – 3rd quartile.

Table 3. Scoring aberrations in chromosomal breakage test with mitomycin C (MMC)

Type of aberration	Break events, n
Chromatid/chromosome break (chtb)	1
Acentric fragment (ace)	1
Dicentric chromosome (dic)	2
Triradial figure	2
Tetradial figure	2
Complex reciprocal chromatid exchange (chte)	sum of centromeres and open breaks

The most reliable results were obtained using the highest MMC concentration (300 nM), with an increased aberration rate in FA patients. Moreover, statistically significant differences in aberration rates were observed between patient and control blood samples (Fig. 2,3).

In the present study, the maximal percentage of MMC-induced breaks/aberrant cell at 300-nM MMC was 100%. The median number of MMC-induced chromosome breaks/cell for the FA patients was 4.86, with a Q1 value of 4.24 and a Q3 value of 8.34. The MMC-induced breaks/

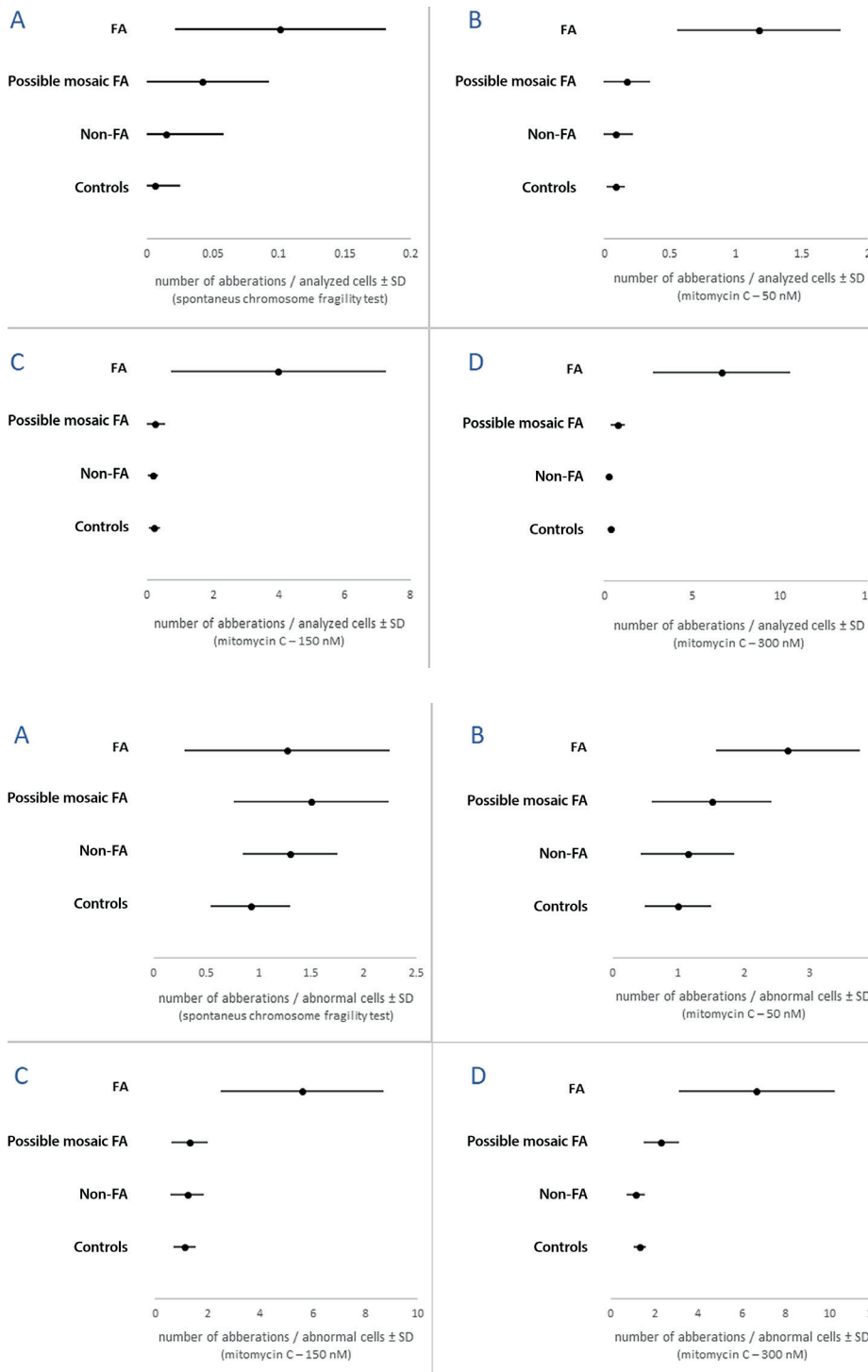


Fig. 2. Differentiation between Fanconi anemia (FA) and other groups by comparing mean breaks/cell observed in the different study groups after treatment with various concentrations of mitomycin C (MMC). A. Culture without MMC; B. Culture with 50 nM of MMC; C. Culture with 150 nM of MMC; D. Culture with 300 nM of MMC

SD – standard deviation.

Fig. 3. Differentiation between Fanconi anemia (FA) and other groups by comparing mean breaks/abnormal cell values in the different study groups after treatment with various concentrations of mitomycin C (MMC). A. Culture without MMC; B. Culture with 50 nM of MMC; C. Culture with 150 nM of MMC; D. Culture with 300 nM of MMC

SD – standard deviation.

aberrant cell ranged from 3.44 to 16.18, while the median was 6.18 (Q1 = 5.14, Q3 = 8.34) (Table 2). Meanwhile, patients who presented with possible mosaic FA had a median breaks/cell value of 0.64 (Q1 = 0.55, Q3 = 1.02) and median MMC-induced breaks/aberrant cell value of 2.18 (Q1 = 1.92, Q3 = 2.74) (Table 2). Patients with no MMC hypersensitivity (non-FA group) had a median breaks/cell value of 0.18 (Q1 = 0.10, Q3 = 0.30) and a median MMC-induced breaks/aberrant cell value of 1.00 (Q1 = 0.79, Q3 = 1.31) (Table 2). In the control group, the median breaks/cell was 0.30 (Q1 = 0.16, Q3 = 0.54), and the median MMC-induced breaks/aberrant cell was 1.22 (Q1 = 1.00, Q3 = 1.28) (Table 2).

Data from other cultures (0-nM, 50-nM and 150-nM MMC) were analyzed similarly. Patients with FA were visibly different from non-FA individuals and those with possible mosaic FA (Table 2). The statistical analysis showed significant differences between the FA group and other groups ($p < 0.01$ for all comparisons using the Mann–Whitney U test with Bonferroni correction).

Discussion

Fanconi anemia is a rare human genetic condition associated with hematological manifestations and a high risk of solid tumors. The clinical picture of FA may present with hypopigmentation or hyperpigmentation of the skin, short stature, skeletal defects of the limbs such as radial aplasia and hand and thumb abnormalities, congenital heart defects, and kidney malformations. Bone marrow failure usually develops between 7 and 10 years of age, while neoplasms can occur in up to 20% of patients. Acute myeloid leukemia is most frequent in adolescence, while head and neck tumors usually develop in adulthood.^{2,13}

The chromosome breakage protocol used in the present study has been widely applied to detect FA for around 30 years. It requires a time-consuming analysis and specialized laboratory staff. The DNA cross-linking agents such as MMC, DEB and cis-diamminedichloroplatinum(II) (cisplatin) are used to demonstrate the hypersensitive phenotype of FA cells. According to the International Fanconi Anemia Registry (IFAR), DEB sensitivity is much more accurate for FA diagnosis than other cross-linking agents. However, most laboratories perform chromosome break induction in lymphocyte cultures of possible FA patients using MMC, since DEB is on the Special Health Hazard Substance List, as it is a volatile carcinogen that should be handled with great caution. In contrast, MMC and cisplatin are clinically approved chemotherapeutic agents that undergo rigorous quality control and are stable when stored in the vials provided by the manufacturer.^{10,19}

Diagnosing patients with somatic hematopoietic mosaicism is challenging since a subset of their peripheral blood cells undergoes a molecular event in which 1 *FANC* allele reverts to normal while the second allele remains mutated.

Furthermore, mosaicism presenting in the blood or bone marrow of those with FA does not protect from the development of clonal chromosome abnormalities, hematologic malignancies or solid tumors.¹⁵

In the present study, the results of the MMC breakage test revealed a higher percentage of MMC-induced aberrant cells in FA patients compared to non-FA patients and possible mosaic FA patients. The study revealed that 13 (13%) out of 100 examined patients had a cellular FA phenotype with increased MMC-induced chromosome fragility. The number of MMC-induced breaks/cell after 300-nM MMC treatment was more than 23 times higher in FA patients than in non-FA patients, and a clear discrimination was observed between FA and non-FA subgroups.

According to the IFAR study, significant differences were observed between the FA and non-FA groups based on DEB-induced chromosome breaks. Also, patients from the possible mosaic FA group had lower chromosome fragility than FA patients. However, there was an overlap between the possible mosaic FA group, non-FA group and controls. These findings may have resulted from a low number of cells with substantial breaks and/or radials in healthy individuals, a phenomenon also described by Castella et al.²⁰

According to the current study, the incidence of FA is lower in the Polish population than in other European countries,^{3,17} which may result from the routine testing of children, but not adults, with a clinical suspicion of FA in Poland. Moreover, it would be reasonable to perform simultaneous blood and skin tests in all patients with suspected FA at the beginning of the diagnostic process to detect those with mosaic FA.

Limitations

An important limitation of our work is that we only performed a cytogenetic study on peripheral blood T-lymphocytes to distinguish possible mosaic FA patients from definite FA patients. Chromosome breakage tests on skin fibroblasts and *FANC* gene sequencing of blood and skin in possible mosaic FA patients are necessary for the next step of our research. However, the strength of our study is that it is the first to directly compare cytogenetic results of patients classified as FA, possible mosaic FA and non-FA in a Polish population with suspected FA.

Conclusions

The results of the current study highlight the importance of performing standard diagnostic MMC tests in patients with suspected FA. The role of FA laboratory tests in this regard is extensive:

1. The heterogenic nature of FA is often the reason for late clinical diagnosis. Moreover, 3 well-known syndromes can yield positive results in the chromosomal breakage test,

including Warsaw breakage syndrome, Nijmegen breakage syndrome and Roberts syndrome, though all are characterized by specific chromosomal aberrations¹⁰;

2. Patient control and care by hematologists, oncologists and other specialists are required for life-long monitoring and treatment of FA^{21,22};

3. Positive MMC-induced breakage results are crucial for patients requiring bone marrow transplantation or chemotherapy. Patients with FA require a modified pretransplantation conditioning protocol, with a lower than usual dose of chemotherapeutic agents²¹;

4. The results of the present study indicate that testing MMC-induced chromosome breakage is useful for distinguishing FA patients from others manifesting some FA clinical features. An accurate diagnosis in these patients is critical for therapeutic decision-making.

ORCID iDs

Anna Repczyńska  <https://orcid.org/0000-0003-2595-6909>
 Katarzyna Jułga  <https://orcid.org/0000-0002-2995-5658>
 Andżelika Lorenc  <https://orcid.org/0000-0002-1474-7864>
 Jolanta Skalska-Sadowska  <https://orcid.org/0000-0002-6785-8664>
 Mariusz Wysocki  <https://orcid.org/0000-0003-2546-6272>
 Agnieszka Zaucha-Prażmo  <https://orcid.org/0000-0001-5332-7996>
 Katarzyna Drabko  <https://orcid.org/0000-0002-7094-9129>
 Artur Bossowski  <https://orcid.org/0000-0002-6316-5342>
 Bożena Dembowska-Bagińska  <https://orcid.org/0000-0002-3845-5380>
 Jacek Wachowiak  <https://orcid.org/0000-0002-4680-603X>
 Adam Buciński  <https://orcid.org/0000-0002-0558-9139>
 Olga Haus  <https://orcid.org/0000-0002-5206-0553>

References

- Dokal I, Vulliamy T. Inherited bone marrow failure syndromes. *Haematologica*. 2010;95(8):1236–1240. doi:10.3324/haematol.2010.025619
- Taylor AMR, Rothblum-Oviatt C, Ellis NA, et al. Chromosome instability syndromes. *Nat Rev Dis Primers*. 2019;5(1):64. doi:10.1038/s41572-019-0113-0
- Toksoy G, Uludağ Alkaya D, Bagirova G, et al. Clinical and molecular characterization of Fanconi anemia patients in Turkey. *Mol Syndromol*. 2020;11(4):183–196. doi:10.1159/000509838
- Chowdhry M, Makroo RN, Srivastava P, et al. Clinicohematological correlation and chromosomal breakage analysis in suspected Fanconi anemia patients of India. *Indian J Med Paediatr Oncol*. 2014;35(1):21–25. doi:10.4103/0971-5851.133706
- Niraj J, Färkkilä A, D'Andrea AD. The Fanconi anemia pathway in cancer. *Annu Rev Cancer Biol*. 2019;3:457–478. doi:10.1146/annurev-cancerbio-030617-050422
- Digweed M, Hoehn H, Sperling K. Milestones in Fanconi anemia research. In: *Monographs in Human Genetics*. Basel, Switzerland: Karger; 2007:23–38. doi:10.1159/000102546
- Amenábar JM, Torres-Pereira CC, Tang KD, Punyadeera C. Two enemies, one fight: An update of oral cancer in patients with Fanconi anemia. *Cancer*. 2019;125(22):3936–3946. doi:10.1002/ncr.32435
- Merfort LW, Lisboa MDO, Cavalli LR, Bonfim CMS. Cytogenetics in Fanconi anemia: The importance of follow-up and the search for new biomarkers of genomic instability. *Int J Mol Sci*. 2022;23(22):14119. doi:10.3390/ijms232214119
- De Winter JP, Joenje H. The genetic and molecular basis of Fanconi anemia. *Mutat Res*. 2009;668(1–2):11–19. doi:10.1016/j.mrfmmm.2008.11.004
- Oostra AB, Nieuwint AWM, Joenje H, De Winter JP. Diagnosis of Fanconi anemia: Chromosomal breakage analysis. *Anemia*. 2012;2012:238731. doi:10.1155/2012/238731
- Schroeder TM. Cytogenetic finding and etiology of Fanconi's anemia. A case of Fanconi's anemia without hexokinase deficiency [in German]. *Humangenetik*. 1966;3(1):76–81. doi:10.1007/BF00273021
- Schoder C, Liehr T, Velleuer E, et al. New aspects on chromosomal instability: Chromosomal break-points in Fanconi anemia patients co-localize on the molecular level with fragile sites. *Int J Oncol*. 2010;36(2):307–312. doi:10.3892/ijo_00000501
- García-de-Teresa B, Rodríguez A, Frias S. Chromosome instability in Fanconi anemia: From breaks to phenotypic consequences. *Genes (Basel)*. 2020;11(12):1528. doi:10.3390/genes11121528
- Nicoletti E, Rao G, Bueren JA, et al. Mosaicism in Fanconi anemia: Concise review and evaluation of published cases with focus on clinical course of blood count normalization. *Ann Hematol*. 2020;99(5):913–924. doi:10.1007/s00277-020-03954-2
- Fargo JH, Rochowski A, Giri N, Savage SA, Olson SB, Alter BP. Comparison of chromosome breakage in non-mosaic and mosaic patients with Fanconi anemia, relatives, and patients with other inherited bone marrow failure syndromes. *Cytogenet Genome Res*. 2014;144(1):15–27. doi:10.1159/000366251
- Solomon PJ, Margaret P, Rajendran R, et al. A case report and literature review of Fanconi anemia (FA) diagnosed by genetic testing. *Ital J Pediatr*. 2015;41:38. doi:10.1186/s13052-015-0142-6
- Risitano AM, Marotta S, Calzone R, Grimaldi F, Zatterale A. Twenty years of the Italian Fanconi Anemia Registry: Where we stand and what remains to be learned. *Haematologica*. 2016;101(3):319–327. doi:10.3324/haematol.2015.133520
- Fiesco-Roa MÓ, García-de Teresa B, Leal-Anaya P, et al. Fanconi anemia and dyskeratosis congenita/telomere biology disorders: Two inherited bone marrow failure syndromes with genomic instability. *Front Oncol*. 2022;12:949435. doi:10.3389/fonc.2022.949435
- Auerbach AD. Fanconi anemia and its diagnosis. *Mutat Res*. 2009;668(1–2):4–10. doi:10.1016/j.mrfmmm.2009.01.013
- Castella M, Pujol R, Callén E, et al. Chromosome fragility in patients with Fanconi anaemia: Diagnostic implications and clinical impact. *J Med Genet*. 2011;48(4):242–250. doi:10.1136/jmg.2010.084210
- Fanconi Anemia Clinical Care Guidelines. Fanconi Anemia Research Fund; 2020. https://www.fanconi.org/images/uploads/other/Fanconi_Anemia_Clinical_Care_Guidelines_5thEdition_web.pdf.
- Dufour C. How I manage patients with Fanconi anaemia. *Br J Haematol*. 2017;178(1):32–47. doi:10.1111/bjh.14615

Association between clinical features and course of systemic sclerosis and serum interleukin-8, vascular endothelial growth factor, basic fibroblast growth factor, and interferon alpha

Joanna Kosałka-Węgiel^{1,2,A–F}, Sabina Lichołai^{2,B,E}, Sylwia Dziędzina^{2,B}, Mamert Milewski^{1,2,B}, Piotr Kuzmiersz^{1,2,B}, Anna Korona^{2,B}, Mariusz Korkosz^{1,C,E,F}, Jolanta Gąsior^{2,B}, Aleksandra Matyja-Bednarczyk^{1,2,B}, Helena Kwiatkowska^{3,B}, Andżelika Siwiec-Koźlik^{1,2,B,C}, Wojciech Sydor^{1,2,B}, Joanna Wilańska^{2,B}, Lech Zaręba^{4,C}, Weronika Pocij-Marciak^{5,6,B}, Jerzy Dropiński^{2,B}, Marek Sanak^{2,C,E,F}, Jacek Musiał^{2,E,F}, Stanisława Bazan-Socha^{1,2,A,B,E,F}

¹ Department of Rheumatology and Immunology, Jagiellonian University Medical College, Kraków, Poland

² Second Department of Internal Medicine, Jagiellonian University Medical College, Kraków, Poland

³ Department of Dermatology, University Hospital, Kraków, Poland

⁴ Interdisciplinary Centre for Computational Modelling, College of Natural Sciences, University of Rzeszów, Poland

⁵ Division of Ophthalmology and Ocular Oncology, Department of Ophthalmology, Faculty of Medicine, Jagiellonian University Medical College, Kraków, Poland

⁶ Department of Ophthalmology and Ocular Oncology, University Hospital, Kraków, Poland

A – research concept and design; B – collection and/or assembly of data; C – data analysis and interpretation;

D – writing the article; E – critical revision of the article; F – final approval of the article

Advances in Clinical and Experimental Medicine, ISSN 1899–5276 (print), ISSN 2451–2680 (online)

Adv Clin Exp Med. 2024;33(4):369–377

Address for correspondence

Joanna Kosałka-Węgiel

E-mail: joanna.kosalka@uj.edu.pl

Funding sources

This publication was supported by the Polish Ministry of Science and Higher Education (grant No. K/DSC/002086 awarded to Joanna Kosałka-Węgiel).

Conflict of interest

None declared

Received on January 7, 2023

Reviewed on March 14, 2023

Accepted on June 23, 2023

Published online on August 4, 2023

Cite as

Kosałka-Węgiel J, Lichołai S, Dziędzina S, et al. Association between clinical features and course of systemic sclerosis and serum interleukin-8, vascular endothelial growth factor, basic fibroblast growth factor, and interferon alpha.

Adv Clin Exp Med. 2024;33(4):369–377.

doi:10.17219/acem/168724

DOI

10.17219/acem/168724

Copyright

Copyright by Author(s)

This is an article distributed under the terms of the Creative Commons Attribution 3.0 Unported (CC BY 3.0) (<https://creativecommons.org/licenses/by/3.0/>)

Abstract

Background. Certain mediators, such as soluble growth factors and cytokines, among others, are implicated in the immunopathogenesis of systemic sclerosis (SSc).

Objectives. This study aimed to examine the association between serum levels of vascular endothelial growth factor (VEGF), interleukin-8 (IL-8), interferon alpha (IFN- α), and basic fibroblast growth factor (bFGF) and the clinical presentation and course of SSc.

Materials and methods. This longitudinal, observational study included 43 patients with SSc and 24 healthy subjects. Serum concentrations of VEGF, IL-8, IFN- α , and bFGF were measured at baseline in patients previously treated for SSc. Medical history of patients was analyzed retrospectively at the time of cytokine measurement to infer clinical correlations, and during follow-up for a median of 5 years, assessing the incidence of death or cancer.

Results. The bFGF and IFN- α concentrations differed between SSc patients and controls ($p < 0.01$). In turn, organ involvement and SSc phenotypes did not impact studied cytokine concentrations, similar to systemic steroid and/or immunosuppressant use at enrollment. However, we have documented a positive correlation between the current oral steroid dose and serum levels of IL-8 and bFGF. Furthermore, patients with a VEGF level ≥ 95.7 pg/mL and IFN- α level ≥ 3.6 pg/mL required cyclophosphamide therapy more often, currently or in the past (approx. 3-fold and 4-fold, respectively). Substantially elevated VEGF and IFN- α concentrations at baseline were associated with higher cancer occurrence ($n = 4$) during follow-up, while elevated circulating IL-8 level was associated with an increased risk of death ($n = 9$).

Conclusions. The SSc group was characterized by higher serum concentrations of bFGF and IFN- α compared to healthy controls. Patients treated with cyclophosphamide or receiving higher systemic steroid doses, thus suffering from a more severe disease type, had increased cytokine levels. Elevated circulating IFN- α and VEGF levels might be correlated with cancer, whereas raised IL-8 levels may be associated with an increased risk of death. However, further research is needed to verify our findings.

Key words: systemic sclerosis, vascular endothelial growth factor, interleukin-8, interferon alpha, basic fibroblast growth factor

Background

Systemic sclerosis (SSc) is a chronic autoimmune process characterized by the dysfunction of the endothelium, defective neovascularization and pathologic tissue fibrosis.^{1–6} Clinically, it is subdivided into 2 large subtypes.^{2–4,7} The first type of the disease, namely diffuse cutaneous SSc (dcSSc), is characterized by proximal cutaneous involvement, whereas the second type, limited cutaneous SSc (lcSSc), is associated with skin hardening of the distal parts of the.^{2–4,8,9} In dcSSc, the incidence of renal injury, pulmonary fibrosis and generalized skin involvement are more frequent. In contrast, pulmonary arterial hypertension of a primarily vascular origin is more typical for lcSSc.^{2,3,9,10} Despite recent progress in understanding the etiology of SSc, the primary causes or molecular mechanisms underlying the disease onset, progression and outcomes remain to be fully elucidated.^{1,11} Some researchers claim that the pathogenesis of SSc is a consequence of endothelial destruction with consecutive activation of immune cells and fibroblasts, causing an undue accumulation of extracellular matrix (ECM) proteins.¹² Certain mediators, including soluble growth factors and cytokines, are implicated in the immunopathogenesis of SSc.^{1,12}

Basic fibroblast growth factor (bFGF) is a stimulating factor of angiogenesis.^{1,13} It is expressed by many tissues and organs, and is a strong mitogen for cells of mesodermal and neuroectodermal origin, including fibroblasts and endothelial cells.^{13,14} It has been suggested that bFGF might be released by exocytosis.¹⁴ After its release, bFGF remains bound to the ECM, therefore, the intensity of its release might regulate angiogenesis and fibrosis.^{13,14} Vascular endothelial growth factor (VEGF) is another mediator modulating various steps of angiogenesis, vasodilation and endothelial cell permeability. It activates the proliferation and migration of cells from the endothelium and causes perivascular ECM remodeling.^{13,15–19} Vascular endothelial growth factor is excreted by many cells, including activated macrophages and keratinocytes,¹³ and its biological effects are extremely dose- and time-dependent.^{15,16,20}

Interferon alpha (IFN- α) is a cytokine that plays a fundamental role in inflammation, immunoregulation, recognition of tumor cells, and T-cell activation. Additionally, its high expression promotes cellular and humoral autoimmunity.^{5,8,21}

Interleukin-8 (IL-8), the main neutrophil stimulator, is also suggested to take part in the pathogenesis of autoimmune disorders. It was found to promote pulmonary fibrosis, a complication of SSc.²² Moreover, it is a tumor-promoting cytokine, thus it might have a prognostic and/or predictive role as a cancer biomarker.^{23,24}

Objectives

Given their involvement in the pathogenetic processes relevant to SSc, we sought to assess serum concentrations

of IL-8, VEGF, bFGF, and IFN- α in a group of SSc patients to determine whether the cytokine profile correlates with disease manifestation, clinical course, comorbidities, treatment modalities, and laboratory results.

Materials and methods

Study subjects

We conducted an observational, cross-sectional study with longitudinal follow-up and comparison to healthy cases.

The case group consisted of 43 adult patients with SSc (33 women and 10 men). The SSc patients were recruited during a 5-year period (2014–2018) at the Outpatient Clinic of the Second Department of Internal Medicine (University Hospital, Kraków, Poland). The individuals were diagnosed with SSc based on the 2013 European League Against Rheumatism/American College of Rheumatology (EULAR/ACR) classification criteria or those proposed by LeRoy and Medsger for early SSc (EaSSc) diagnosis.^{25,26} All SSc patients were clinically stable at enrollment, with no change in therapy during the last 6 months. The interstitial lung disease associated with SSc (SSc-ILD) was confirmed by high-resolution computed tomography (HRCT) of the lungs and was considered clinically significant if forced vital capacity (FVC), measured using spirometry, was lower than 70% of the predicted value. Probable pulmonary artery hypertension (PAH) was defined with high probability when systolic pressure values evaluated with the use of transthoracic echocardiography were greater than 45 mm Hg.² This noninvasive method has a 97% specificity as compared to right heart catheterization (100%).²⁷ Scleroderma renal crisis was diagnosed as a new onset of renal insufficiency, however, other causes must be excluded (e.g., multiple organ dysfunction syndrome, infections, etc.). Digital ulcers were described as lesions with concomitant loss of tissue, occurring at the distal parts of fingers and toes. Patients were excluded from the study if they had an active acute or chronic infection, including viral hepatitis, other active chronic inflammatory disease (e.g., rhinosinusitis), confirmed cancer, or if they were pregnant or in the postpartum period.

Scleroderma cases were followed up for a median of 5 years to record cancer and death incidence and their potential association with cytokines measured at baseline.

The healthy group was comprised of 24 individuals (14 men and 10 women), with a median age of 32 (22–40) years. The study was conducted in accordance with the Declaration of Helsinki and was approved by the Bioethics Committee at the Jagiellonian University Medical College (approval No. KBET/235/B/2013; date of approval: September 26, 2013).

Laboratory analysis

Blood samples were obtained from a peripheral vein with minimal tourniquet pressure. Complete blood cell (CBC)

count, plasma fibrinogen, lipid profile, and serum levels of C-reactive protein (CRP), alanine and aspartate transaminases (ALT and AST, respectively), bilirubin, alkaline phosphatase, urea, and creatinine with estimated glomerular filtration rate (eGFR, using Modification of Diet in Renal Disease formula) were measured using routine laboratory techniques. Antinuclear antibodies (ANA) were evaluated using indirect immunofluorescence assay in Hep-2 cell lines (EUROIMMUN, Lübeck, Germany). They were positive if the titer was at least 1:160. We also utilized immunoblot techniques specific for autoantibodies against topoisomerase I, centromeres, PM-Scl, RNA polymerase III, Ku, NOR 90, PDGFR, fibrillarin, and Ro-52 (EUROIMMUN). After blood sample centrifugation in separation tubes at $2000 \times g$ for 10 min at room temperature within 2 h of collection, cytokine levels were measured, and serum supernatant was immediately frozen and stored at a temperature of -70°C until analysis.

Serum cytokines

Serum levels of VEGF, IL-8, IFN- α , and bFGF were measured using Luminex ProcartaPlex Immunoassays (eBioscience, San Diego, USA), according to the manufacturer's protocol, as well as the MAGPIX[®] platform (Luminex Corp., Austin, USA) and xPonent software (Luminex Corp.). The array was chosen based on the earlier information about circulating biomarkers in SSc. Results below the detection threshold were assigned a value of the lower assay limits.

Statistical analyses

The results were analyzed using STATISTICA 13.3 software (TIBCO Software, Palo Alto, USA) and R software (R Foundation for Statistical Computing, Vienna, Austria). According to the Shapiro–Wilk test, continuous variables were all non-normally distributed. They are presented as median with interquartile range (25Q–75Q).

The variables were compared using the Mann–Whitney U test to check the statistical significance of the rank distribution. A one-way covariance analysis (ANCOVA) was performed to adjust for potential confounders, including sex, age and body mass index (BMI). Categorical variables were reported as percentages and compared using the χ^2 test. To evaluate the relationship between continuous variables, Spearman's rank correlation tests were performed. Independent determinants of serum cytokine levels were established using multiple linear regression models. The R^2 was assessed as a measure of the variance. The collinearity of predictors in multiple linear regression models was checked using Pearson linear correlation coefficient and variance inflation factor (VIF). The backward stepwise regression method was used to select predictors for the regression model. To calculate the odds ratio (OR) with a 95% confidence interval (95% CI), the cut-off points were determined based on receiver operating

characteristic (ROC) curves, using the Youden method. We attempted to distinguish clusters of patients based on laboratory test results, including cytokine profiles that could indicate the existence of distinct disease phenotypes. The cluster analysis was performed using the k-means method. Statistical significance was set at a p-value <0.05 .

Results

Characteristics of the SSc patients

Table 1 presents the demographic characteristics of the SSc patients. Table 2 demonstrates the clinical parameters and autoantibody profiles of the SSc group. Briefly, at enrollment, the median duration of the disease was 4 (range: 1–11) years, and more than half of the patients ($n = 26$, 60.5%) were diagnosed with dcSSc. The most frequent feature of the disease was Raynaud's phenomenon ($n = 41$, 95.3%). The SSc-ILD was confirmed in 69.8% of patients, whereas other symptoms of SSc, including digital ulcers, dysphagia and probable PAH, were rare (Table 2). At enrollment, 16 SSc patients (37.2%) were treated with steroids, and 7 individuals (16.3%) were receiving immunosuppressive drugs, such as cyclophosphamide (3 patients), methotrexate (2 patients), mycophenolate mofetil (1 patient), and azathioprine (1 patient). The median daily methylprednisolone dose was 0 (range: 0–4) mg (Table 2). Other medications used, such as antihypertensive drugs, vasodilators and statins, are listed in Table 2.

The ANA were detected in the serum of all SSc patients. The most frequent were anti-topoisomerase I antibodies (Scl-70), confirmed in 24 cases (55.8%), followed by anti-Ro52 and anti-centromeric antibodies (ACA) (25.6% and 23.3%, respectively). Other types of ANA, such as anti-RNA polymerase III, anti-NOR, anti-PM/Scl, anti-Ku, and anti-Th/To, had a much lower prevalence.

Table 1. Demographic and clinical characteristics of systemic sclerosis group

Variables	Patients (n = 43)
Age [years]	59 (44–65)
Male gender, n	10
Body mass index [kg/m ²]	23.6 (22.2–26.1)
Smoking in the past, n	15
Smoking [packs/year]	0 (0–5)

Categorical variables are presented as number (percentage), and continuous variables are presented as median and interquartile range (25Q–75Q).

SSc patients had higher serum bFGF and IFN- α levels than controls

Table 3 compares the serum levels of IL-8, VEGF, bFGF, and IFN- α between the control group and the whole SSc cohort. The bFGF and IFN- α levels were approx.

Table 2. Clinical characteristics and antinuclear antibodies in systemic sclerosis patients

Clinical characteristics	Patients (n = 43)
Duration of the disease [years]	4 (1–11)
Limited disease, n (%)	17 (39.5)
Diffuse disease, n (%)	26 (60.5)
Antinuclear antibodies, n (%)	43 (100)
Anti-Scl-70 antibodies, n (%)	24 (55.8)
Anti-PM/Scl antibodies, n (%)	7 (16.3)
Anti-centromeric antibodies, n (%)	10 (23.3)
Anti-NOR antibodies, n (%)	2 (4.7)
Anti-Ro52 antibodies, n (%)	11 (25.6)
RNA polymerase III antibodies, n (%)	1 (2.3)
Anti-Th/To antibodies, n (%)	1 (2.3)
Anti-Ku antibodies, n (%)	1 (2.3)
Organ involvement	
Digital ulcers, n (%)	14 (32.6)
Abnormal nailfold capillaries, n (%)	26 (60.5)
Telangiectasia, n (%)	12 (27.9)
Raynaud's phenomenon, n (%)	41 (95.3)
Dysphagia, n (%)	10 (23.3)
Interstitial lung disease, n (%)	30 (69.8)
Pulmonary arterial hypertension, n (%)	10 (23.3)
Characteristics of the treatment	
Current steroid therapy, n (%)	16 (37.2)
Current steroid dose, recalculated to methylprednisolone [mg/day]	0 (0–4)
Systemic steroid therapy [years]	0 (0–3)
Immunosuppressive treatment (currently or in the past)	
Azathioprine, n (%)	5 (11.6)
Cyclophosphamide, n (%)	16 (37.2)
Methotrexate, n (%)	12 (27.9)
Mycophenolate mofetil, n (%)	5 (11.6)
Comorbidities	
Hypertension, n (%)	18 (41.9)
Diabetes mellitus, n (%)	3 (7)
Hypercholesterolemia, n (%)	18 (41.9)
Medications	
Angiotensine converting enzyme inhibitors or angiotensin receptor antagonists, n (%)	21 (48.8)
Statins, n (%)	13 (30.2)
Beta-blockers, n (%)	10 (23.3)
Diuretics, n (%)	10 (23.3)
Calcium channel blockers, n (%)	26 (60.5)

Categorical variables are presented as number (percentage), and continuous variables are presented as median and interquartile range (25Q–75Q).

1.2-fold and 2.4-fold higher in SSc than in healthy controls ($p < 0.01$). We found a similar trend of increased serum VEGF levels in the SSc group, however, the difference was

not statistically significant ($p = 0.0501$). Median IL-8 levels were similar in patients and controls. However, the highest levels of IL-8 and VEGF were observed in SSc patients (Fig. 1). Furthermore, there were no differences in the median levels of circulating IL-8, VEGF, bFGF, and IFN- α between diffuse and limited SSc phenotypes (Fig. 2) and regarding organ involvement, such as digital ulcers, abnormal nailfold capillaries, telangiectasia, SSc-ILC, or probable PAH. In addition, internal comorbidities such as arterial hypertension and hypercholesterolemia did not alter cytokine concentrations.

Serum cytokine levels at enrollment were associated with current steroid doses and were higher in patients treated with cyclophosphamide currently or in the past

Expectedly, circulating IFN- α correlated positively with biomarkers of inflammation, such as CRP ($r = 0.42$, $p = 0.005$) and white blood cell count ($r = 0.31$, $p = 0.005$). On the other hand, patients treated with systemic steroids ($n = 16$, 37.2%) or other immunosuppressants at enrollment ($n = 7$, 16.3%) did not differ in terms of studied cytokine levels (Table 4). However, we have documented a positive correlation between the current oral steroid dose and serum levels of IL-8 ($r = 0.46$, $p = 0.002$) and bFGF ($r = 0.34$, $p = 0.025$). Furthermore, patients with IL-8 ≥ 6.02 pg/mL were approx. 3 times more often treated with systemic steroids. Interestingly, patients with VEGF levels ≥ 95.7 pg/mL ($n = 12$) and IFN- $\alpha \geq 3.6$ pg/mL ($n = 14$) required cyclophosphamide therapy more often currently or in the past (approx. 3-fold and 4-fold, respectively).

Other medications used, such as antihypertensives, vasodilators and statins, did not influence studied cytokine levels (data not shown).

Higher circulating VEGF and IFN- α levels at baseline were associated with increased cancer risk, whereas higher IL-8 was documented in patients who died during follow-up

Circulating VEGF elevated by ≥ 232.5 pg/mL and an increase in IFN- α level by ≥ 3.6 pg/mL at baseline were linked with a higher risk of developing a neoplastic disease. During the follow-up for a median of 5 years, 4 SSc patients had been diagnosed with the following: lung cancer ($n = 2$), squamous cell carcinoma of unknown origin ($n = 1$), and multiple myeloma with concomitant breast cancer ($n = 1$).

Furthermore, those with IL-8 levels ≥ 15.3 pg/mL had a 4 times (95% CI: 1.7–10.3) higher risk of death. Nine SSc patients died during the follow-up period. The causes of death included lung cancer ($n = 2$), renal crisis ($n = 1$), multiple-organ failure ($n = 1$), and in 5 cases, the reason of death was unknown.

Table 3. Serum cytokine levels of the study subjects

Studied cytokine	Patients (n = 43)	Controls (n = 24)	Z	p-value
IL-8 [pg/mL]	6.9 (3.5–15.3)	5.2 (4.7–6.6)	0.949	0.3457
VEGF [pg/mL]	87 (55.5–162.9)	60.9 (44.6–84.9)	1.495	0.0501
bFGF [pg/mL]	2.2 (1.8–3.9)	1.8 (0.9–1.8)	2.654	0.0081*
IFN-α [pg/mL]	3.6 (2.3–3.6)	1.5 (0.7–1.5)	5.730	<0.0001*

Continuous variables are presented as median and interquartile range (25Q–75Q). The statistically significant results are marked with an asterisk (*). The value of the z test statistic for the Mann–Whitney U test was presented. bFGF – basic fibroblast growth factor; IFN-α – interferon alpha; IL-8 – interleukin-8; VEGF – vascular endothelial growth factor.

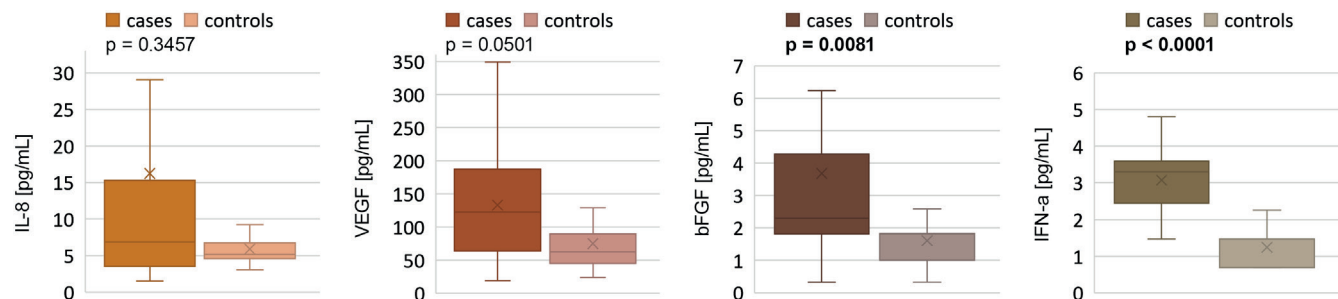


Fig. 1. Serum cytokines of the study subjects. The p-value of the Mann–Whitney U test

bFGF – basic fibroblast growth factor; IFN-α – interferon alpha; IL-8 – interleukin-8; n – number; VEGF – vascular endothelial growth factor. The chart columns represent the range (whiskers), interquartile range (box), median (line), and mean values (X mark).

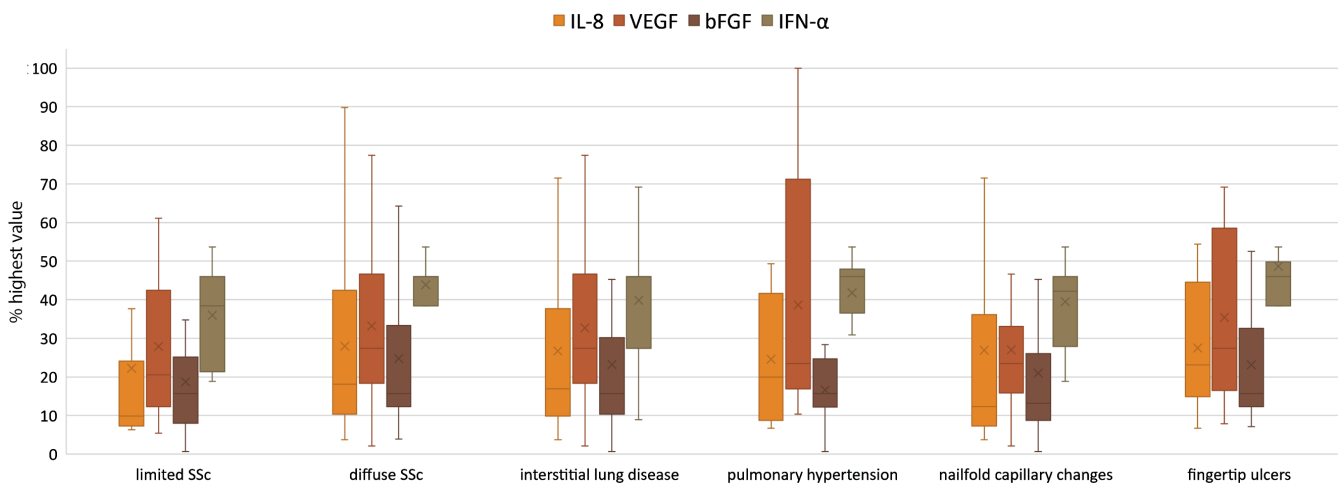


Fig. 2. Relative cytokine levels (% highest value) in different clinical manifestations of systemic sclerosis (SSc)

bFGF – basic fibroblast growth factor; IFN-α – interferon alpha; IL-8 – interleukin-8; n – number; VEGF – vascular endothelial growth factor. The chart columns represent the range (whiskers), interquartile range (box), median (line), and mean values (X mark).

Table 4. Comparison of cytokine levels between patients treated with steroids and immunosuppressants compared to those not receiving these medications at enrollment

Studied cytokine	Patients on steroids (n = 16)	Patients not receiving steroids (n = 27)	z	p-value	Patients on immunosuppressive treatment other than steroids (n = 7)	Patients not receiving immunosuppressive treatment other than steroids (n = 36)	z	p-value
IL-8 [pg/mL]	10.02 (7.09–21.03)	4.37 (2.96–9.79)	2.579	0.27	7.34 (3.54–17.85)	6.85 (3.34–14.65)	0.231	0.997
VEGF [pg/mL]	113.26 (80.11–179.08)	74.34 (51.16–144.16)	1.37	0.38	87.64 (66.62–152.39)	83.54 (55.16–162.93)	0.313	0.56
bFGF [pg/mL]	2.74 (1.81–6.35)	1.86 (1.57–3.31)	1.401	0.47	3.91 (1.81–6.18)	2.15 (1.69–3.46)	0.893	0.14
INF-α [pg/mL]	3.6 (3–3.6)	3 (1.87–3.6)	0.812	0.78	1.48 (1.48–3.6)	3.6 (3–3.6)	–1.705	0.13

Continuous variables are presented as median and interquartile range (25Q–75Q). bFGF – basic fibroblast growth factor; IFN-α – interferon alpha; IL-8 – interleukin-8; VEGF – vascular endothelial growth factor.

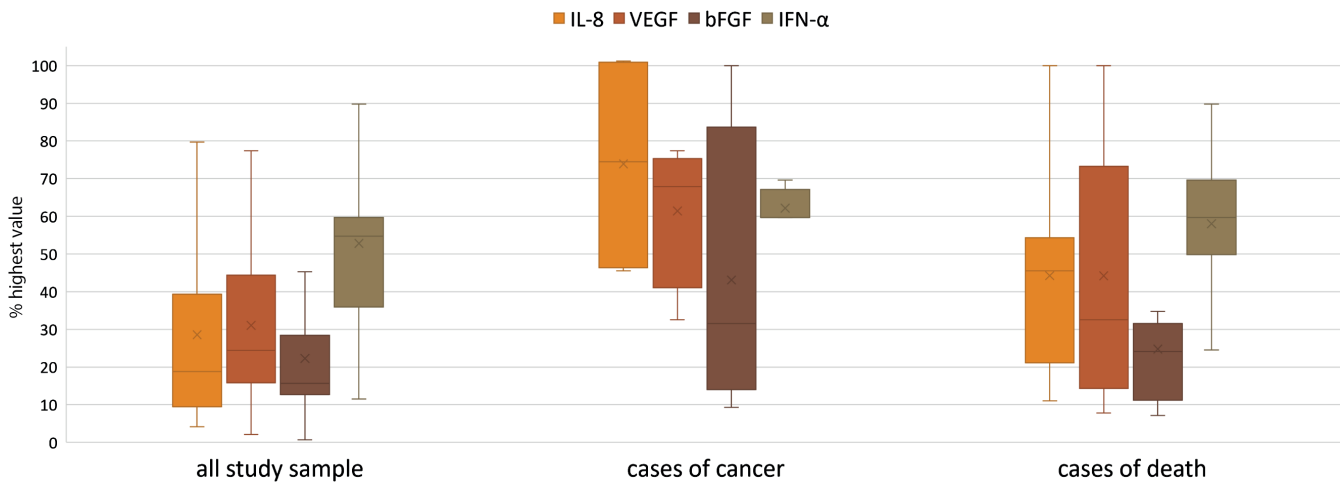


Fig. 3. Relative cytokine levels (% highest value) in different outcomes at follow-up

bFGF – basic fibroblast growth factor; IFN- α – interferon alpha; IL-8 – interleukin-8; VEGF – vascular endothelial growth factor. The chart columns represent the range (whiskers), interquartile range (box), median (line), and mean values (X mark).

The relative levels of the measured cytokines and outcomes at follow-up are presented in Fig. 3.

Independent determinants of higher serum cytokine levels in SSc patients

Multiple linear regression models demonstrated that in SSc, blood hemoglobin concentration was the most potent independent determinant of higher IL-8 levels (Table 5). On the other hand, VEGF correlated with elevated CRP, ALT, and, interestingly, higher maximal pulmonary artery pressure (mPAP) (Table 5). In addition, CRP was the most potent positive predictor of higher bFGF and IFN- α concentrations (Table 5).

Cluster analysis of SSc patients revealed 2 different phenotypes

In a cluster analysis based on laboratory test results, we have distinguished 2 clearly defined phenotypes characterized in Table 6. Both had similar clinical presentation of the disease, but cluster 2 was characterized by a higher ANA titer, increased CRP levels, and elevated levels of all the serum cytokines (Table 6). Patients in cluster 2 were also administered higher oral corticosteroid doses ($p = 0.054$). Furthermore, this cluster contained all but 1 cancer patient (Table 6).

Table 5. Multiple linear regression models showing associations between interleukin-8 (IL-8), vascular endothelial growth factor (VEGF), basic fibroblast growth factor (bFGF), and interferon alpha (IFN- α), with basic laboratory variables and selected clinical features of systemic sclerosis

Studied cytokine	Predictors of cytokine concentration	β	95% CI	R ²	F	p-value
IL-8	Hb [g/dL]	0.399	(0.23–0.57)	0.20	2.89	0.045
	glucose [mmol/L]	–0.243	(–0.4––0.09)			
	lymphocytes [thous/uL]	–0.346	(–0.52––0.18)			
VEGF	CRP [mg/L]	0.228	(0.07–0.38)	0.27	2.97	0.03
	mPAP [mm Hg]	0.286	(0.13–0.44)			
	triglycerides [mmol/L]	–0.309	(–0.47––0.15)			
	ALT [U/L]	0.249	(0.09–0.41)			
bFGF	CRP [mg/L]	0.416	(0.27–0.56)	0.30	5.05	0.005
	ALT [U/L]	0.337	(0.19–0.48)			
	mPAP [mm Hg]	–0.189	(–0.33––0.05)			
IFN- α	CRP [mg/L]	0.575	(0.42–0.73)	0.36	5.01	0.006
	HDL [mmol/L]	0.260	(0.11–0.41)			
	lymphocytes [thous/uL]	0.320	(0.17–0.47)			

For all multiple regressions and all predictors, variance inflation factor (VIF) was <1.3 ; β – standardized regression coefficient; ALT – alanine transaminase; CI – confidence interval; CRP – C-reactive protein; Hb – hemoglobin; HDL – high density lipoprotein; mPAP – maximal pulmonary artery pressure.

Table 6. Two clusters among systemic sclerosis (SSc) patients based on the cytokine profile, clinical features and cancer frequency

Analytes and features		Cluster 1	Cluster 2	p-value
Analyte	IL-8 [pg/mL]	8.22 (4.67–11.77)	34.76 (6.76–76.29)	0.00063*
	VEGF [pg/mL]	67.58 (55.65–79.52)	209.37 (174.74–244)	<0.00001*
	bFGF [pg/mL]	2.41 (1.77–3.06)	4.84 (2.5–7.18)	0.054
	IFN- α [pg/mL]	3.02 (2.46–3.58)	3.59 (3.08–4.1)	0.033*
Feature	age [years]	54.3 (49.32–59.28)	59.31 (52.55–66.07)	0.24
	body mass index [kg/m ²]	24.67 (23.17–26.16)	24.55 (21.94–27.16)	0.93
	duration of the disease [years]	5.95 (3.35–8.55)	6.15 (2.41–9.9)	0.93
	pulmonary artery systolic pressure [mm Hg]	36.19 (33.99–38.38)	39.17 (33.66–44.68)	0.2
	daily methylprednisolone dose [mg/day]	1.47 (0.54–2.39)	4.46 (0.06–8.99)	0.054
	max. ANA [titer]	1:12,000 (1:9,000–15,000)	1:18,000 (1:17,000–21,000)	0.006*
	C-reactive protein [mg/L]	7.22 (4.83–9.6)	13.73 (4.77–22.69)	0.0049*
Patients without cancer, n		28	8	0.025*
Patients with cancer, n		1	3	

Continuous variables are presented as median and interquartile range (25Q–75Q). Categorical variables are presented as numbers. The statistically significant results are marked with an asterisk (*). ANA – antinuclear antibodies; bFGF – basic fibroblast growth factor; IFN- α – interferon alpha; IL-8 – interleukin-8; VEGF – vascular endothelial growth factor.

Discussion

The present study documents that SSc patients have higher serum bFGF and IFN- α levels compared to healthy controls. Furthermore, there was an association between all studied cytokine levels and immunosuppressive treatment. Finally, elevated baseline VEGF and IFN- α levels predisposed to an increased cancer risk, whereas elevated IL-8 was associated with a higher incidence of death during follow-up for a median of 5 years. An increase in pro-angiogenic growth factors, such as bFGF and VEGF, may represent the extent of endothelial damage and an ongoing attempt at angiogenic tissue.²⁸ Previous studies concerning bFGF seem to be controversial. Hummers et al. and Kadono et al. noted that the levels of bFGF in SSc patients were statistically significantly higher than the values found in controls, while Distler et al. did not confirm that observation.^{20,28,30} In line with our results, Hummers et al. did not find bFGF to correlate with any clinical measures, including concomitant vascular disease.²⁸ Other researchers have demonstrated the elevation of circulating VEGF in SSc patients, that can normalize during immunosuppressive therapy.^{16,18,20,31–34} Hummers et al. indicated that higher serum levels of VEGF are more frequent in the earliest stages of the disease and in those without peripheral ulcers, therefore, VEGF plays a protective role against ischemic manifestations.²⁸ Choi et al. highlighted that patients with dcSSc had elevated levels of serum VEGF compared to lcSSc.³² Compared to Hashimoto et al., they underlined that circulating VEGF levels positively correlated with the extent of skin involvement and were inversely correlated with nailfold capillary density.^{32,34} However, similar to our results, no significant differences were found by Hummers et al. and Choi et al. in the levels

of circulating VEGF between SSc patients with and without organ involvement.^{28,32} Papaioannou et al. reported an association between serum VEGF levels and systemic pulmonary artery pressure (sPAP), suggesting a potential role of this growth factor in the pathogenesis of PAH in the course of SSc,¹⁶ which was in line with our results. De Santis et al. confirmed an association between elevated VEGF levels and ILD.³³ Unlike previous studies, we did not find a relationship between VEGF and disease subtype or SSc duration.^{16,28,29,32,34}

Also, we did not find any correlation between IFN- α , elevated in the SSc cases, and clinical manifestations of the disease or basic laboratory abnormalities. On the contrary, data presented by Kim et al. suggest that IFN- α may be higher in dcSSc as compared to lcSSc patients, and higher in cases of SSc-associated lung fibrosis, suggesting that IFN- α may play a role in tissue injury.⁸ These observations are in line with results presented by Chizzolini et al.,^{5,8} stating that ubiquitous antigens, including topoisomerase-1, promote the production of IFN- α , probably by interacting with Toll-like receptors.⁵ Interestingly, Black et al. claimed that the treatment with IFN- α may, in fact, be deleterious in SSc.⁷

Opposite to our findings, data presented by Wu et al. show that SSc patients seem to have a higher incidence of elevated IL-8 levels compared to unaffected controls.³⁵ Gourh et al. stated that higher IL-8 level was associated with more severe restrictive lung disease at the baseline visit,³⁶ consistent with the results of Schmidt et al., who found that elevated IL-8 in bronchoalveolar lavage was correlated with SSc-ILD and worse results of lung function tests.³⁷ In contrast, we could not find any correlation of IL-8 with organ involvement, similar to McMahan et al., who found no significant associations between serum IL-8 levels and skin score or disease duration.³⁸

In our dataset, SSc patients with elevated VEGF and IFN- α levels had a higher frequency of cancers, which was not described by other authors.^{16,18,20,28,31–34} Previous investigations have confirmed that VEGF is a crucial mediator in cancer development affecting angiogenesis in patients without SSc, and is upregulated by oncogene expression, many growth factors and hypoxia.^{24,39–41} In turn, IFN- α is a central immunomodulatory agent relevant in all stages of cancer development, conferring effects from an anti-tumor enhancement of the immune response in early stages to immunosuppressive function exploited through deregulated transcription of pro-tumorigenic IFN-stimulated genes, thus contributing to cancer escape in later stages.⁴²

The higher incidence of death in SSc patients with elevated baseline IL-8 levels merits comment. The analogous observation was described in patients with cancers and without coexisting SSc.^{23,24} Moreover, Ma et al. suggested that elevated serum IL-8 levels might help identify patients with a poor prognosis due to cancer, who may benefit from more aggressive disease management.²⁴ However, only 2 out of 9 fatal outcomes in our follow-up could be attributed to cancer. Further studies are needed to assess whether smoking and diabetes alter the clinical course of the disease and whether the studied cytokines may serve as biomarkers of disease progression or the need for immunosuppressive treatment as well as predictors of prognosis or risk of cancer in SSc patients.

Limitations

Our research included a limited number of patients and underpowered statistical tests used in the subgroup analyses, which may be the cause for the lack of clinical correlations that have been previously found in the datasets of other authors. Additionally, patients underwent different immunosuppressive treatments, therefore, the drugs might have impacted our results. Finally, it was challenging to provide the time of first SSc symptoms since many of them are silent or unspecific for that disease (e.g., weakness, arthralgia, dyspnea). Therefore, we could not reliably report their beginning, including the Raynaud's phenomenon.

The observational design of the study does not allow for inferring of causal relations between the studied cytokines and clinical outcomes.

Conclusions

In summary, SSc is characterized by elevated bFGF and IFN- α serum levels, regardless of organ involvement. Furthermore, elevated IFN- α and VEGF serum levels might be linked with the development of cancer, whereas elevated IL-8 levels are associated with a higher death risk during a 5-year follow-up. Further research studies are necessary to verify our findings.

ORCID iDs

Joanna Kosalka-Węgiel  <https://orcid.org/0000-0003-1013-2253>
 Sabina Lichołai  <https://orcid.org/0000-0001-7008-2492>
 Sylwia Dziejczak  <https://orcid.org/0000-0002-7760-9864>
 Piotr Kuzmierz  <https://orcid.org/0000-0002-2031-6657>
 Anna Korona  <https://orcid.org/0000-0001-7590-7318>
 Mariusz Korkosz  <https://orcid.org/0000-0002-1749-9739>
 Aleksandra Matyja-Bednarczyk  <https://orcid.org/0000-0003-4038-5016>
 Andżelika Siwiec-Koźlik  <https://orcid.org/0000-0003-2258-0248>
 Wojciech Sydor  <https://orcid.org/0000-0002-5323-3890>
 Joanna Wilańska  <https://orcid.org/0000-0001-8914-1042>
 Lech Zaręba  <https://orcid.org/0000-0002-2221-614X>
 Weronika Pocij-Marciak  <https://orcid.org/0000-0003-1766-1035>
 Jerzy Dropiński  <https://orcid.org/0000-0002-0768-5597>
 Marek Sanak  <https://orcid.org/0000-0001-7635-8103>
 Jacek Musiał  <https://orcid.org/0000-0002-0955-1808>
 Stanisława Bazan-Socha  <https://orcid.org/0000-0001-9634-0963>

References

- Romano E, Rosa I, Fioretto BS, Guiducci S, Manetti M, Matucci-Cerinic M. A new avenue in the pathogenesis of systemic sclerosis: The molecular interface between the endothelial and the nervous systems. *Clin Exp Rheumatol*. 2019;37 Suppl 119(4):133–140. PMID:31025932.
- Kuzmierz P, Pacholczak-Madej R, Siwiec A, et al. Thrombin generation potential is enhanced in systemic sclerosis: Impact of selected endothelial biomarkers. *Clin Exp Rheumatol*. 2021;39 Suppl 131(4):13–19. doi:10.55563/clinexprheumatol/d03dnc
- Cantero-Nieto L, Álvarez-Cienfuegos A, García-Gómez JA, Ríos-Fernández R, Robledo G, Ortego-Centeno N. Association between FGF-23 levels and risk of fracture in women with systemic sclerosis. *J Clin Densitom*. 2021;24(3):362–368. doi:10.1016/j.jocd.2020.05.010
- Cantero-Nieto L, Alvarez-Cienfuegos A, García-Gómez JA, Martin J, González-Gay MA, Ortego-Centeno N. Role of fibroblast growth factor-23 in calcinosis in women with systemic sclerosis. *Acta Reumatol Port*. 2020;45(4):259–264. PMID:33420766.
- Chizzolini C, Brembilla NC, Montanari E, Truchetet ME. Fibrosis and immune dysregulation in systemic sclerosis. *Autoimmun Rev*. 2011;10(5):276–281. doi:10.1016/j.autrev.2010.09.016
- Rentka A, Hársfalvi J, Berta A, et al. Vascular endothelial growth factor in tear samples of patients with systemic sclerosis. *Mediators Inflamm*. 2015;2015:573681. doi:10.1155/2015/573681
- Black CM, Silman AJ, Herrick AL, et al. Interferon-alpha does not improve outcome at one year in patients with diffuse cutaneous scleroderma: Results of a randomized, double-blind, placebo-controlled trial. *Arthritis Rheum*. 1999;42(2):299–305. doi:10.1002/1529-0131(199902)42:2<299::AID-ANR12>3.0.CO;2-R
- Kim D, Peck A, Santer D, et al. Induction of interferon- α by scleroderma sera containing autoantibodies to topoisomerase I: Association of higher interferon- α activity with lung fibrosis. *Arthritis Rheum*. 2008;58(7):2163–2173. doi:10.1002/art.23486
- Pacholczak-Madej R, Kuzmierz P, Bazan-Socha S, et al. Endothelial dysfunction in patients with systemic sclerosis. *Postepy Dermatol Alergol*. 2020;37(4):495–502. doi:10.5114/ada.2019.83501
- Ahmadi R, Hajjalilo M, Ghorbanihaghjo A, et al. FGF-23, klotho and vitamin D levels in scleroderma. *Iran J Public Health*. 2017;46(4):530–536. PMID:28540270.
- Iannone F, Praino E, Rotondo C, et al. Body mass index and adipokines/cytokines dysregulation in systemic sclerosis. *Clin Exp Immunol*. 2021;206(2):153–160. doi:10.1111/cei.13651
- Shirai Y, Okazaki Y, Inoue Y, et al. Elevated levels of pentraxin 3 in systemic sclerosis: Associations with vascular manifestations and defective vasculogenesis. *Arthritis Rheumatol*. 2015;67(2):498–507. doi:10.1002/art.38953
- Kikuchi K, Hoashi T, Kanazawa S, Tamaki K. Angiogenic cytokines in serum and cutaneous lesions of patients with polyarteritis nodosa. *J Am Acad Dermatol*. 2005;53(1):57–61. doi:10.1016/j.jaad.2005.02.018
- Lawrence A, Khanna D, Misra R, Aggarwal A. Increased expression of basic fibroblast growth factor in skin of patients with systemic sclerosis. *Dermatol Online J*. 2006;12(1):2. PMID:16638370.
- Müller-Ladner U, Distler O, Ibba-Manneschi L, Neumann E, Gay S. Mechanisms of vascular damage in systemic sclerosis. *Autoimmunity*. 2009;42(7):587–595. doi:10.1080/08916930903002487

16. Papaioannou AI, Zakyntinos E, Kostikas K, et al. Serum VEGF levels are related to the presence of pulmonary arterial hypertension in systemic sclerosis. *BMC Pulm Med*. 2009;9:18. doi:10.1186/1471-2466-9-18
17. Ding S, Liang Y, Zhao M, et al. Decreased microRNA-142-3p/5p expression causes CD4+ T cell activation and B cell hyperstimulation in systemic lupus erythematosus. *Arthritis Rheum*. 2012;64(9):2953–2963. doi:10.1002/art.34505
18. Zhan H, Li H, Liu C, Cheng L, Yan S, Li Y. Association of circulating vascular endothelial growth factor levels with autoimmune diseases: A systematic review and meta-analysis. *Front Immunol*. 2021;12:674343. doi:10.3389/fimmu.2021.674343
19. Allanore Y, Borderie D, Airo P, et al. Lack of association between three vascular endothelial growth factor gene polymorphisms and systemic sclerosis: Results from a multicenter EUSTAR study of European Caucasian patients. *Ann Rheum Dis*. 2007;66(2):257–259. doi:10.1136/ard.2006.054346
20. Distler O, Del Rosso A, Giacomelli R, et al. Angiogenic and angiostatic factors in systemic sclerosis: Increased levels of vascular endothelial growth factor are a feature of the earliest disease stages and are associated with the absence of fingertip ulcers. *Arthritis Res*. 2002;4(6):R11. doi:10.1186/ar596
21. De Ceuninck F, Duguet F, Aussy A, Laigle L, Moingeon P. IFN- α : A key therapeutic target for multiple autoimmune rheumatic diseases. *Drug Discov Today*. 2021;26(10):2465–2473. doi:10.1016/j.drudis.2021.06.010
22. Nielepkowicz-Goździńska A, Fendler W, Robak E, et al. Exhaled IL-8 in systemic lupus erythematosus with and without pulmonary fibrosis. *Arch Immunol Ther Exp (Warsz)*. 2014;62(3):231–238. doi:10.1007/s00005-014-0270-5
23. Schalper KA, Carleton M, Zhou M, et al. Elevated serum interleukin-8 is associated with enhanced intratumor neutrophils and reduced clinical benefit of immune-checkpoint inhibitors. *Nat Med*. 2020;26(5):688–692. doi:10.1038/s41591-020-0856-x
24. Ma Y, Ren Y, Dai ZJ, Wu CJ, Ji YH, Xu J. IL-6, IL-8 and TNF- α levels correlate with disease stage in breast cancer patients. *Adv Clin Exp Med*. 2017;26(3):421–426. doi:10.17219/acem/62120
25. Van Den Hoogen F, Khanna D, Fransen J, et al. 2013 classification criteria for systemic sclerosis: An American College of Rheumatology/European League against Rheumatism collaborative initiative. *Arthritis Rheum*. 2013;65(11):2737–2747. doi:10.1002/art.38098
26. LeRoy EC, Medsger TA. Criteria for the classification of early systemic sclerosis. *J Rheumatol*. 2001;28(7):1573–1576. PMID:11469464.
27. Mukerjee D, St George D, Knight C, et al. Echocardiography and pulmonary function as screening tests for pulmonary arterial hypertension in systemic sclerosis. *Rheumatology (Oxford)*. 2004;43(4):461–466. doi:10.1093/rheumatology/keh067
28. Hummers LK, Hall A, Wigley FM, Simons M. Abnormalities in the regulators of angiogenesis in patients with scleroderma. *J Rheumatol*. 2009;36(3):576–582. doi:10.3899/jrheum.080516
29. Rajkumar VS, Sundberg C, Abraham DJ, Rubin K, Black CM. Activation of microvascular pericytes in autoimmune Raynaud's phenomenon and systemic sclerosis. *Arthritis Rheum*. 1999;42(5):930–941. doi:10.1002/1529-0131(199905)42:5<930::AID-ANR11>3.0.CO;2-1
30. Kadono T, Kikuchi K, Kubo M, Fujimoto M, Tamaki K. Serum concentrations of basic fibroblast growth factor in collagen diseases. *J Am Acad Dermatol*. 1996;35(3 Pt 1):392–397. doi:10.1016/S0190-9622(96)90603-9
31. Mittag M, Beckheirich P, Hausteil UF. Systemic sclerosis-related Raynaud's phenomenon: Effects of iloprost infusion therapy on serum cytokine, growth factor and soluble adhesion molecule levels. *Acta Derm Venereol*. 2001;81(4):294–297. doi:10.1080/00015550152572976
32. Choi JJ, Min DJ, Cho ML, et al. Elevated vascular endothelial growth factor in systemic sclerosis. *J Rheumatol*. 2003;30(7):1529–1533. PMID:12858453.
33. De Santis M, Ceribelli A, Cavaciocchi F, et al. Nailfold videocapillaroscopy and serum VEGF levels in scleroderma are associated with internal organ involvement. *Autoimmun Highlights*. 2016;7(1):5. doi:10.1007/s13317-016-0077-y
34. Hashimoto N, Iwasaki T, Kitano M, Ogata A, Hamano T. Levels of vascular endothelial growth factor and hepatocyte growth factor in sera of patients with rheumatic diseases. *Mod Rheumatol*. 2003;13(2):129–134. doi:10.3109/s10165-002-0211-8
35. Wu B, Wang W, Zhan Y, et al. CXCL13, CCL4, and sTNFR as circulating inflammatory cytokine markers in primary and SLE-related autoimmune hemolytic anemia. *J Transl Med*. 2015;13:112. doi:10.1186/s12967-015-0474-4
36. Gourh P, Arnett FC, Assassi S, et al. Plasma cytokine profiles in systemic sclerosis: Associations with autoantibody subsets and clinical manifestations. *Arthritis Res Ther*. 2009;11(5):R147. doi:10.1186/ar2821
37. Schmidt K, Martinez-Gamboa L, Meier S, et al. Bronchoalveolar lavage fluid cytokines and chemokines as markers and predictors for the outcome of interstitial lung disease in systemic sclerosis patients. *Arthritis Res Ther*. 2009;11(4):R111. doi:10.1186/ar2766
38. McMahan Z, Schoenhoff F, Van Eyk JE, Wigley FM, Hummers LK. Biomarkers of pulmonary hypertension in patients with scleroderma: A case-control study. *Arthritis Res Ther*. 2015;17(1):201. doi:10.1186/s13075-015-0712-4
39. Carmeliet P. VEGF as a key mediator of angiogenesis in cancer. *Oncology*. 2005;69 Suppl 3:4–10. doi:10.1159/000088478
40. Frezzetti D, Gallo M, Maiello MR, et al. VEGF as a potential target in lung cancer. *Expert Opin Ther Targets*. 2017;21(10):959–966. doi:10.1080/14728222.2017.1371137
41. Alevizakos M, Kaltsas S, Syrigos KN. The VEGF pathway in lung cancer. *Cancer Chemother Pharmacol*. 2013;72(6):1169–1181. doi:10.1007/s00280-013-2298-3
42. Vidal P. Interferon α in cancer immunoediting: From elimination to escape. *Scand J Immunol*. 2020;91(5):e12863. doi:10.1111/sji.12863

Distal symmetrical polyneuropathy in diabetes mellitus patients: Proposition of a new scoring system based on electroneurography findings

Jakub Stepień^{1,A,B-D}, Żanna Pastuszek^{2,A-C,E,F}

¹ Insula Clinical Trials Center, Warsaw, Poland

² Laboratory of Preclinical Research and Environmental Agents, Mossakowski Medical Research Institute, Polish Academy of Sciences, Warsaw, Poland

A – research concept and design; B – collection and/or assembly of data; C – data analysis and interpretation; D – writing the article; E – critical revision of the article; F – final approval of the article

Advances in Clinical and Experimental Medicine, ISSN 1899–5276 (print), ISSN 2451–2680 (online)

Adv Clin Exp Med. 2024;33(4):379–385

Address for correspondence

Jakub Stepień
E-mail: jakub.stepien@o2.pl

Funding sources

None declared

Conflict of interest

None declared

Received on December 20, 2022

Reviewed on April 5, 2023

Accepted on June 19, 2023

Published online on July 24, 2023

Abstract

Background. Neuropathy affects 25% of people with diabetes mellitus. The evaluation of disease severity is still a challenge for modern medicine. Many screening instruments are based primarily on clinical criteria. There is a lack of a simple, reliable and precise scoring system that could improve the classification of neuropathy and monitor disease progression using not only clinical criteria but also electroneurography. There is a need to find sensitive neurography parameters that reflect peripheral nerve impairments in this group of patients.

Objectives. This study aimed to create a scoring system for diabetic neuropathy, based on electroneurography criteria, that reflects the natural course of the disease. A new scoring system will improve the treatment of patients with diabetes mellitus.

Materials and methods. A total of 113 patients with distal symmetrical polyneuropathy (DSPN) were involved in the study. Median, ulnar, sural, tibial, and peroneal nerves were examined. Parameters such as amplitude, conduction velocity, distal latency, and F wave latency were analyzed. The results of nerve conduction studies in the investigated group were compared to those of the control group, which consisted of 61 healthy volunteers.

Results. The most sensitive parameter of peripheral nerve impairment severity was a reduction of the sensory action potential amplitude in the peroneal nerve by 72.8% ($p < 0.05$). The observation of changes in sensory action potential amplitudes in the peroneal nerve is the most important element of our scoring system.

Conclusions. A new electroneurography scoring system of DSPN severity should be based on sensory and motor action potential amplitudes that reflect axonal loss in the examined nerves and the nature of the disease.

Key words: diabetes mellitus, classification, peroneal nerve, nerve conduction studies, diabetic neuropathies

Cite as

Stepień J, Pastuszek Ż. Distal symmetrical polyneuropathy in diabetes mellitus patients: Proposition of a new scoring system based on electroneurography findings.

Adv Clin Exp Med. 2024;33(4):379–385.

doi:10.17219/acem/168504

DOI

10.17219/acem/168504

Copyright

Copyright by Author(s)

This is an article distributed under the terms of the Creative Commons Attribution 3.0 Unported (CC BY 3.0) (<https://creativecommons.org/licenses/by/3.0/>)

Background

Neuropathy affects 25% of people with diabetes mellitus. This disease is the leading known cause of neuropathy in developed countries and is implicated in 50–75% of nontraumatic amputations.^{1–4} Distal symmetrical polyneuropathy (DSPN) is the most common presentation of the disease. A glove–stocking distribution of numbness, sensory loss, dysesthesia, loss of reflexes, and nighttime pain are the most common symptoms.^{5,6} Ulcers, infections, as well as fractures of the knees, ankles or feet are the most common complications of the disease. Distal symmetrical polyneuropathy is associated with significant morbidity and increased mortality. The most important risk factor for developing DSPN in type 1 diabetes mellitus is poor glycemic control.^{7–9} Pathophysiology of the disease remains elusive, but nerve biopsies from patients with diabetic neuropathy revealed degeneration of both myelinated and unmyelinated fibers.^{10–12} Peripheral nerve impairment in patients with diabetes mellitus may be connected to mitochondrial malfunction. This organelle is responsible for the production of energy. Its dysfunction is connected to the activation of the tryptophan–kynurenine metabolic system that has an impact on tryptophan metabolism.^{13–15} Tryptophan is an endogenous amino acid necessary for protein synthesis and a precursor to the synthesis of bioactive molecules, including nicotinamide adenine dinucleotide.¹⁶ It undergoes transformations, leading to the formation of kynurenines, the role of which is to regulate the excitability of neurons as well as the response of immune cells.¹⁷ Kynurenine has a role in processing neurogenic inflammation by affecting glutamate receptors.^{18–20}

In another study, the increased plasma levels of proinflammatory factors such as tumor necrosis factor alpha (TNF- α) and intercellular adhesion molecule 1 (ICAM-1) were connected to polyneuropathy incidence in diabetes patients.²¹ Metabolic changes induced by hyperglycemia lead to dysregulation of cytokine control. Another study revealed that in patients with DSPN, interleukin (IL)-1, IL-6, leukemia inhibitory factor (LIF), ciliary neurotrophic factor (CNTF), and transforming growth factor beta (TGF- β) production is more intense than in healthy patients.^{22,23} A study by Behse and Buchthal revealed that in the blood of patients with diabetic polyneuropathy, the levels of IL-10 were lower than in healthy individuals.²⁴ A clinical investigation of nerve biopsies in neuropathic patients revealed upregulated TNF- α expression in human Schwann cells.²⁵

The diagnosis of DSPN is primarily clinical, and its most important part is the physical examination, including neurologic testing. Nerve conduction studies (NCSs) play an important role in the diagnostic process, especially in patients with minimal or no objective symptoms, and are the most useful in patients with large fiber neuropathy.^{26–29} Other forms of neuropathy that occur in diabetes mellitus include mononeuropathies, cranial neuropathies,

plexopathies, radiculopathy, amyotrophy, autonomic neuropathy, and small fiber neuropathy. Moreover, chronic inflammatory demyelinating neuropathy is more common in diabetic patients.^{30–32}

Many screening instruments based mainly on clinical criteria have been developed to evaluate the severity of diabetic neuropathy. Most of them are time-consuming and require a precise neurological examination. There is a lack of a simple, objective scoring system using electro-neurographic parameters that could help monitor disease progression with the use of objective criteria, especially in patients in the initial stage of DSPN.^{33,34}

Objectives

This study aimed to confirm the hypothesis that DSPN affects primarily sensory nerve fibers in the legs and leads mainly to axonal loss.^{35,36} Our study is an attempt to create a simple scoring system with the use of objective parameters of nerve conduction that will reflect the natural course of the disease.³⁷ We propose a simple, clear system of the classification of the severity of neuropathy that can be used by neurologists and other clinical practitioners to evaluate the severity of neuropathy and monitor disease progression in patients with DSPN.³⁸

Materials and methods

This retrospective study investigated a group of 113 patients (53 females and 60 males) with DSPN due to diabetes mellitus. All patients in the investigated group were diagnosed at the Electromyography and Nerve Conduction Laboratory in Warsaw, Poland. The mean age in the group was 59.27 years (standard deviation (SD) \pm 13.66). Additionally, a control group of 61 healthy volunteers with a mean age of 41.70 (\pm 18.37) years were included. The size of the study and control groups was estimated based on statistical methodology. Patients with alcohol addiction, post-oncologic treatment, kidney and thyroid diseases, and other potential causes of peripheral nerve impairments were excluded from the study. In all patients, a NCS was performed after obtaining the approval of the Bioethical Committee of Military Institute of Medicine (approval No. 14/WIM/2021). The median, ulnar, sural, tibial, and peroneal nerves were examined. Parameters such as amplitude, conduction velocity, distal latency, and F wave latency were analyzed.

Sensory studies were performed antidromically. In the case of the ulnar nerve sensory action potential, the recording electrode was placed on the 5th finger, while for the median nerve, it was placed on the 2nd finger. The sural nerve was stimulated on the posterolateral aspect of the lower third of the leg, and the distance between the recording electrode and the stimulating one

was approx. 14 cm. For ulnar nerve motor fibers, the recording electrode was placed over the abductor digiti minimi muscle. In the case of median nerve motor fibers, the recording electrode was placed over the abductor pollicis brevis muscle. For the peroneal nerve, the recording electrode was placed over the extensor digitorum brevis, whereas the abductor hallucis muscle was used for the placement of the recording electrode for the tibial nerve. The distance between the recording electrode and the stimulating electrode was 8 cm in the testing of all motor nerves. Locations of stimulating and recording electrodes in the case of all examined nerves were typical, as presented in previous studies.^{39,40} Motor and sensory NCSs were performed in an environment with a temperature of 21–25°C, as are the optimal parameters for electroneurography.⁴¹

The results of the NCSs in the investigated group were compared to those of the controls. Nerves were ranked depending on the degree of impairment to create the scoring system. Normal distribution of variables was obtained in the case of the conduction velocity in sensory fibers, as well as F wave latency of the median nerve, F wave latency of the ulnar nerve, conduction velocity in sensory fibers of the peroneal nerve, and conduction velocity in sensory fibers of the sural nerve. In the remaining cases, the distribution of variables was non-normal. Student's t-test or Mann–Whitney U tests were used to statistically analyze the data.

Results

The analysis with the use of the Mann–Whitney U test revealed that both amplitude and conduction velocity of sensory action potentials of the sural, peroneal, median, and ulnar nerves were reduced in the investigated group when compared to controls. Moreover, the analysis with the use of the same test revealed a reduction in the amplitude and conduction velocity, as well as elongation of distal latency and F wave latency of motor action potentials in the tibial, peroneal, median, and ulnar nerves in comparison to controls. Based on that data, we have created diagnostic criteria for the impairment of all investigated nerves (Tables 1–5). In the case of the conduction velocity of sensory action potentials, the differences between the 2 analyzed groups were compared using the Student's t-test (regarding the peroneal and sural nerves). The Mann–Whitney U test was used in the case of all other nerves (Table 3).

The mean amplitude of sensory action potentials in the investigated group was significantly lower in comparison to controls. The most significant reduction of amplitude in the investigated group compared to controls was observed in the peroneal nerve (72.8%, $p < 0.05$ using the Mann–Whitney U test).

Moreover, the values of sensory action potential amplitudes for the sural, peroneal, median, and ulnar nerves where impairment was present are depicted in Table 1 and Fig. 1.

Table 1. Amplitude of sensory action potential in investigated and control groups [μV] using Mann–Whitney U test

Nerve	Group	n	M	95% CI	95% CI	Me	Q1	Q3	Statistical significance
Median	investigated	113	12.82	10.51	15.12	10.00	4.00	18.00	U = -5.58615, p = 0.000000
	control	61	20.87	18.52	23.23	20.00	15.00	23.00	
Ulnar	investigated	110	12.86	10.36	15.36	9.00	5.00	16.00	U = -6.72478, p = 0.000000
	control	61	22.96	20.83	25.09	23.00	17.00	27.00	
Peroneal	investigated	113	3.19	2.58	3.80	2.00	0.50	5.00	U = -9.56193, p = 0.000000
	control	61	10.73	9.72	11.75	9.00	7.30	14.00	
Sural	investigated	112	4.91	3.98	5.83	4.00	1.00	8.00	U = -8.37706, p = 0.000000
	control	61	13.11	11.63	14.59	12.00	9.00	16.00	

95% CI – 95% confidence interval; Me – median; M – mean.

Table 2. Amplitude of motor action potential in investigated and control groups [mV] using Mann–Whitney U test

Nerve	Group	n	M	95% CI	95% CI	Me	Q1	Q3	Statistical significance
Median	investigated	112	7.07	6.61	7.54	6.90	5.60	8.80	U = -2.31339, p = 0.020702
	control	61	8.31	7.62	9.00	7.80	6.00	10.30	
Ulnar	investigated	110	8.87	8.26	9.47	9.35	7.10	11.20	U = -4.04598, p = 0.000052
	control	61	10.93	10.43	11.43	11.00	9.40	12.20	
Peroneal	investigated	113	7.94	6.95	8.93	8.10	4.00	11.20	U = -7.21846, p = 0.000000
	control	61	14.62	13.46	15.78	14.70	11.00	17.90	
Tibial	investigated	113	3.73	3.29	4.17	3.50	2.10	5.60	U = -3.54290, p = 0.000396
	control	61	5.04	4.59	5.49	4.70	4.00	5.70	

95% CI – 95% confidence interval; Me – median; M – mean.

Table 3. Conduction velocity of sensory action potentials in investigated and control groups [ms] using Mann–Whitney U test (median, ulnar nerves) and Student's t test (peroneal, sural nerves)

Nerve	Group	n	M	95% CI	95% CI	Me	Q1	Q3	Statistical significance
Median	investigated	98	44.79	43.55	46.02	45.00	40.00	49.00	U = 9.28889, p = 0.000000
	control	61	55.72	54.64	56.81	56.00	52.00	59.00	
Ulnar	investigated	97	43.27	42.17	44.36	43.00	40.00	47.00	U = 9.56644, p = 0.000000
	control	61	54.25	53.25	55.25	54.00	51.50	57.00	
Peroneal	investigated	84	41.48	40.29	42.67	42.00	37.50	45.00	t = -8.05598, p = 0.000000
	control	61	48.50	47.29	49.72	48.00	45.00	52.00	
Sural	investigated	85	42.56	41.48	43.65	43.00	39.00	46.00	t = -7.14204, p = 0.000000
	control	61	48.12	47.09	49.15	48.00	45.00	50.00	

95% CI – 95% confidence interval; Me – median; M – mean.

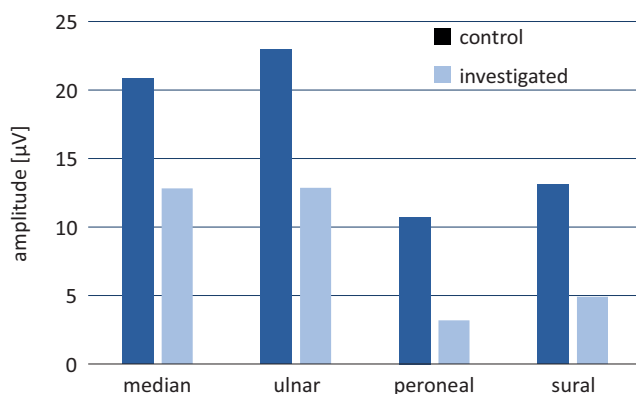
Table 4. Conduction velocity of motor action potentials in investigated and control group [ms] using Mann–Whitney U test

Nerve	Group	n	M	95% CI	95% CI	Me	Q1	Q3	Statistical significance
Median	investigated	110	51.43	50.26	52.60	52.00	48.00	55.00	U = -7.99026, p = 0.000000
	control	61	58.70	57.84	59.56	58.00	56.00	61.00	
Ulnar	investigated	108	53.44	52.09	54.79	53.50	50.00	58.00	U = -3.59515, p = 0.000324
	control	61	57.68	56.27	59.09	58.00	53.00	61.00	
Tibial	investigated	101	40.18	39.14	41.23	41.00	37.00	44.00	U = -7.86278, p = 0.000000
	control	61	47.45	46.38	48.51	47.00	44.00	50.00	
Peroneal	investigated	101	42.62	41.52	43.73	44.00	39.00	46.00	U = -6.55305, p = 0.000000
	control	61	48.53	47.45	49.61	48.20	46.00	51.00	

95% CI – 95% confidence interval; Me – median; M – mean.

Table 5. Distal symmetrical polyneuropathy (DSPN) scoring system

Neuropathy severity	Criteria
Grade I (minimal)	reduction of sensory action potential amplitude of peroneal and sural nerves
Grade II (mild)	reduction of sensory action potential amplitude of peroneal and sural nerves and of sensory fibers in at least 1 nerve in upper limbs
Grade III (moderate)	reduction of sensory action potential amplitude of peroneal and sural nerves and of sensory fibers in at least 1 nerve in upper limbs; additionally, the reduction of motor potential amplitude in peroneal or tibial nerves must be observed
Grade IV (severe)	reduction of sensory action potential amplitude of peroneal and sural nerves and of sensory fibers in at least 1 nerve in upper limbs; additionally, the reduction of motor potential amplitude in peroneal, tibial as well as median or ulnar nerves must be observed
Grade V (extremal)	no response from sensory and motor fibers in lower limbs and in sensory fibers in upper limbs; response in motor fibers in upper limbs may be observed

**Fig. 1.** Mean amplitude of sensory action potential in investigated and control groups [µV]

The mean amplitude of motor action potentials in the investigated group was statistically significantly lower in comparison to controls. The most significant reduction of amplitude in the investigated group compared to controls was observed in the peroneal nerve (45%, $p < 0.05$ using the Mann–Whitney U test). Moreover, the values of motor action potential amplitudes for tibial, peroneal, median, and ulnar nerve impairments are presented in Table 2.

Mean conduction velocity of sensory action potentials in the investigated group was statistically significantly lower in comparison to controls. The most significant reduction of conduction velocity in the investigated group compared to controls was observed in the median nerve

(19.6%, $p < 0.05$, Mann–Whitney U test). Moreover, the values of sensory action potential conduction velocities for sural, peroneal, median, and ulnar nerve impairments are presented in Table 3.

The mean conduction velocity of motor action potentials was statistically significantly lower in the investigated group when compared to controls. The most significant reduction of conduction velocity in the investigated group compared to controls was observed in the median (12.38%) and peroneal (12.17%) nerves ($p < 0.05$, Mann–Whitney U test). Values for tibial, peroneal, median, and ulnar nerve impairments are presented in Table 4.

The mean distal latency of motor action potentials in the investigated group was statistically significantly lower in comparison to controls. The most significant reduction of distal latency in the investigated group compared to controls was observed in the median nerve (24.1%, $p < 0.05$, Mann–Whitney U test; data not shown).

The mean F wave latency of motor action potentials in the investigated group was statistically significantly longer in comparison to controls. The most significant reduction of F wave latency in the investigated group compared to controls was observed in the median nerve (13%, $p < 0.05$, Mann–Whitney U test; data not shown).

In the present study, the biggest difference in conduction parameters between the examined nerves in the investigated group was observed in the amplitude of both motor and sensory action potentials. The most sensitive parameter of the severity of peripheral nerve impairments was the reduction of sensory action potential amplitude in the peroneal nerve. Similar observations were made for the amplitude of sensory and motor action potentials in other examined nerves. In the case of the conduction velocity as well as distal and F wave latencies, that connection was not so evident.

Taking those data into consideration, we have created a simple scoring system presented in Table 5. We propose the working name “SAP (sensory amplitude potential) – reduction scale” for this scoring scale with stratification of severity.

Discussion

The evaluation of severity of neuropathy remains a challenge for modern medicine.⁴² Many scales have been proposed to resolve this problem, but each of them has its limitations. In many cases, a relationship between a patient’s clinical status and NCS results does not exist. Severely disabled patients with neuropathies can have mild NCS results, and the converse relationship is also often observed. Moreover, the ideal scoring system should reflect the natural disease course and include only objective parameters. Distal symmetrical polyneuropathy is the most common polyneuropathy among patients with diabetes mellitus. Electromyography plays an important role in the diagnosis

and disease progression monitoring, especially in patients in the initial phases of neuropathy when symptoms can be subtle.^{43–45} Moreover, clinical evaluation of disease progression can also be subjective and new objective and more precise methods should be evaluated. Our study is an attempt to create a simple scoring system based on electro-neurography criteria that could improve the standards of medical care and positively impact the cooperation between electromyography administrators and neurologists, as well as other specialists such as cardiologists, nephrologists and rehabilitation therapists.

Many screening instruments with numerous composite scores are used to evaluate the severity of neuropathy. One of the most frequently used systems of classification is Neuropathy Disability Score (NDS) that examines temperature, vibration perception and presence of reflexes.^{46,47} Another scale is the Neuropathy Impairment Score (NIS) which includes the examination of sensory functions and reflexes but also the evaluation of motor function impairments.^{48,49} Disease symptoms, reflexes and sensory symptoms are found in the Toronto Clinical Neuropathy Scoring System.^{50,51} Using the systems of classification presented above allows physicians to assign patients to different disease levels; however, it is important to notice that the clinical features of one patient may not be directly comparable to those of another one, even if the same degree of neuropathy has been established in both cases. The explanation of this observation derives from the fact that symptoms of neuropathy may vary from patient to patient. Foot deformities are often seen in neuropathies, especially hereditary ones. Additionally, asymmetric motor and sensory symptoms can make the evaluation more difficult.^{52,53} Many scores were developed for screening for a particular type of neuropathy or to evaluate disease severity. For example, the Michigan Neuropathy Screening Instrument questionnaire (MNSIq) contains symptoms, sensory disturbances and reflex disturbances, and is used in screening for diabetic neuropathy, similar to the Clinical Neuropathy Examination (CNE).^{54–56} The indubitable advantage of those scales is that they do not require specific knowledge or appropriate professional training, and can be performed by clinicians other than neurologists. Unfortunately, they also include some criteria that can make the objective assessment of disease progression difficult.

In the present study, among all the parameters evaluated in the NCS, the most significant reduction was observed in the case of sensory and motor action potential amplitudes. It confirms the hypothesis that in cases of DSPN, axonal loss plays an important role in the pathogenesis of the disease. Features of the demyelinating process were also observed in these patients, but they were far less increased. Due to that, conduction velocity and distal and F wave latencies, which are the parameters of demyelination, were not reduced as much as the amplitude of motor and sensory action potentials. The presented results also confirm the hypothesis that sensory nerves are more

affected by the disease than motor nerves. In our study, the most sensitive parameter of peripheral nerve impairment severity was the reduction of sensory action potential amplitude in the peroneal nerve. It seems that the reduction of sensory action potential amplitude in this nerve is the first sign of disease. Patients with diabetes and isolated impairment of peroneal nerve sensory fibers should be monitored for DSPN. Symptoms of DSPN usually start in the lower limbs and sensory fibers. In our study, the most significant reduction was observed in both the amplitude of sensory action potentials and conduction velocities. The presented scale seems to reflect the nature of the disease with the proposed sensory nerve evaluation. Our scoring system may be very useful not only for neurologists but also for diabetologists. Electromyography studies are safe for the patient and can be performed in every hospital.

Limitations

The limitation of our study is that the correlation between our scoring system and classifications was based on clinical criteria that were not evaluated. The next step of our investigations will be the assessment of this classification system in different types of neuropathies.

Conclusions

Proper polyneuropathy systems of classification seem to be inevitable in routine neurological practice. Not only could they improve the organization of medical research, but also they could help monitor disease progression and treatment effects. The majority of scores involve sensory perception, motor functions, reflexes, and disease symptoms. If the scale is too subtle or does not reflect the severity of the disease, the symptomatology alone is insufficient. Electroneurographic studies have a high sensitivity in the diagnosis of polyneuropathy, as well as play a big role in the evaluation of disease progression. Although numerous, the attempts of creating new scores have failed to be widely used in clinical practice. The presented classification is a simple and objective scoring system based only on electroneurographic parameters and can be used in patients with DSPN who have experienced disease progression. In our study, the most significant reductions were in the amplitude of sensory action potentials. This finding is connected to axonal degeneration and Schwann cell damage that were observed during nerve biopsies in patients with diabetes mellitus polyneuropathy in previous studies.^{57–60} There is a strong correlation between electroneurographic results and histopathological findings; thus, a scoring system based on electroneurographic criteria reflects the natural disease course. The presented paper is a pilot study, and further studies evaluating the correlation between our classification and those based on clinical criteria are in progress.

ORCID iDs

Jakub Stępień  <https://orcid.org/0000-0001-5789-8518>

Żanna Pastuszek  <https://orcid.org/0000-0002-1806-1587>

References

1. Snyder MJ, Gibbs LM, Lindsay TJ. Treating painful diabetic peripheral neuropathy: An update. *Am Fam Physician*. 2016;94(3):227–234. PMID:27479625.
2. Hicks CW, Selvin E. Epidemiology of peripheral neuropathy and lower extremity disease in diabetes. *Curr Diab Rep*. 2019;19(10):86. doi:10.1007/s11892-019-1212-8
3. Hammi C, Yeung B. Neuropathy. In: *StatPearls*. Treasure Island, USA: StatPearls Publishing; 2022. <https://www.ncbi.nlm.nih.gov/books/NBK542220/>. Accessed October 15, 2022.
4. Papanas N, Ziegler D. Risk factors and comorbidities in diabetic neuropathy: An update 2015. *Rev Diabet Stud*. 2015;12(1–2):48–62. doi:10.1900/RDS.2015.12.48
5. Kaku M, Vinik A, Simpson DM. Pathways in the diagnosis and management of diabetic polyneuropathy. *Curr Diab Rep*. 2015;15(6):609. doi:10.1007/s11892-015-0609-2
6. Boulton AJM, Kempler P, Ametov A, Ziegler D. Whither pathogenetic treatments for diabetic polyneuropathy? *Diabetes Metab Res Rev*. 2013;29(5):327–333. doi:10.1002/dmrr.2397
7. Liu S, Kuja-Halkola R, Larsson H, et al. Poor glycaemic control is associated with increased risk of neurodevelopmental disorders in childhood-onset type 1 diabetes: A population-based cohort study. *Diabetologia*. 2021;64(4):767–777. doi:10.1007/s00125-020-05372-5
8. Archer AG, Watkins PJ, Thomas PK, Sharma AK, Payan J. The natural history of acute painful neuropathy in diabetes mellitus. *J Neurol Neurosurg Psychiatry*. 1983;46(6):491–499. doi:10.1136/jnnp.46.6.491
9. Bril V, Perkins BA. Validation of the Toronto Clinical Scoring System for diabetic polyneuropathy. *Diabetes Care*. 2002;25(11):2048–2052. doi:10.2337/diacare.25.11.2048
10. Goel J, Anadure RK, Nair MD, Nair S, Yasha TC. A study correlating nerve biopsy with clinical diagnosis and its impact on improving management in peripheral neuropathies. *Interdiscip Neurosurg*. 2021; 25:101237. doi:10.1016/j.inat.2021.101237
11. McArthur JC, Stocks EA, Hauer P, Cornblath DR, Griffin JW. Epidermal nerve fiber density: Normative reference range and diagnostic efficiency. *Arch Neurol*. 1998;55(12):1513–1520. doi:10.1001/archneur.55.12.1513
12. Lehmann HC, Wunderlich G, Fink GR, Sommer C. Diagnosis of peripheral neuropathy. *Neurol Res Pract*. 2020;2:20. doi:10.1186/s42466-020-00064-2
13. Yu Y. Gold standard for diagnosis of DPN. *Front Endocrinol (Lausanne)*. 2021;12:719356. doi:10.3389/fendo.2021.719356
14. Bryleva EY, Brundin L. Suicidality and activation of the kynurenine pathway of tryptophan metabolism. In: *Inflammation-Associated Depression: Evidence, Mechanisms and Implications*. Vol 31. Current Topics in Behavioral Neurosciences. Cham, Switzerland: Springer International Publishing; 2016:269–284. doi:10.1007/7854_2016_5
15. Sharma KR, Cross J, Farronay O, Ayyar D, Shebert R, Bradley W. Demyelinating neuropathy in diabetes mellitus. *Arch Neurol*. 2002;59(5): 758–765. doi:10.1001/archneur.59.5.758
16. Fatehi F, Nafissi S, Basiri K, Amiri M, Soltanzadeh A. Chronic inflammatory demyelinating polyneuropathy associated with diabetes mellitus. *J Res Med Sci*. 2013;18(5):438–441. PMID:24174953.
17. Igelhorst BA, Niederkinkhaus V, Karus C, Lange MD, Dietzel ID. Regulation of neuronal excitability by release of proteins from glial cells. *Philos Trans R Soc Lond B Biol Sci*. 2015;370(1672):20140194. doi:10.1098/rstb.2014.0194
18. Yang Z, Chen R, Zhang Y, et al. Scoring systems to screen for diabetic peripheral neuropathy. *Cochrane Database Syst Rev*. 2018;2018(7): CD010974. doi:10.1002/14651858.CD010974.pub2
19. Carmichael J, Fadavi H, Ishibashi F, Shore AC, Tavakoli M. Advances in screening, early diagnosis and accurate staging of diabetic neuropathy. *Front Endocrinol (Lausanne)*. 2021;12:671257. doi:10.3389/fendo.2021.671257
20. Koop L, Tadi P. Neuroanatomy, sensory nerves. In: *StatPearls*. Treasure Island, USA: StatPearls Publishing; 2022. <https://www.ncbi.nlm.nih.gov/books/NBK539846/>. Accessed July 25, 2022.

21. Feldman EL, Callaghan BC, Pop-Busui R, et al. Diabetic neuropathy. *Nat Rev Dis Primers*. 2019;5(1):42. doi:10.1038/s41572-019-0097-9
22. Peltier AC, Myers MI, Artibee KJ, et al. Evaluation of dermal myelinated nerve fibers in diabetes mellitus. *J Peripher Nerv Syst*. 2013;18(2):162–167. doi:10.1111/jns5.12027
23. Jin HY, Park TS. Can nerve conduction studies detect earlier and predict clinical diabetic neuropathy? *J Diabetes Invest*. 2015;6(1):18–20. doi:10.1111/jdi.12236
24. Behse F, Buchthal F. Normal sensory conduction in the nerves of the leg in man. *J Neurol Neurosurg Psychiatry*. 1971;34(4):404–414. doi:10.1136/jnnp.34.4.404
25. Ghiasvand F, Ghadimi M, Ghadimi F, Safarpour S, Hosseinzadeh R, SeyedAlinaghi S. Symmetrical polyneuropathy in coronavirus disease 2019 (COVID-19). *IDCases*. 2020;21:e00815. doi:10.1016/j.idcr.2020.e00815
26. Rutkove SB. Effects of temperature on neuromuscular electrophysiology. *Muscle Nerve*. 2001;24(7):867–882. doi:10.1002/mus.1084
27. Hange N, Poudel S, Ozair S, et al. Managing chronic neuropathic pain: Recent advances and new challenges. *Neurol Res Int*. 2022;2022:8336561. doi:10.1155/2022/8336561
28. Burgess J, Frank B, Marshall A, et al. Early detection of diabetic peripheral neuropathy: A focus on small nerve fibres. *Diagnostics (Basel)*. 2021;11(2):165. doi:10.3390/diagnostics11020165
29. Dunker Ø, Nilsen KB, Olsen SE, Åsvold BO, Bjørgaas MRR, Sand T. Which combined nerve conduction study scores are best suited for polyneuropathy in diabetic patients? *Muscle Nerve*. 2022;65(2):171–179. doi:10.1002/mus.27445
30. Petropoulos IN, Ponirakis G, Khan A, Almuhammad H, Gad H, Malik RA. Diagnosing diabetic neuropathy: Something old, something new. *Diabetes Metab J*. 2018;42(4):255–269. doi:10.4093/dmj.2018.0056
31. Service FJ, Rizza RA, Daube JR, O'Brien PC, Dyck PJ. Near normoglycaemia improved nerve conduction and vibration sensation in diabetic neuropathy. *Diabetologia*. 1985;28(10):722–727. doi:10.1007/BF00265018
32. Yang Z, Zhang Y, Chen R, et al. Simple tests to screen for diabetic peripheral neuropathy. *Cochrane Database Syst Rev*. 2018;2018(7):CD010975. doi:10.1002/14651858.CD010975.pub2
33. Dyck PJ, Davies JL, Litchy WJ, O'Brien PC. Longitudinal assessment of diabetic polyneuropathy using a composite score in the Rochester Diabetic Neuropathy Study cohort. *Neurology*. 1997;49(1):229–239. doi:10.1212/WNL.49.1.229
34. Dyck PJ, Kincaid JC, Dyck PJB, et al. Assessing mNIS+7Ioni and international neurologists' proficiency in a familial amyloidotic polyneuropathy trial. *Muscle Nerve*. 2017;56(5):901–911. doi:10.1002/mus.25563
35. Vas PR, Sharma S, Rayman G. Distal sensorimotor neuropathy: Improvements in diagnosis. *Rev Diabet Stud*. 2015;12(1–2):29–47. doi:10.1900/RDS.2015.12.29
36. Abraham A, Barnett C, Katzberg HD, Lovblom LE, Perkins BA, Bril V. Toronto Clinical Neuropathy Score is valid for a wide spectrum of polyneuropathies. *Eur J Neurol*. 2018;25(3):484–490. doi:10.1111/ene.13533
37. Picon AP, Ortega NRS, Watari R, Sartor C, Sacco ICN. Classification of the severity of diabetic neuropathy: A new approach taking uncertainties into account using fuzzy logic. *Clinics (Sao Paulo)*. 2012;67(2):151–156. doi:10.6061/clinics/2012(02)10
38. Baets J, Deconinck T, De Vriendt E, et al. Genetic spectrum of hereditary neuropathies with onset in the first year of life. *Brain*. 2011;134(Pt 9):2664–2676. doi:10.1093/brain/awr184
39. Valk GD, De Sonnaville JJJ, Van Houtum WH, et al. The assessment of diabetic polyneuropathy in daily clinical practice: Reproducibility and validity of Semmes Weinstein monofilaments examination and clinical neurological examination. *Muscle Nerve*. 1997;20(1):116–118. doi:10.1002/(SICI)1097-4598(199701)20:1<116::AID-MUS19>3.0.CO;2-2
40. Van De Poll-Franse LV, Valk GD, Renders CM, Heine RJ, Van Eijk JTM. Longitudinal assessment of the development of diabetic polyneuropathy and associated risk factors. *Diabet Med*. 2002;19(9):771–776. doi:10.1046/j.1464-5491.2002.00778.x
41. Herman WH, Pop-Busui R, Braffett BH, et al. Use of the Michigan Neuropathy Screening Instrument as a measure of distal symmetrical peripheral neuropathy in type 1 diabetes: Results from the Diabetes Control and Complications Trial/Epidemiology of Diabetes Interventions and Complications. *Diabet Med*. 2012;29(7):937–944. doi:10.1111/j.1464-5491.2012.03644.x
42. Tanaka M, Szabó Á, Spekker E, Polyák H, Tóth F, Vécsei L. Mitochondrial impairment: A common motif in neuropsychiatric presentation? The link to the tryptophan–kynurenine metabolic system. *Cells*. 2022;11(16):2607. doi:10.3390/cells11162607
43. Zheng H, Sun W, Zhang Q, et al. Proinflammatory cytokines predict the incidence of diabetic peripheral neuropathy over 5 years in Chinese type 2 diabetes patients: A prospective cohort study. *EClinicalMedicine*. 2020;31:100649. doi:10.1016/j.eclinm.2020.100649
44. Skundric DS, Lisak RP. Role of neurotrophic cytokines in development and progression of diabetic polyneuropathy: From glucose metabolism to neurodegeneration. *Exp Diabetes Res*. 2003;4(4):303–312. doi:10.1155/EDR.2003.303
45. Behse F, Buchthal F, Carlsen F. Nerve biopsy and conduction studies in diabetic neuropathy. *J Neurol Neurosurg Psychiatry*. 1977;40(11):1072–1082. doi:10.1136/jnnp.40.11.1072
46. Younger DS. Diabetic neuropathy: A clinical and neuropathological study of 107 patients. *Neurol Res Int*. 2010;2010:140379. doi:10.1155/2010/140379
47. Dyck PJB, Engelstad J, Norell J, Dyck PJ. Microvasculitis in non-diabetic lumbosacral radiculoplexus neuropathy (LSRPN): Similarity to the diabetic variety (DLSRPN). *J Neuropathol Exp Neurol*. 2000;59(6):525–538. doi:10.1093/jnen/59.6.525
48. Woltman H, Wilder R. Diabetes mellitus: Pathogenic changes in the spinal cord and peripheral nerves. *Arch Intern Med (Chic)*. 1929;44:576–603. doi:10.1001/archinte.1929.00140040114010
49. Krendel DA, Costigan DA, Hopkins LC. Successful treatment of neuropathies in patients with diabetes mellitus. *Arch Neurol*. 1995;52(11):1053–1061. doi:10.1001/archneur.1995.00540350039015
50. Younger DS, Rosoklija G, Hays AP, Trojaborg W, Latov N. Diabetic peripheral neuropathy: A clinicopathologic and immunohistochemical analysis of sural nerve biopsies. *Muscle Nerve*. 1996;19(6):722–727. doi:10.1002/(SICI)1097-4598(199606)19:6<722::AID-MUS6>3.0.CO;2-C
51. Ciapała K, Mika J, Rojewska E. The kynurenine pathway as a potential target for neuropathic pain therapy design: From basic research to clinical perspectives. *Int J Mol Sci*. 2021;22(20):11055. doi:10.3390/ijms222011055
52. Tajti J, Szok D, Csáti A, Szabó Á, Tanaka M, Vécsei L. Exploring novel therapeutic targets in the common pathogenic factors in migraine and neuropathic pain. *Int J Mol Sci*. 2023;24(4):4114. doi:10.3390/ijms24044114
53. Perini F, D'Andrea G, Galloni E, et al. Plasma cytokine levels in migraineurs and controls. *Headache*. 2005;45(7):926–931. doi:10.1111/j.1526-4610.2005.05135.x
54. Baka P, Escolano-Lozano F, Birklein F. Systemic inflammatory biomarkers in painful diabetic neuropathy. *J Diabetes Complications*. 2021;35(10):108017. doi:10.1016/j.jdiacom.2021.108017
55. Zilliox LA, Ruby SK, Singh S, Zhan M, Russell JW. Clinical neuropathy scales in neuropathy associated with impaired glucose tolerance. *J Diabetes Complications*. 2015;29(3):372–377. doi:10.1016/j.jdiacom.2015.01.011
56. Badawy AAB. Kynurenine pathway of tryptophan metabolism: Regulatory and functional aspects. *Int J Tryptophan Res*. 2017;10:1178646917691938. doi:10.1177/1178646917691938
57. Tanaka M, Török N, Tóth F, Szabó Á, Vécsei L. Co-players in chronic pain: Neuroinflammation and the tryptophan–kynurenine metabolic pathway. *Biomedicines*. 2021;9(8):897. doi:10.3390/biomedicines9080897
58. Meacham K, Shepherd A, Mohapatra DP, Haroutounian S. Neuropathic pain: Central vs. peripheral mechanisms. *Curr Pain Headache Rep*. 2017;21(6):28. doi:10.1007/s11916-017-0629-5
59. Savitz J. The kynurenine pathway: A finger in every pie. *Mol Psychiatry*. 2020;25(1):131–147. doi:10.1038/s41380-019-0414-4
60. Rojewska E, Piotrowska A, Makuch W, Przewlocka B, Mika J. Pharmacological kynurenine 3-monooxygenase enzyme inhibition significantly reduces neuropathic pain in a rat model. *Neuropharmacology*. 2016;102:80–91. doi:10.1016/j.neuropharm.2015.10.040

Changes in the scar tissue structure after cesarean section as a result of manual therapy

Katarzyna Olszewska^{1,A–D}, Agnieszka Ptak^{1,E,F}, Agnieszka Rusak^{2,E}, Agnieszka Dębiec-Bąk^{1,D}, Małgorzata Stefańska^{1,B,C,E,F}

¹ Faculty of Physiotherapy, Wrocław University of Health and Sport Sciences, Poland

² Department of Human Morphology and Embryology, Division of Histology and Embryology, Wrocław Medical University, Poland

A – research concept and design; B – collection and/or assembly of data; C – data analysis and interpretation;

D – writing the article; E – critical revision of the article; F – final approval of the article

Advances in Clinical and Experimental Medicine, ISSN 1899–5276 (print), ISSN 2451–2680 (online)

Adv Clin Exp Med. 2024;33(4):387–395

Address for correspondence

Agnieszka Rusak

E-mail: agnieszka.rusak@umw.edu.pl

Funding sources

None declared

Conflict of interest

None declared

Received on January 18, 2023

Reviewed on May 11, 2023

Accepted on July 5, 2023

Published online on September 4, 2023

Abstract

Background. Available statistical data from 2015 show that 28% of pregnancies in developed countries end in cesarean section (CC). Discomfort associated with the scar after surgery is a common complication.

Objectives. This study aimed to evaluate the changes in the structure of the cesarean scar after the application of a scheme of manual therapy.

Materials and methods. The study included 15 women in the treatment group (TG) and 15 in the control group (CG). The scars were evaluated twice at 5-week intervals with the use of quantitative scales: the Vancouver Scar Scale (VSS), the Manchester Scar Scale (MSS) and the Patient and Observer Scar Assessment Scale (POSAS). During each examination, the scar was compared, using the specified criteria, to the physiological skin, i.e., the tissues directly bordering the incision. During therapy, 8 manual techniques were used during a 4-week program consisting of 30-minute sessions 3 times per week.

Results. Patients in the TG showed a statistically significant improvement in all of the analyzed characteristics of the scar. A statistically significant difference was also observed between the results obtained during the 2nd examination (after the therapy) in the TG and the CG.

Conclusions. As a result of the therapy, the condition of the scar in the TG significantly improved. Onerous scar-related symptoms were alleviated. The vascularity, hyperpigmentation and distortion of the scar were reduced. The elasticity and pliability of the scar increased, and the height of the scar decreased. The texture, finish and contour of the scar improved. Obtained results suggest that manual therapy of the scar after CC should be a part of the treatment in women during the postpartum period.

Key words: cesarean section, women's health, scar therapy

Cite as

Olszewska K, Ptak A, Rusak A, Dębiec-Bąk A, Stefańska M. Changes in the scar tissue structure after cesarean section as a result of manual therapy.

Adv Clin Exp Med. 2024;33(4):387–395.

doi:10.17219/acem/169236

DOI

10.17219/acem/169236

Copyright

Copyright by Author(s)

This is an article distributed under the terms of the Creative Commons Attribution 3.0 Unported (CC BY 3.0) (<https://creativecommons.org/licenses/by/3.0/>)

Background

According to the recommendations of the World Health Organization (WHO), the percentage of pregnancies delivered by cesarean section (CC) should not exceed 10–30%. Statistical data show that in Organization for Economic Cooperation and Development (OECD) countries (36 highly developed countries of the world), the number of deliveries ending in CC increased from 20% in 2000 to 27.9% in 2015.¹ Globally, the CC rate has also been rising – it grew from 12.1% in 2005 to 21.1% in 2015. In Western Europe, 19.6% of pregnancies were delivered by CC in 2000, and by 2015, this rate increased to 26.9%.²

The decision to perform a CC is made more frequently due to the early detection of hazards, an increasing number of multiple gestations and preterm births, as well as late births (in terms of the mother's age). In addition to obstetric indications, the procedure is performed for indications related to ophthalmic, orthopedic, cardiac, neurological, and psychiatric issues.^{1,3} Pregnant women are often convinced that a CC is the easier, safer and painless method of delivery, better than natural childbirth. The most frequently employed technique is the transperitoneal CC, involving a transverse lower abdominal incision through the skin, the subcutaneous tissue, the peritoneum over the uterus, and the uterus. Cutting through muscle fibers is currently avoided.⁴ The findings of Cromi et al.³ demonstrated that the type and technique of surgical closure used following the procedure has no impact on the appearance of the scar evaluated using the Vancouver Scar Scale (VSS) and the Patient and Observer Scar Assessment Scale (POSAS).

The wound healing and scar formation processes begin with hemostasis, followed by inflammation, proliferation and remodeling. They take place over a period of up to 2 years, and their duration depends on the etiology of the wound. The process consists of the conversion of type III collagen to type I collagen. The finer and less ordered structure of type I collagen both strengthens the tissue and decreases its elasticity. This process can be distorted by several factors.⁵

Remodeling abnormalities can cause the formation of hypertrophic, keloid or atrophic scars. Women who underwent a CC are at an increased risk of developing pathological lesions due to hormonal activity, taking care of an infant, a change in the body's center of gravity, and genetic makeup.

Despite a growing interest in pregnancy and childbirth, women often overlook the needs of their own bodies, focusing instead on the everyday chores related to taking care of a baby. Such situation can cause the changes in the locomotor system that solidify during pregnancy. Painful scar and a reflex to protect the injured area cause the woman to assume antalgic positions, enhancing and solidifying incorrect posture patterns.⁶ Additionally, pain predisposes the woman to assume a forward flexion posture and avoid tensing the abdominal wall muscles, which causes further

weakening of the muscles that become stretched during pregnancy. Women report various scar-related complaints, such as itching, pulling, pain, numbness (hypoesthesia) or hyperesthesia in the scar area, pricking, burning, tingling, and stinging.

There are no uniform standards for procedures in cesarean scar therapy. Literature mentions the beneficial impact of massage on the rate of scar remodeling and pain alleviation.^{7,8} Wong et al. reported the effectiveness of delicate scar mobilization in combination with exercises for chronic pain.⁹

Scar-related complaints can cause physical problems and psychological issues, consisting of malaise and a lack of acceptance of the scar and oneself. In critical situations, the patients see the scar as a non-existent, unaesthetic element of their body that restricts their functioning.¹⁰ Physical complaints and a lack of acceptance of oneself can also cause women to limit or discontinue physical exercises.¹¹ Postoperative scars are often overlooked in the postoperative period. Currently, numerous operations are carried out in the abdominal area. Not all possible ailments caused by the presence of scars are unequivocally investigated. Cesarean section is one of the most numerous operations. Each interruption in tissue communication is traumatic for the body and results in psychosocial and purely physical ailments. One of the research directions related to scar treatment is manual therapy, which, due to its nature, is one of the simplest, cheapest and most accessible methods. According to the available literature, there are indications of the effects of manual therapy on scars, but the research results are inconsistent. The evidence for the use of scar massage is weak, the regimens vary, and the measured results are neither normalized nor objective. Although scar massage is anecdotally effective, there is limited scientific data in the literature to support it.¹² The review by Wasserman et al. shows preliminary strong evidence of the benefit of soft tissue mobilization for symptoms associated with acute postoperative adhesions, preliminary moderate evidence of the benefit of soft tissue mobilization for symptoms of chronic inoperable adhesions, and moderate evidence of the benefit of using soft tissue mobilization for symptoms associated with chronic postoperative adhesions.¹³ Although most postoperative adhesions are clinically silent, the consequences of adhesion formation can be a lifelong problem, including chronic abdominal pain, recurrent bowel obstructions requiring multiple hospitalizations, and infertility. Moreover, adhesion disease can become a chronic condition with significant morbidity, and lacks effective treatment. Despite recent advances in surgical techniques, there is no reliable strategy to treat postoperative adhesions.¹⁴ It is vital to look at the human body comprehensively. With the increasing number of CCs, the impact of scarring on the overall health of patients is increasingly observed. Abdominal stretch marks and cesarean scars are considered important predictors of intraperitoneal

adhesions. Women with significant stretch marks had thick intraperitoneal adhesions. Women with intraperitoneal adhesions had more vascularized, discolored, less flexible, and raised scars. Therefore, verifying the effect of scars and the possibility of their modification, for example, to reduce adhesions, is of utmost importance.¹⁵ Tapes, used in the prevention of surgical scars, effectively reduce scars and display features of growth, color and itching.^{16,17} An overview of the methods used in physical therapy on scars is discussed in the review by Deflorin et al.¹⁸ Overall, 1 meta-analysis showed that the effect on the scar by different physiotherapeutic means has a significantly positive influence on pain, pigmentation, suppleness, itching, surface area, and scar thickness.¹⁸ There are reports stating that therapy has a clear positive effect on the state of scars and the overall wellbeing of patients.¹⁹ The current state of research does not allow for a direct transfer of the above research results to clinical treatment of patients with big scars. However, the continued clinical implementation of the results obtained in studies with respect to the mechanical sensitivity of isolated fibroblasts and continuous adaptation of manual techniques created an evidence basis for manual scar therapy. Manual doses are adapted to the physiology of the tissue and the respective phases of wound healing. Clinical observations show improved mobility of affected areas and fewer relapses of the inflammatory phase due to mechanical overload.²⁰

Objectives

This study aimed to evaluate the changes in the structure of the cesarean scar as a result of an applied scheme of manual therapy.

Materials and methods

Study design

This study was designed to investigate the influence of our scheme of manual therapy on scar recurrence after a CC. In this study, vascularity, pigmentation, pliability, height pain, itching, color, stiffness, thickness, texture, and overall condition of the scar were evaluated in patients using subjective scales.

Setting

The trial has been registered and allocated in the Australian New Zealand Clinical Trials Registry (No. ACTRN12620000115932, registration date: February 7, 2020). Data were collected from January 7, 2019 to May 12, 2019. The first participant's enrollment date was January 7, 2019, and the enrollment date of the last participant was April 12, 2019.

Participants

The criterion for inclusion in the treatment group (TG) was the lack of any prior work on the CC scar. All participants (n = 30) were randomly assigned to 2 same-sized groups – the TG that participated in the therapy of the scar and the control group (CG) that did not undergo therapy. Demographic characteristics of both groups are presented in Table 1. Patients were recruited according to the diagram depicted in Fig. 1, but the sample size was established a priori using G*Power 3.1 software (v. 3.1.9.2; G*Power, Kiel, Germany).²¹ The expected effect size (ES) was set at 0.85 (Cohen's f), the α level was set at 0.05 and the power was set at 0.8.²² The minimum group size was 10 participants, but the final recruitment consisted of 15 women in each group.²¹

Table 1. Demographic characteristics of patients included in the manual therapy and control groups

Parameter	Average value for the treatment group	Average value for the control group
Sex	female	female
Age [years]	33 ±4	30 ±4
Height [cm]	164.5 ±7	169.2 ±5
Body mass [kg]	64.1 ±18	69.1 ±13
Nationality	Polish	Polish
City population	>500,000	>500,000
Time after cesarean section [months]	14 ±8	14 ±9
Group size	15	15

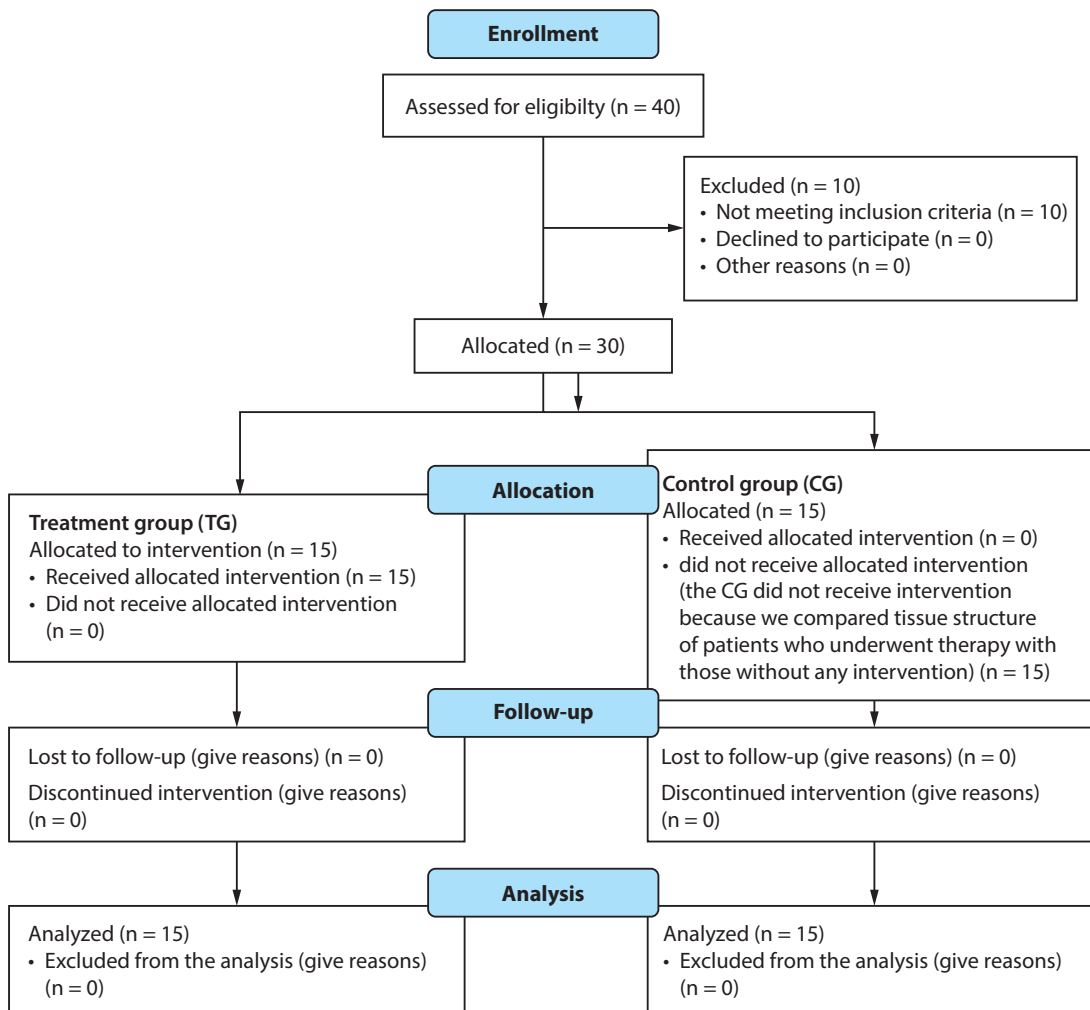
Variables

The experiment consisted of 2 examination meetings and 12 therapy sessions. During the examination meetings, the scar of each participant was assessed visually and by touch using quantitative scar evaluation scales: VSS and Manchester Scar Scale (MSS). Additionally, the scar was assessed by each patient using the POSAS Patient Scale. The VSS was used to evaluate vascularity, pigmentation, pliability, and height. The MSS evaluated color, finish, contour, distortion, and texture. The subjective POSAS Patient Scale was utilized to evaluate pain, itching, color, stiffness, thickness, texture, and the overall condition of the scar.²³

Data measurement

The patients from the TG underwent scar therapy 3 times per week for 4 weeks. The therapy consisted of twelve 30-minute sessions carried out 3 times per week. During each session, the therapist applied 8 manual techniques in the following order: stroking, superficial rubbing using spiral and transverse motions, deep rubbing using spiral and transverse motions, moving, rolling, breaking up, and pinching. The order and intensity of the techniques were adjusted to the condition and the response of the treated

Fig. 1. Flow diagram of patient recruitment



tissues. The visualization of the scars before and after therapy was conducted using a thermal imaging camera FLIR T335 (Merlin Lazer, Crowborough, UK).

Bias

The only criterion for inclusion in the study was the absence of any previous work on the cesarean scar to avoid misinterpretation of the obtained results.

Study size

The study size was determined by the preliminary character of this project. An investigation conducted on a larger group of patients is currently under consideration as a part of a dedicated grant.

The therapy and all examinations were carried out at the Scientific and Research Laboratory of the Faculty of Physiotherapy at Wroclaw University of Health and Sport Sciences (Poland). The trial was approved by the Senate Committee on Ethics of Scientific Research at the Wroclaw University of Health and Sport Sciences (approval No. ACTRN12620000115932).

Quantitative variables

The MSS and VSS were used to evaluate the scar before and after the therapy. On both scales, each characteristic of the scar was given a specific score. The higher the final score, the worse the condition of the scar. The maximum score on the MSS was 18 points, and on the VSS it was 13 points. The subjective scar-related experiences of the participants were evaluated twice with the use of the POSAS Patient Scale.²³ Each described characteristic was given a score from 1 to 10 (the higher the score, the worse the result). The maximum score on that scale was 70. The median was calculated for the results obtained before and after the therapy in both evaluated groups.

Statistical analyses

The statistical calculations were made using Statistica v. 13.1 (StatSoft, Inc., Tulsa, USA). The Shapiro–Wilk test was used to check the distribution of all quantitative variables. Due to the ordered nature of the survey results and the lack of normality in the distribution of the quantitative

variables, the median was used as a measure of central tendency, and the interquartile range (IQR) as a measure of dispersion.

The results were analyzed with the use of statistical tests for ordinal variables: the Mann–Whitney U test and the Wilcoxon matched-pairs test. The statistical significance of the differences in the appearance and structure of the scar in both groups before and after the therapy, as well as between the TG and CG before and after the therapy, were assessed. Due to the occurrence of multiple comparisons, the Bonferroni correction was applied to reduce the risk of a type I error. The assumed significance level (0.05) was divided by the number of comparisons (4). The adjusted significance level was set at 0.0125.

Results

The median was calculated for each analyzed parameter in both evaluated groups (Fig. 2,3). Using the MSS, we observed that the color, finish, contour, distortion, and texture were statistically significantly improved. According to the VSS, vascularity, pigmentation, pliability, and height were statistically significantly improved. According to the POSAS Patient Scale, color, stiffness, thickness, texture, and overall opinion were statistically significantly improved. Pain and itching did not change. The median was calculated for the results obtained before and after the therapy in both evaluated groups (Fig. 4).

The MSS, VSS and POSAS Patient Scale scores obtained during the first examination were not statistically significantly different between the TG and CG. Statistically significant differences were observed between the groups during 2nd examination. The scores obtained during both

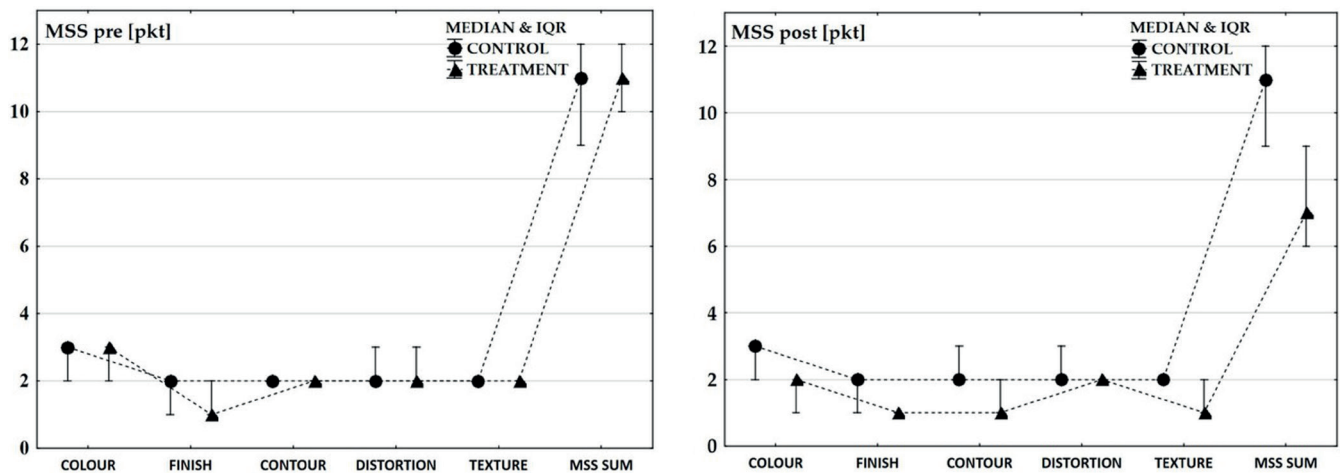


Fig. 2. Manchester Scar Scale (MSS) scores in the form of a median calculated for each analyzed parameter in the treatment group and the control group before and after the therapy

IQR – interquartile range.

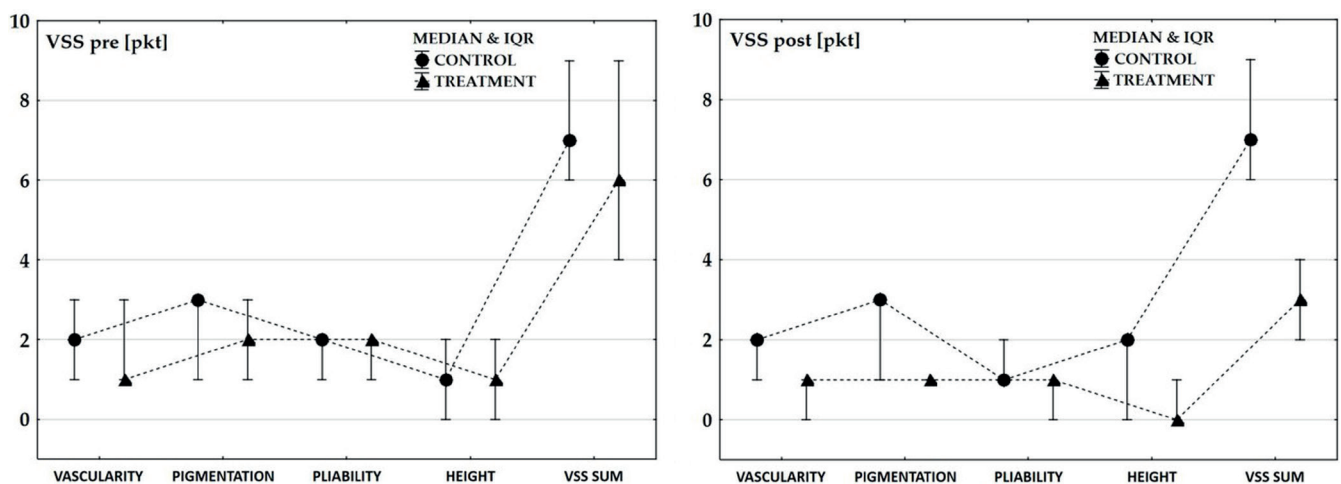


Fig. 3. Vancouver Scar Scale (VSS) scores in the form of a median calculated for each analyzed parameter in the treatment group and the control group before and after the therapy

IQR – interquartile range.

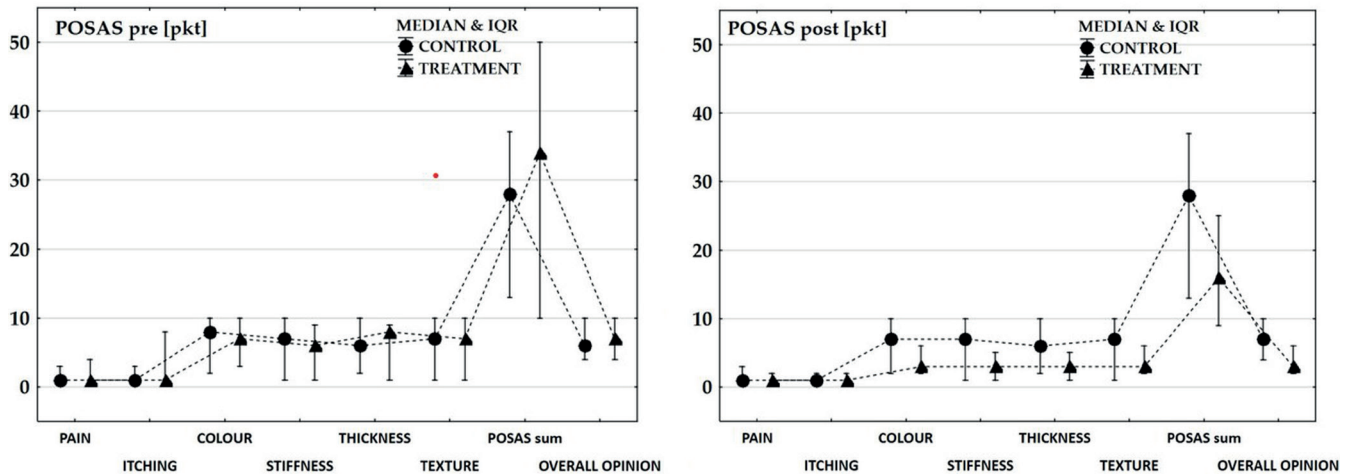
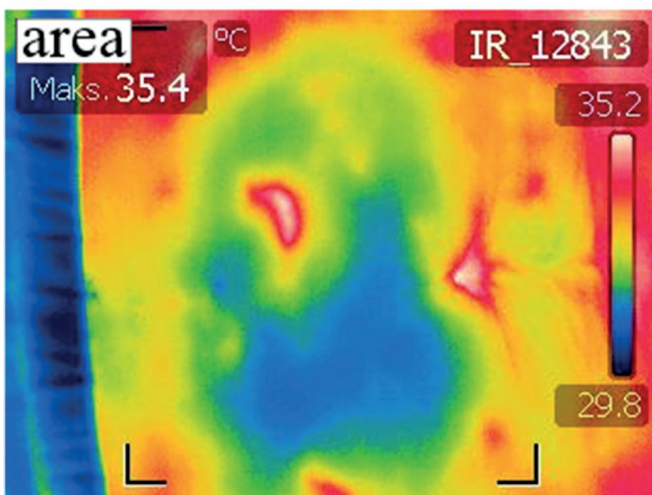


Fig. 4. Patient and Observer Scar Assessment Scale (POSAS) scores in the form of a median calculated for each analyzed parameter in the treatment group and the control group before and after the therapy

IQR – interquartile range.

BEFORE THERAPY



AFTER THERAPY

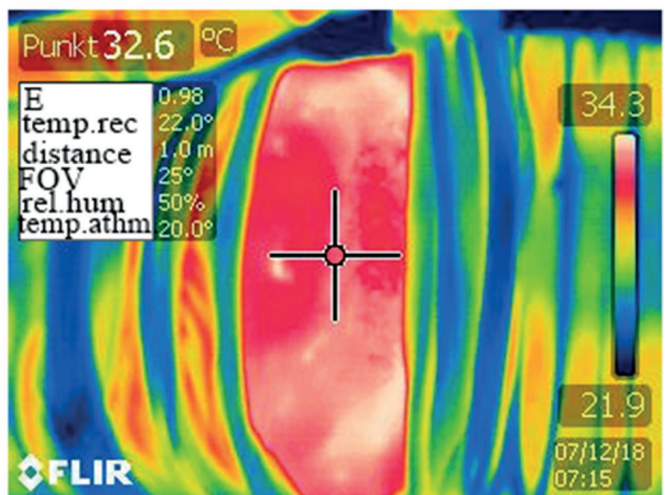


Fig. 5. Evaluation of the effects of manual therapy on representative photos of the patient's scar remodeling. On the left – the patient's scar area before manual therapy; on the right – the patient's scar area after manual therapy (thermal imaging camera FLIR T335). The figure shows the temperature (thermvision) scale (for each patient, it was different in terms of maximum and minimum temperatures), which varies from the darkest blue to its lighter shades, green, yellow, orange through red to white. White indicates the areas with the highest temperature relative to the other elements. Dark blue indicates the areas with the lowest temperature relative to the other areas covered by the thermal image. The difference between the indicated area before and after treatments was taken into account to verify the effectiveness of the therapy

FOV – field of view.

examinations for each of the scales were different in a statistically significant manner only in the TG (Table 2,3). Representative photos of the results of manual therapy are presented in Fig. 5. Generally, as a result of therapy, the condition of the scar in the TG significantly improved. Onerous scar-related symptoms were alleviated. The vascularity, hyperpigmentation and distortion of the scar were reduced, the height of the scar decreased, and the elasticity and pliability of the scar increased. The texture, finish and contour of the scar improved.

Following the results from the thermal imaging camera, these were pilot studies. So far, the thermal imaging camera

has been used, for example, to verify the effect of thermal factors on the scar and the course of the wound healing process,^{24,25} but not to verify the effect of manual therapy. The effects of therapy on temperature changes cannot be unequivocally determined due to the different types of scars.

Atrophic, hypertrophic and keloid scars differ in their initial temperature distribution. In addition, the use of manual methods varies in proportion over time. To draw specific conclusions, the study group should be broadened and differentiated according to the types of scars.

No statistically significant changes were observed, but a certain trend in temperature change was noted, which

Table 2. Results of tests and p-values of the Mann–Whitney U test and the Wilcoxon matched-pairs test calculated for each parameter evaluated using the Manchester Scar Scale (MSS) and the Vancouver Scar Scale (VSS) before and after the therapy in the treatment group and the control group

Parameter		PRE vs. POST				Treatment group vs. control group			
		treatment group		control group		PRE		POST	
		T	p-value	T	p-value	U	p-value	U	p-value
MSS	color	<0.01	0.0015*	3.50	0.1422	107.50	0.8519	53.50	0.0152
	finish	<0.01	0.0277*	1.50	1.0000	75.00	0.1249	37.50	0.0020*
	contour	<0.01	0.0033*	6.00	0.3454	94.50	0.4679	54.00	0.0161
	distortion	<0.01	0.0077*	NA	1.0000	108.00	0.8682	67.50	0.0649
	texture	<0.01	0.0033*	2.50	0.3613	90.00	0.3615	64.50	0.0488
	MSS sum	<0.01	0.0007*	5.50	0.2945	112.50	0.9835	28.50	0.0005*
VSS	vascularity	<0.01	0.0015*	4.00	0.7150	87.50	0.3095	16.00	0.0001*
	pigmentation	<0.01	0.0051*	2.50	0.3613	98.50	0.5755	50.50	0.0107*
	pliability	<0.01	0.0010*	6.00	0.6858	101.00	0.6482	47.50	0.0075*
	height	<0.01	0.0051*	4.00	0.7150	107.50	0.8519	59.50	0.0294
	VSS sum	<0.01	0.0007*	0.00	0.1088	99.00	0.5897	19.00	0.0001*

NA – not available; *statistically significant value, $p < 0.0125$.

Table 3. Results of tests and p-values for the Mann–Whitney U test and the Wilcoxon matched-pairs test calculated for each parameter and evaluated using the Patient and Observer Scar Assessment Scale (POSAS) before and after the therapy in the treatment group and the control group

Parameter		PRE vs. POST				Treatment group vs. control group			
		treatment group		control group		PRE		POST	
		T	p-value	T	p-value	U	p-value	U	p-value
Pain	6.00	0.1763	0.00	0.1797	105.50	0.7603	110.50	0.9362	
Itching	5.50	0.2945	1.00	0.6547	107.50	0.8238	102.50	0.6465	
Color	0.00	0.0015*	0.00	0.1797	111.50	0.9832	36.00	0.0015*	
Stiffness	1.50	0.0009*	NA	1.0000	105.00	0.7687	39.00	0.0022*	
Thickness	0.00	0.0010*	NA	1.0000	101.00	0.6406	22.00	0.0002*	
Texture	2.00	0.0015*	1.50	1.0000	95.50	0.4831	44.50	0.0044*	
Sum	0.00	0.0007*	1.50	0.4227	89.50	0.3491	28.00	0.0005*	
Overall opinion	0.00	0.0007*	NA	NA	106.50	0.8152	18.50	0.0001*	

NA – not available; *statistically significant value, $p < 0.0125$.

requires further investigation. In all cases, the temperature of the scar area after treatment was close to that of the surrounding tissues.

We are planning to conduct a research in a larger group of patients, taking into account various diagnostic and therapeutic methods to compare their effectiveness.

Discussion

Globally, 21.1% of pregnancies were delivered by CC in 2015.² Women are not educated on scar care and the possible side effects of failing to undergo or discontinuing therapy. The scar- and adhesion-related symptoms are not associated with the presence of those lesions in any way by the physician or patient.²⁶ Onerous symptoms included a pulling sensation and pain during the performance of everyday chores, as well as pain originating

in the lumbar vertebral column, the gastrointestinal tract and the scar itself. Furthermore, an important complaint related to the cesarean scar is the aesthetic aspect, i.e., the lack of acceptance of a part of the patient’s own body that has a negative impact on everyday functioning.¹⁰

According to the research performed by Chochowska et al.,²⁶ the aforementioned complaints are alleviated or reduced after the scar therapy. Twenty-four months after the procedure, scar treatment may be less effective. Chochowska et al.²⁶ noticed that postoperative adhesions cannot be eliminated during therapy, and each subsequent surgery increases the risk of their formation. They cause onerous symptoms resulting from the decreased glide between tissues, which may give rise to pain in the head, vertebral column, pelvis, and other regions. Pilot studies on the use of Myofascial Induction Therapy (MIT) showed that the aforementioned activities effectively change the structure of the scar despite the completion of the remodeling process.²⁷

The most recent research suggests that it is possible to change the structure of adhesions.²⁸ Ault et al. focused on hypertrophic burn scars.²⁹ They claimed that massage is an effective treatment that impacts the height, vascularity, elasticity, pain, itching, and depression of scars. Anthonissen et al. compared the effectiveness of various types of therapy: pressure, silicone, massage, moisturizing creams, physical activity, and mobilization.³⁰ They questioned the accuracy of the analyzed projects due to the small size of the evaluated groups and the lack of a detailed description of the therapy. Many authors suggest that both objective and subjective scales should be used.^{3,29,30} In our research, the changes that occurred during therapy were assessed using the VSS, MSS and POSAS Patient Scale.

The improvement in the parameters such as pigmentation, color or elasticity may result from the massage stimulating the reconstruction of connective tissue by increasing the number of collagen fibers while reducing their diameter and cross-section.³¹ In our research, according to the VSS, MSS and POSAS Patient Scale, scar therapy improved all evaluated parameters. It is possible that pain and itching require a different type of treatment than the ones used. O'Reilly et al. observed a reduction in itching within the studied scars.¹⁶ In our studies, no statistically significant changes were observed in these parameters. According to the results of other experiments, pain decreased after scar therapy.^{12,13,18} However, these results are not conclusive. The evidence for the use of scar massage is still not sufficient, the regimes vary, and the measured outcomes are neither standardized nor objective. However, the effectiveness of the therapy appears to be greater in postoperative scars than in traumatic or post-burn scars. Although scar massage is known to be effective, there are little scientific data in the literature to support it.¹² Recently, the clinical impact of scar management has been studied more intensively.^{19,20} It is important to analyze and continue research in order to determine the best procedures affecting scars. Moreover, it is worth clarifying and differentiating which therapy protocol is most effective as well as verifying what affects the effectiveness of the performed treatments, in order to improve the abovementioned parameters and the comfort of a patient's life.

Andrzejewski noticed increased blood flow in the skin and muscles, as well as the normalization of the autonomic nervous system after scar massage.³² The results achieved during therapy indicated that massage in the form of rubbing increases the level of fibroblast growth factor (FGF) in the tissue, which causes structural changes in collagen fibers.

Another method used in scar therapy is Kinesiology Taping.^{16,17,33} The research on various types of pathological scars was conducted in 54 patients. Following a 7-day application, a change in the tissue color, an increase in its mobility and improved satisfaction were demonstrated in the majority of subjects.³³

It is becoming increasingly common to use various types of topical formulations that the patients can self-administer

on the scar. However, there are no solid scientific studies that would corroborate the positive influence of such formulations on the tissues.

A few studies concerning cesarean scar therapy and an increasing rate of surgical births encourage further attempts to develop standards for cesarean scar management. Abdominal striae and a cesarean scar on intraperitoneal adhesions were significant predictors of scar adhesion type. It has been observed that women with severe stretch marks had thicker intraperitoneal adhesions, whereas women with intraperitoneal adhesions had more vascularized, discolored, less pliable, and raised scars.¹⁵ Results obtained by our team could have implications for physiotherapy practice. Currently, the use of various topical preparations of varying efficacy is becoming more common in scar therapy. In many cases, they are not sufficient due to persistent scar-related ailments. The growing percentage of surgical deliveries and a small number of scientific studies on the treatment of scars after CC prompts the development of therapeutic management standards. We have obtained interesting results using a thermal imaging camera to assess scar conditions after CC. Siah and Childs noted that heat is a sign of surgical wound infection in the wound assessment criteria, but no diagnostic tool is used in clinical practice to assess the skin temperature of surgical wounds.²⁴ Observations made by other authors showed that thermovision is a valuable tool in scar management²⁵ and, in our opinion, it has clinically useful potential in the rehabilitation of cesarean scars. It is worth noting that postoperative adhesions, although clinically silent, can cause chronic pain and infertility¹⁴; thus, new methods of scar management are needed.

The results of our research indicate significantly positive effects of using manual techniques in scar therapy. They can be used in perinatal care, as well as in broadly understood surgery, plastic surgery, orthopedics, and traumatology, wherever scars are common.

Limitations

Our work presents the results of a preliminary study, and for this reason, the sample size was not numerous. It is worth expanding the groups of patients in the future studies and checking whether the time elapsed since the CC affects the influence of therapy over long-time follow-up. In conducted research, subjective assessment methods were used, which should be complemented by objective (quantitative) methods, allowing for a better comparison with results obtained by other researchers.

Conclusions

As a result of the manual therapy, the condition of the scar in the TG significantly improved. The presented scheme of manual therapy has the potential to be a simple and effective treatment for women after a CC.

ORCID iDs

Katarzyna Olszewska  <https://orcid.org/0000-0002-4521-8105>
 Agnieszka Ptak  <https://orcid.org/0000-0002-8396-5267>
 Agnieszka Rusak  <https://orcid.org/0000-0001-9587-0575>
 Agnieszka Dębiec-Bąk  <https://orcid.org/0000-0001-7005-3018>
 Małgorzata Stefańska  <https://orcid.org/0000-0003-2070-8535>

References

1. Organisation for Economic Co-operation and Development (OECD). Health at a Glance 2017: OECD Indicators. Paris, France: OECD Publishing; 2017. doi:10.1787/health_glance-2017-en
2. Boerma T, Ronsmans C, Melesse DY, et al. Global epidemiology of use of and disparities in caesarean sections. *Lancet*. 2018;392(10155):1341–1348. doi:10.1016/S0140-6736(18)31928-7
3. Cromi A, Ghezzi F, Gottardi A, Cherubino M, Uccella S, Valdatta L. Cosmetic outcomes of various skin closure methods following cesarean delivery: A randomized trial. *Am J Obstet Gynecol*. 2010;203(1):36.e1–36.e8. doi:10.1016/j.ajog.2010.02.001
4. Bordoni B, Zanier E. Skin, fascias, and scars: Symptoms and systemic connections. *J Multidiscip Healthc*. 2013;7:11–24. doi:10.2147/JMDH.S52870
5. Guo S, DiPietro LA. Factors affecting wound healing. *J Dent Res*. 2010;89(3):219–229. doi:10.1177/0022034509359125
6. Kouwenberg CAE, Bijlard E, Timman R, Hovius SER, Busschbach JJV, Mureau MAM. Emotional quality of life is severely affected by keloid disease: Pain and itch are the main determinants of burden. *Plast Reconstr Surg*. 2015;136(4S):150–151. doi:10.1097/01.prs.0000472474.17120.84
7. Cho YS, Jeon JH, Hong A, et al. The effect of burn rehabilitation massage therapy on hypertrophic scar after burn: A randomized controlled trial. *Burns*. 2014;40(8):1513–1520. doi:10.1016/j.burns.2014.02.005
8. Loghmani MT, Warden SJ. Instrument-assisted cross fiber massage increases tissue perfusion and alters microvascular morphology in the vicinity of healing knee ligaments. *BMC Complement Altern Med*. 2013;13:240. doi:10.1186/1472-6882-13-240
9. Wong YY, Smith RW, Koppenhaver S. Soft tissue mobilization to resolve chronic pain and dysfunction associated with postoperative abdominal and pelvic adhesions: A case report. *J Orthop Sports Phys Ther*. 2015;45(12):1006–1016. doi:10.2519/jospt.2015.5766
10. Brown BC, McKenna SP, Siddhi K, McGrouther DA, Bayat A. The hidden cost of skin scars: Quality of life after skin scarring. *J Plast Reconstr Aesthet Surg*. 2008;61(9):1049–1058. doi:10.1016/j.bjps.2008.03.020
11. Alvira-Lechuz J, Espiau MR, Alvira-Lechuz E. Treatment of the scar after arthroscopic surgery on a knee. *J Bodyw Mov Ther*. 2017;21(2):328–333. doi:10.1016/j.jbmt.2016.07.013
12. Shin TM, Bordeaux JS. The role of massage in scar management: A literature review. *Dermatol Surg*. 2012;38(3):414–423. doi:10.1111/j.1524-4725.2011.02201.x
13. Wasserman JB, Copeland M, Upp M, Abraham K. Effect of soft tissue mobilization techniques on adhesion-related pain and function in the abdomen: A systematic review. *J Bodyw Mov Ther*. 2019;23(2):262–269. doi:10.1016/j.jbmt.2018.06.004
14. Moris D, Chakedis J, Rahnama-Azar AA, et al. Postoperative abdominal adhesions: Clinical significance and advances in prevention and management. *J Gastrointest Surg*. 2017;21(10):1713–1722. doi:10.1007/s11605-017-3488-9
15. ElPrince M, Taha OT, Ibrahim ZM, et al. Prediction of intraperitoneal adhesions using striae gravidarum and scar characteristics in women undergoing repeated cesarean sections. *BMC Pregnancy Childbirth*. 2021;21(1):286. doi:10.1186/s12884-021-03763-z
16. O'Reilly S, Crofton E, Brown J, Strong J, Ziviani J. Use of tape for the management of hypertrophic scar development: A comprehensive review. *Scars Burn Heal*. 2021;7:205951312110292. doi:10.1177/20595131211029206
17. Klingenstein A, Garip-Kuebler A, Muth DR, Hintschich C. A prospective randomized pilot study evaluating the scar outcome after gluteal dermis fat graft with and without kinesiotaping. *Int Ophthalmol*. 2022;42(8):2563–2571. doi:10.1007/s10792-022-02304-7
18. Deflorin C, Hohenauer E, Stoop R, van Daele U, Clijsen R, Taeymans J. Physical management of scar tissue: A systematic review and meta-analysis. *J Altern Complement Med*. 2020;26(10):854–865. doi:10.1089/acm.2020.0109
19. Gianatasio C, Abrouk M, Waibel JS. Treatment approaches for treating hypertrophic scars and keloids. *Dermatol Rev*. 2021;2(1):11–22. doi:10.1002/der2.64
20. Koller T. Mechanosensitive aspects of cell biology in manual scar therapy for deep dermal defects. *Int J Med Sci*. 2020;21(6):2055. doi:10.3390/ijms21062055
21. Faul F, Erdfelder E, Lang AG, Buchner A. G*Power 3: A flexible statistical power analysis program for the social, behavioral, and biomedical sciences. *Behav Res Methods*. 2007;39(2):175–191. doi:10.3758/BF03193146
22. Cohen J. *Statistical Power Analysis for the Behavioral Sciences*. Hillsdale, USA: Lawrence Erlbaum Associates; 1988. doi:10.4324/9780203771587
23. Bringeland NE, Boeger D. *Terapia blizn metody stymulujące gojenie się ran i usprawniające funkcjonowanie układu powięziowego*. Wrocław, Poland: MedPharm Polska; 2020. ISBN:978-83-7846-111-1.
24. Siah CJR, Childs C. Thermographic mapping of the abdomen in healthy subjects and patients after enterostoma. *J Wound Care*. 2015;24(3):112;114–120. doi:10.12968/jowc.2015.24.3.112
25. Riquet D, Houel N, Bodnar JL. Stimulated infrared thermography applied to differentiate scar tissue from peri-scar tissue: A preliminary study. *J Med Eng Technol*. 2016;40(6):307–314. doi:10.1080/03091902.2016.1193239
26. Chochowska M, Marcinkowski J, Klimberg A. *Terapia manualna w pracy z blizną po operacji cięcia cesarskiego*. <http://www.h-ph.pl/hyg.php?opc=AR&lng=pl&art=636>. *Hygeia Public Health*. 2017;52(2):151–156. Accessed April 10, 2023.
27. Chamorro Comesaña A, Suárez Vicente M del P, Docampo Ferreira T, Pérez-La Fuente Varela M del M, Porto Quintáns MM, Pilat A. Effect of myofascial induction therapy on post-c-section scars, more than one and a half years old. Pilot study. *J Bodyw Mov Ther*. 2017;21(1):197–204. doi:10.1016/j.jbmt.2016.07.003
28. Bove GM, Chapelle SL, Hanlon KE, Diamond MP, Mokler DJ. Attenuation of postoperative adhesions using a modeled manual therapy. *PLoS One*. 2017;12(6):e0178407. doi:10.1371/journal.pone.0178407
29. Ault P, Plaza A, Paratz J. Scar massage for hypertrophic burns scarring: A systematic review. *Burns*. 2018;44(1):24–38. doi:10.1016/j.burns.2017.05.006
30. Anthonissen M, Daly D, Janssens T, van den Kerckhove E. The effects of conservative treatments on burn scars: A systematic review. *Burns*. 2016;42(3):508–518. doi:10.1016/j.burns.2015.12.006
31. Kassolik K, Andrzejewski W, Dziegieł P, et al. Massage-induced morphological changes of dense connective tissue in rat's tendon. *Folia Histochem Cytobiol*. 2013;51(1):103–106. doi:10.5603/FHC.2013.0014
32. Andrzejewski W. Mechanotransduction as one of potential mechanisms of impact of massage on the organism. *Physiotherapy*. 2014;22(4):44–49. doi:10.1515/physio-2014-0024
33. Karwacińska J, Kiebzak W, Stepanek-Finda B, et al. Effectiveness of kinesiotaping on hypertrophic scars, keloids and scar contractures. *Pol Ann Med*. 2012;19(1):50–57. doi:10.1016/j.poamed.2012.04.010

Gene expression profile of hiPSC-derived cells differentiated with growth factors, forskolin and conditioned medium from human adrenocortical cell line

Ewelina Stelcer^{1,A–D}, Karol Jopek^{1,B,C,F}, Małgorzata Blatkiewicz^{1,B,C,F}, Anna Olechnowicz^{1,2,B,C,F}, Kacper Kamiński^{1,2,B,C,F}, Marta Szyszka^{1,B,C,F}, Wiktoria Maria Suchorska^{3,4,A,C,E}, Marcin Ruciński^{1,A,C,E}

¹ Department of Histology and Embryology, Poznan University of Medical Sciences, Poland

² Doctoral School, Poznan University of Medical Sciences, Poland

³ Department of Electroradiology, Poznan University of Medical Sciences, Poland

⁴ Radiobiology Lab, Greater Poland Cancer Centre, Poznań, Poland

A – research concept and design; B – collection and/or assembly of data; C – data analysis and interpretation;

D – writing the article; E – critical revision of the article; F – final approval of the article

Advances in Clinical and Experimental Medicine, ISSN 1899–5276 (print), ISSN 2451–2680 (online)

Adv Clin Exp Med. 2024;33(4):397–407

Address for correspondence

Ewelina Stelcer

E-mail: ewelina.stelcer@ump.edu.pl

Funding sources

National Science Centre grant No. UMO-2017/25/

B//NZ4/00065

Conflict of interest

None declared

Received on February 19, 2023

Reviewed on April 6, 2023

Accepted on June 20, 2023

Published online on August 4, 2023

Cite as

Stelcer E, Jopek K, Blatkiewicz M, et al. Gene expression profile of hiPSC-derived cells differentiated with growth factors, forskolin and conditioned medium from human adrenocortical cell line. *Adv Clin Exp Med.* 2024;33(4):397–407. doi:10.17219/acem/168603

DOI

10.17219/acem/168603

Copyright

Copyright by Author(s)

This is an article distributed under the terms of the Creative Commons Attribution 3.0 Unported (CC BY 3.0) (<https://creativecommons.org/licenses/by/3.0/>)

Abstract

Background. Adrenocortical carcinoma (ACC) affects approx. 2 in 1,000,000 individuals in the USA, and is more common in females than males. Adrenocortical carcinoma often presents with severe symptoms, such as abdominal pain, high blood pressure, acne, hair overgrowth, and voice deepening.

Objectives. Research on ACC constitutes a large body of published data. There is an increased need for easy access to ACC-derived biological material. Moreover, there are limited numbers of human cell lines available. For this reason, we attempted to differentiate human induced pluripotent stem cells (hiPSCs) into adrenocortical-like cells to establish a new functional cell line.

Materials and methods. We conducted a long-term differentiation process (35 and 70 days) in the presence of growth factors (GFs), forskolin and conditioned medium collected from the human adrenal carcinoma (HAC15) cell line. Then, we analyzed the gene expression profile of the differentiated cells.

Results. The obtained cells possess features characteristic of all 3 primary germ layers. Interestingly, the differentiated cells demonstrated an extremely high level of gene expression for those involved in endocrine processes, namely glycoprotein hormones, alpha polypeptide (CGA), insulin receptor substrate 4 (IRS4), and pancreatic progenitor cell differentiation and proliferation factor-like protein (PPDPFL).

Conclusions. The results of the study indicate that we obtained progenitors derived from endoderm with some characteristics of pancreatic-like cells. The endodermal derivative differentiation is a very challenging and complicated process; thus, the results presented in this study deserve closer consideration.

Key words: human induced pluripotent stem cells, endoderm, adrenal cells, forskolin

Background

Adrenocortical tumors are quite frequent, with an incidence of 3–10% in the population.¹ These tumors can be divided into adrenocortical adenoma and adrenocortical carcinoma (ACC).² Adrenocortical carcinoma is sporadic, with a reported prevalence of 2 cases per 1,000,000 individuals/year, and is most frequently diagnosed in women (55–60% of cases) in their 4th or 5th decade of life.^{2,3} The main substance currently approved for the treatment of ACC is mitotane (2,4'-dichlorodiphenyl)dichloroethane, 1-(2-chlorophenyl)-1-(4-chlorophenyl)-2,2-dichloroethane, with a recommended therapeutic plasma mitotane level of 14–20 mg/L (~50 µM).³ However, the efficacy of this drug is limited due to its low pharmacokinetic properties and dose-limiting toxicity.³

Commercially available ACC human cell lines have a limited production capacity for mineralocorticoids, glucocorticoids and adrenal androgens. Furthermore, they show a limited response to angiotensin II (Ang II), adrenocorticotrophic hormone (ACTH) and potassium ions. Even so, they play an important role as a screening tool for cancer therapies.^{4,5} Researchers mainly rely on 2 commonly used ACC cell lines, namely NCI-H295R and SW-13. Importantly, both cell lines are characterized by TP53 loss-of-function alterations.⁶ Conversely to the non-hormone-producing SW-13 cells, NCI-H295R cells can produce steroid hormones and retain a gain-of-function Catenin beta 1 mutation.^{6,7} A 3rd cell line, the human adrenal carcinoma (HAC15), can respond to Ang II, potassium and ACTH, being the first adrenal cell line capable of such responses.⁸ Significant advances made in the last few years have changed the preclinical landscape for ACC. The new experimental models of ACC cells, namely MUC-1, CU-ACC1, CU-ACC2, JIL-2266, and TVBF-7, together with the commonly used NCI-H295R cell line, give researchers the instruments that are consistent with the well-defined heterogeneity of this disease and have the potential to disclose yet unknown patient subtype characteristics.⁹ In particular, the usefulness of CU-ACC1 and CU-ACC2 cells as models to improve the search for targets and drug efficacy in the treatment of ACC has been demonstrated.¹⁰ Nevertheless, there is a need to establish an ACC cell line that will show complete hormonal responses, steroidogenesis and expression of steroid-metabolizing enzymes.¹¹

Objectives

The objective of this study was to obtain cells that possess features of adrenal cells using human induced pluripotent stem cell (hiPSC) differentiation. We aimed to establish an easily accessible protocol, and for this reason, we relied on endo- and exogenous additives instead of previously described procedures, such as the overexpression of steroidogenic factor-1 (SF-1).¹² Because the cortex of the adrenal

gland is derived from mesoderm,¹³ whereas the medulla is derived from the neural crest and is of ectodermal origin,¹⁴ we decided to conduct long-term hiPSC differentiation via embryoid bodies (EBs) with all 3 primary germ layers for 35 days and 70 days in the presence of forskolin, growth factors (GFs) and conditioned media collected from the HAC15 cell line.

Materials and methods

Medium conditioning

A standard culture medium, consisting of Dulbecco's modified Eagle's medium/Nutrient Mixture F-12 (DMEM/F-12) (Thermo Fisher Scientific, Waltham, USA), 10% Cosmic Calf Serum (Hyclone; GE Healthcare, Westborough, USA) and 1% Insulin-Transferrin-Selenium (ITS) Premix Universal Culture Supplement (Corning Inc., Corning, USA), was used for conditioning. The medium was used for the HAC15 (ATCC® CRL-3301TM; American Type Cell Culture (ATCC), Manassas, USA) cells. The conditioned medium was collected after 24 h.

Adrenal differential medium

Adrenal media consisted of DMEM/F-12, 10% fetal bovine serum (Biowest, Nuaillé, France), 10 µM of forskolin (Merck Millipore, Burlington, USA), 1% ITS Premix Universal Culture Supplement (Corning Inc.), 50 µM of ascorbic acid and 10⁻⁷ M of dexamethasone (both from Merck Millipore), 10 ng/mL epidermal growth factor (EGF) and 10 ng/mL insulin-like growth factor 1 (IGF-1; both from STEMCELL Technologies, Cologne, Germany). All components of the medium were chosen based on previous adrenal-related literature.^{16–20}

hiPSC differentiation

We used 2 hiPSC cell lines, namely the purchased ND41658*H (Coriell Cell Repository, Camden, USA) and GPCCi001-A, previously described by our group.²¹ The cell lines formed EBs that were transferred onto 6-well plates coated with 0.1% gelatin (Merck Millipore, Darmstadt, Germany). On the 2nd day, the media were replaced with a 1:1 ratio of adrenal media and conditioned medium. The cells were collected 35 and 70 days after differentiation.

Microarray study

The total RNA was isolated from both undifferentiated and differentiated hiPSC cell lines. The following variants were obtained: control (GPCCi001-A and ND41658*H pooled into one) (i), 35 days differentiation (ii) and 70 days differentiation (iii). The whole procedure of preparing RNA for hybridization was conducted using the GeneChip™

WT PLUS Reagent Kit (Affymetrix Inc., Santa Clara, USA). The complete procedure has been described previously.^{22–26} Briefly, a two-step cDNA synthesis reaction was carried out with 100 ng of RNA using random primers extended by the T7 RNA polymerase promoter sequence. The cRNA was synthesized by the in vitro transcription for 16 h at 40°C. Then, the cRNA was purified and re-transcribed into cDNA. Next, the cDNA was biotin-labeled and fragmented using the Affymetrix GeneChip WT Terminal Labeling and Hybridization kit (Affymetrix Inc.). Biotin-labeled fragments of cDNA were hybridized using the Affymetrix Human Gene 2.1 ST ArrayStrip (20 h, 48°C), and the microarrays were stained with the aid of the Affymetrix GeneAtlas Fluidics Station (Affymetrix Inc.). Finally, the array strips were scanned using a GeneAtlas Imaging Station (Thermo Fisher Scientific). The preliminary analysis of the scanned chips was carried out with the use of Affymetrix GeneAtlas Operating Software (Affymetrix Inc.), and the quality of gene expression data was verified using the software's quality control criteria.

The obtained CEL files were analyzed using the R statistical language (R Foundation for Statistical Computing, Vienna, Austria) and Bioconductor package, including the selected Bioconductor libraries. The Robust Multi-array Average (RMA) normalization algorithm implemented in the “Affy” library was applied for the normalization, background correction and calculation of the expression values of the analyzed genes. A complete gene data table, including normalized gene expression values, gene symbols, gene names, and Entrez IDs was prepared based on the assigned biological annotations taken from the pd.hugene.2.1.st library. Linear microarray data models with moderated t statistics included in the “limma” library were applied for the expression and statistical assessment. The established cutoff criteria were as follows: the absolute value of expression fold change (FC) >2 and false discovery rate (FDR) adjusted $p \leq 0.01$. Genes fulfilling those criteria were considered differentially expressed genes (DEGs) and were subjected to further analyses. The result of such selection was presented as a volcano plot, showing the total number of up- and downregulated genes.

Variances were calculated for the entire gene expression dataset, and the top 1000 genes with the highest variance were subjected to principal component analysis (PCA). Principal component analysis of gene expression dataset was performed and visualized using factextra library²⁷ with default parameters ($n = \text{“auto”}$, $\text{rotation} = \text{“none”}$, $\text{center} = \text{TRUE}$, $\text{scale} = \text{TRUE}$).

The entire set of DEGs was subjected to functional annotation and clustering using the Database for Annotation, Visualization, and Integrated Discovery (DAVID) bioinformatics tool.²⁸ All gene IDs of DEGs were uploaded to DAVID with the use of the RDAVIDWebService Bioconductor library,²⁹ where they were assigned to relevant Gene Ontology (GO) terms, with a subsequent selection

of significantly enriched GO terms from the GO BP FAT database. The kappa statistics p-values of selected GO terms were corrected using Benjamini–Hochberg procedure, and were described as adjusted p-values. Differentially expressed genes from each comparison were visualized with a heatmap using the ComplexHeatmap library.³⁰

Gene set enrichment analysis (GSEA) was carried out using the clusterProfiler Bioconductor library.³¹ The analysis aimed to identify the level of depletion or enrichment in GO terms by calculating normalized enrichment score (NES) with a relevant p-value. Normalized FC values from all genes were \log_2 -transformed, sorted and used as an argument for the gseGO function. The gene set enrichment was performed regarding the “biological process” GO category, assuming the minimum size of each geneSet for analyzing = 100 and Fisher exact p-value ≤ 0.001 . Ten ontology groups with the highest enrichment score (the highest NES value) and 10 groups with the most depleted enrichment score (the lowest NES value) were visualized in a bar chart. Enrichment plots for 5 of the most enriched and 5 of the most depleted GO terms were also presented.

Technical descriptions with raw and normalized data files were deposited in the Gene Expression Omnibus (GEO) repository at the National Center for Biotechnology Information (<http://www.ncbi.nlm.nih.gov/geo/>), under the GEO accession No. GSE150775.

Real-time quantitative polymerase chain reaction analysis

Real-time quantitative polymerase chain reaction (qPCR) was carried out using the PrimePCR™ SYBR® Green Assay (Bio-Rad, Hercules, USA) and the specific synthesized primers for pancreatic progenitor cell differentiation as well as glycoprotein hormones, alpha polypeptide (CGA), and insulin receptor substrate 4 (*IRS4*).

Immunohistochemistry

After 70 days of differentiation, GPCCi001-A cells were fixed using 4% phosphate-buffered formalin, embedded in paraffin and sectioned. The samples were then stained using anti-CGA (ABIN3021817, 1:200) and anti-pancreatic progenitor cell differentiation and proliferation factor-like protein (PPDPFL) (NBP2-31818, 1:20) antibodies, according to the manufacturer's instructions.

Results

The 2 hiPSC cell lines undergoing 70-day differentiation changed their morphology during differentiation in vitro from cells forming colonies of EBs to spindle-like cells (Fig. 1A,B). Furthermore, they demonstrated active

proliferation during differentiation. The morphology of both differentiated hiPSC-derived cell lines was very similar.

To perform a complete comparison of differentiated cells and hiPSC transcriptomic profiles, we analyzed whole genome expression using Affymetrix Human Gene 2.1 ST ArrayStrips. Principal component analysis (Supplementary Fig. 1A) indicated clear segregation of cells before and after differentiation. After both 35-day and 70-day differentiation, there were distinct groups of hiPSCs visible. Moreover, both differentiation time points shared 30.7% of upregulated and 27.5% of downregulated genes, which corresponds to 47 and 56 genes, respectively (Supplementary Fig. 1B).

The general profile of whole gene expression in the differentiated ND41658*H/GPCCi001-A and undifferentiated groups is shown in a volcano plot (Fig. 2A), with each dot representing the mean expression level ($n = 3$) of a single gene obtained from a microarray normalized dataset. The selection criteria aimed at determining significantly altered gene expression were based on the absolute expression fold difference >2 and an adjusted $p \leq 0.01$. Genes above the cutoff value are differentially expressed and presented as orange (downregulated genes) or blue (upregulated genes) dots. Based on these criteria, 62 genes were significantly downregulated, and 100 genes were upregulated in the differentiated group compared to the hiPSCs 70 days after differentiation. Ten genes with the highest and 10 genes with the lowest FC values are presented in table format displaying the gene symbol, gene name, FC, and adjusted p-value (Fig. 2B). These genes were characterized by high FC values, especially for upregulated genes (range for upregulated genes: 79.90–5.89, and for downregulated genes: -5.76 – -2.98). This group

of genes includes glycoprotein hormones, namely *CGA* (FC = 79.90), *IRS4* (FC = 22.31), phosphoenolpyruvate carboxykinase 1 (*PCK1*) (FC = 7.24), synaptotagmin-like 5 (*SYTL5*) (FC = -5.76), Kelch-like family member 4 (*KLHL4*) (FC = -4.56), and gamma-aminobutyric acid type A receptor subunit epsilon (*GABRE*) (FC = -4.41).

We also compared gene expression profiles of cells after 35 days of differentiation to hiPSCs, and 70 days to 35 days after differentiation (Supplementary Fig. 2A,B). Interestingly, in 35-day cells, the high expression of *CGA*, *IRS4* and *PPDPFL* was notable. We found 198 genes significantly downregulated, and 99 were upregulated in the treated group compared to the hiPSCs 35 days after differentiation. The 2nd stage of differentiation (day 70 compared to day 35) resulted in minimal gene expression changes. No genes were downregulated and 8 genes were upregulated.

A bioinformatic evaluation of transcriptomic modulation was performed using GSEA (Fig. 3). This approach was based on the full transcriptomic profile analysis, regardless of the predefined cutoff criteria ($FC > 2$, $p \leq 0.01$). In this method, genes pre-ranked by logarithmic FC values were employed to determine enrichment (positive NES) or depletion (negative NES) in the GO-BP database after hiPSC differentiation. The largest cluster of enriched or depleted terms was related to “cell GTPase cell-cell involved”, “histone internal peptidyl-lysine acetylation”, “hormone-mediated intracellular steroid hormone”, “regulation of mRNA metabolic process” and “anion chloride transport” (Fig. 3A).

The 70-day differentiation led to the enrichment of genes involved in the regulation of steroid biosynthetic process (NES: 2.436), endocrine process (NES: 2.304) and mitochondrial adenosine triphosphate (ATP) synthesis coupled electron transport (NES: 2.328), as well as to the depletion

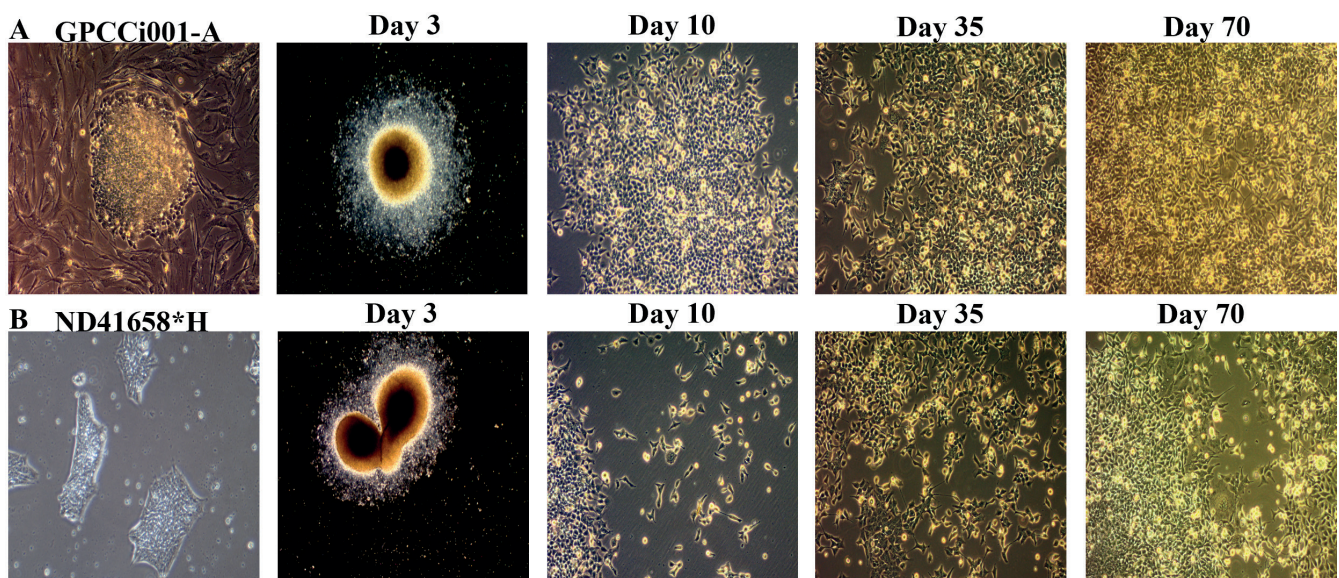


Fig. 1. Two human induced pluripotent stem cell (hiPSC) cell lines: GPCCi001-A (A) and ND41658*H (B), were differentiated via embryoid bodies (EBs) for 70 days in the presence of growth factors (GFs): epidermal growth factor (EGF) and insulin-like growth factor 1 (IGF-1), forskolin and conditioned medium collected from a human adrenal carcinoma (HAC15) cell line. They lost the ability to form colonies and took a spindle-like shape

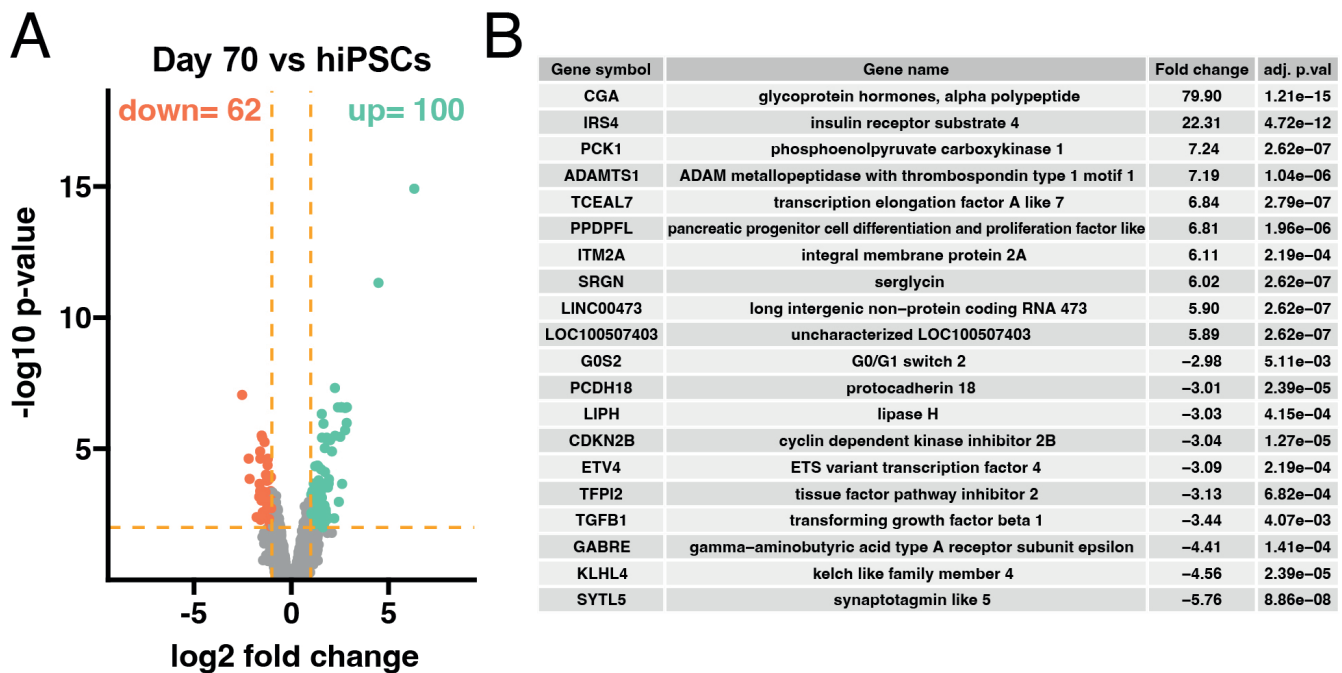


Fig. 2. The general profile of whole gene expression in the differentiated ND41658*H/GPCCI001-A and undifferentiated (untreated ND41658*H/GPCCI001-A) groups is shown in a volcano plot (A), with each dot on the graph corresponding to 1 transcript. Genes above the cutoff value are differentially expressed and shown as orange (downregulated genes) or blue (upregulated ones) dots. Seventy days after differentiation, 62 genes were significantly downregulated, and 100 genes were upregulated in the differentiated group compared to the human induced pluripotent stem cells (hiPSCs). Ten genes with the highest and 10 genes with the lowest fold change (FC) values are presented in tabular format displaying the gene symbol, gene name, FC, and adjusted p-value (B)

of genes related to, e.g., hormone-mediated signaling pathway (NES: -2.050), chloride transport (NES: -2.088) and histone H3-K4 methylation (NES: -2.155), among others (Fig. 3B).

The GSEA analysis also showed a significant decrease in the expression of genes closely related to cell-cell junction organization and intracellular steroid hormone receptor signaling pathway. These groups are comprised of genes with very low logFC values, thus their expression is suppressed during differentiation (Fig. 3C).

The interaction network between genes with the highest impact on “endocrine process”, “regulation of steroid biosynthetic process” and “mitochondrial respiratory chain complex” is presented in Fig. 3D. The expression of all presented genes increased after differentiation, suggesting that this process affects the physiological function of hiPSCs in a hormone-dependent manner.

Then, GO terms were assigned to the DEGs (Fig. 4). The GO analysis showed that the differentiation of hiPSCs significantly alters the expression of certain genes that play an essential role in the regulation of transcription, DNA-templated (GO: 0006351), regulation of vascular development (GO: 1901342), regulation of angiogenesis (GO: 0045765), epithelium development (GO: 0060429), cell death (GO: 0008219), and blood vessel development (GO: 0001568). Interestingly, at the differentiation midpoint (day 35), we observed a large decrease in the expression of genes involved in response to growth factor (GO: 0070848), regulation of cell communication (GO:

0010646), circulatory system development (GO: 0072359), cell migration (GO: 0016477), and blood vessel development (GO: 0001568). This suggests that circulatory-like features are developed in cells after 35 days of differentiation. The comparison between day 70 and day 35 did not show crucial gene expression changes.

Due to the structure of the GO database, single genes can often be assigned to many ontological terms. For this reason, the relationship between genes and GO terms with visualization of logFC values and gene symbols was demonstrated. To better show all dependencies, the results were compiled in a heatmap involving gene expression of all groups (day 70 compared to hiPSCs, day 35 compared to hiPSCs and day 70 compared to day 35) (Supplementary Fig. 3).

We also investigated the expression of genes involved in the 3 primary germ layers and stemness using qPCR *GATA4* (FC = 1.98, $p \leq 0.05$) as an endodermal marker, α -smooth muscle actin (α -SMA) (FC = 0.28, $p \leq 0.001$) and Brachyury as mesodermal markers, Vimentin and paired box 6 (*PAX6*) (FC = 0.872, $p > 0.05$) as ectodermal markers, as well as *CD133* (FC = 0.61, $p \leq 0.05$), *CD117* (FC = 0.989, $p > 0.05$), *CD44* (FC = 0.46, $p \leq 0.01$), and SRY-box transcription factor 2 (*SOX2*) (FC = 0.639, $p > 0.05$) as stem and/or cancer cell markers after 70-day differentiation (Supplementary Fig. 4). To confirm or refute our hypothesis, we have also examined features characteristic of adrenocortical-like cells. After 70 days of differentiation, the cells did not demonstrate expression of markers characteristic of adrenal cells such as steroidogenic acute

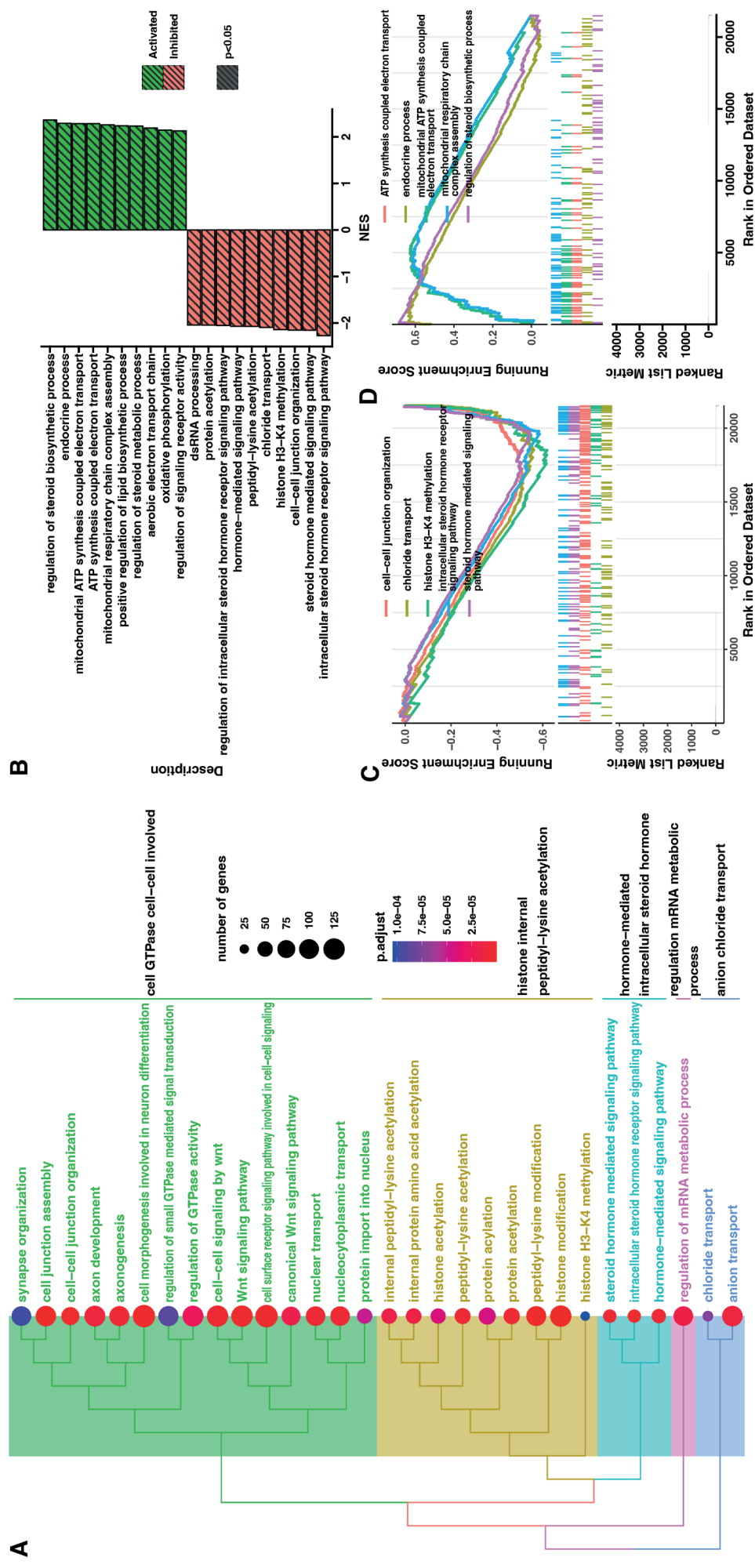


Fig. 3. A bioinformatic evaluation of transcriptome modulation was performed using gene set enrichment analysis (GSEA). Genes pre-ranked using logarithmic fold change (FC) values were employed to determine enrichment (positive normalized enrichment score (NES)) or depletion (negative NES) in the GO-BP database. The largest cluster of enriched or depleted terms was related to “cell GTPase cell-cell involved”, “histone internal peptidyl-lysine acetylation”, “hormone-mediated intracellular steroid hormone”, “regulation mRNA metabolic process”, and “anion chloride transport” (A). Differentiation of cells led, i.a., to the enrichment of genes involved in the regulation of steroid biosynthetic process and endocrine process, and to the depletion of genes related to, e.g., hormone-mediated signaling pathway (B). GSEA analysis also showed a significant decrease in the expression of genes closely related to cell-cell junction organization and intracellular steroid hormone receptor signaling pathway (C). The interaction network between genes with the highest impact on, i.a., endocrine process and regulation of steroid biosynthetic process are presented (D)

ATP – adenosine triphosphate.



Fig. 4. Differentially expressed genes from an investigated group (day 70 compared to human induced pluripotent stem cells (hiPSCs)) were then assigned to Gene Ontology (GO) terms. The GO analysis showed that differentiation alters the expression of genes that play an essential role in the regulation of signaling pathways, e.g., regulation of vascular development, regulation of angiogenesis, epithelium development, and blood vessel development. Halfway through differentiation (day 35), a high decrease in the expression of genes involved in, i.a., response to growth factor, regulation of cell communication, circulatory system development, cell migration, and blood vessel development was observed

regulatory protein (*STAR*), cytochrome P450, family 11, subfamily A, polypeptide 2 (*CYP11A2*), or cytochrome P450 family 11 subfamily B member 2 (*CYP11B2*) (data not shown), and based on enzyme-linked immunosorbent assay (ELISA), they did not secrete the primary hormones involved in steroidogenesis (aldosterone and cortisol; data not shown). The most upregulated genes, *CGA* and *IRS4*, were subjected to further qPCR evaluation in both hiPSCs cell lines separately (Supplementary Fig. 5A,B). The differentiated hiPS ND41658*H cells demonstrated elevated gene expression of *CGA* (FC = 573.6, $p > 0.05$) and *IRS4* (FC = 255.5, $p \leq 0.01$). In turn, hiPS GPCCi001-A cells were characterized by increased gene expression levels of *CGA* (FC = 564, $p \leq 0.05$) and *IRS4* (FC = 220.2, $p \leq 0.05$) after 70 days of differentiation. Based on these data, we confirmed the expression of *CGA* and PDPFL at the protein level using immunohistochemistry in the hiPSC GPCCi001-A cell line, revealing statistical significance in the case of both *CGA* and *IRS4* gene expression levels (Supplementary Fig. 5C).

Discussion

Adrenocortical carcinoma research constitutes a large body of published data, although there is only limited information available on human cell lines. Therefore, there is still a strong need to establish a functional ACC cell line. The main aim of this study was to obtain cells with features characteristic of adrenal cells via long-term differentiation in vitro. To verify our hypothesis, 2 hiPSC cell lines were subjected to differentiation in the presence of GFs, forskolin and ACC-conditioned medium (Fig. 1). The gene expression profile of differentiated cells differs significantly from undifferentiated and partially differentiated hiPSCs (Supplementary Fig. 1,2). Our findings demonstrated that instead of adrenocortical-like cells, we obtained cells with some endodermal features. Below, we discuss our results in the context of the differentiation of stem cells (SCs) into endodermal precursors and adrenocortical-like cells (originating from mesoderm).

Yazawa et al. revealed that mesenchymal stem cells (MSCs) can be differentiated into steroidogenic cells by expressing nuclear receptor 5A subfamily proteins (SF-1 and liver receptor homolog-1 (LRH-1)) in the presence of cyclic adenosine monophosphate (cAMP).³² Notably, the authors highlighted that there is a strong need to establish efficient protocols for inducing SF-1 and LRH-1 expression in SCs without gene transfer.³²

Another interesting approach was demonstrated by Li et al., who differentiated hiPSCs into adrenal cells with high efficiency toward androgen-producing Leydig cells.³³ They used 2 systems, namely MesenCult™-ACF Attachment Substrate-coated plates for generating adrenal cells

and plates coated with Collagen I rat protein solution for obtaining Leydig cells. These 2 systems involve deriving mesenchymal progenitors and overexpression of SF-1 in the presence of dibutyryl-cAMP, desert hedgehog and human chorionic gonadotropin.³³

Sonoyama et al. differentiated human embryonic stem cells (hESCs) and hiPSCs into steroid-producing cells involving the multistep method.¹² First, SCs were differentiated into the mesodermal lineage cells with the aid of BIO, a glycogen synthase kinase-3 beta inhibitor. Then, the mesodermal cells were transfected with plasmid DNA which encodes SF-1. The transfectants were further differentiated under the addition of 8-bromoadenosine 3',5'-cyclic monophosphate.¹²

The aforementioned studies show that the majority of protocols are based on forced overexpression of SF-1 in SCs. Our aim was to obtain adrenocortical-like cells without using genetic engineering tools. We focused on the influence of ACC-conditioned medium and exogenous addition of adrenal-related factors to the hiPSC-derived EBs. As a result, the cells acquired spindle-like morphology after long-term differentiation (Fig. 1) and were characterized by an altered gene expression profile (Fig. 2). They did not demonstrate the expression of genes involved in steroidogenesis (Supplementary Fig. 3) and did not secrete hormones after stimulation. Based on that, we can assume that our cells do not possess the features of adrenocortical cells.

The endodermal cells are challenging to grow in vitro, while the acquisition of primary tissues is often problematic and ethically questionable, especially from healthy donors. Consequently, basic research, disease modeling and regenerative medicine applications are limited by the lack of high-quality endodermal cells. Thus, the production of endodermal derivatives has been a major focus in the field of human pluripotent stem cells (hPSCs) for over 20 years.¹⁵

Organs derived from definitive endoderm, like the pancreas, are of great interest. Thus, D'Amour et al. described the production of enriched cultures of definitive endoderm derived from hESCs in the presence of activin A and low serum.³⁴ The transplantation of these cells under the kidney capsule resulted in their further differentiation into more mature cells with characteristics of endodermal organs.³⁴

Moreover, Bogacheva et al. demonstrated the influence of biomaterial properties on the endodermal differentiation process and the importance of spheroid size control for successful hiPSC differentiation.³⁵ The spheroid size determines the availability of growth factors as well as the supply of nutrients and oxygen to all cells. Suspension culture ensures sufficient mass transfer and thus provides more effective definitive endoderm differentiation in the presence of B-27 and activin A than nanofibrillar cellulose hydrogel-based culture.³⁵

Kopper and Benvenisty differentiated hESC-derived EBs into endodermal progenitors in the presence of activin A and fibroblast growth factor-2 (FGF2).³⁶ According them, once endoderm progenitor cells are isolated from other cell types and create their niche, they differentiate into hepatic, bile and colon tissues.³⁶

Fang and Li described a simplified but highly efficient procedure to induce hESC-based endoderm differentiation with crotonate, a precursor of crotonyl-CoA for histone crotonylation deposition on endodermal genes.³⁷ In this method, the addition of crotonate in different endodermal differentiation media significantly improved the differentiation efficiency and substantially diminished the number of required reagents.³⁷

A protocol based on the addition of all-trans-retinoic acid, basic FGF and dibutyryl-cAMP may result in obtaining definitive endoderm from murine ESCs in the absence of EB formation. Those cells may serve as pancreatic precursors and display an increased SOX17 and FOXA2 expression, consistent with definitive endoderm production.³⁸

To understand the distinctions between endodermal derivatives and other lineage-specific progenitors, the transcriptomes of 2-day mouse embryonic stem cells (mESCs) differentiated with bone morphogenetic protein 4 (BMP4), activin A and CHIR99021 were examined with scRNA-seq. The analysis revealed an endodermal-specific signature that is enriched for NODAL and Wingless-INT (WNT) signaling pathways, as well as metabolism-related gene expression.³⁹

Based on those studies, we believe that our results are of high scientific quality. Since differentiation toward mesodermal lineage was not our primary aim, we did not use activin A and FGF, which seems to be crucial in endodermal differentiation. On the contrary, the use of ACC-conditioned medium, forskolin, ascorbic acid, dexamethasone, EGF, and IGF-1 resulted in extremely high expression of genes characteristic for pancreatic-like cells, namely *CGA*, *IRS4* and *PPDPFL* (Fig. 2 and Supplementary Fig. 3). Moreover, we have demonstrated the presence of those markers at the protein level (Supplementary Fig. 5). Notably, our results indicate that signaling pathways connected with the circulatory system originating from mesoderm are activated in the obtained cells (Fig. 3,4). However, the qPCR analysis did not confirm higher expression of mesodermal markers α -SMA and Brachyury (Supplementary Fig. 4), and thus in this study, we focus on endodermal-like properties, which are more challenging to induce.

Limitations

We are aware that the results presented in this study are contrary to the assumed hypothesis. Nevertheless, we demonstrated comprehensive research, which provides new knowledge in the fields of cell biology and regenerative medicine. Apart from that, the in vitro research should be confirmed through in vivo experiments.

Conclusions

Herein, we presented an interesting outcome of long-term hiPSC differentiation in the presence of a conditioned medium collected from human ACCs, forskolin and other GFs. The gene expression profile revealed that obtained cells had features of all primary germ layers. We revealed that the gene expression profile of cells following 70-day differentiation differs from those differentiated for 35 days, as well as from undifferentiated hiPSCs. Moreover, we observed the elevated expression of endodermal markers like GATA Binding Protein 4 (GATA4). In the near future, they may have the potential to serve as endoderm precursors, such as pancreatic-like cells. Because the differentiation of SCs into endodermal derivatives is a challenging task, we believe that the work presented in our study will contribute to the improvement in generating specialized hiPSC-derived cells. Those cells could constitute a promising approach to tissue engineering in the future.

Supplementary data

The supplementary materials are available at <https://doi.org/10.5281/zenodo.7933236>. The package contains the following files:

Supplementary Fig. 1. PCA (A) indicates clear segregation of cells before and after differentiation. Cells after 35-day and 70-day differentiation create groups very distinct from hiPSCs. It is also noticeable that cells at both differentiation time points share 30.7% of upregulated and 27.5% of downregulated genes (B).


Supplementary Fig. 2. 35 days after differentiation, 198 genes were significantly downregulated and 99 were upregulated in the treated group compared to the hiPSCs (A). The 2nd stage of differentiation (day 70 compared to day 35) resulted in barely noticeable gene expression changes: 0 genes were downregulated and 8 genes were upregulated (B).

Supplementary Fig. 3. The connection between genes and GO terms with visualization of logFC values and gene symbols was demonstrated. To better show all dependencies, those results were compiled in a heatmap involving gene expression of all compared groups (day 70 compared to hiPSCs, day 35 compared to hiPSCs and day 70 compared to day 35).

Supplementary Fig. 4. GATA4 (FC = 1.98, $p \leq 0.05$) as an endodermal marker (i), α -SMA (FC = 0.28, $p \leq 0.001$) and Brachyury as mesodermal markers (ii), vimentin and PAX6 (FC = 0.872, $p > 0.05$) as ectodermal markers (iii), as well as CD133 (FC = 0.61, $p \leq 0.05$), CD117 (FC = 0.989, $p > 0.05$), CD44 (FC = 0.46, $p \leq 0.01$), SOX2 (FC = 0.639, $p > 0.05$) as stem and/or cancer cell markers (iv) after 70-day differentiation. The median, interquartile range (IQR) and mean (as diamond) are marked on the plots.

Supplementary Fig. 5. The most upregulated genes, *CGA* and *IRS4*, were subjected to further qPCR evaluation in both hiPSC cell lines separately (A,B). The differentiated hiPS ND41658*H cells demonstrated elevated gene expression as follows: *CGA* (FC = 573.6, $p > 0.05$) and *IRS4* (FC = 255.5, $p \leq 0.01$). The hiPS GPCCi001-A cells after 70-day differentiation were characterized by increased gene expression levels in the following manner: *CGA* (FC = 564, $p \leq 0.05$) and *IRS4* (FC = 220.2, $p \leq 0.05$). Based on that, we confirmed the expression of *CGA* and *PPDPFL* at the protein level by immunohistochemistry in the hiPSC GPCCi001-A cell line (C). The median, interquartile range (IQR) and mean (as diamond) are marked on the plots.

ORCID iDs

Ewelina Stelcer  <https://orcid.org/0000-0003-0077-9539>
 Karol Jopek  <https://orcid.org/0000-0002-7399-0303>
 Małgorzata Blatkiewicz  <https://orcid.org/0000-0001-5506-2397>
 Anna Olechnowicz  <https://orcid.org/0000-0001-6043-5637>
 Kacper Kamiński  <https://orcid.org/0000-0003-0641-1444>
 Marta Szyszka  <https://orcid.org/0000-0003-0150-3665>
 Wiktoria Maria Suchorska  <https://orcid.org/0000-0003-4742-2465>
 Marcin Ruciński  <https://orcid.org/0000-0002-2525-5777>

References

- Mete O, Erickson LA, Juhlin CC, et al. Overview of the 2022 WHO Classification of Adrenal Cortical Tumors. *Endocr Pathol.* 2022;33(1):155–196. doi:10.1007/s12022-022-09710-8
- Libé R. Adrenocortical carcinoma (ACC): Diagnosis, prognosis, and treatment. *Front Cell Dev Biol.* 2015;3:45. doi:10.3389/fcell.2015.00045
- Tsai WH, Chen TC, Dai SH, Zeng YH. Case report: Ectopic adrenocortical carcinoma in the ovary. *Front Endocrinol (Lausanne).* 2021;12:662377. doi:10.3389/fendo.2021.662377
- Wang T, Rainey WE. Human adrenocortical carcinoma cell lines. *Mol Cell Endocrinol.* 2012;351(1):58–65. doi:10.1016/j.mce.2011.08.041
- Alyateem G, Nilubol N. Current status and future targeted therapy in adrenocortical cancer. *Front Endocrinol (Lausanne).* 2021;12:613248. doi:10.3389/fendo.2021.613248
- Nicolson NG, Korah R, Carling T. Adrenocortical cancer cell line mutational profile reveals aggressive genetic background. *J Mol Endocrinol.* 2019;62(4):179–186. doi:10.1530/JME-18-0262
- Cheng JY, Brown TC, Murtha TD, et al. A novel FOXO1-mediated dedifferentiation blocking role for DKK3 in adrenocortical carcinogenesis. *BMC Cancer.* 2017;17(1):164. doi:10.1186/s12885-017-3152-5
- Parmar J, Key RE, Rainey WE. Development of an adrenocorticotropin-responsive human adrenocortical carcinoma cell line. *J Clin Endocrinol Metab.* 2008;93(11):4542–4546. doi:10.1210/jc.2008-0903
- Sigala S, Rossini E, Abate A, Tamburello M, Bornstein SR, Hantel C. An update on adrenocortical cell lines of human origin. *Endocrine.* 2022;77(3):432–437. doi:10.1007/s12020-022-03112-w
- Nanba K, Blinder AR, Rainey WE. Primary cultures and cell lines for in vitro modeling of the human adrenal cortex. *Tohoku J Exp Med.* 2021;253(4):217–232. doi:10.1620/tjem.253.217
- Sigala S, Bothou C, Penton D, et al. A comprehensive investigation of steroidogenic signaling in classical and Nex experimental cell models of adrenocortical carcinoma. *Cells.* 2022;11(9):1439. doi:10.3390/cells11091439
- Sonoyama T, Sone M, Honda K, et al. Differentiation of human embryonic stem cells and human induced pluripotent stem cells into steroid-producing cells. *Endocrinology.* 2012;153(9):4336–4345. doi:10.1210/en.2012-1060
- Xing Y, Lerario AM, Rainey W, Hammer GD. Development of adrenal cortex zonation. *Endocrinol Clin North Am.* 2015;44(2):243–274. doi:10.1016/j.ecl.2015.02.001
- Gordon J, Wilson VA, Blair NF, et al. Functional evidence for a single endodermal origin for the thymic epithelium. *Nat Immunol.* 2004;5(5):546–553. doi:10.1038/ni1064
- Yiangou L, Ross ADB, Goh KJ, Vallier L. Human pluripotent stem cell-derived endoderm for modeling development and clinical applications. *Cell Stem Cell.* 2018;22(4):485–499. doi:10.1016/j.stem.2018.03.016
- Manna PR, Huhtaniemi IT, Wang XJ, Eubank DW, Stocco DM. Mechanisms of epidermal growth factor signaling: Regulation of steroid biosynthesis and the steroidogenic acute regulatory protein in mouse Leydig tumor cells. *Biol Reprod.* 2002;67(5):1393–1404. doi:10.1095/biolreprod.102.007179
- Sicard F, Ehrhart-Bornstein M, Corbeil D, et al. Age-dependent regulation of chromaffin cell proliferation by growth factors, dehydroepiandrosterone (DHEA), and DHEA sulfate. *Proc Natl Acad Sci U S A.* 2007;104(6):2007–2012. doi:10.1073/pnas.0610898104
- Kinyua AW, Doan KV, Yang DJ, et al. Insulin regulates adrenal steroidogenesis by stabilizing SF-1 activity. *Sci Rep.* 2018;8(1):5025. doi:10.1038/s41598-018-23298-2
- Willenberg HS, Haase M, Papewalis C, Schott M, Scherbaum WA, Bornstein SR. Corticotropin-releasing hormone receptor expression on normal and tumorous human adrenocortical cells. *Neuroendocrinology.* 2005;82(5–6):274–281. doi:10.1159/000093126
- Zatelli MC, Rossi R, Degli Uberti EC. Androgen influences transforming growth factor-beta1 gene expression in human adrenocortical cells. *J Clin Endocrinol Metab.* 2000;85(2):847–852. doi:10.1210/jcem.85.2.6350
- Lach MS, Wroblewska JP, Augustyniak E, Kulcenty K, Suchorska WM. A feeder- and xeno-free human induced pluripotent stem cell line obtained from primary human dermal fibroblasts with epigenetic repression of reprogramming factors expression: GPCCi001-A. *Stem Cell Res.* 2017;20:34–37. doi:10.1016/j.scr.2017.02.004
- Stelcer E, Milecka P, Komarowska H, et al. Adropin stimulates proliferation and inhibits adrenocortical steroidogenesis in the human adrenal carcinoma (HAC15) cell line. *Front Endocrinol (Lausanne).* 2020;11:561370. doi:10.3389/fendo.2020.561370
- Budna J, Chachuła A, Kaźmierczak D, et al. Morphogenesis-related gene-expression profile in porcine oocytes before and after in vitro maturation. *Zygote.* 2017;25(3):331–340. doi:10.1017/S096719941700020X
- Golkar-Narenji A, Antosik P, Nolin S, et al. Gene ontology groups and signaling pathways regulating the process of avian satellite cell differentiation. *Genes (Basel).* 2022;13(2):242. doi:10.3390/genes13020242
- Rucinski M, Zok A, Guidolin D, De Caro R, Malendowicz LK. Expression of precerebellins in cultured rat calvaria osteoblast-like cells. *Int J Mol Med.* 2008;22(4):553–558. PMID:18813864.
- Stelcer E, Komarowska H, Jopek K, et al. Biological response of adrenal carcinoma and melanoma cells to mitotane treatment. *Oncol Lett.* 2022;23(4):120. doi:10.3892/ol.2022.13240
- Kassambara A, Mundt F. Factoextra: Extract and visualize the results of multivariate data analyses. <https://cran.r-project.org/web/packages/factoextra/index.html>. Accessed July 27, 2023.
- Dennis G, Sherman BT, Hosack DA, et al. DAVID: Database for annotation, visualization, and integrated discovery. *Genome Biol.* 2003;4(5):P3. PMID:12734009.
- Fresno C, Fernandez EA. RDAVIDWebService: A versatile R interface to DAVID. *Bioinformatics.* 2013;29(21):2810–2811. doi:10.1093/bioinformatics/btt487
- Gu Z, Eils R, Schlesner M. Complex heatmaps reveal patterns and correlations in multidimensional genomic data. *Bioinformatics.* 2016;32(18):2847–2849. doi:10.1093/bioinformatics/btw313
- Yu G, Wang LG, Han Y, He QY. clusterProfiler: An R package for comparing biological themes among gene clusters. *OMICS.* 2012;16(5):284–287. doi:10.1089/omi.2011.0118
- Yazawa T, Imamichi Y, Miyamoto K, Umezawa A, Taniguchi T. Differentiation of mesenchymal stem cells into gonad and adrenal steroidogenic cells. *World J Stem Cells.* 2014;6(2):203–212. doi:10.4252/wjsc.v6.i2.203
- Li L, Li Y, Sottas C, et al. Directing differentiation of human induced pluripotent stem cells toward androgen-producing Leydig cells rather than adrenal cells. *Proc Natl Acad Sci U S A.* 2019;116(46):23274–23283. doi:10.1073/pnas.1908207116
- D'Amour KA, Agulnick AD, Eliazar S, Kelly OG, Kroon E, Baetge EE. Efficient differentiation of human embryonic stem cells to definitive endoderm. *Nat Biotechnol.* 2005;23(12):1534–1541. doi:10.1038/nbt1163

35. Bogacheva MS, Harjumäki R, Flander E, et al. Differentiation of human pluripotent stem cells into definitive endoderm cells in various flexible three-dimensional cell culture systems: Possibilities and limitations. *Front Cell Dev Biol.* 2021;9:726499. doi:10.3389/fcell.2021.726499
36. Kopper O, Benvenisty N. Stepwise differentiation of human embryonic stem cells into early endoderm derivatives and their molecular characterization. *Stem Cell Res.* 2012;8(3):335–345. doi:10.1016/j.scr.2011.12.006
37. Fang Y, Li X. A simple, efficient, and reliable endoderm differentiation protocol for human embryonic stem cells using crotonate. *STAR Protoc.* 2021;2(3):100659. doi:10.1016/j.xpro.2021.100659
38. Kim PTW, Hoffman BG, Plesner A, et al. Differentiation of mouse embryonic stem cells into endoderm without embryoid body formation. *PLoS One.* 2010;5(11):e14146. doi:10.1371/journal.pone.0014146
39. Tu X, Zhang Q, Zhang W, Zou X. Single-cell data-driven mathematical model reveals possible molecular mechanisms of embryonic stem-cell differentiation. *Math Biosci Eng.* 2019;16(5):5877–5896. doi:10.3934/mbe.2019294

At what point are we on the way to optimally treat multiple myeloma patients over 75 years of age in 2023?

Agata Tyczyńska^{A–F}, Jan Zaucha^{A,C–F}

Department of Hematology and Transplantology, University Clinical Center, Medical University of Gdańsk, Poland

A – research concept and design; B – collection and/or assembly of data; C – data analysis and interpretation; D – writing the article; E – critical revision of the article; F – final approval of the article

Advances in Clinical and Experimental Medicine, ISSN 1899–5276 (print), ISSN 2451–2680 (online)

Adv Clin Exp Med. 2024;33(4):409–418

Address for correspondence

Jan Zaucha

E-mail: jan.zaucha@gumed.edu.pl

Funding sources

None declared

Conflict of interest

None declared

Received on April 11, 2023

Reviewed on June 14, 2023

Accepted on June 22, 2023

Published online on August 14, 2023

Abstract

Several novel drugs for multiple myeloma, including monoclonal and bispecific antibodies, immunomodulatory agents, and newer-generation proteasome inhibitors, have been introduced over the last decade. Based on the results of randomized clinical trials, the drugs have been incorporated into current treatment recommendations, with the most substantial changes observed in patients under the age of 75. However, new therapeutic options have been indirectly proposed for patients over 75, despite the lack of conclusive data from randomized prospective trials. This paper outlines the development of myeloma therapy and summarizes the current treatment recommendations for patients over 75 by systematically reviewing the most crucial studies involving this group of individuals, with a focus on evaluating treatment safety and efficacy. Melphalan–prednisone (MP), bortezomib plus MP (VMP), lenalidomide–dexamethasone (Rd), and bortezomib plus Rd (VRd) regimens have evolved over the past few years as therapies of choice for the first-line treatment of these patients. A breakthrough came with daratumumab, which increased response rates, extended median progression-free survival (PFS) and overall survival (OS) in the absence of significantly increased toxicity when added to the above regimens.

Key words: multiple myeloma, elderly, frailty, daratumumab, over 75 years of age

Cite as

Tyczyńska A, Zaucha J. At what point are we on the way to optimally treat multiple myeloma patients over 75 years of age in 2023?. *Adv Clin Exp Med.* 2024;33(4):409–418. doi:10.17219/acem/168685

DOI

10.17219/acem/168685

Copyright

Copyright by Author(s)

This is an article distributed under the terms of the Creative Commons Attribution 3.0 Unported (CC BY 3.0) (<https://creativecommons.org/licenses/by/3.0/>)

Background

Multiple myeloma patients over 75 years of age are an eminently heterogeneous group, ranging from very frail to relatively fit and independent. Tolerance of oncological treatments decreases with age and, as one ages, the presence of additional burdens, such as comorbidities, reduced compensatory capacity of internal organs, slower recovery, lower tolerance to adverse effects, simultaneous use of multiple drugs, psychomotor limitations, and less physical activity, develop. For these reasons, potential therapeutic options in this group of patients are limited. In addition, it is very difficult to predict individual tolerance to planned treatments. Myeloma-dedicated frailty status indices, such as the Myeloma Frailty Score, are helpful in treatment planning. Defining the intensity of treatment for an elderly myeloma patient should not only depend on the risk of the disease but also require an assessment of the mental, social and physical condition, an estimation of the life expectancy of the patient with and without myeloma, and predicting how the treatment and disease impact the patient's quality of life. Therefore, the goal of therapy in this group of patients is not only to achieve a profound response and extend time free from disease progression but also to maintain intellectual and physical independence. The treatment of the elderly often requires a third person in terms of availability and organization of care.^{1–11}

Objectives

This literature review encompasses the available results of clinical trials published from 1960 to 2022 that involved patients over 75 years of age. An attempt was made to propose practical guidelines for clinicians on individualizing therapy in these patients in order to safely achieve the longest possible survival time with a preserved quality of life.

Epidemiology

Multiple myeloma accounts for approx. 13% of hematologic malignancies and 2% of all cancers in humans.^{2–4} Among the most common lymphoid tissue neoplasms, multiple myeloma is 2nd to chronic lymphocytic leukemia,^{1–3,8,9} and is one of the most common indications for hospitalization in hematology departments.^{2,3}

Multiple myeloma incidence increases with age, though its occurrence rates are influenced by increasing accessibility to a faster and earlier diagnosis.^{2–5,8} The highest incidence rates are observed in Australia and New Zealand (age-standardized incidence rates of 37.7/100,000 for males and 29.4/100,000 for females) and North America (16.4/100,000 for males and 11.7/100,000 for females), and the lowest in Asia (0.2/100,000 for both males and

females in China), while in Europe the incidence rate is at 4.5–6/100,000. The incidence rate observed in Poland is similar to the European one: 4.36/100,000, including 4.84 for males and 3.89 for females.^{8,9} The median age at diagnosis is 70 years,^{1–4,9} with more than 60% of patients over 65 and approx. 32–38% over 75 years of age.^{6,7} The indications for treating multiple myeloma in elderly patients are the same as for younger patients. According to the International Myeloma Working Group (IMWG) guidelines, initiating treatment requires that symptomatic multiple myeloma is diagnosed along with Calcium Renal Anemia Bone (CRAB) symptoms with a score of 1–4 points, or one of the following changes are found in laboratory tests (so-called SLiM-Sixty, Light Chain, magnetic resonance imaging (MRI) criteria: points 5–7)¹:

1. Hypercalcemia: serum calcium ≥ 1 mg/dL over the normal upper limit or >11 mg/dL (sign C);
2. Occurrence of renal failure associated with myeloma: creatinine >2 mg/dL or a glomerular filtration rate (GFR) <40 mL/min (sign R);
3. Anemia defined as a hemoglobin concentration of 2 g/dL below the normal lower limit or <10 g/dL (sign A);
4. Presence of bone disease in the course of myeloma (a minimum of 1 osteolytic focus detected by positron emission tomography (PET) or computed tomography (CT)) (sign B);
5. The percentage of clonal plasma cells in the bone marrow $\geq 60\%$;
6. A clonal to non-clonal light chain ratio >100 , with a clonal light chain concentration of at least 100 mg/L;
7. Presence of at least 2 focal lesions on MRI of a minimum of 5 mm.

Treatment of elderly patients

The challenge in choosing the optimal treatment is to tailor it to the individual biology of the disease and the patient's general condition. The first regimen used to treat multiple myeloma in elderly patients and those ineligible for an autotransplantation procedure was the melphalan–prednisone (MP) regimen, which has been in use since the 1960s.¹² The addition of the first immunomodulatory drug, thalidomide, to the MP regimen (MPT) in 1999 increased progression-free survival (PFS) by approx. 6 months (from 18.5 to 24.1 months), and was based on a meta-analysis of 5 clinical trials (Table 1)^{13–19} that demonstrated overall survival (OS) to be prolonged by approx. 15 months.¹⁴ However, the improved treatment results were burdened by more than a 2.5-fold higher rate of grade 3 and 4 non-hematologic complications, mainly related to the use of thalidomide (the recommended dose at the time was as high as 200 mg/day), thromboembolic complications, peripheral polyneuropathies, lethargy, and skin lesions.^{13,14,19} The incidence of thromboembolic events was reduced in the GIMEMA and HOVON 49 trials

Table 1. Characteristics of registration trials for the melphalan–prednisone–thalidomide and melphalan–prednisone regimens for people aged over 75 years

Characteristics	Study group				
	GIMEMA	HOVON	IFM-II	NMSG	TMSG
Name of the study, reference	GIMEMA ¹⁸	HOVON 49 ¹⁵	IFM01/01 ¹⁷	NMSG12 ¹⁹	TMSG ¹⁶
Country/region	Italy	The Netherlands, Belgium	France	Northern Europe	Turkey
Number of patients	331	333	229	357	114
Years of recruitment	2002–2005	2002–2007	2002–2006	2002–2007	2006–2009
Age [years]	>65	>65	>75	>65	>55
Patients ≥75 years of age, n (%)	110 (33%)	121 (36%)	227 (99%)	159 (45%)	36 (31%)
Advancement, according to Durie–Salmon staging	II, III	Ib, II, III	II, III, and I high-risk	I–III symptoms	I–III symptoms
WHO status (ECOG)	0–4	0–3	0–4	0–4	0–2
Placebo	no	no	yes	yes	no
Dose of melphalan	4 mg/m ² day 1–4	0.25 mg/kg day 1–5	0.20 mg/kg day 1–4	0.25 mg/kg day 1–4	9 mg/m ² day 1–4
Dose of prednisone	40 mg/m ² day 1–7	1 mg/kg day 1–5	2 mg/kg day 1–4	100 mg day 1–4	60 mg/m ² day 1–4
Number of cycles/cycle length [weeks]	6/4	8/4	12/6	up to the plateau period/6	8/6
Thalidomide [mg/day]	100	200	100	200–400	100
Duration of treatment	until progression	8 cycles	12 cycles	until progression	8 cycles
Shift to MPT from MP	no	no	no	no	18%
Median OS MP vs. MPT [months]	47.6 vs. 45	31 vs. 40	29.1 vs. 44	32 vs. 29	26 vs. 28
Median PFS MP vs. MPT [months]	14.5 vs. 21.8	11 vs. 15	24.1 vs. 29	14 vs. 15	N/A

ECOG – Eastern Cooperative Oncology Group; MP – melphalan–prednisone; MPT – melphalan–prednisone–thalidomide; OS – overall survival; WHO – World Health Organization; N/A – not applicable.

by acetylsalicylic acid or low-molecular-weight heparin (2% to 3%) prophylaxis.^{13,17} The IFM 01/01 study confirmed the safety and efficacy of the MPT regimen in patients older than 75, showing a prolonged median OS for MPT (44 months) compared to MP (29.1 months),^{14,20} and it has been the recommended regimen in this age group since 2002.

In view of the relatively high toxicity of the 3-drug MPT regimen, an attempt was made to compare the 2-drug MP regimen to the thalidomide with dexamethasone (TD) regimen^{20–24} in elderly patients (trial No. NCT00205751). However, OS and PFS were shorter, despite achieving better responses in the experimental TD arm (19.8 months and 16.7 months compared to 41.3 months and 20.7 months for MP). In addition, the number of complications such as thromboembolic events, polyneuropathy, fatigue, infections, psychiatric disorders, and constipation was higher for the TD arm, mainly in patients over 75, which was probably related to the high doses of thalidomide and dexamethasone (the average dose administered was 200 mg/day of thalidomide and 40 mg of dexamethasone for the first 4 days of the cycle). The results indicated that the 3-drug regimen was more effective in older patients, but it was at the expense of greater toxicity, so the choice of the optimal treatment was still an open question.

New opportunities to determine optimal treatment in the elderly were created in 2005 with the registration of lenalidomide, a 2nd-generation immunomodulatory drug with less toxicity, especially in polyneuropathy and thrombotic events. The MM-015 trial, performed in patients over 65 and ineligible for transplantation, compared 3 regimens, namely MP, melphalan, prednisolone and lenalidomide (MPR) and MPR in the induction phase and maintenance treatment (MPR-R).^{22,25,26} The induction phase included 9 cycles of 28 days. The primary study endpoint was achieved, and there was a marked improvement in median PFS time with the MPR-R regimen (≥31 months) compared to MPR (14 months) and MP (13 months). The MPR regimen outperformed MP as an induction regimen in terms of response rate, quality of response and overall response rate. However, in patients older than 75, the median time of PFS for MPR-R was 19 months, for MPR – 12 months, and for MP – 15 months. The failure to demonstrate better efficacy using MPR in this age group may have been due to an increased incidence of adverse effects, particularly hematologic toxicity, which was associated with a more frequent need for dose modifications. The most important observation of this study was that maintenance treatment with lenalidomide (10 mg) alone, administered on days 1 to 21 over a 28-day cycle, was associated with improvements in PFS regardless of age

(median PFS time of 31 months, and 19 months for patients >75 years old) and an acceptable rate of hematologic adverse events in the form of asymptomatic cytopenias.

Another attempt aimed at determining the optimal treatment in elderly patients was made during the EMN01 trial between 2009 and 2012, which randomized newly diagnosed myeloma patients aged over 65 to 3 treatment arms: lenalidomide–dexamethasone (Rd), MPR, and cyclophosphamide, lenalidomide and prednisone (CRP).²⁵ The PFS time after a 31-month follow-up period was 23 months for Rd, 27 months for MPR and 23 months for CPR (Rd compared to MPR, $p = 0.216$; Rd compared to CPR, $p = 0.872$; MPR compared to CPR, $p = 0.148$), while the PFS time in the subgroup of patients older than 75 was 22 months for Rd, 18 months for MPR and 21 months for CPR (Rd compared to MPR, $p = 0.572$; Rd compared to CPR, $p = 0.699$; MPR compared to CPR, $p = 0.914$).²⁶ Adding an alkylating drug (melphalan or cyclophosphamide) to the lenalidomide and steroid combination showed no benefit in terms of PFS time in all patients. In contrast, the MPR regimen was burdened with a more than 60% rate of hematologic complications.^{26,27} The above study clearly indicated that the 3-drug treatment is recommended for younger patients and that the optimal treatment approach for patients aged >75 years is a 2-drug regimen, such as lenalidomide plus a steroid. However, the decision over which type of steroid to use (dexamethasone in lower doses (20 mg once a week) or appropriately dosed prednisone) remained an unresolved issue.^{26–28}

The NCT00098475 study provided important guidance on the treatment of the elderly, and its main goal was to identify the optimal dose of dexamethasone combined with lenalidomide. Two 28-day, 2-drug regimens of lenalidomide with dexamethasone were compared, with 1 arm receiving high doses of dexamethasone (40 mg for 4 days with 4 days off) and the other receiving 40 mg every 7 days. The lenalidomide dosage was 25 mg in both arms. The study was terminated early due to the significant safety advantage of lower doses of dexamethasone. High doses of dexamethasone yielded higher response rates for complete remission and had a very good partial response; however, this did not result in an improved PFS time. Indeed, the median PFS time for the high dose was 19.1 months (15.7–26.3), while the low dose resulted in PFS time of 25.3 months (22.3 – not reached, $p = 0.026$),²⁶ and there was no correlation between the depth of response and the length of response. However, the trial was stopped after 1 year due to the better OS achieved with low-dose dexamethasone compared to the high dose. Nonetheless, it should be remembered that in certain cases, such as acute renal failure due to myeloma nephropathy, myeloma cord compression or aggressive refractory disease, high-dose steroids still play an important role in therapy.

Based on the results of the study outlined above, the Frontline Investigation of Lenalidomide + Dexamethasone versus Standard Thalidomide Trial-MM-020/IFM

07 01 (FIRST) study was designed for patients over 65 years of age and compared MPT (12 cycles of 42 days), Rd (18 cycles, Rd18) and Rd continuous regimens until disease progression (Table 2). In the Rd arms, doses of lenalidomide (25 mg) and dexamethasone (40 mg) were administered on days 1, 8, 15, and 22. Approximately 1/3 of the study participants were older than 75 years.^{28,29} After 3 years of follow-up, the median PFS was 26 months for the Rd continuous regimen, 21 months for Rd18, and 21.9 months for MPT. Meanwhile, the median OS time was 59.1 months for the Rd continuous arm, 62.3 months for Rd18, and 49.1 months for MPT. The highest rate of hematologic complications was observed with the MPT regimen (45%).³⁰ The most important achievement of this study was that it demonstrated the highest efficacy in terms of the number of achieved responses (overall response rate (ORR) = 75.1%) and the duration of response in patients older than 75. As such, the Rd continuous regimen extended the time to 2nd progression or death to 35 months, prolonged PFS to 26 months, and significantly increased OS to 59 months. Since publishing the results of the FIRST study, the Rd continuous regimen has been the recommended treatment for patients ineligible for autologous transplantation and the elderly. A significant advantage of this treatment option is the oral route of drug administration.

Unfortunately, the Rd regimen is not sufficiently effective in all elderly patients. Therefore, attempts have been made to determine the role of proteasome inhibitors in treating this group. Bortezomib was the first effective proteasome inhibitor and is still recommended for the treatment of both younger and older patients.¹ Its main advantage over lenalidomide is the lack of nephrotoxicity, though it induces polyneuropathy in some patients, which is not dose-dependent, as with thalidomide. The VISTA study compared bortezomib plus MP (VMP) and MP regimens, with 30% of patients being over 75 years of age.^{29–31} Median PFS was prolonged to approx. 22 months in the VMP arm compared to 16.6 months in the MP arm (Table 2).^{28–40} However, better PFS outcomes were burdened by a higher number of non-hematologic adverse events, mainly peripheral polyneuropathy. Subsequent studies evaluating the safety and efficacy of multidrug regimens using bortezomib for transplant-ineligible patients (VMP and bortezomib, thalidomide dexamethasone (VTd)), namely the GIMEMA BIW, GIMEMA Q7 and GEM2005MAS655 trials (in all studies, patients over 75 years of age accounted for 30%, 26% and 32%, respectively), demonstrated the same efficacy. The VISTA (21.7 months), GIMEMA BIW (25.2 months), GIMEMA QW (22.2 months), and GEM2005MAS65 trials (38 months) reported an increased median PFS, which was associated with once-weekly bortezomib maintenance treatment for up to 3 years instead of twice-weekly administration.⁴⁰ The peripheral neuropathy (grade 3 and 4) incidence in the VISTA study was 13%, 14% in the GIMEMA BIW trial, 7% in the GEM2005MAS65 trial, and 2% in the GIMEMA QW trial.⁴¹

Table 2. Registration trials of currently used treatment regimens

Name of the study, year	Regimens used	Regimen details	Median progression-free survival (mPFS) [months]	Median overall survival (mOS) [months]
VISTA, 2008 ²⁹	VMP 9 cycles, 42 days	bortezomib: 1.3 mg/m ² IV; days 1, 4, 8, 11, 22, 25, 29, 32 (cycles 1–4); days 1, 8, 22, 29 (cycles 5–9)	24	56.4
	MP 9 cycles, 42 days	melphalan: 9 mg/m ² ; days 1–4 prednisolone: 60 mg/m ² ; days 1–4; continuous	18	43
FIRST, 2014 ^{27,28,30}	Rd continuous, 28 days	28-day regimen: lenalidomide: 25 mg; days 1–21 dexamethasone: 40 mg; days 1, 8, 15, 22	26	59.1
	Rd 18 cycles, 28 days	lenalidomide: 25 mg; days 1–21 dexamethasone: 40 mg; days 1, 8, 15, 22	21	62.3
	MPT 12 cycles, 42 days	melphalan: 0.25 mg/kg; days 1–4 prednisolone: 2 mg/kg; days 1–4 thalidomide: 200 mg daily	21.9	49.1
UPFRONT, 2015 ³¹	VD 8 cycles, 21 days	bortezomib: 1.5 mg/m ² IV; days 1, 4, 8, 11 dexamethasone: 20 mg; days 1, 2, 4, 5, 8, 9, 11, 12 (cycles 1–4); days 1, 2, 4, 5 (cycles 5–8)	14.7	49.8
	VTd 8 cycles, 21 days	bortezomib: 1.5 mg/m ² IV; days 1, 4, 8, 11 dexamethasone: 20 mg; days 1, 2, 4, 5, 8, 9, 11, 12 (cycles 1–4); days 1, 2, 4, 5 (cycles 5–8) thalidomide: 100 mg; days 1–21	15.4	51.5
	VMP 8 cycles, 21 days; maintenance with bortezomib IV 1.5 mg/m ² , days 1, 8, 15, 22	bortezomib: 1.5 mg/m ² IV; days 1, 4, 8, 11 prednisolone: 60 mg/m ² ; days 1–4 melphalan: 9 mg/m ² ; days 1–4	17.3	53.1
SWOG S07777, 2017 ³⁴	VRd 8 cycles, 21 days	bortezomib: 1.3 mg/m ² IV; days 1, 4, 8, 11 lenalidomide: 25 mg; days 1–14 dexamethasone: 20 mg; days 1, 2, 4, 5, 8, 9, 11, 12	43	75
	Rd 6 cycles, 28 days	lenalidomide: 25 mg; days 1–21 dexamethasone: 40 mg; days 1, 8, 15, 22	30	64
CLARION, 2019 ³⁵	KMP 9 cycles, 42 days	carfilzomib: 20 mg/m ² IV on days 1 and 2 in cycle 1, 36 mg/m ² IV in others; days 1, 2, 8, 9, 22, 23, 29, 30 melphalan: 9 mg/m ² ; days 1–4 prednisolone: 60 mg/m ² ; days 1–4	22.3	no data
	VMP 9 cycles, 42 days	bortezomib: 1.3 mg/m ² SC or IV on days 1, 4, 8, 11, 22, 25, 29, 32 (cycles 1–4); days 1, 8, 22, 29 (cycles 5–9) melphalan: 9 mg/m ² ; days 1–4 prednisolone: 60 mg/m ² ; days 1–4	22.1	no data
ALCYONE, 2018 ^{37,38}	DaraVMP 9 cycles, 42 days	daratumumab: 16 mg/kg IV/week in cycle 1; every 3 weeks until cycle 29, then every 4 weeks bortezomib: 1.3 mg/m ² SC or IV on days 1, 4, 8, 11, 22, 25, 29, 32 (cycles 1–4); days 1, 8, 22, 29 (cycles 5–9) melphalan: 9 mg/m ² ; days 1–4 prednisolone: 60 mg/m ² ; days 1–4	not reached	under evaluation
	VMP 9 cycles, 42 days	bortezomib: 1.3 mg/m ² SC or IV on days 1, 4, 8, 11, 22, 25, 29, 32 (cycles 1–4); days 1, 8, 22, 29 (cycles 5–9) melphalan: 9 mg/m ² ; days 1–4 prednisolone: 60 mg/m ² ; days 1–4	19.3	under evaluation
MAIA, 2019 ³⁶	Dara-Rd 28-day cycles	daratumumab: 16 mg/kg IV/week (cycles 1 and 2); every 2 weeks (cycles 3–6); then every 4 weeks lenalidomide: 25 mg; days 1–21 dexamethasone: 40 mg weekly	not reached	under evaluation
	Rd continuous, 28-day cycles	lenalidomide: 25 mg; days 1–21 dexamethasone: 40 mg weekly	31.9	under evaluation
TOURMALINE-MM2 ^{32,39}	IRd 9 cycles, 28 days	ixazomib: 4 mg; days 1, 8, 15 lenalidomide: 25 mg; days 1–21 dexamethasone: 40 mg; days 1, 8, 15, and 22 (20 mg for patients >75 years old)	35.3	no data
	Rd 9 cycles, 28 days	lenalidomide: 25 mg; days 1–21 dexamethasone: 40 mg; days 1, 8, 15, and 22 (20 mg for patients >75 years old)	21.8	no data
VRd lite, 2014 ³³	VRd 35 days	bortezomib: 1.3 mg/m ² IV; days 1, 8, 15, 22 lenalidomide: 15 mg; days 1–21 dexamethasone: 20 mg; days 1, 2, 8, 9, 15, 16, 22, 23	35.1	not reached

MP – melphalan–prednisone; VMP – bortezomib plus MP; Rd – lenalidomide–dexamethasone; MPT – melphalan–prednisone–thalidomide; VTd – bortezomib–thalidomide–dexamethasone; VRd – bortezomib plus RD; KMP – carfilzomib–melphalan–prednisone; IV – intravenous; SC – subcutaneous; VD – bortezomib–dexamethasone; IRd – ixazomib–lenalidomide–dexamethasone.

The UPFRONT trial, dedicated to determining the role of bortezomib in the treatment of the elderly (half of the patients were >75 years old), randomized participants into bortezomib dexamethasone (Vd), VTd and VMP arms.³¹ The median PFS time was similar for each regimen, that being 14.7 months for Vd, 15.4 months for VTd, and 17.3 months for VMP, with no significant differences in the incidence in grade 3 and 4 peripheral polyneuropathies in the Vd (24%), VTd (29%) or VMP (21%) arms.^{31,34} As such, the study indicated the possibility of using a 2-drug regimen (Vd) in elderly patients, as it provided the same benefit as 3-drug regimens. However, it should be noted that it was possible to reduce the incidence of neurological complications by using bortezomib once a week.^{29–31,42,43}

The above studies, similar to those evaluating lenalidomide, demonstrated the advantages of 2-drug regimens in patients over 75 years of age. However, the partners for lenalidomide and bortezomib were alkylating drugs (melphalan or Endoxan) or the relatively toxic thalidomide (VTd). In this regard, a key study in the elderly, in which patients over 75 accounted for 25.5% of participants, was the US SWOG S0777 trial comparing the bortezomib plus Rd (VRd) regimen (bortezomib, lenalidomide and dexamethasone) to the Rd regimen (lenalidomide and dexamethasone).³⁴ Median PFS for patients over 75 treated with VRd was 39 months, compared to 20 months for those treated with the Rd regimen ($p = 0.0037$), while the median OS time was 63 months (VRd) compared to 31 months (Rd, $p = 0.0250$) (Table 2).³⁴ Grade 3 adverse events occurred in 82% of patients in the VRd arm and in 75% of patients in the Rd arm. The most common hematologic adverse events attributed to the treatments were \geq grade 3 cytopenias in all 4 cell lines, and the most common \geq grade 3 non-hematologic adverse events were muscle weakness, fatigue, cardiac disorders, hyperglycemia, thrombosis, embolism, and diarrhea. As expected, neurological events graded 3 or higher, mainly peripheral polyneuropathy, were more frequent in the VRd (33%) group than in the Rd group (11%, $p < 0.0001$), though there was a balance between the 2 groups for all other events.

The SWOG 0777 study unequivocally showed improved PFS, OS, depth of response, and response rates using the VRd regimen while maintaining a relatively comparable safety profile to the Rd regimen.³⁴ In addition, lower toxicity and additional improvements in survival can be expected with weekly subcutaneous administration of bortezomib.⁴³

The results of the presented studies indicate that it is possible to safely use a 3-drug regimen in patients over 75 years of age, as the treatment offers the greatest benefit, with long OS and relatively well-tolerated drug toxicity. The VRd appears to be the safest of the 3-drug regimens. On the other hand, the Rd regimen, in an indirect comparison with VTd and VMP, provides similar benefits with less toxicity and is a good alternative in the absence

of a 3-drug regimen, mainly in the presence of contraindications to bortezomib. However, using the VRd regimen in the elderly, despite its advantages, is not appropriate for all patients, primarily due to the risk of developing polyneuropathy and causing a decline in quality of life.

An attractive proposal for improving the efficacy of the 2-drug Rd regimen was the addition of daratumumab, which has a completely different mechanism of action than the drugs used so far. Daratumumab (D) is a human monoclonal antibody of the immunoglobulin (Ig)G1 class and is effective against the cluster of differentiation (CD)38 antigen. After binding to CD38, it strongly inhibits cell growth and cell adhesion to the microenvironment and has a direct anti-tumor effect. In addition, it is highly immunologically active and uses complement-dependent cytotoxicity (CDC) to induce tumor cell lysis and tumor cell death through an effector function mediated, for example, by natural killer (NK) cells, which it activates by cross-binding with the Fc receptor (ADCC). Moreover, daratumumab induced antibody-dependent cellular phagocytosis (ADCP), in which macrophages play a major role. In addition, it exhibits immunomodulatory properties by increasing the levels of CD4⁺ and CD8⁺ T cells in the blood and bone marrow. The antibody also reduces the number of regulatory T cells (CD38⁺Tregs), B cells (CD38⁺Bregs) and myeloid-derived suppressor cells (CD38⁺MDSCs).

The comparison of the randomized MAIA Rd with the D-Rd trial, in which 43.2% of patients were over 75 years old, was crucial for results concerning older people. The median PFS time was not reached in the experimental arm after a 56-month follow-up, but it was reached in the control group after 34.4 months.^{36,42,44} Furthermore, the proportion of patients who had a complete response, or better, an almost doubled response, and negative or minimal residual disease was more than 3 times higher for the daratumumab group than the control group.^{36,44–49} However, reporting of grade 3 and 4 adverse events was more frequent in the daratumumab arm and included neutropenia (54% compared to 37%), pneumonia (19% compared to 11%) and lymphopenia (16% compared to 11%). Furthermore, treatment-related deaths were slightly higher in the daratumumab arm (4%) than in the control group (3%), and no new complications were observed.^{36,45–49}

An alternative partner to dexamethasone, instead of Rd, is the MPV regimen, which was used in the ALCYONE trial comparing daratumumab plus VMP (D-VMP) to VMP (29.9% were patients older than 75 years).^{37,38,46–48} As expected, PFS analyses showed consistent superiority of D-VMP over VMP across all subgroups, which included those over 75 years of age and prognostic factors (stage III ISS disease, renal failure or high-risk cytogenetic profile). Additionally, as in the MAIA trial, they did not reach the median PFS, but the PFS of 18.1 months was reported for the control group (values similar to the FIRST

trial).^{27,28,36,50} Grade 3 and 4 hematologic complications included neutropenia (39.9% of D-VMP patients compared to 38.7% of control patients), anemia (15.9% of D-VMP patients compared to 19.8% of control patients) and thrombocytopenia (34.4% of D-VMP patients compared to 37.6% of control patients). In addition, the percentage of grade 3 and 4 infections was higher in the D-VMP group (23.1%) than in the control group (14.7%). The most frequent grade 3 or 4 infection was pneumonia, which occurred more often in the D-VMP group (11.3%) than in the control group (4.0%), while peripheral polyneuropathy was more common in the control group (34.2% compared to 28.3%), with grade 3 and 4 infections occurring at 4% for the VMP and 1.4% for the D-VMP groups. Of course, it is important to keep in mind the adverse events associated with daratumumab administration, of which grades 1 and 2 affected 1 in 4 patients, and grades 3 and 4 occurred in 4.9% of patients. However, the number and quality of daratumumab-related events have been effectively minimized, with the introduction of a subcutaneous form. The efficacy and safety of a fixed dose (1800 mg) of subcutaneous daratumumab were demonstrated in the PLEIADES trial, in which all events associated with subcutaneous daratumumab administration accounted for 7.5% (15/199), with 1 case involving grade 3 and the rest grade 1 or 2.⁵¹ Furthermore, no drug-related events were reported with the 2nd administration, and only 3 grade 1 and 2 cases (1.5%; 3/199) were reported in subsequent administrations.

Overall toxicity did not increase when using daratumumab in combination with VMP. Except for respiratory tract infections (3 times more common in the daratumumab group), there was a balance between the daratumumab and control groups in terms of adverse events, although peripheral sensory neuropathy rates were lower in the daratumumab group. In addition, in the ALCYONE trial evaluating patients' quality of life, both arms showed early and sustained improvements in health-related quality of life (HRQoL), function and reduced disease symptoms.³⁷

Both D-Rd and D-VMP regimens can be used in patients over 75 years of age, but due to toxicity, the D-Rd regimen is the safer and more convenient form of treatment. A study comparing the D-Rd regimen with VRD lite is currently being planned, the results of which may change the sequence of recommended regimens (study No. NCT05561387).

Carfilzomib is a novel selective and irreversible proteasome inhibitor recommended for refractory multiple myeloma and/or relapse. A phase I/II trial for a first-line treatment of patients over 65 years of age, combining carfilzomib with melphalan and prednisone (KMP) reported a PFS of 21 months and a response rate of 90%. The study formed the basis for the Phase 3 CLARION trial, which directly compared VMP and KMP arms. The study included 31.3% of patients over 75 years of age and confirmed the safety of carfilzomib as first-line treatment, primarily in terms of polyneuropathy incidence (incidence

of minimum grade 2 polyneuropathy was 2.5% in the KMP arm and 35.1% in the VMP arm), but showed no statistical differences in PFS time (22.3 months for KMP compared to 22.1 months for VMP).³⁵ In contrast, the ENDURANCE trial compared VRd to carfilzomib, lenalidomide and dexamethasone (KRd). The study included 32% of patients over 70 years of age and showed no increase in PFS time after carfilzomib treatment. The regimen was more toxic in this group of patients.⁵²

Ixazomib is an oral proteasome inhibitor (like 2nd-generation carfilzomib) that was studied in the first-line treatment of transplant-ineligible patients (those over 75 years of age accounted for 43.5%). The TOURMALINE-MM2 study compared ixazomib in combination with Rd to Rd alone, and the results suggested a clinically significant PFS benefit for this group of patients, with a median PFS in the ixazomib arm of 27.9 months and 20.5 months for Rd, and a hazard ratio (HR) of 0.87, but this was not statistically significant.³⁹ The PFS benefit of ixazomib-Rd was observed primarily in patients with renal failure, high-risk cytogenetics and grade 3 injury severity score (ISS). Furthermore, the toxicity profile was acceptable but markedly higher in the ixazomib group, though it did not reduce the patient's quality of life, with rash and diarrhea grade 3 and above being more common in the investigational regimen group. The ixazomib regimen in combination with Rd may be considered in patients who can only take oral medications, are high-risk, or those with renal failure.

Studies evaluating the safety and efficacy of regimens combining lenalidomide and dexamethasone with ixazomib, elotuzumab, isatuximab, bispecific antibodies, or chimeric antigen receptor (CAR)-T therapy for first-line treatment are currently underway, and some studies may include patients aged over 75.

The results of the CAR-T therapies, namely idecabtagene vicleucel (ide-target) and ciltacabtagene autoleucel (ciltacel), both targeting the myeloma B-cell maturation antigen (BCMA), are eagerly awaited. Both therapies are undergoing intensive first-line trials in transplant-ineligible patients, such as CARTITUDE 5. However, patients over 80 are not included in the study (NCT04923893). Bispecific antibodies, on the other hand, are most often administered subcutaneously cyclically (every 1–4 weeks) and do not require time-consuming production for each patient. For this antibody (bispecific antibodies), one target is CD3 on T cells, and the other is an antigen found on myeloma cells such as BCMA (teclistamab, elranatamab, linvoseltamab), GPRC5D (talquetamab) and FcRH5 (cevestamab). Importantly, the trials on teclistamab and elranatamab (EudraCT No. 2021-000803-20) for non-transplant patients as first-line treatment have recently been started, with no age limit.⁵³ The most serious complications of both therapies are infectious complications accompanied by hypogammaglobulinemia, cytokine release syndrome (CRS) and neurological disorders (ICONS). From the data

obtained so far, the percentage of grade 3 and 4 complications is acceptable.

Patients over 75 have the highest mortality rate, which did not significantly improve in the analysis up to 2012.⁵⁴ Factors that increase the risk of death, along with early death (up to 12 months after the diagnosis of the disease), include limited function according to the Eastern Cooperative Oncology Group (ECOG) status,^{55–57} advanced disease (ISS 3), and comorbidities such as cardiovascular diseases, including hypertension and chronic kidney disease.^{58–60} In a retrospective meta-analysis of 4 randomized trials, it was shown that patients older than 75 have an increased risk of death (HR: 1.44, 95% confidence interval (95% CI): 1.20–1.72, $p < 0.001$).⁴⁴ Additionally, the aggressiveness of the therapy contributes to this state of affairs. Indeed, there was a 3.02-fold increase in patients receiving VTd/bortezomib–melphalan–prednisone–thalidomide (VMPT), a 1.62-fold increase in patients receiving VMP, and a slight increase in those receiving MP/MPT.^{20,21,41,50,61}

Conclusions

The treatment of multiple myeloma patients, including elderly patients over 75 years of age, has undergone significant changes over the past 20 years. The MPT regimen based on the FIRST trial, which was groundbreaking in the early 2000s, has been replaced by the Rd regimen. The VRD 3-drug regimen, its “light” version in particular, has been considered an equally interesting option. However, based on the ALCYONE and MAIA trials, the D-Rd regimen is the most effective and safest treatment option.

The Rd regimen with ixazomib did not show a significant benefit over Rd in patients over 75, although it is an attractive treatment option due to its complete ambulatory nature (all drugs are administered orally). In contrast, there are no data on the use of the Rd regimen with carfilzomib as a first-line therapy in patients over 75, as the ENDURANCE trial only included patients between the ages of 70 and 75. The only available treatment recommendations for patients over 75 are those by the National Comprehensive Cancer Network (NCCN). The NCCN panel does not recommend separate treatment for patients over 75 years of age; however, for frail patients, the VRD lite regimen is recommended.

Therapeutic decisions should be made after assessing the risk of the disease, the severity of CRAB symptoms, especially renal failure, and other comorbidities, as well as the patient’s situation (place of residence, commuting, availability of care by a third person, for example). The treatment of renal failure patients who do not yet need renal replacement therapy may be a challenge, though VTd can be considered for this group. The VTd regimen may also be appropriate for patients at high risk of thromboembolism. Switching from lenalidomide to melphalan can be considered (VMP regimen based on the UPFRONT and CLARION trials).


Regimens with bortezomib are recommended for patients with high cytogenetic or thromboembolic risks, those with renal failure, and those with a contraindication to anticoagulants. The neurotoxicity of bortezomib can be reduced without affecting OS if administered once a week.^{38,50,62} On the other hand, lenalidomide is indicated for patients with pre-existing polyneuropathy.

Undoubtedly, patients over 75 constitute a minority in clinical trials, and those over 80 are often ineligible for trials. Therefore, the access to clinical data collected by treatment centers is also important to build real treatment guidelines for this group of patients.

Given that age alone increases the risk of death in elderly patients, deciding on the type of therapy remains a challenge and requires further follow-up and prospective analyses.

ORCID iDs

Agata Tyczyńska  <https://orcid.org/0000-0002-2067-2715>

Jan Zaucha  <https://orcid.org/0000-0002-0986-8936>

References

1. Dimopoulos MA, Moreau P, Terpos E, et al. Multiple myeloma: EHA-ESMO Clinical Practice Guidelines for diagnosis, treatment and follow-up. *Ann Oncol*. 2021;32(3):309–322. doi:10.1016/j.annonc.2020.11.014
2. Suska A, Jurczyszyn A. Epidemiology and etiopathogenesis of multiple myeloma and monoclonal gammopathy of undetermined significance. *Postepy Hig Med Dosw*. 2018;72:953–965. doi:10.5604/01.3001.0012.7296
3. Kyle RA, Rajkumar SV. Multiple myeloma. *Blood*. 2008;111(6):2962–2972. doi:10.1182/blood-2007-10-078022
4. Padala SA, Barsouk A, Barsouk A, et al. Epidemiology, staging, and management of multiple myeloma. *Med Sci (Basel)*. 2021;9(1):3. doi:10.3390/medsci9010003
5. Jurczyszyn A, Suska A. Multiple myeloma. In: *Reference Module in Biomedical Sciences*. Elsevier; 2019:461–478. doi:10.1016/B978-0-12-801238-3.11412-6
6. National Cancer Institute. *Cancer Stat Facts: Myeloma*. Rockville, USA: National Cancer Institute; 2021. <https://seer.cancer.gov/statfacts/html/mulmy.html>. Accessed October 6, 2021.
7. Polish National Cancer Registry. *Multiple Myeloma and Malignant Plasma Cell Neoplasms – 2019*. https://onkologia.org.pl/sites/default/files/Multiple_myeloma_and_malignant_plasma_cell_neoplasms.pdf.
8. Szumera-Ciećkiewicz A, Wojciechowska U, Didkowska J, et al. Population-based epidemiological data of follicular lymphoma in Poland: 15 years of observation. *Sci Rep*. 2020;10(1):14610. doi:10.1038/s41598-020-71579-6
9. Kazandjian D. Multiple myeloma epidemiology and survival: A unique malignancy. *Semin Oncol*. 2016;43(6):676–681. doi:10.1053/j.seminoncol.2016.11.004
10. Manapuram S, Hashmi H. Treatment of multiple myeloma in elderly patients: A review of literature and practice guidelines. *Cureus*. 2018; 10(12):e3669. doi:10.7759/cureus.3669
11. Tuchman SA, Shapiro GR, Ershler WB, et al. Multiple myeloma in the very old: An IASIA conference report. *J Natl Cancer Inst*. 2014;106(5):dju067. doi:10.1093/jnci/dju067
12. Alexanian R, Haut A, Khan A, et al. Treatment for multiple myeloma: Combination chemotherapy with different melphalan dose regimens. *JAMA*. 1969;208(9):1680–1685. doi:10.1001/jama.1969.03160090040009
13. Palumbo A, Waage A, Hulin C, et al. Safety of thalidomide in newly diagnosed elderly myeloma patients: A meta-analysis of data from individual patients in six randomized trials. *Haematologica*. 2013; 98(1):87–94. doi:10.3324/haematol.2012.067058

14. Hulin C, Facon T, Rodon P, et al. Efficacy of melphalan and prednisone plus thalidomide in patients older than 75 years with newly diagnosed multiple myeloma: IFM 01/01 trial. *J Clin Oncol*. 2009; 27(22):3664–3670. doi:10.1200/JCO.2008.21.0948
15. Wijermans P, Schaafsma M, Termorshuizen F, et al. Phase III study of the value of thalidomide added to melphalan plus prednisone in elderly patients with newly diagnosed multiple myeloma: The HOVON 49 Study. *J Clin Oncol*. 2010;28(19):3160–3166. doi:10.1200/JCO.2009.26.1610
16. Beksac M, Haznedar R, Firatli-Tuglular T, et al. Addition of thalidomide to oral melphalan/prednisone in patients with multiple myeloma not eligible for transplantation: Results of a randomized trial from the Turkish Myeloma Study Group. *Eur J Haematol*. 2011;86(1):16–22. doi:10.1111/j.1600-0609.2010.01524.x
17. Ludwig H, Hajek R, Tóthová E, et al. Thalidomide-dexamethasone compared with melphalan-prednisolone in elderly patients with multiple myeloma. *Blood*. 2009;113(15):3435–3442. doi:10.1182/blood-2008-07-169565
18. Palumbo A, Bringhen S, Liberati AM, et al. Oral melphalan, prednisone, and thalidomide in elderly patients with multiple myeloma: Updated results of a randomized controlled trial. *Blood*. 2008; 112(8):3107–3114. doi:10.1182/blood-2008-04-149427
19. Waage A, Gimsing P, Fayers P, et al. Melphalan and prednisone plus thalidomide or placebo in elderly patients with multiple myeloma. *Blood*. 2010;116(9):1405–1412. doi:10.1182/blood-2009-08-237974
20. Fayers PM, Palumbo A, Hulin C, et al. Thalidomide for previously untreated elderly patients with multiple myeloma: Meta-analysis of 1685 individual patient data from 6 randomized clinical trials. *Blood*. 2011;118(5):1239–1247. doi:10.1182/blood-2011-03-341669
21. Palumbo A, Falco P, Corradini P, et al. Melphalan, prednisone, and lenalidomide treatment for newly diagnosed myeloma: A report from the GIMEMA – Italian Multiple Myeloma Network. *J Clin Oncol*. 2007;25(28):4459–4465. doi:10.1200/JCO.2007.12.3463
22. Palumbo A, Magarotto V, Bringhen S, et al. A randomized phase 3 trial of melphalan-lenalidomide-prednisone (MPR) or cyclophosphamide-prednisone-lenalidomide (CPR) vs lenalidomide plus dexamethasone (Rd) in elderly newly diagnosed multiple myeloma patients. *Blood*. 2013;122(21):536. doi:10.1182/blood.V122.21.536.536
23. Palumbo A, Hajek R, Delforge M, et al. Continuous lenalidomide treatment for newly diagnosed multiple myeloma. *N Engl J Med*. 2012; 366(19):1759–1769. doi:10.1056/NEJMoa1112704
24. Magarotto V, Bringhen S, Musto P, et al. Doublet vs triplet lenalidomide-containing regimens in newly diagnosed myeloma patients, younger or older than 75 years: Subgroup analysis of a phase III study. *Blood*. 2014;124(21):2110. doi:10.1182/blood.V124.21.2110.2110
25. Bringhen S, Offidani M, Musto P, et al. Long-term outcome of lenalidomide-dexamethasone (Rd) vs melphalan-lenalidomide-prednisone (MPR) vs cyclophosphamide-prednisone-lenalidomide (CPR) as induction followed by lenalidomide-prednisone (RP) vs lenalidomide (R) as maintenance in a community-based newly diagnosed myeloma population: Updated analysis of EMN01 phase III study. *Blood*. 2017;130(Suppl 1):901. doi:10.1182/blood.V130.Suppl_1.901.901
26. Rajkumar SV, Jacobus S, Callander NS, et al. Lenalidomide plus high-dose dexamethasone versus lenalidomide plus low-dose dexamethasone as initial therapy for newly diagnosed multiple myeloma: An open-label randomised controlled trial. *Lancet Oncol*. 2010;11(1): 29–37. doi:10.1016/S1470-2045(09)70284-0
27. Facon T, Dimopoulos MA, Dispenzieri A, et al. Initial phase 3 results of the first (Frontline Investigation Of Lenalidomide + Dexamethasone Versus Standard Thalidomide) trial (MM-020/IFM 07 01) in newly diagnosed multiple myeloma (NDMM) patients (Pts) ineligible for stem cell transplantation (SCT). *Blood*. 2013;122(21):2. doi:10.1182/blood.V122.21.2
28. Facon T, Dimopoulos MA, Dispenzieri A, et al. Final analysis of survival outcomes in the phase 3 FIRST trial of up-front treatment for multiple myeloma. *Blood*. 2018;131(3):301–310. doi:10.1182/blood-2017-07-795047
29. Mateos MV, Richardson PG, Schlag R, et al. Bortezomib plus melphalan and prednisone compared with melphalan and prednisone in previously untreated multiple myeloma: Updated follow-up and impact of subsequent therapy in the phase III VISTA trial. *J Clin Oncol*. 2010;28(13):2259–2266. doi:10.1200/JCO.2009.26.0638
30. Mateos MV, Bringhen S, Richardson PG, et al. Bortezomib cumulative dose, efficacy, and tolerability with three different bortezomib-melphalan-prednisone regimens in previously untreated myeloma patients ineligible for high-dose therapy. *Haematologica*. 2014; 99(6):1114–1122. doi:10.3324/haematol.2013.099341
31. Niesvizky R, Flinn IW, Rifkin R, et al. Community-based phase IIIB trial of three UPFRONT bortezomib-based myeloma regimens. *J Clin Oncol*. 2015;33(33):3921–3929. doi:10.1200/JCO.2014.58.7618
32. Stege CAM, Nasserinejad K, Van Der Spek E, et al. Efficacy and tolerability of ixazomib, daratumumab and low dose dexamethasone (Ixa Dara dex) in unfit and frail newly diagnosed multiple myeloma (NDMM) patients; Results of the interim efficacy analysis of the phase II HOVON 143 study. *Blood*. 2019;134(Suppl 1):695. doi:10.1182/blood-2019-121694
33. O'Donnell EK, Laubach JP, Yee AJ, et al. A phase 2 study of modified lenalidomide, bortezomib and dexamethasone in transplant-ineligible multiple myeloma. *Br J Haematol*. 2018;182(2):222–230. doi:10.1111/bjh.15261
34. Durie BGM, Hoering A, Abidi MH, et al. Bortezomib with lenalidomide and dexamethasone versus lenalidomide and dexamethasone alone in patients with newly diagnosed myeloma without intent for immediate autologous stem-cell transplant (SWOG S0777): A randomised, open-label, phase 3 trial. *Lancet*. 2017;389(10068):519–527. doi:10.1016/S0140-6736(16)31594-X
35. Facon T, Lee JH, Moreau P, et al. Carfilzomib or bortezomib with melphalan-prednisone for transplant-ineligible patients with newly diagnosed multiple myeloma. *Blood*. 2019;133(18):1953–1963. doi:10.1182/blood-2018-09-874396
36. Facon T, Kumar SK, Plesner T, et al. Daratumumab, lenalidomide, and dexamethasone versus lenalidomide and dexamethasone alone in newly diagnosed multiple myeloma (MAIA): Overall survival results from a randomised, open-label, phase 3 trial. *Lancet Oncol*. 2021;22(11):1582–1596. doi:10.1016/S1470-2045(21)00466-6
37. Mateos MV, Cavo M, Blade J, et al. Overall survival with daratumumab, bortezomib, melphalan, and prednisone in newly diagnosed multiple myeloma (ALCYONE): A randomised, open-label, phase 3 trial. *Lancet*. 2020;395(10218):132–141. doi:10.1016/S0140-6736(19)32956-3
38. Knop S, Mateos MV, Dimopoulos MA, et al. Health-related quality of life in patients with newly diagnosed multiple myeloma ineligible for stem cell transplantation: Results from the randomized phase III ALCYONE trial. *BMC Cancer*. 2021;21(1):659. doi:10.1186/s12885-021-08325-2
39. Facon T, Venner CP, Bahlis NJ, et al. Oral ixazomib, lenalidomide, and dexamethasone for transplant-ineligible patients with newly diagnosed multiple myeloma. *Blood*. 2021;137(26):3616–3628. doi:10.1182/blood.202008787
40. Moreau P, Kolb B, Attal M, et al. Phase 1/2 study of carfilzomib plus melphalan and prednisone in patients aged over 65 years with newly diagnosed multiple myeloma. *Blood*. 2015;125(20):3100–3104. doi:10.1182/blood-2015-02-626168
41. Kuhr K, Wirth D, Srivastava K, Lehmacher W, Hellmich M. First-line therapy for non-transplant eligible patients with multiple myeloma: Direct and adjusted indirect comparison of treatment regimens on the existing market in Germany. *Eur J Clin Pharmacol*. 2016;72(3): 257–265. doi:10.1007/s00228-015-1998-5
42. Mateos MV, Oriol A, Martínez-López J, et al. Bortezomib, melphalan, and prednisone versus bortezomib, thalidomide, and prednisone as induction therapy followed by maintenance treatment with bortezomib and thalidomide versus bortezomib and prednisone in elderly patients with untreated multiple myeloma: A randomised trial. *Lancet Oncol*. 2010;11(10):934–941. doi:10.1016/S1470-2045(10)70187-X
43. Reeder CB, Reece DE, Kukreti V, et al. Once- versus twice-weekly bortezomib induction therapy with CyBORd in newly diagnosed multiple myeloma. *Blood*. 2010;115(16):3416–3417. doi:10.1182/blood-2010-02-271676
44. Bringhen S, Mateos MV, Zweegman S, et al. Age and organ damage correlate with poor survival in myeloma patients: Meta-analysis of 1435 individual patient data from 4 randomized trials. *Haematologica*. 2013;98(6):980–987. doi:10.3324/haematol.2012.075051
45. Dimopoulos MA, Oriol A, Nahi H, et al. Daratumumab, lenalidomide, and dexamethasone for multiple myeloma. *N Engl J Med*. 2016;375(14): 1319–1331. doi:10.1056/NEJMoa1607751

46. Palumbo A, Bringhen S, Mateos MV, et al. Geriatric assessment predicts survival and toxicities in elderly myeloma patients: An International Myeloma Working Group report. *Blood*. 2015;125(13):2068–2074. doi:10.1182/blood-2014-12-615187
47. Palumbo A, Chanan-Khan A, Weisel K, et al. Daratumumab, bortezomib, and dexamethasone for multiple myeloma. *N Engl J Med*. 2016;375(8):754–766. doi:10.1056/NEJMoa1606038
48. Mateos MV, Dimopoulos MA, Cavo M, et al. Daratumumab plus bortezomib, melphalan, and prednisone for untreated myeloma. *N Engl J Med*. 2018;378(6):518–528. doi:10.1056/NEJMoa1714678
49. Facon T, Kumar S, Plesner T, et al. Daratumumab plus lenalidomide and dexamethasone for untreated myeloma. *N Engl J Med*. 2019;380(22):2104–2115. doi:10.1056/NEJMoa1817249
50. Bringhen S, Offidani M, Palmieri S, et al. Early mortality in myeloma patients treated with first-generation novel agents thalidomide, lenalidomide, bortezomib at diagnosis: A pooled analysis. *Crit Rev Oncol Hematol*. 2018;130:27–35. doi:10.1016/j.critrevonc.2018.07.003
51. Chari A, Rodriguez-Otero P, McCarthy H, et al. Subcutaneous daratumumab plus standard treatment regimens in patients with multiple myeloma across lines of therapy (PLEIADES): An open-label Phase II study. *Br J Haematol*. 2021;192(5):869–878. doi:10.1111/bjh.16980
52. Kumar SK, Jacobus SJ, Cohen AD, et al. Carfilzomib or bortezomib in combination with lenalidomide and dexamethasone for patients with newly diagnosed multiple myeloma without intention for immediate autologous stem-cell transplantation (ENDURANCE): A multicentre, open-label, phase 3, randomised, controlled trial. *Lancet Oncol*. 2020;21(10):1317–1330. doi:10.1016/S1470-2045(20)30452-6
53. Martin T, Usmani SZ, Berdeja JG, et al. Ciltacabtagene autoleucel, an anti-B-cell maturation antigen chimeric antigen receptor T-cell therapy, for relapsed/refractory multiple myeloma: CARTITUDE-1 2-year follow-up. *J Clin Oncol*. 2023;41(6):1265–1274. doi:10.1200/JCO.22.00842
54. Costa LJ, Brill IK, Omel J, Godby K, Kumar SK, Brown EE. Recent trends in multiple myeloma incidence and survival by age, race, and ethnicity in the United States. *Blood Adv*. 2017;1(4):282–287. doi:10.1182/bloodadvances.2016002493
55. Krzemieniecki K. Comprehensive geriatric assessment and its clinical impact in oncology: Systematic literature review [in Polish]. *Onkol Prak Klin*. 2010;6(3):91–95. https://journals.viamedica.pl/oncology_in_clinical_practice/article/view/9204. Accessed August, 2021.
56. Lawton MP. Scales to measure competence in everyday activities. *Psychopharmacol Bull*. 1988;24(4):609–614. PMID:3074322.
57. Łacko A. Peculiarities of treatment of elderly cancer patients [in Polish]. *Old Age Med*. 2012;2(1):7–11. https://journals.viamedica.pl/medycyna_wieku_podeszlego/article/view/19209. Accessed June 21, 2021.
58. Mohty M, Cavo M, Fink L, et al. Understanding mortality in multiple myeloma: Findings of a European retrospective chart review. *Eur J Haematol*. 2019;103(2):107–115. doi:10.1111/ejh.13264
59. Xia J, Wang L, Zhou X, Wang J, Wang H, Guo H. Early mortality in elderly patients undergoing treatment for multiple myeloma in real-world practice. *J Int Med Res*. 2018;46(6):2230–2237. doi:10.1177/0300060518757640
60. Warren JL, Harlan LC, Stevens J, Little RF, Abel GA. Multiple myeloma treatment transformed: A population-based study of changes in initial management approaches in the United States. *J Clin Oncol*. 2013;31(16):1984–1989. doi:10.1200/JCO.2012.46.3323
61. Piechotta V, Jakob T, Langer P, et al. Multiple drug combinations of bortezomib, lenalidomide, and thalidomide for first-line treatment in adults with transplant-ineligible multiple myeloma: A network meta-analysis. *Cochrane Database Syst Rev*. 2019;2019(11):CD013487. doi:10.1002/14651858.CD013487
62. Cook J, Johnson I, Higgins A, et al. Outcomes with different administration schedules of bortezomib in bortezomib, lenalidomide and dexamethasone (VRd) as first-line therapy in multiple myeloma. *Am J Hematol*. 2021;96(3):330–337. doi:10.1002/ajh.26074